AD NUMBER

AD850243

NEW LIMITATION CHANGE

TO

Approved for public release, distribution unlimited

FROM

Distribution authorized to U.S. Gov't. agencies and their contractors; Administrative/Operational Use; Dec 1968. Other requests shall be referred to Air Force Materials Lab., Air Force Systems Command, Wright-Patterson AFB, OH 45433.

AUTHORITY

AFML ltr, 12 Jan 1972

AFML-TR-68-210

DEVELOPMENT OF FUSED SLURRY SILICIDE COATINGS FOR THE ELEVATED-TEMPERATURE OXIDATION PROTECTION OF COLUMBIUM AND TANTALUM ALLOYS

S. Priceman
L. Sama
Sylvania Electric Products Inc.
Hicksville, New York

Technical Report AFML-TR-68-210
December 1968

Air Force Materials Laboratory
Air Force Systems Command
Wright-Patterson Air Force Base, Ohio

NOTICES

When Government drawings, specifications, or other data are used for any purpose other than in connection with a definitely related Government procurement operation, the United States Government thereby incurs no responsibility nor any obligation whatsoever; and the fact that the Government may have formulated, furnished, or in any way supplied the said drawings, specifications, or other data, is not to be regarded by implication or otherwise as in any manner licensing the holder or any other person or corporation, or conveying any rights or permission to manufacture, use, or sell any patented invention that may in any way be related thereto.

This document is subject to special export controls and each transmittal to foreign governments or foreign nationals may be made only with prior approval of the Metals and Ceramics Division (MAMP), Air Force Materials Laboratory, Wright-Patterson Air Force Base, Ohio 45433.

Distribution of this report is limited because the report contains technology identifiable with items on the strategic embargo lists excluded from export under the U.S. Export Control Act, as implemented by AFR 310-2 and AFSC 80-20.

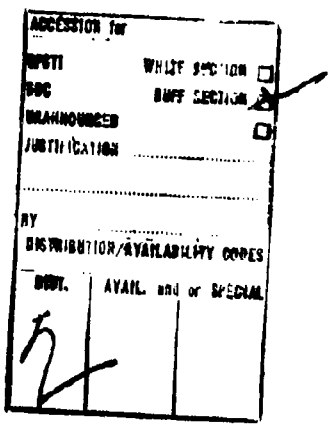

Copies of this report should not be returned unless return is required by security considerations, contractual obligations, or notice on a specific document.

AFML-TR-68-210

DEVELOPMENT OF FUSED SLURRY SILICIDE COATINGS FOR THE ELEVATED-TEMPERATURE OXIDATION PROTECTION OF COLUMBIUM AND TANTALUM ALLOYS

S. Priceman
L. Sama

FOREWORD

This final summary report was prepared by the High Temperature Composites Laboratory, Chemical and Metallurgical Division, Sylvania Electric Products Inc. under USAF Contract No. AF 33(615)-3272. This contract was initiated under Project No. 7312, "Metals Surface Deterioration and Protection", Task No. 731201 "Metal Surface Protection." This work was administered under the direction of the Air Force Materials Laboratory, Air Force Systems Command, with Mr. Norman Geyer (MAMP) as the project engineer.

This report covers the results of an experimental program conducted from October 1965 to June 1968.

The authors wish to acknowledge the contributions of their colleagues at the General Telephone & Electronics Laboratories: H. Woods for all the metallographic studies and P. Lublin, E. Rittershaus and W. Sutkowski for the x-ray diffraction and electron microbeam probe analyses. The coatings applications and evaluation procedures were performed by A. Zarnowski and F. Klimuck.

This technical report has been reviewed and is approved.

I. PERLMUTTER
Chief, Metals Branch
Metals and Ceramics Division
Air Force Materials Laboratory

ABSTRACT

Improved fused silicide coatings for columbium alloys were selected on the basis of slow cyclic oxidation tests. Several coating compositions were broadly characterized in terms of their structure and chemistry by means of x-ray diffraction and electron microbeam probe techniques and in terms of their applicability and performance by experimental analyses of wettability and flowability, faying surface penetration, coating repair, mechanical property tests, slow thermal cycling, furnace and torch oxidation, arc plasma tests, low temperature cycling, low pressure - high temperature exposures, re-entry simulation and statistical reliability analyses. The coating composition Si-20Cr-20Fe was the best for columbium alloys using the above combined criteria. More than 40 typical full scale columbium alloy aerospace structural panels were coated for reentry evaluation. During the course of the program several experimental compositions were utilized and procedures modified in accordance with panel fabrication requirements. These included stripping and repair brazing. Improved coating compositions and application techniques were used in the latter stages on virgin panels. Demonstrations are also presented which show the applicability of the process to the coating of threaded fasteners.

The compositions Si-20Ti-10Mo and Si-20Cr-1/2B_4Si were identified as better compositions for tantalum and molybdenum alloys on the bases of various higher temperature tests. The maximum useful temperature of these systems is approximately 3200°F.

The feasibility of using the fused silicides as a one-step combination coating-braze was demonstrated, and shear strength tests on such joints were carried out at temperatures in the range of room temperature to 3000°F.

This abstract is subject to special export controls and each transmittal to foreign governments or foreign nationals may be made only with prior approval of the Air Force Materials Laboratory (MAMP), Wright Patterson AFB, Ohio, 45433.

TABLE OF CONTENTS

TABLE OF CONTENTS (Cont)

TABLE OF CONTENTS (Cont)

LIST OF ILLUSTRATIONS

LIST OF ILLUSTRATIONS (Cont)

LIST OF ILLUSTRATIONS (Cont)

LIST OF ILLUSTRATIONS (Cont)

LIST OF ILLUSTRATIONS (Cont)

LIST OF ILLUSTRATIONS (Cont)

LIST OF ILLUSTRATIONS (Cont)

LIST OF ILLUSTRATIONS (Cont)

LIST OF ILLUSTRATIONS (Cont)

LIST OF TABLES

LIST OF TABLES (Cont)

LIST OF TABLES (Cont)

SECTION I

INTRODUCTION

Under a previous Air Force sponsored program (1), Sylvania developed a new series of coatings designated as "fused silicide slurry coatings." Those coatings have a number of advantages over coatings applied by other processes, which make them potentially very attractive for application to aerospace structures and other complex or large hardware. The coatings are essentially silicon alloy brazes based on the near-eutectic, binary compositions of Si-20w/oCr and Si-20w/oTi to which many ternary and higher-order additions have been made. In this previous program, the coatings were evaluated by broad-spectrum testing, which included high- and low-temperature cyclic oxidation resistance, slow cyclic oxidation, and resistance to degradation in or by low-pressure, high-temperature environments. This evaluation demonstrated that the coatings had excellent overall oxidation-protective properties, equal to or better than all other coatings developed to date.

Of equal importance, however, is the fact that the nature of the process makes it reasonable to assume that the properties demonstrated on small, simple, sheet specimens can be realized on large complex configurations; such is not the case with the pack cementation process. With the slurry process, the achievement of uniform coatings over large areas is due primarily to the absence of large masses of insulating pack materials, and to the wetting ability of the molten silicon alloy. The wetting and fluxing properties of the molten silicon alloy, which are obviously superior to those of the silicon halide vapors formed in pack coatings, result in a coating with an inherently superior reliability. Furthermore, the apparently great capillary attraction between the molten coating alloy and refractory metal surfaces causes the fused silicides to be drawn into deep recesses, faying surfaces and small holes. The coating of such surfaces by any other known process remains a serious problem. Improved edge coverage also results with the fused silicide process, because an appreciable portion of the coating-substrate reaction takes place while the coating is still liquid. A number of other processing and performance advantages of fused silicide coatings are summarized in reference (1).

The program covered by this report, which was a logical extension of the work summarized in reference (1), had as its major objective the further development of fused slurry silicide coatings to provide reliable protection to columbium and tantalum alloys in earth reentry environments. Emphasis was directed toward characterizing and improving a number of single-cycle coating compositions for use on columbium alloy sheet.

Significant secondary goals were

(1) the development of successful duplex coating systems using fused slurry compositions and techniques as a basis for improved reliability, and

(2) the investigation and development of fused slurry silicide compositions as braze alloys.

Effort was also directed toward the development of thicker, potentially longer-lived coatings, the use of fused silicides for coating repair, and the area of process development.

SECTION II

EXPERIMENTAL PROCEDURES AND RESULTS

This section describes the experimental and analytical investigations carried out as part of the program covered by this report. Most of this work was aimed at the immediate achievement of fused silicide coatings with improved properties and the characterization of these improved coatings in the broadest manner. A substantial effort was also directed toward clarifying the basic phenomena controlling the coating formation process, and the operative, protective, and failure mechanisms.

The work was not necessarily performed chronologically in the order presented below. The compositional optimization study, in fact, was continued throughout most of the program. Consequently, many test evaluations or characterization studies were initiated before improved compositions were identified. In many cases, these evaluations were repeated on the improved compositions. A somewhat reverse situation occurred toward the end of the program when more comprehensive and advanced evaluation procedures were employed. Although the "more optimum" compositions had now been identified, it was decided to apply these procedures to earlier widely-used compositions as well, since they had been previously factored into other programs and had received a considerable amount of independent evaluation.

1. MATERIALS

The substrate alloys selected for use on the program were D-43, Cb-752, T-111, T-222, and TZM. Ingot analyses of the materials used are given in Table I.

2. COATING PROCEDURES

The fused silicide slurries are made by mixing the elemental or prealloyed powders in a V Blender and then mixing these powders with lacquer by mechanical stirring. The columbium or tantalum surfaces to be coated may be cleaned by dry abrasive blasting with iron or alumina grit, or by acid pickling for one minute in a solution of one part concentrated HF, one part concentrated HNO_3 and one part water. Molybdenum and its alloys were similarly prepared for coating by grit blasting or acid pickling. The acid mixture used for these materials however was composed of equal parts of concentrated HCL, HNO_3 and water. There is no preferred cleaning method insofar as wettability or protectiveness of the coating is concerned. The method used, therefore, will depend on other factors such as convenience, availability of suitable equipment, and accessibility of the surface to be coated.

The slurry is applied to the cleaned surface by spraying, dipping, or brushing. If all surfaces are readily accessible, spraying is the preferred method.

TABLE I

INGOT ANALYSES OF ALLOYS

Element	D-43 Heat 389-21	Cb-752 Heat 53242	T-222 Heat 65034	T-111 Heat 2691	TZM Heat 7428
Cb	Bal.	Bal.	--	--	--
Ta	--	--	Bal.	Bal.	--
Mo	--	--	--	--	Bal.
W	10.2 w/o	10.0 w/o	9.5 w/o	7.1 w/o	--
Zr	1.0	2.5	--	--	0.087
Ti	--	--	--	--	0.42
Hf	--	--	2.4	1.6	--
Fe	--	--			10 ppm
Ni	--	--			10
C	0.1	60 ppm	160 ppm	18 ppm	160
O	186 ppm	65	50	10	3
H	3	--	2	--	1
N	48	78	22	22	3

After air drying, the coated part is placed in a cold-wall vacuum furnace on quartz, alumina, or alundum pads, or it is suspended by refractory metal wires, and fired at 2500 to 2600°F. The normal fusion-diffusion treatment was carried out for one hour.

3. SCREENING TEST PROCEDURES

A difficult problem in many development programs is to devise a rapid, but meaningful screening test. That is, when a process parameter or the chemical composition is varied, how can one simply determine if the resulting coating is significantly better or worse? The best test is not necessarily the most rigorous test or

the highest temperature test, but the one that most nearly ranks the candidate coatings in the order that would be obtained in actual use.

In most applications for coated refractory metals, large temperature gradients will be encountered. Furthermore, in some applications, cooling and heating rates will be such that the coating will be subjected to a broad temperature spectrum in use. The screening test should ideally evaluate the protective ability of the coating over the whole temperature range of interest.

It is a current general practice to subject coated specimens to one-hour cycles from some elevated temperature to room temperature. With coatings for columbium alloys, 2500°F has usually been chosen as the screening test temperature. However, tests may also be performed at 2200, 1800 and/or 1400°F, presumably in an effort to uncover any anomalous low- to intermediate-temperature oxidation behavior. Even testing at four or five temperatures involves a considerable effort in sample preparation and test performance and thereby limits the number of variations that can be screened. Also, from the considerable experience gathered over the last several years, it is clear that the intermetallic aluminides and silicides, on which practically all protective coatings for refractory metals are based, are all susceptible in varying degree to more rapid oxidation at some low-to-intermediate temperature than at 2500°F. The minimum life temperature, however, will vary from coating to coating, and even within a specific coating process the life nadir will be shifted up or down by slight changes in processing conditions or chemistry. Therefore, whether one tests at four temperatures or eight temperatures, most of the temperature spectrum is still being neglected.

A much more meaningful test is the slow cyclic oxidation test which consists of heating and cooling the specimens slowly through a broad temperature profile. The test, which is both simple and economical, is performed in a vertical mullite tube furnace heated by four Globar elements. This furnace, shown in Figure 1, is maintained at a constant temperature of 2500°F in the hot zone. The test specimens are suspended from a quartz hook, attached to a Pt-40w/oRh wire, which is in turn attached to a flexible chain. The chain goes over an idler pulley and is affixed to an adjustable crank arm driven by a 1/60 rpm instrument motor and gear reducer unit. The motor and crank turn one complete revolution in one hour. This causes the samples to be slowly lowered into and raised out of the hot zone over this period. During the initial calibration a thermocouple was attached near the test samples and the output was fed into a strip chart recorder, yielding the curve shown in Figure 2. The test is usually continued until there is visual evidence of the initiation of oxidation of the base metal. Duplicate samples are usually employed, and the variation of lifetimes within each pair of duplicates has been sufficiently small to demonstrate that the results are characteristic of the experimental sample batches tested.

This test closely simulates the type of temperature profile that a coated, refractory-metal, reentry vehicle would be subjected to in actual use. Since reentry vehicle applications constitute a prime potential use for coated refractory

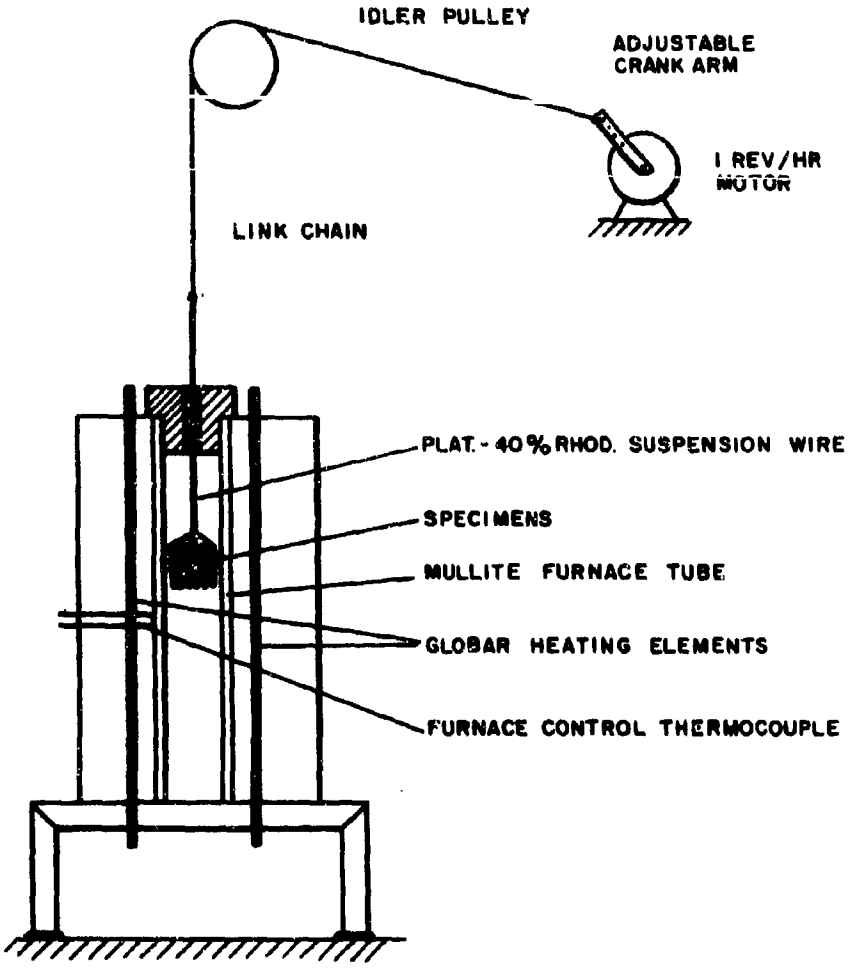

Figure 1 Schematic Drawing of Slow Cyclic Oxidation Test Apparatus.

metals, it is obvious that this test is valid not only as a screening test, but also as a partially simulating environmental test.

4. COATINGS FOR COLUMBIUM ALLOYS

a. Compositional Optimization Study

The objective of this study was first to evaluate and compare the slow cyclic oxidation performance of the most promising fused silicide coating compositions, and then to optimize the composition on the basis of further slow cyclic tests. Since there had previously been indications that longer heat treatments might be beneficial, the effect of heat treatment time was also included in the study. Eleven compositions

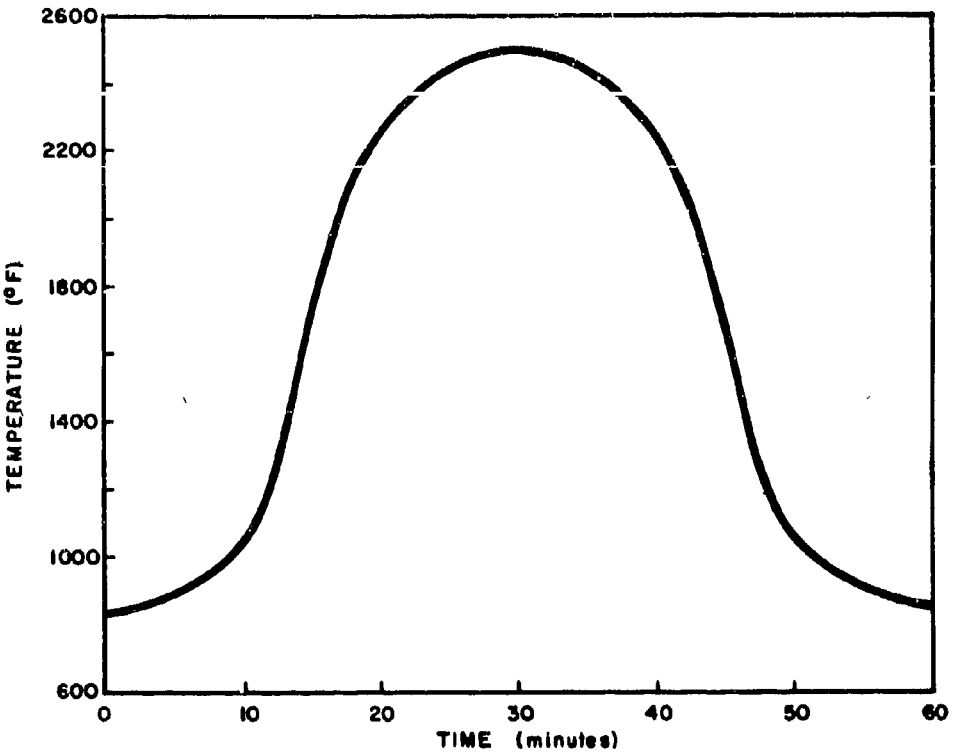

Figure 2 Temperature Versus Time for Slow-Cycling Oxidation Tests.

were initially selected along with three heat treatments: 1, 2, and 4 hours at 2580°F. Five small coupons of D-43 were coated with each of the 33 compositional heat-treatment combinations and evaluated by metallographic examination and slow cyclic oxidation. Photomicrographs of all the different compositions in the 1-hour and 4-hour diffusion-treatment conditions are shown in Figure 3. As would be expected, the longer heat treatments generally resulted in some additional growth of the lower layers. It is significant, however, that the structures of all the coatings are quite similar, even though the chemical compositions vary considerably.

During the slow cyclic test, each sample was weighed after each cycle, and unit weight gain versus cyclic oxidation time curves were constructed for many of the coatings. A secondary object of these tests was to determine if there is any correlation between the weight change during slow cycling and the time-to-failure.

Table II lists the number of cycles, or time-to-failure for each system together with coating weights and selected weight gain data. Curves of weight gain versus oxidation time for the 11 compositions given the one-hour standard diffusion treatment are plotted in Figure 4. The two- and four-hour diffusion treatments invariably resulted in similarly sloped curves with slightly higher weight gains.

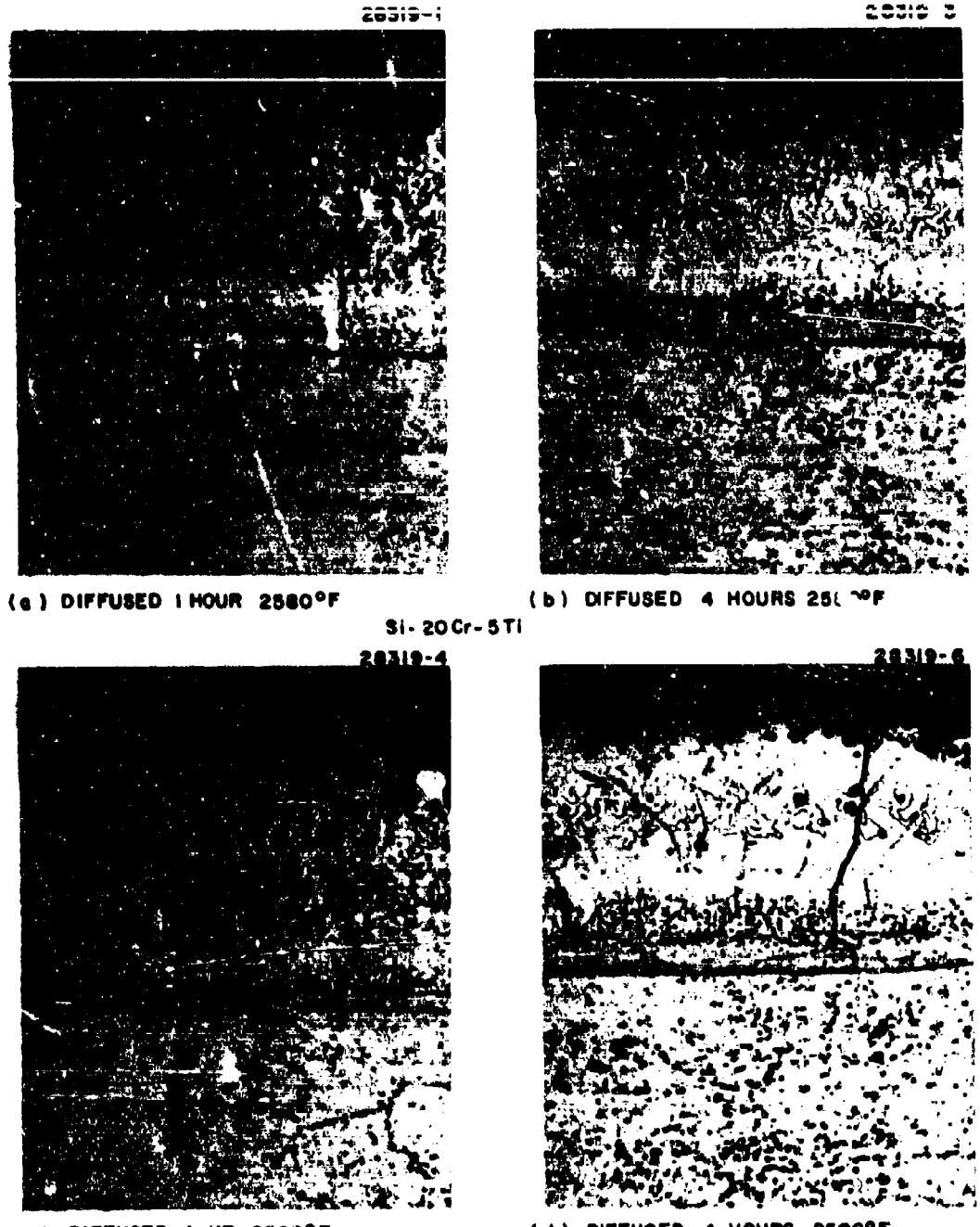

Figure 3 Photomicrographs of Fused Silicide Coated D43 Showing Various Coating Compositions and Diffusion Treatments (500X).

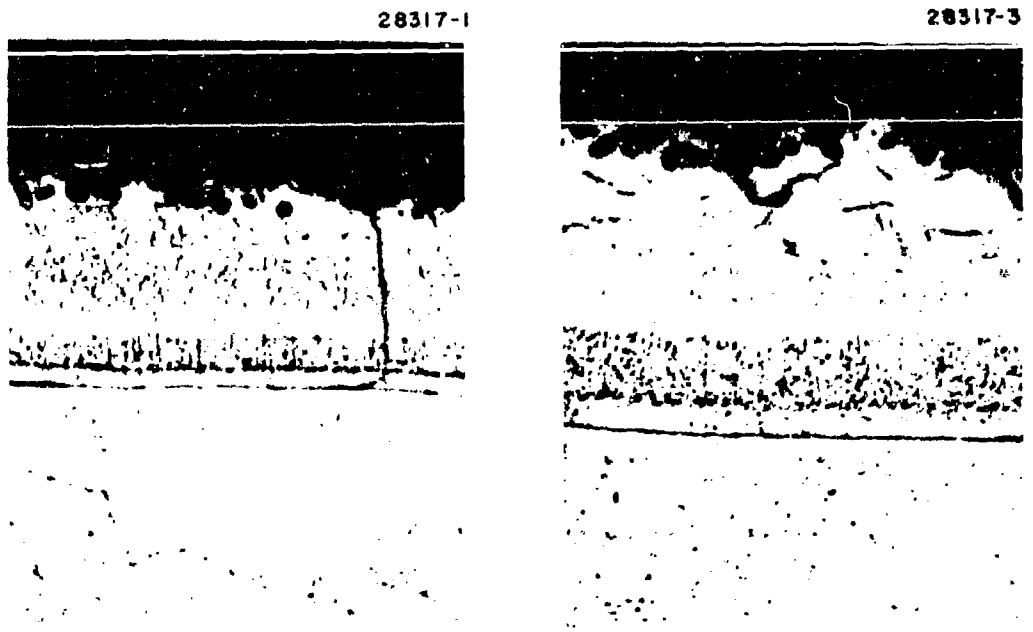

(e) DIFFUSED 1 HOUR 2580° F

(f) DIFFUSED 4 HOURS 2580° F

Si-20Cr-20Ti

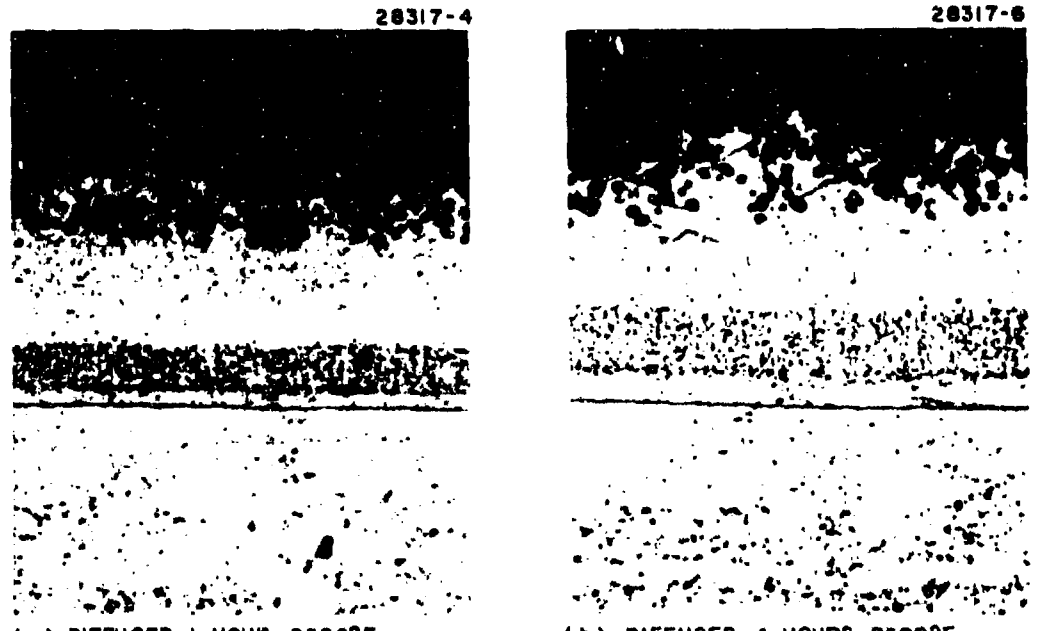

(g) DIFFUSED 1 HOUR 2580°F

(h) DIFFUSED 4 HOURS 2580°F

Si-20Ti-10Cr

Figure 3---Continued

(i) DIFFUSED 1 HOUR 2580°F

(j) DIFFUSED 4 HOURS 2580°F

Si-20Cr-5V

(k) DIFFUSED 1 HOUR 2580°F

(l) DIFFUSED 4 HOURS 2580°F

Si-20-10V

Figure 3---Continued

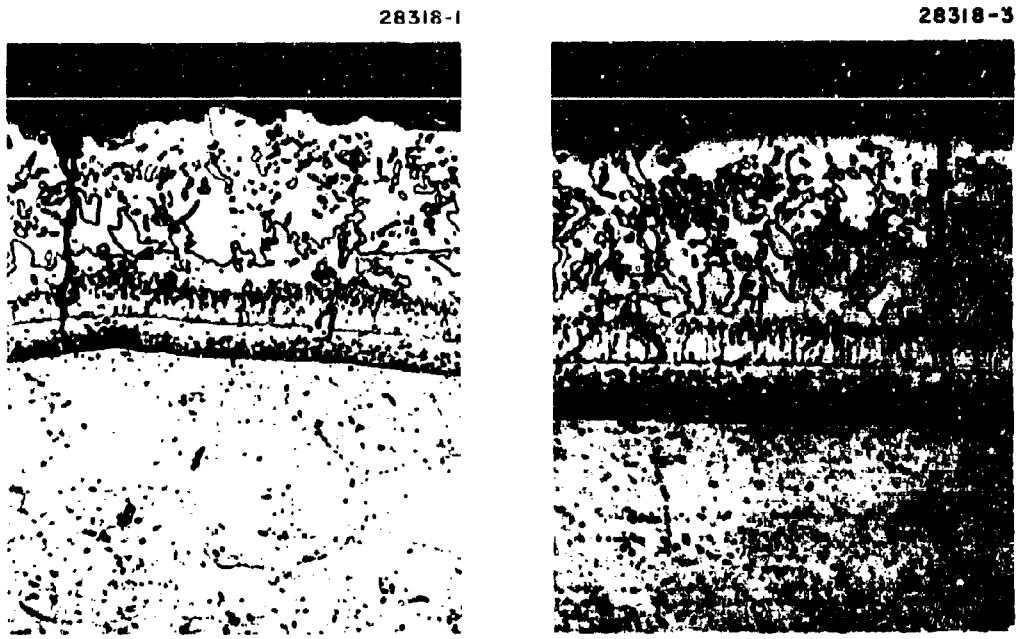

(m) DIFFUSED 1 HOUR 2580°F (n) DIFFUSED 4 HOURS 2580°F

Si-20Cr-2Al

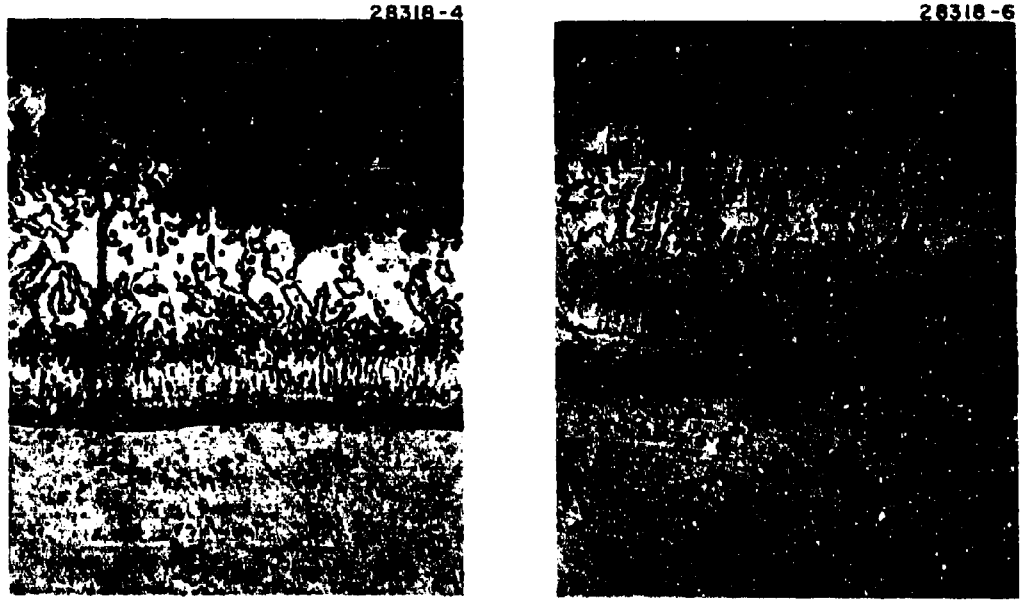

(o) DIFFUSED 1 HOUR 2580°F (p) DIFFUSED 4 HOURS 2580°F

Si-20Cr-5Ti_1-10VSi_2

Figure 3---Continued

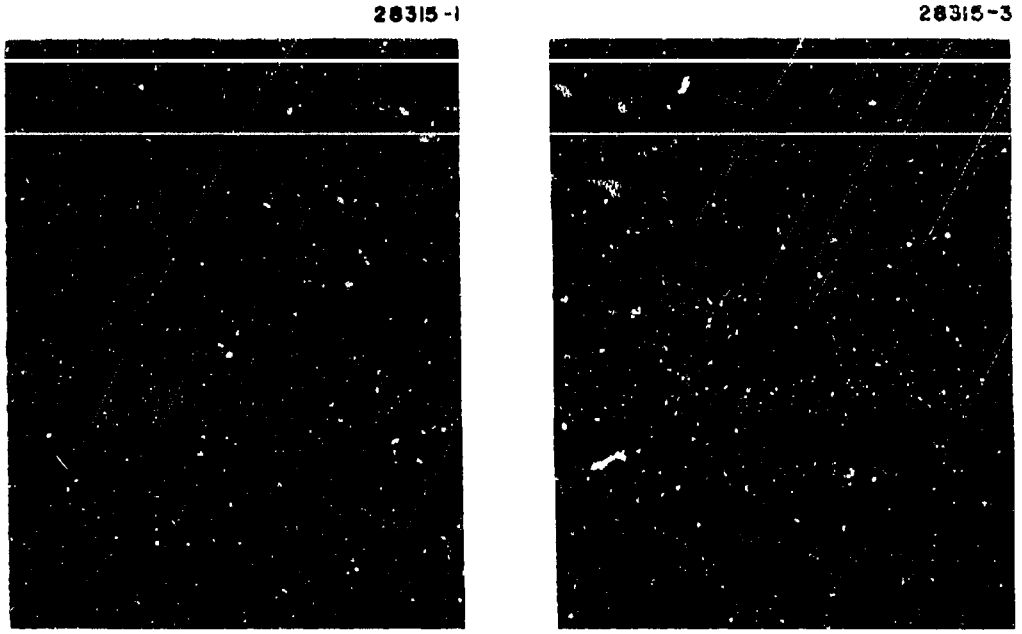

(q) DIFFUSED 1 HOUR 2580°F (r) DIFFUSED 4 HOURS 2580°F

Si-20Cr-5Ti-10Fe-10VSi_2

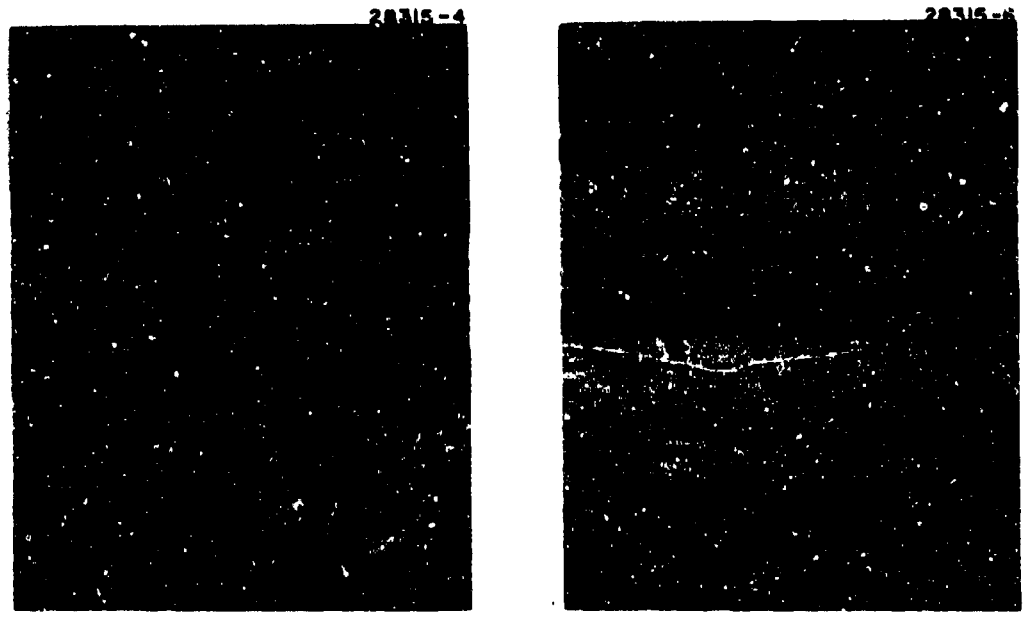

(s) DIFFUSED 1 HOUR 2580°F (t) DIFFUSED 4 HOURS 2580°F

Si-20Cr-10Mo

Figure 3---Continued

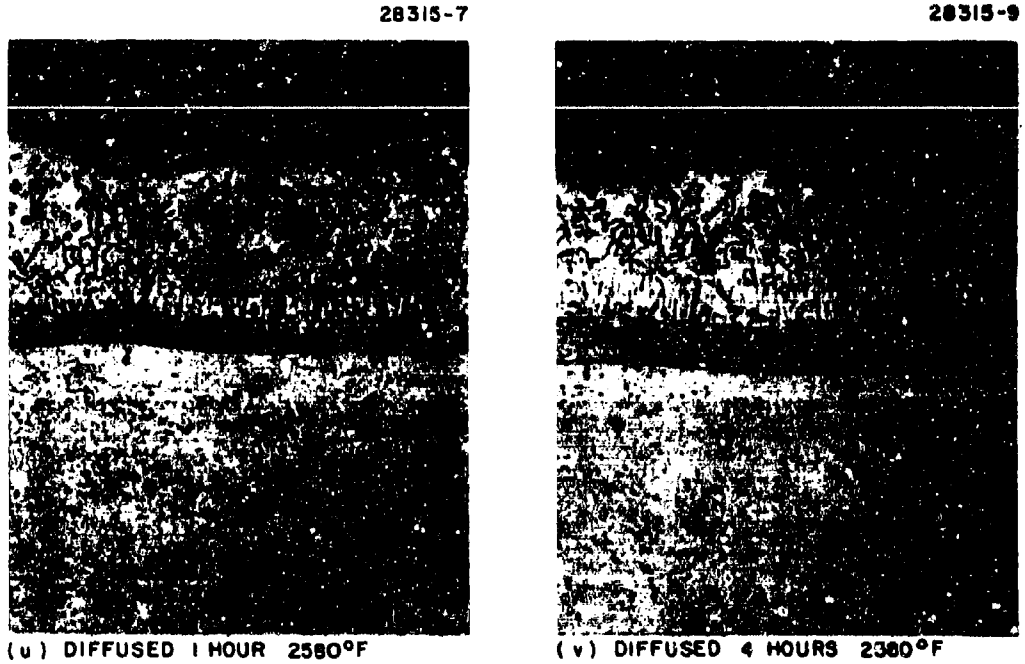

Si-20Cr-10W

Figure 3---Concluded

It is significant that the coating displaying the highest initial weight gain rate and greatest absolute weight gain also had by far the lowest slope and the longest lifetime. It may well be that the relatively high oxidation rate of the outer layer of this coating, coupled with improved ductility of the scale due to alloying, quickly and effectively seals the thermal stress cracks in the coating. With the more-oxidation-resistant compositions, oxidation of the surfaces of the thermal stress cracks proceeds at too slow a rate to seal them. Oxidation of the lower, less-oxidation-resistant phases of the coating can then proceed, resulting in severe stress and ultimately in spalling of the coating at the edges.

With several systems such as Si-Cr-V, Si-Cr-Al, and Si-Cr-W, although failure occurred primarily at the edges, the coatings were generally oxidized. Coatings in the Si-Cr-Ti, Si-Cr-Ti-V, and Si-Cr-Ti-Fe-V systems generally were not severely oxidized, and with the exception of Si-20Cr-5Ti, the craze cracking pattern was not obvious except under polarized light at 100X or higher magnifications. These coatings also failed at the edges, and cracks in the coating were noted near the edges after failure. It seems clear that thermal stress cracking and oxidation in these cracks, particularly at or near sheet edges, is responsible for most oxidation failures, and that this phenomenon is accelerated during slow cycling oxidation exposure.

TABLE II

SLOW CYCLIC OXIDATION TEST DATA

Diff. Time (hr)	Composition	Applied Coat. Wt. (mg/cm^2)	No. Cycles to Fail.	Total Unit Weight Gain (mg/cm^2)	
				1 hr	8 hr
1	Si-20Cr-5Ti	16.5	9^e, 10^e	0.64	1.32
2		15.9	9^e, 10^e	0.74	1.43
4		16.6	9^e, 10^e	1.15	1.82
1	Si-20Cr-10Ti	19.3	8^e, 8^e	0.64	1.11
2		18.8	8^e, 8^e	0.75	1.28
4		16.0	9^e, 7^e	0.98	1.75
1	Si-20Cr-20Ti	21.9	7^e, 10^e	0.66	1.45 (7 hr)
2		19.3	9^e, 8^e	0.75	1.52
4		18.6	4^e, 3^e	0.66	-
1	Si-20Ti-10Cr	18.7	8^e, 10^e	0.96	1.50
2		15.6	8^e, 10^e	1.20	1.75
4		15.1	7^e, 9^e	1.52	1.94 (7 hr)
1	Si-20Cr-5V	17.4	8^e, 9^e	0.79	1.82
2		15.7	11^e, 9^e	1.15	2.52
4		12.8	6^e, 6^s	1.67	-
1	Si-20Cr-10V	20.8	16^{es}, 12^e	1.26	1.67
2		17.2	8^e, 10^s	1.54	4.96 (7 hr)
4		19.5	7^g, 6^e	2.00	6.85 (6 hr)

TABLE II (Cont)

SLOW CYCLIC OXIDATION TEST DATA

Diff. Time (hr)	Composition	Applied Coat. Wt. (mg/cm^2)	No. Cycles to Fail.	Total Unit Weight Gain (mg/cm^2)	
				1 hr	6 hr
1	Si-20Cr-2Al	21.8	8^e, 11^e	0.62	1.45
2		19.1	8^e, 10^e	0.79	2.31
4		18.4	7^e, 8^e	0.96	3.01 (7 hr)
1	Si-20Cr-5Ti-10VSi_2	22.3	11^e, 10^e	0.86	1.26
2		21.0	9^e, 10^e	1.35	1.69
4		19.7	8^e, 10^e	1.75	4.31 (7 hr)
1	Si-20Cr-5Ti-10Fe-10VSi_2	19.2	28^e, 24^g	1.62	2.07
2		17.0	15^e, 16^e	2.09	2.50
4		16.6	16^e, 17^e	2.69	1.62
1	Si-20Cr-10Mo	15.4	13^e, 17^e	0.45	0.66
2		15.9	13^e, 13^e	0.60	0.75
4		13.5	13^e, 13^e	0.75	0.23
1	Si-20Cr-10W	17.1	14^e, 13^e	0.60	1.62
2		14.2	13^e, 12^e	0.79	2.03
4		16.0	14^e, 10^e	1.07	3.27

^{e} Edge failure

^{g} General failure

^{s} Surface failure

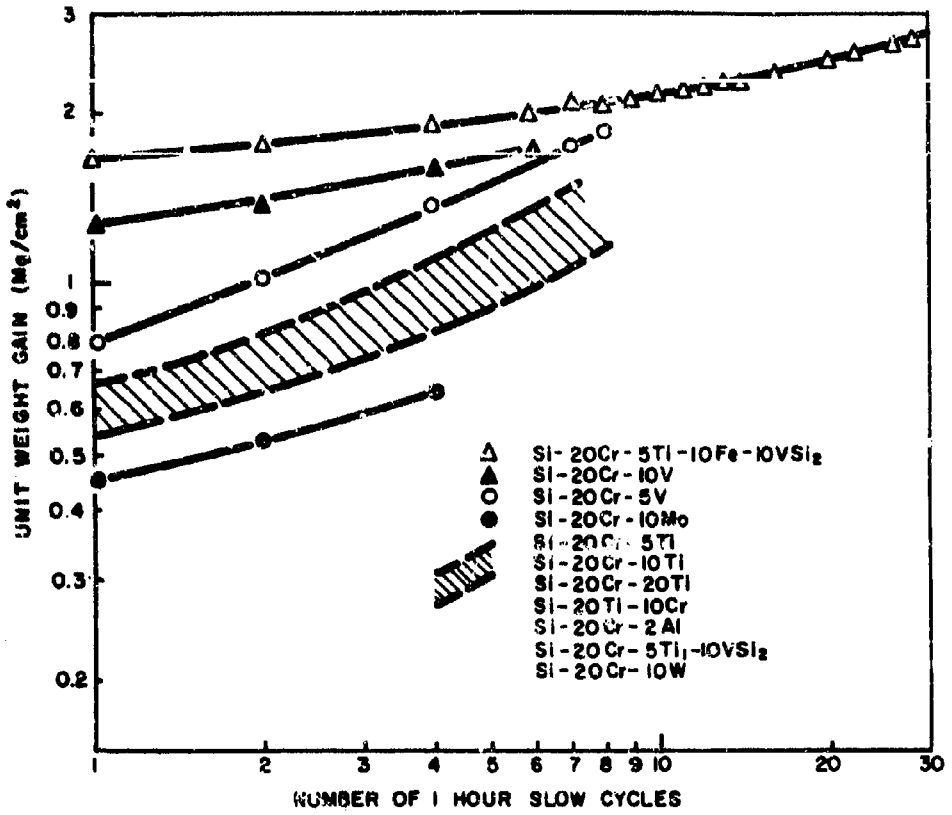

Figure 4 Weight Change During Slow Cyclic Oxidation From 800 to 2500°F.

The results of the initial screening tests demonstrated that the complex Si-20Cr-5Ti-10Fe-10VSi_2 coating was superior to the other compositions tested. This finding, moreover, was consistent with the results of the previous program (1). Consequently, twenty-five compositions in the Si-Cr-Ti-Fe-V system were selected for study aimed at optimization of the composition in relation to slow cyclic oxidation life. This experiment represented a full factorial plan based on two levels of Cr, Ti, Fe, and V concentrations plus nine additional compositions based on a third (zero) titanium level and two additional (zero and 5%) VSi_2 levels. The D-43 alloy was also used in this experiment. Table III lists the coating compositions studied and the corresponding slow cyclic test results. The data are broken down in Tables IV, V, VI, and VII to show the effect of variation in each specific additive. It is clear that 20Cr, 0Ti, and 10VSi_2 levels result in significantly greater lives than do the higher concentrations of these elements. The greatest improvement resulted from the elimination of titanium from the coating. The data for iron are not as conclusive as for the other elements. The optimum compositions based on this analysis of the data would be Si-20Cr-20Fe-10VSi_2 and Si-20Cr-20Fe. These compositions also displayed the longest slow cyclic lives of all those tested.

Photomicrographs of selected coating compositions are shown in both the as-coated and tested conditions in Figure 5.

TABLE III

CYCLIC OXIDATION TEST RESULTS OF COMPOSITIONAL OPTIMIZATION STUDY

Composition	Applied Coating (mg/cm^2)	No. Cycles to Failure
Si-20Cr-5Ti-10Fe-10VSi_2	19.3	17^e, 20^e
Si-20Cr-5Ti-10Fe-20VSi_2	23.6	17^e, 20^e
Si-20Cr-5Ti-20Fe-10VSi_2	20.6	34^e, 21^s
Si-20Cr-5Ti-20Fe-20VSi_2	19.8	15^e, 17^e
Si-20Cr-10Ti-10Fe-10VSi_2	19.7	10^{es}, 11^e
Si-20Cr-10Ti-10Fe-20VSi_2	23.2	8^e, 9^e
Si-20Cr-10Ti-20Fe-10VSi_2	18.5	8^e, 9^e
Si-20Cr-10Ti-20Fe-20VSi_2	24.8	1^e, 10^e
Si-30Cr-5Ti-10Fe-10VSi_2	16.4	7^s, 12^{es}
Si-30Cr-5Ti-10Fe-20VSi_2	19.4	7^{es}, 9^{es}
Si-30Cr-5Ti-20Fe-10VSi_2	21.9	20^s, 22^s
Si-30Cr-5Ti-20Fe-20VSi_2	24.7	10^s, 18^s
Si-30Cr-10Ti-10Fe-10VSi_2	19.7	8^{es}, 10^e
Si-30Cr-10Ti-10Fe-20VSi_2	15.7	1^e, 3^e
Si-30Cr-10Ti-20Fe-10VSi_2	20.9	3^{es}, 5^{es}
Si-30Cr-10Ti-20Fe-20VSi_2	24.6	2^e, 2^e
Si-20Cr-10Fe-10VSi_2	20.0	44^e, 33^e
Si-20Cr-20Fe-10VSi_2	20.6	44^e, 42^e
Si-30Cr-20Fe-10VSi_2	18.0	40^e, 33^s
Si-30Cr-10Fe-10VSi_2	21.0	37^s, 37^e
Si-20Cr-20Fe-5VSi_2	20.8	28^e, 40^e
Si-20Cr-10Fe-5VSi_2	21.9	35^e, 11^e
Si-10Cr-20Fe-10VSi_2	19.5	23^e, 45^s
Si-20Cr-20Fe	21.3	45^e, 45^e
Si-20Cr-10Fe	19.0	48^e, 33^e

^{e} Edge Failure ^{s} Surface Failure

TABLE IV

COMPARISON OF SLOW CYCLIC DATA FOR EFFECT OF CHROMIUM CONCENTRATION IN COATING

Base Coating Composition +	Slow Cyclic Oxidation Life (No. of 1-hour cycles)	
	20 Cr	30 Cr
Si-5Ti-10Fe-10VSi_2	17, 20	7, 12
Si-5Ti-10Fe-20VSi_2	17, 20	7, 9
Si-5Ti-20Fe-10VSi_2	34, 21	20, 22
Si-5Ti-20Fe-20VSi_2	15, 17	10, 18
Si-10Ti-10Fe-10VSi_2	10, 11	8, 10
Si-10Ti-10Fe-20VSi_2	8, 9	1, 3
Si-10Ti-20Fe-10VSi_2	8, 9	3, 5
Si-20Ti-20Fe-20VSi_2	1, 10	2, 2
Si-0Ti-10Fe-10VSi_2	42, 33	37, 37
Si-0Ti-20Fe-20VSi_2	44, 42	40, 33
Total	388	286
Average	19.4	14.3

TABLE V

COMPARISON OF SLOW CYCLIC DATA FOR EFFECT OF TITANIUM CONCENTRATION IN COATING

Base Coating Composition +	Slow Cyclic Oxidation Life (No. of 1-hour cycles)		
	0 Ti	5 Ti	10 Ti
Si-20Cr-10Fe-10VSi_2	42, 43	17, 20	10, 11
Si-20Cr-10Fe-20VSi_2	-	17, 20	8, 9
Si-20Cr-20Fe-10VSi_2	44, 42	34, 21	8, 9
Si-20Cr-20Fe-20VSi_2	-	15, 17	1, 10
Si-20Cr-10Fe-10VSi_2	37, 37	7, 12	8, 10
Si-20Cr-10Fe-20VSi_2	-	7, 9	1, 3
Si-30Cr-20Fe-10VSi_2	40, 33	20, 22	3, 5
Si-30Cr-20Fe-20VSi_2	-	10, 18	2, 2
Total	308	266	100
Average	38.5	16.6	6.3

TABLE VI

COMPARISON OF SLOW CYCLIC DATA FOR EFFECT OF IRON CONCENTRATION IN COATING

Base Coating Composition +	Slow Cyclic Oxidation Life (No. of 1-hour cycles)	
	10 Fe	20 Fe
Si-20Cr-5Ti-10VSi_2	17, 20	34, 21
Si-20Cr-5Ti-20VSi_2	17, 20	15, 17
Si-20Cr-10Ti-10VSi_2	10, 11	8, 9
Si-20Cr-10Ti-20Vsi_2	8, 9	1, 10
Si-30Cr-5Ti-10VSi_2	7, 12	20, 22
Si-30Cr-5Ti-20VSi_2	7, 9	10, 18
Si-30Cr-10Ti-10VSi_2	8, 10	3, 5
Si-30Cr-10Ti-20VSi_2	1, 3	2, 2
Si-20Cr-0Ti-10VSi_2	42, 33	44, 42
Si-30Cr-0Ti-20VSi_2	37, 37	40, 33
Si-20Cr-0Ti-5VSi_2	35, 11	40, 28
Si-20Cr-0Ti-0VSi_2	48, 33	45, 45
Total	445	514
Average	18.5	21.4

TABLE VII

COMPARISON OF SLOW CYCLIC DATA FOR EFFECT OF VSi_2 CONCENTRATION IN COATING

Base Coating Composition +	Slow Cyclic Oxidation Life (No. of 1-hour cycles)	
	10 VSi_2	20 VSi_2
Si-20Cr-5Ti-10Fe	17, 20	17, 20
Si-20Cr-5Ti-20Fe	34, 21	15, 17
Si-20Cr-10Ti-10Fe	10, 11	8, 9
Si-20Cr-10Ti-20Fe	8, 9	1, 10
Si-30Cr-5Ti-10Fe	7, 12	7, 9
Si-30Cr-5Ti-20Fe	20, 22	10, 18
Si-30Cr-10Ti-10Fe	8, 10	1, 3
Si-30Cr-10Ti-20Fe	3, 5	2, 2
Total	217	156
Average	13.6	9.3

	0 VSi_2	5 VSi_2	10 VSi_2
Si-20Cr-0Ti-20Fe	45, 45	28, 40	44, 42
Si-20Cr-0Ti-10Fe	43, 33	35, 11	21, 35
Total	166	114	142
Average	41.5	28.5	35.5

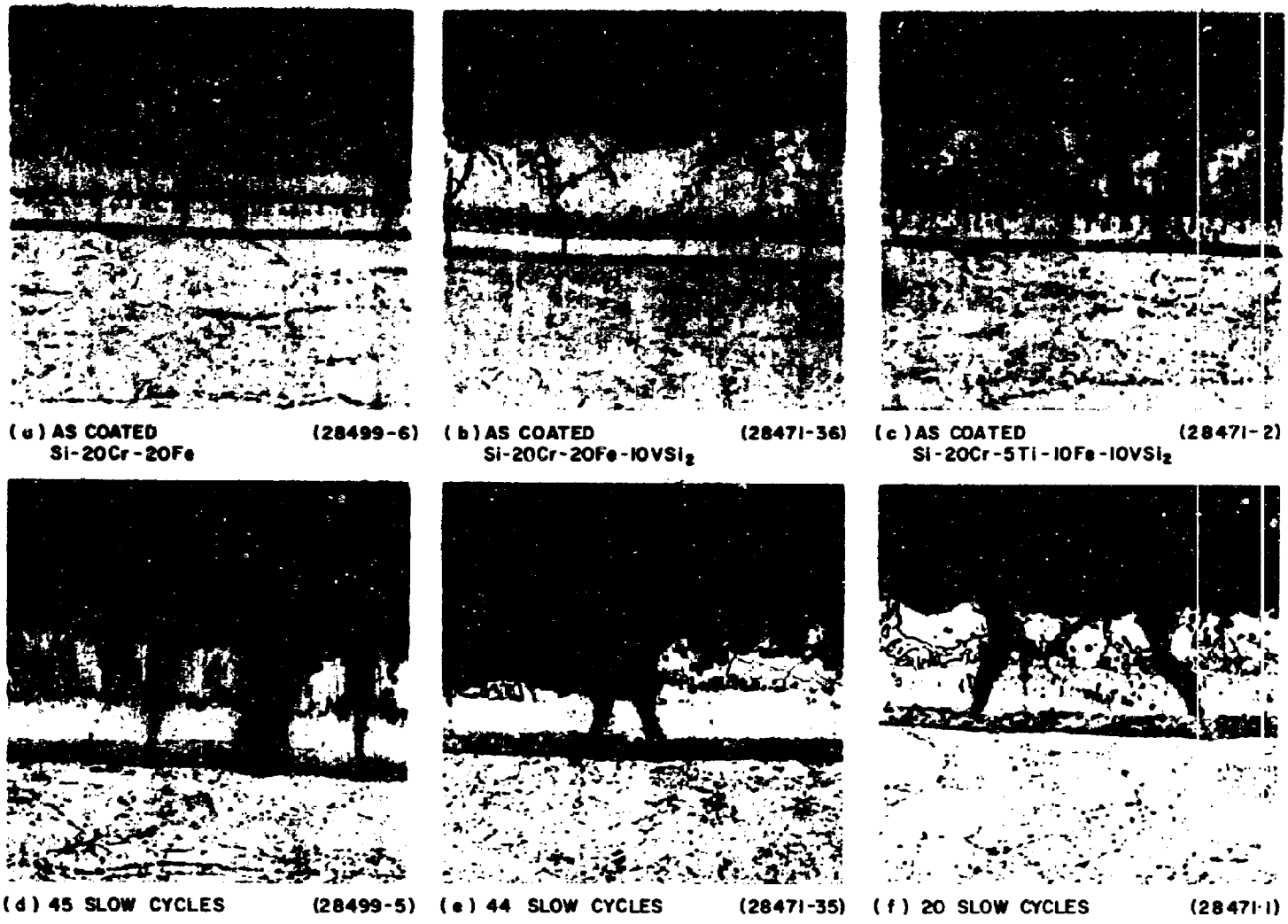

Figure 5 Photomicrographs of Selected Coating Compositions From Coating Optimization Study (300X).

b. Optimization of Coating Composition in the Si-Cr-Fe System

It was observed during the slow cyclic oxidation testing of the Si-20Cr-20Fe coatings on D43 that a yellowish, nonadherent, dusting, oxide scale formed on the surface somewhere after around 10 cycles and continued to form for about 10 to 20 additional cycles. If the samples were brushed clean after 30 cycles, no additional formation of this powdery scale was observed. On the basis of the X-ray and EMP analysis (see para 1 of this section), it was inferred that this phenomenon was related to the existence of a one mil thick zone of unalloyed $CbSi_2$ at the coating surface.

A brief study was made of the effect of fusion-diffusion time, temperature, and environment on this behavior. Lower temperatures, shorter times, and higher pressure environments (one atmosphere argon in lieu of vacuum) were investigated.

Groups of four coupons each were coated with the Si-20Cr-20Fe slurry and fired using six different sets of conditions. Two coupons of each set were slow-cyclically, oxidation-tested to failure. The samples were examined periodically to observe the times at which dusting commenced and ceased.

Table VIII lists the various heat treatments and visual observations and the time-to-failure for all the test specimens. Although the samples did exhibit some slight variations in appearance during the first six slow cycles, they all tended to exhibit the dusting behavior typical of the system after the sixth slow cycle. At the end of the 27th cycle the oxide "dust" or powder was brushed from the specimen surfaces, and no further dusting was observed. The lifetimes of the 15-minute, 2300°F, vacuum-diffusion treated samples were significantly lower than the lifetime of normally treated samples (70-100 cycles). On the other hand, the lifetimes exhibited by the argon-treated specimens were considerably greater than that normally obtained.

Further efforts were made to eliminate the residual $CbSi_2$ layer by decreasing the silicon concentration in the as-applied coating. The compositions looked at initially were Si-20Cr-25Fe, Si-25Cr-20Fe, Si-25Cr-25Fe and the base composition Si-20Cr-20Fe. Two samples of D43 coated with each of these compositions were slow cyclically oxidation tested. The Si-25Cr-25Fe coating did not exhibit the dusting surfaces characteristic of the Si-20Cr-20Fe coating, while the intermediate compositions did.

This was followed up with a more extensive study encompassing nine compositions, three firing temperatures, and two evaluation tests in a full factorial experiment. The base metal was D43 and the compositions were all in the range (40-60)Si- (20-40) Cr -(20-40)Fe. The firing temperatures studied were 2580, 2625, and 2700°F. The higher firing temperatures were looked at because of earlier indications that some of the more heavily alloyed as-applied coating compositions had higher initial melting points. One sample representing each compositional-diffusion treatment combination was slow cyclically tested to failure and one of each group was cyclically tested at 2400°F to failure.

TABLE VIII

EFFECT OF VARIATIONS IN FUSION-DIFFUSION TREATMENTS ON SLOW CYCLIC OXIDATION BEHAVIOR OF Si-20Cr-20Fe FUSED SILICIDE COATING

Time	Temp. °F	Environment	1st Cycle	2nd Cycle	6th Cycle	10th Cycle	19th Cycle	27th[a] Cycle	30th Cycle	No. of 1-hour slow cycles to failure
15 min.	2300	Vacuum	Green adherent scale	Green adherent scale	Olive drab adherent	Surface dusting	Surface dusting	Surface dusting both yellow & brown powder	Uniform brown adherent scale	27, 32
1 hr.	2300	Vacuum	Green adherent scale	Green adherent scale	Olive drab adherent	Surface dusting	Surface dusting	Surface dusting both yellow & brown powder	Uniform brown adherent scale	107,107
15 min.	2500	Vacuum	Gray adherent scale	Gray & brown adherent scale	Some yellowish oxide	Surface dusting	Surface dusting	Surface dusting both yellow & brown powder	Uniform brown adherent scale	107,100

TABLE VIII (Cont)

EFFECT OF VARIATIONS IN FUSION-DIFFUSION TREATMENTS ON SLOW CYCLIC OXIDATION BEHAVIOR OF Si-20Cr-20Fe FUSED SILICIDE COATING

Time	Temp. °F	Environment	1st Cycle	2nd Cycle	6th Cycle	10th Cycle	19th Cycle	27th[a] Cycle	30th Cycle	No. of 1-hour slow cycles to failure
1 hr.	2500	Vacuum	Gray adherent scale	Gray & brown adherent scale	Some yellowish oxide	Surface dusting	Surface dusting	Surface dusting both yellow & brown powder	Uniform brown adherent scale	124,139
1 hr.	2500	1 atm. argon	Gray adherent scale	Gray & brown adherent scale	Some yellowish oxide	Surface dusting	Surface dusting	Surface dusting both yellow & brown powder	Uniform brown adherent scale	208,203
1 hr.	2580	1 atm. argon	Gray adherent scale	Gray & brown adherent scale	Some yellowish oxide	Surface dusting	Surface dusting	Surface dusting both yellow & brown powder	Uniform brown adherent scale	208,190

[a] Powdery oxides removed from sample surfaces by brushing after 27th cycle.

The dusting oxide scale which has been previously described as characteristic of the Si-20Cr-20Fe coating was observed only with that specific composition. It may be safely concluded, therefore, that compositions containing a minimum of 50 percent (Fe + Cr), with the ratio of these elements ranging from 1:2 to 2:1, will not exhibit this apparently harmless phenomenon.

The oxidation test results are given in Table IX. The most significant conclusion to be drawn from these tests is that all 27 combinations of composition and heat treatment result in coatings with excellent protectiveness. The range of slow cyclic oxidation lifetimes is 52-168 cycles and of the 1-hour 2400°F cyclic test 48-96 cycles. These results are very significant since they point out the relative insensitivity of the Si-Cr-Fe coating system to fairly large compositional and diffusion temperature variations.

Photomicrographs of each coating composition are shown in Figure 6. The coatings shown were those fused at 2625°F. As the silicon content in the coating is reduced, the amount of $CbSi_2$ appears to decrease. With silicon contents below 50 w/o there is apparently no $CbSi_2$ formed. However, it is also very apparent that these coatings generally have very irregular surfaces. Although they have tested out well it still would be very desirable to have smooth surfaces. The coating experiments described in the previous paragraphs appear to indicate that the surfaces were less irregular when produced at the lower firing temperatures. For this reason firing temperatures of 2400 and 2500°F were looked at with two coating compositions, but the results based on visual and metallographic observations do not indicate any marked improvement in surface smoothness.

In the course of other earlier work on this program, aimed at optimizing fused silicide coating compositions for tantalum alloys, a Si-20Ti-10Mo-3V prealloyed powder was prepared and used in an effort to produce a more homogeneous coating. The coating produced was apparently very uniform in thickness and structure, had a very smooth surface, and was superior in these respects to a coating of similar composition prepared from elemental powders. In the light of this experience it was decided to prepare a Si-25Cr-25Fe prealloyed powder, in the hope that coatings made with this powder might have smoother surfaces than coatings of the same composition made with elemental powders.

The prealloyed powders were prepared by vacuum melting and grinding compacted pellets made of blended powders of the proper composition. Grinding was done manually in a steel mortar and pestle, and the powder was passed through a magnetic separator to remove all steel particles. The prealloyed powder slurry was spray-coated on D43 sheet coupons and fired in groups of three each at 2400, 2500, and 2580°F. Unexpectedly, the visual and macroscopic appearance of all three groups of samples was quite nonuniform. It looked as if the coatings were not completely melted and/or wet out well, particularly around the edges. Cold-pressed pellets of the prealloyed powder were used for melting point determinations, and it was conclusively demonstrated that the melting point of the prealloyed powder is somewhere below 2400°F.

TABLE IX

OXIDATION TEST RESULTS OF Si-Cr-Fe FUSED SILICIDE COATINGS

Composition	2580°F Diffusion Temp.		2625°F Diffusion Temp.		2700°F Diffusion Temp.	
	No. 1-hr. Slow Cycles to Failure	No. 1-hr. 2400°F Cycles to Failure	No. 1-hr. Slow Cycles to Failure	No. 1-hr. 2400°F Cycles to Failure	No. 1-hr. Slow Cycles to Failure	No. 1-hr. 2400°F Cycles to Failure
Si-20Cr-20Fe	84	71	91	71	68	53
Si-25Cr-25Fe	84	66	150	66	120	66
Si-20Cr-30Fe	120	66	168	66	168	66
Si-30Cr-20Fe	100	48	117	48	84	50-65
Si-20Cr-35Fe	133	50-65	73	50-65	130	73
Si-35Cr-20Fe	112	73	112	73	103	73
Si-20Cr-40Fe	58	50	88	50	52	50
Si-30Cr-30Fe	118	73	144	73	122	73
Si-40Cr-20Fe	138	92	104	Not tested	127	96

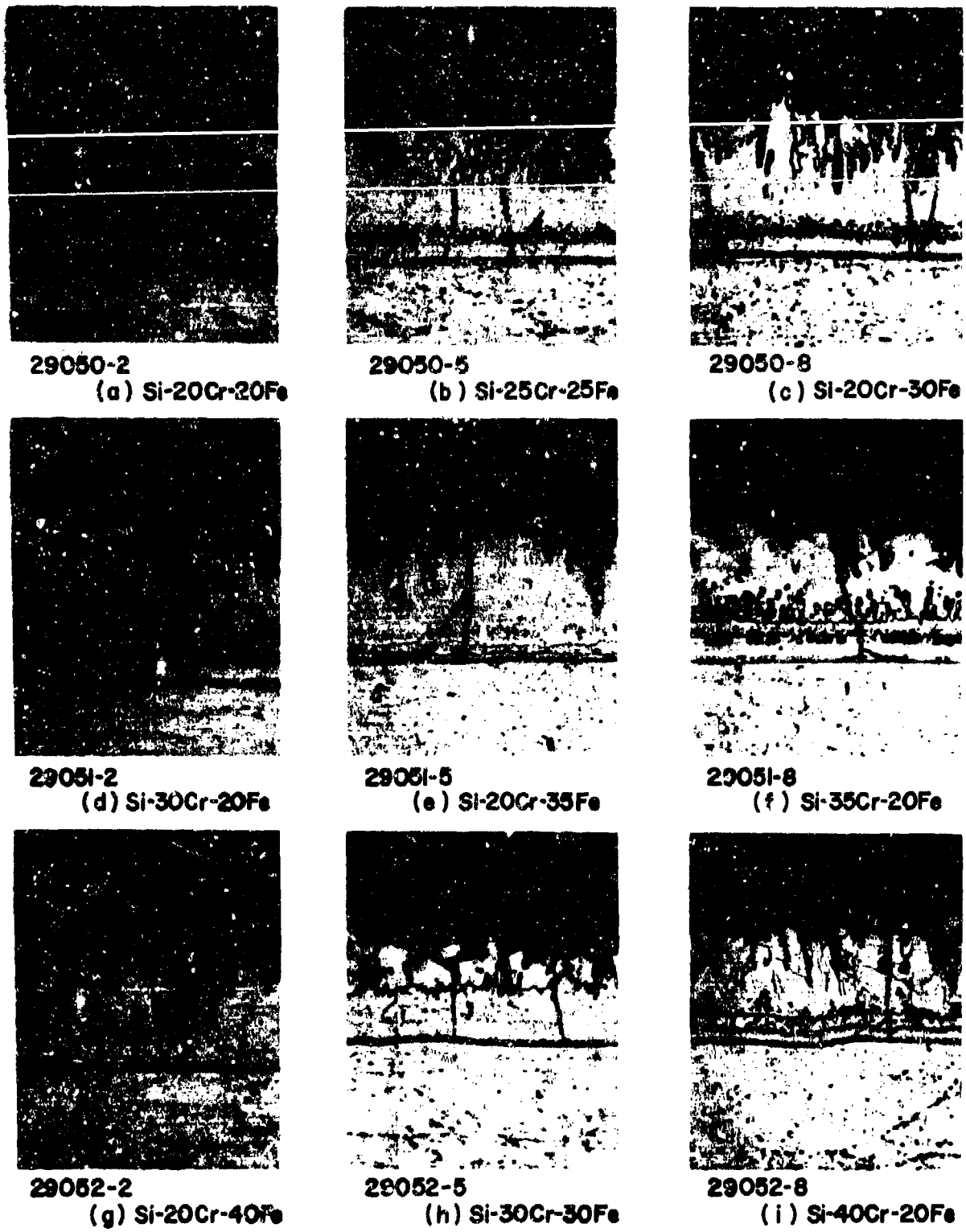

Figure 6 Si-Cr-Fe Fused Silicide Coatings on D43 Alloy (300X)

Slurry coatings composed of 90 percent prealloyed plus 10 percent elemental Si-25Cr-25Fe, and 95 percent prealloyed Si-25Cr-25Fe plus 5 percent elemental silicon were applied to D43 alloy and fired at the usual conditions of 2580°F for one hour in vacuum. These coatings wet out very well in contrast with the 100 percent prealloyed Si-25Cr-25Fe examined previously. Metallographic examination indicated that the 90 percent prealloyed (Si-25Cr-25Fe) 10 w/o Si coating had a fairly regular surface while the others were judged unacceptable in this regard.

Another approach looked at consisted of converting the $CbSi_2$ layer to M_5Si_3 by the application of a second coating. Three compositions, Cr-50Fe, Fe, and Si-20Cr-20Fe were applied and fired over Si-20Cr-20Fe coated Cb752, and all three coatings appeared to wet and react well with the silicide surface. With the duplex coatings, the second coat was applied to a unit weight approximately 25 percent of the first coat weight. The microstructure of these coatings is shown in Figure 7. Double coating Si-20Cr-20Fe results in a porous outer layer. The structure of the Cr-Fe over Si-20Cr-20Fe is remarkably similar to the single-coated Si-20Cr-20Fe. The Fe over Si-20Cr-20Fe has an outer layer that appears to contain less second phase than the others. However the surface of this coating is considerably more jagged than that of the other coatings shown.

One specimen representing each duplex coating plus one normal coated specimen were slow cyclically oxidation tested to failure. The results of these tests are given below in Table X. The results indicate that a second coat of the original composition (Si-20Cr-20Fe) does not eliminate the dusting phenomenon, while a second coat of Cr-50Fe or Fe does. In the case of the Fe overcoat, however, there is a definite decrease in protectiveness of the coating, while with the Cr-50Fe it also appears likely that the protectiveness has been adversely affected.

TABLE X

SLOW CYCLIC OXIDATION LIFE OF DUPLEX FUSED SILICIDE COATINGS

Coating Composition	Slow Cyclic Life (No. of 1-hr. slow cycles to failure)	Remarks
Si-20Cr-20Fe (single coat)	38[e]	Dusting
Si-20Cr-20Fe (double coat)	38[+]	Dusting
Si-20Cr-20Fe - 1st coat Cr-50Fe - 2nd coat	31[e]	No dusting
Si-20Cr-20Fe - 1st coat Fe - 2nd coat	14[s]	No dusting

[e] Edge Failure [s] Surface Failure [+] No Failure - Test Stopped

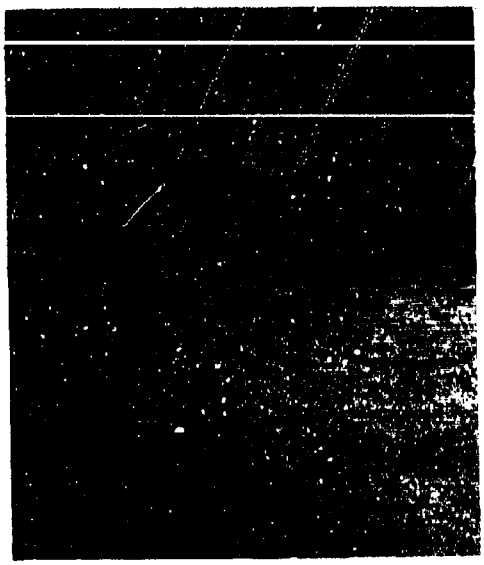

C-185-1 (a) Si-20Cr-20Fe
(SINGLE COAT)

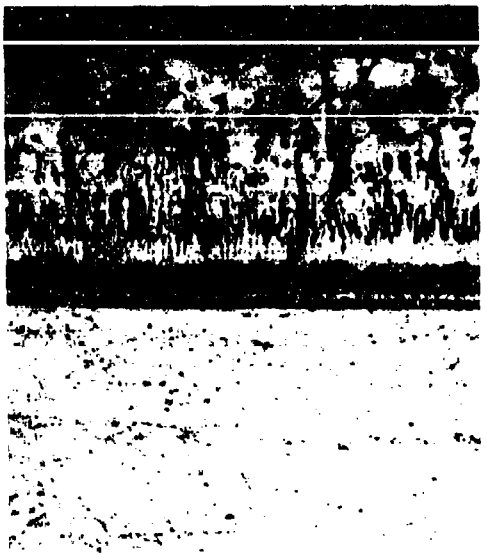

C-185-4 (b) Si-20Cr-20Fe
(DOUBLE COAT)

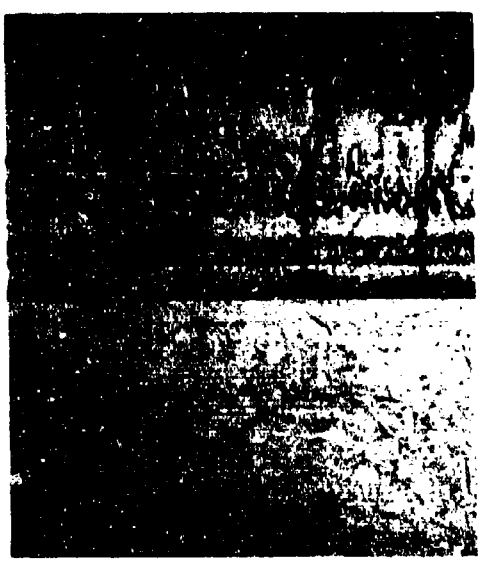

C-185-2 (c) Si-20Cr-20Fe 1st COAT
Cr-50Fe 2nd COAT

C-185-3 (d) Si-20Cr-20Fe 1st COAT
Fe 2nd COAT

Figure 7 Structures of Duplex Fused Silicide Coatings (300X)

c. Statistical Reliability

Use of the Weibull (2) distribution function for evaluating the statistical reliability of protective coatings for refractory metals was initiated by Wurst (3) and has become more or less an accepted standard means of data analysis in this field. In general, however, the variable being analyzed is the oxidation protectiveness (coating life) at a given temperature (most often 2400, 2500 or 2600 °F) during one-hour cyclic furnace testing. In view of the fact that one cannot extrapolate intermetallic-coating, oxidation life data obtained at one temperature to any higher or lower temperature, it is doubtful that any analysis of such data, regardless of the merits of the methods employed, can result in really valid conclusions. However, when this method of analysis is applied to a more meaningful test such as the slow cyclic test, it should yield a valid picture of the protective reliability of coatings, particularly for reentry applications.

Groups of 20 coupons each were coated with Si-20Cr-20Fe and Si-20Cr-20Fe-10VSi_2 and slow cyclically oxidation tested to failure. The Weibull cumulative, failure, distribution data resulting from these tests are plotted in Figure 8. It is obvious that both compositions exhibit a high reliability, as evidenced by a high slope, and a single failure mode (wearout), by the single straight line plots. The Si-20Cr-20Fe coating in particular shows very high lifetimes at very high reliabilities, e.g., 50 slow cycles at 99 percent reliability. The data on which these plots are based are given in Appendix I (p 220).

A metallographic study was made in an effort to determine the mechanism of failure during slow cyclic oxidation testing. Pairs of D-43 coupons coated with Si-20Cr-5Ti-10Fe-10VSi_2 were exposed for 1, 3, 7, 12, 15, 20, 23 and 35 hours (cyclic) in the slow cyclic test equipment. Metallographic examinations were made of both transverse and longitudinal sections through the edges of each of these samples, since failure almost invariably occurs at sample edges. No significant difference was noted in the severity, size, frequency or pattern of cracks in the coating in these two different planes. Photomicrographs (Figure 9) of transverse sections of a number of these specimens show that oxidation in the thermal stress cracks results in a progressive widening of these cracks. It is reasonable to assume that the growth of these oxide wedges results in compressive stresses in the coating of considerable magnitude. On a curved surface, such as that at sheet edges, these stresses may be resolved into tangential and normal components as shown schematically in Figure 10. As oxidation proceeds and the wedges grow, the normal forces on a pie-shaped piece of coating will eventually be sufficient to pull it out, and the coating will fail.

On flat surfaces the compressive stresses caused by oxidation in the cracks have no component normal to the coating-substrate interface, and therefore there is less likelihood of a piece of coating being ejected due to these forces. Since all refractory metal, intermetallic coatings have thermal expansion cracks, it is believed that coated sheet edges are therefore inherently the most likely to be sites of first failures. Coating systems that outperform others and at the same time consistently fail at sheet edges are not displaying an inherent deficiency in the coating process.

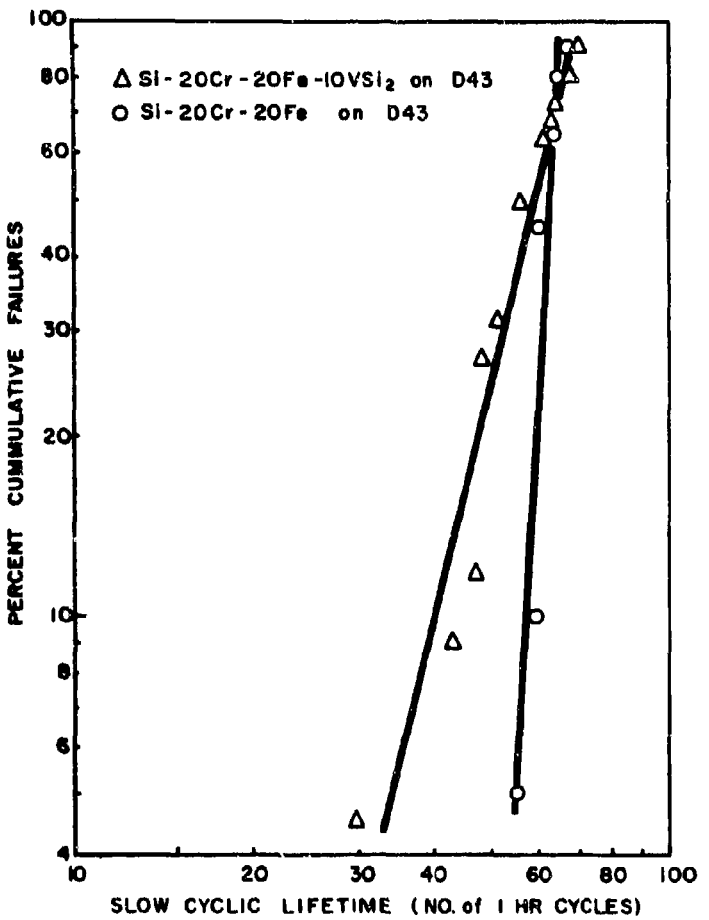

Figure 8 Weibull Plots of Slow Cyclic Oxidation Performance of Fused Silicide Coatings.

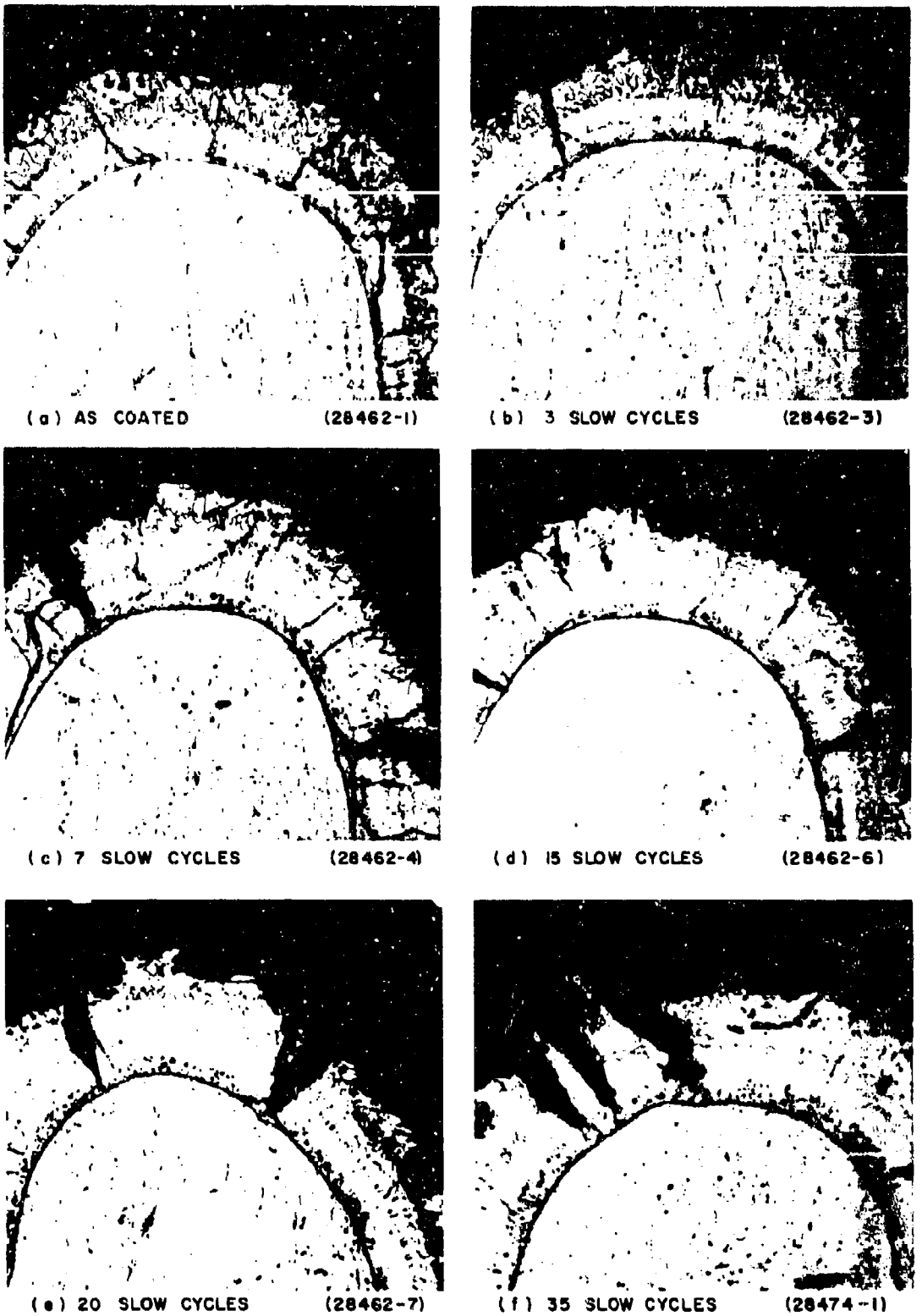

Figure 9 Photomicrographs (300X) Showing Progression of Oxidation in Coating Cracks at Sheet Edges. Si-20Cr-5Ti-10Fe-10VSi_2 Coating on D43 Alloy.

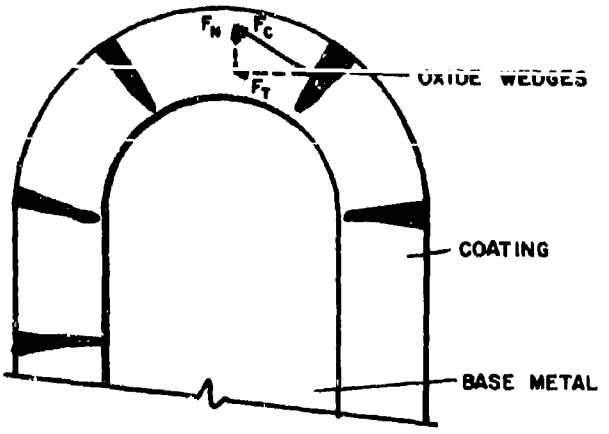

Figure 10 Resolution of Forces at Sheet Edges Due to Lateral Oxidation in Coating Cracks

On the contrary, this behavior is the reflection of a highly reliable process, since failure always occurs at the weakest link due to the mechanical factors explained earlier.

d. Effect of Coating Thickness

A study was made of the effect of coating thickness and post-diffusion heat treatment on the slow cyclic oxidation life of the Si-20Cr-5Ti-10Fe-10VSi_2 coating on D43.

Five nominal coating thicknesses,

10 mg/cm^2,
15 mg/cm^2,
20 mg/cm^2,
30 mg/cm^2, and
40 mg/cm^2,

and two conditions,

as-diffused, and
diffused plus heat-treated for two hours at 2500°F in argon, were chosen for the study. Two samples of each kind were tested to failure in the slow cyclic test. The results, given in Table XI, show marked improvement in life with increasing thickness. It is also obvious that the additional heat treatment is detrimental to coatings 15 mg/cm^2 and thinner, but does not appear to affect significantly the performance of thicker coatings. Data for the as-coated and tested specimens plotted in Figure 11 indicate a linear relationship. In an ideal situation one would expect the life to increase parabolically with increasing coating thickness since the

TABLE XI

EFFECT OF COATING THICKNESS AND HEAT TREATMENT ON SLOW CYCLIC OXIDATION LIFE

Coating Unit Weight (mg/cm^2)	Slow Cyclic Oxidation Life	
	As Coated	2 hour, 2500°F Argon Post-Diffusion Heat Treatment
9.4	8[e]	--
9.4	8[s]	--
9.6	--	1[e]
9.6	--	2[e]
15.4	21[e]	--
14.3	24[s]	--
13.5	--	2[e]
13.7	--	5[e]
21.3	24[e]	--
21.5	24[e]	--
21.8	--	18[e]
21.9	--	24[e]
31.1	36[e]	--
30.5	47[e]	--
30.4	--	60[e]
30.4	--	54[e]
37.9	55[e]	--
37.3	51[e]	--
36.1	--	54[e]
35.7	--	54[e]

[e] Edge failure

[s] Surface failure

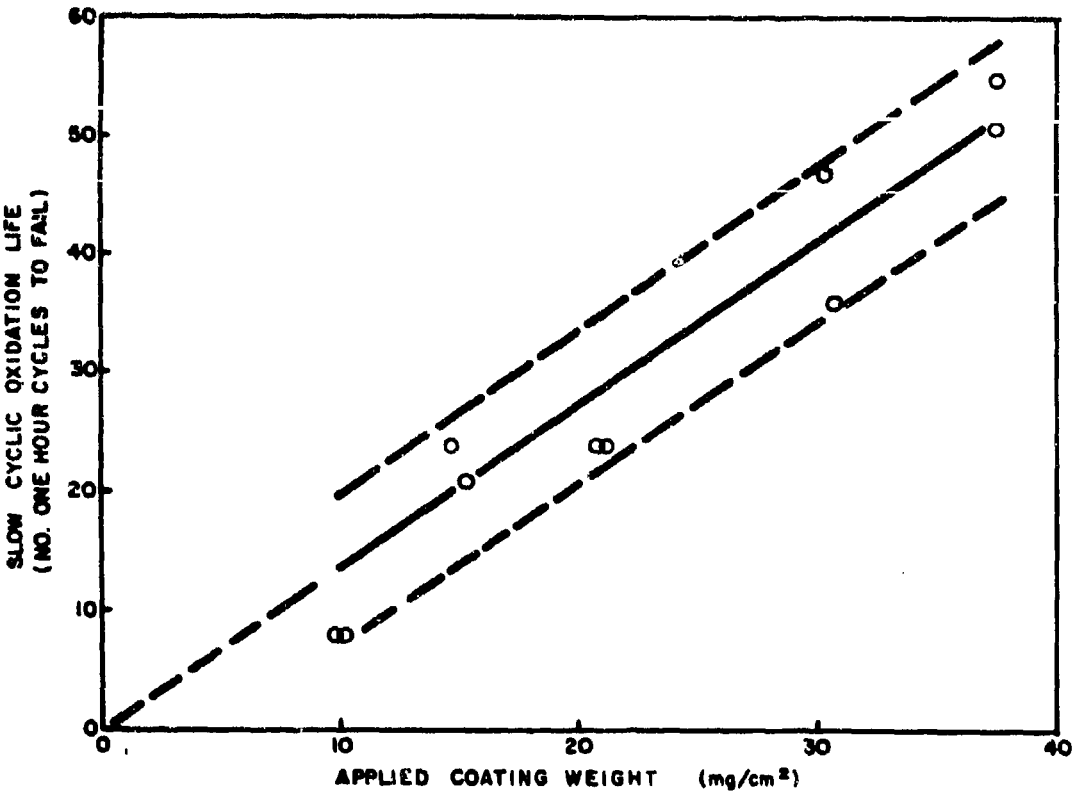

Figure 11 Slow Cyclic Oxidation Life Versus Applied Coating Weight (Si-20Cr-5Ti-10Fe-10VSi_2 on D43).

rates of both the oxidation reaction and the reaction with the substrate are supposedly controlled by the solid-state diffusional rates which are assumed to be parabolic. However, the linear increase in life with thickness over such a large range is quite satisfactory since, in the case of pack cementation coatings, thickness cannot be easily increased beyond two or three mils, and even when it can, no appreciable improvement results due to imperfect edge growth.

Photomicrographs of specimens from these experiments are shown in Figure 12. The two thicker coatings contain appreciably more cracks than do the thinner coatings. The cracks in these thicker coatings are not all of the usual type that are normal to the interface and extend to the surface. Many of these cracks terminate within the coating proper and variously oriented. In some respects these thick coating microstructures resemble the microstructures of the prestressed coatings.

Thickness measurements made from the photomicrographs of Figure 12 are plotted against the applied coating unit weights in Figure 13. The data, as expected, show a linear relationship intersecting the origin.

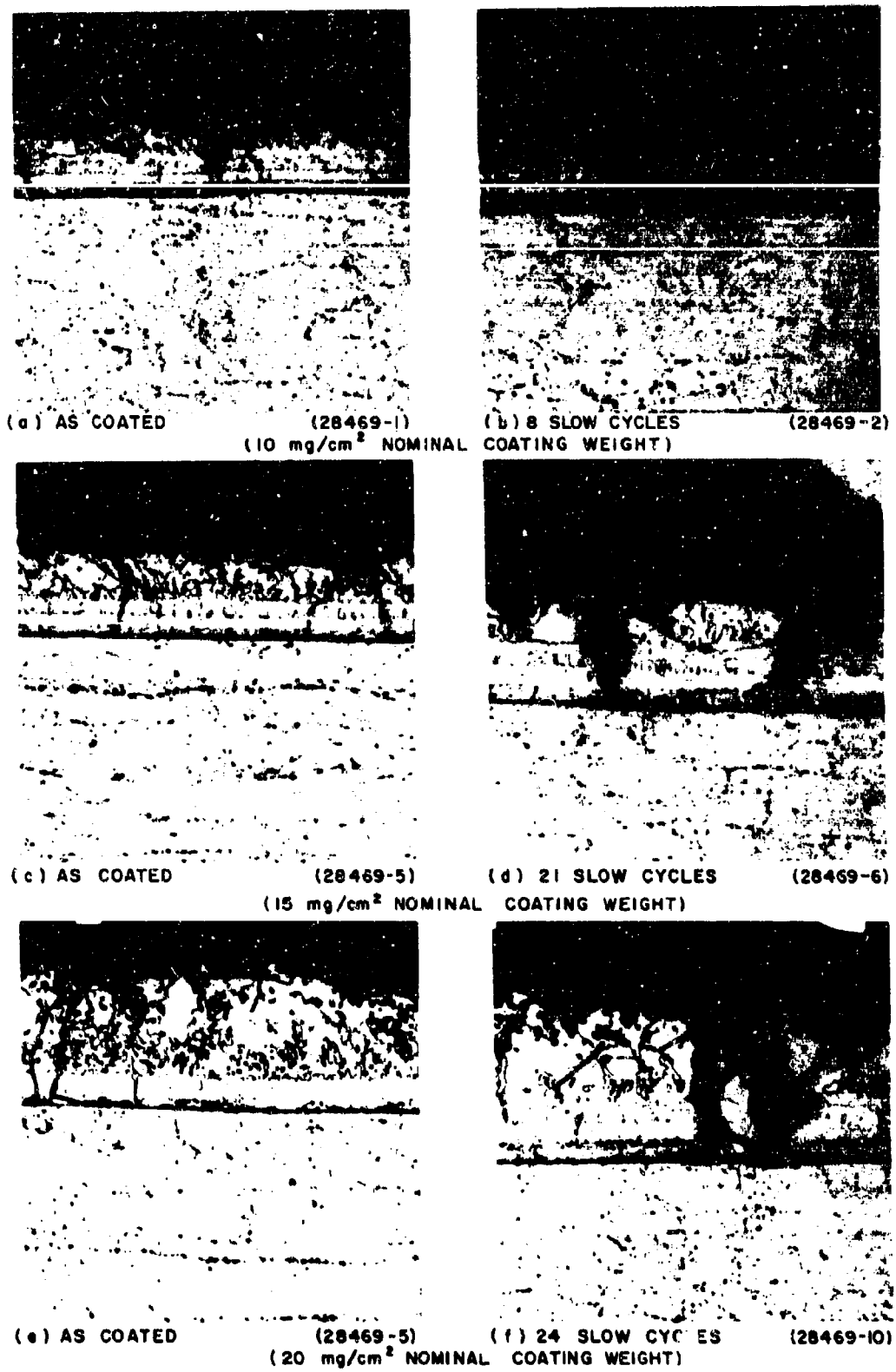

Figure 12 Photomicrographs of As-Coated and Slow Cyclically Oxidation Tested Si-20Cr-5Ti-10Fe-10VSi_2 Coatings of Various Thicknesses on D43 (300X).

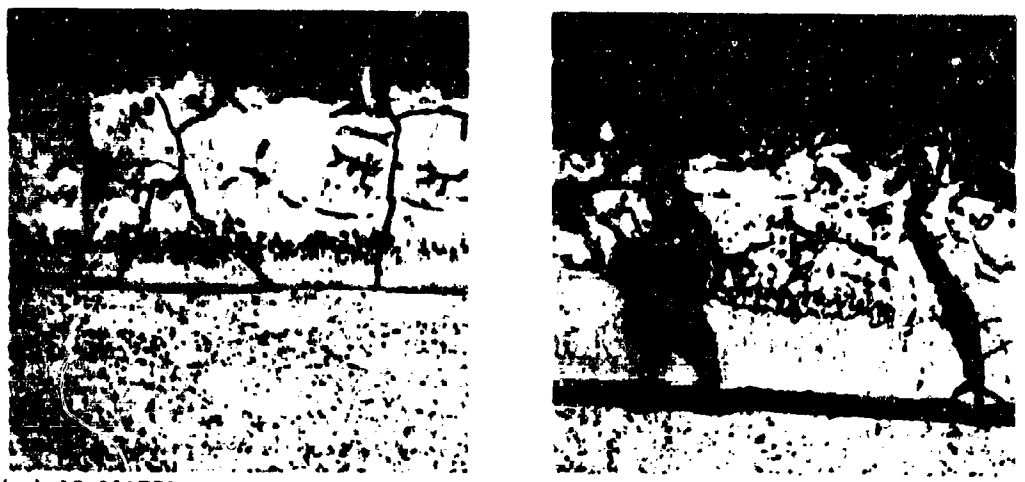

(g) AS COATED (28523-2) (h) 47 SLOW CYCLES (28523-1)

(30 mg/cm² NOMINAL COATING WEIGHT)

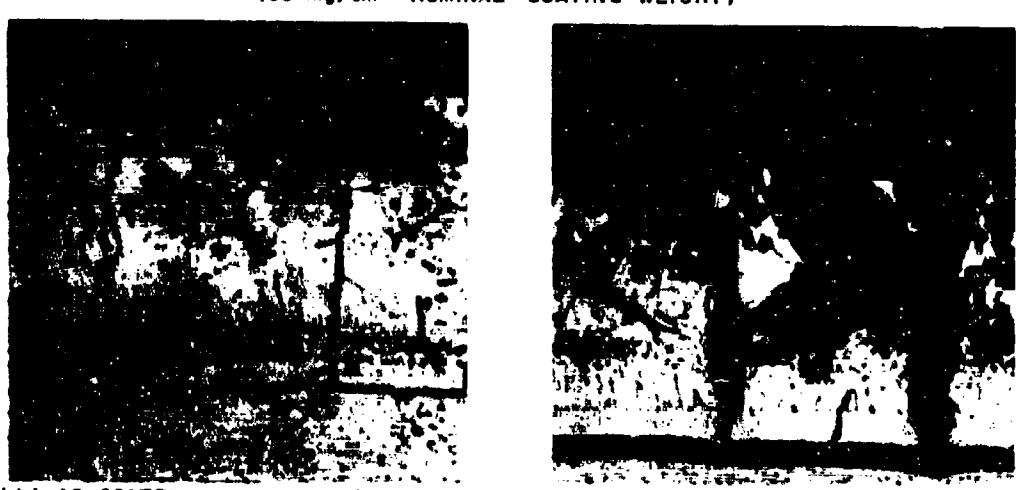

(i) AS COATED (28523-6) (j) 55 SLOW CYCLES (28523-5)

(40 mg/cm² NOMINAL COATING WEIGHT)

Figure 12---Concluded

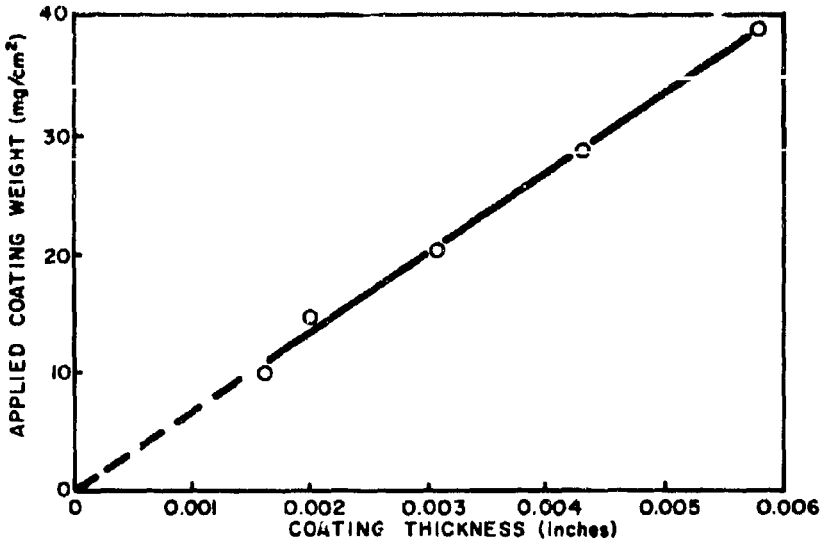

Figure 13 Applied Coating Weight Versus Metallographic Coating Thickness (Si-20Cr-5Ti-10Fe-10VSi_2 Coating on D43).

e. Low-Temperature Cycling

An orbiting earth reentry vehicle may, during the orbiting phase of its mission, experience a low-temperature cycle as it alternates between day and night. During such operation its temperature might vary from 300°F in daylight to -200°F in darkness.

The effect of such cycling on the protectiveness of the fused silicide coating was determined by alternately immersing four Si-20Cr-20Fe-10VSi_2 coated D-43 tabs in liquid nitrogen (-320°F) for two minutes and then placing them in a 300°F oven for two minutes. After 100 such low temperature cycles, two of these tabs were then slow cyclically oxidation tested to failure; they exhibited lives of 51 and 67 cycles. The average slow cyclic lifetime of 20 samples from this batch not previously exposed to the low-temperature was 50 hours, so there was no apparent degradation of protectiveness due to the low-temperature cycling.

Photomicrographs of samples in the as-coated, coated and slow-cycled, low-temperature cycled, and both low-temperature cycled and slow-cycled conditions are shown in Figure 14. On the basis of the test results or microstructures, no adverse effects are apparent as a result of the low-temperature cycling.

(a) AS COATED (28658-4)

(b) AS COATED + 70 SLOW CYCLES (28658-1)

(c) AS COATED + 100 LOW TEMP. CYCLES (-320 TO +300°F) (28658-2)

(d) 100 LOW TEMP. CYCLES + 67 SLOW CYCLES (28684-1)

Figure 14 Photomicrographs of Low Temperature Cyclic Test Specimens (300X).

f. Oxidation in Low-Pressure Environments

Protective coatings for refractory metals were initially developed and optimized on the basis of their oxidation resistance in ambient sea level air.

Since about 1963, a good deal of effort, principally by Perkins, has been directed towards the evaluation of the protectiveness of existing coatings in the low-pressure, high-temperature environment that will be encountered in space reentry applications (4). This work, which served to characterize the performance of most coatings in these kinds of environments, clearly underscored the severely degrading effects of reduced-pressure oxidation. In addition, this work also documented a large body of observations describing the changes brought about in the coatings studied as a result of such exposures.

The work described in the following paragraphs was aimed at characterizing the effect of low-pressure environment in several fused silicide coating systems, and toward identifying the principal mechanisms operable in oxidation processes under these special conditions.

The effect of 26 hour, 2500°F exposures at air pressures of 760, 5, 1 and 0.1 torr on several coating base metal systems was studied metallographically and thermogravimetrically. Two substrate alloys (D43 and Cb752), and three fused silicide coating compositions (Si-20Cr-5Ti, Si-20Cr-20Fe, and Si-20Cr-20Fe-10VSi_2) were selected for this evaluation, making a total of six material systems combinations. The coating weight for all specimens was 22.5 ±2.5 mg/cm^2.

A single specimen of each kind was exposed at each set of conditions in the reentry simulator (Figure 15). The samples were removed for weighing at 1, 2, 3, 4, 5, 10 and 26 hours. No oxidation failures were noted on any of the specimens. The weight change curves are shown in Figures 16 through 21.

There is a great similarity between the two sets of curves representing each coating on the two different alloys. Also, it is significant to note that net weight losses result only with the Si-20Cr-5Ti systems at the lowest pressure (0.1 torr). This is probably attributable to the lower oxidation rate of this coating which results in a lower oxygen pickup and also enables volatiles to diffuse through the thinner scale at a higher rate.

Photomicrographs of the low-pressure-exposed samples are shown in Figures 22 through 27. The pictures reveal that dense oxide scales are grown on all six coating systems at all pressures from 0.1 to 760 torr at 2500°F.

In a short study aimed at identifying the mechanisms operable in the low-pressure oxidation of silicide coated columbium alloys, the fused silicide coating systems were compared with other systems.

Figure 15 Reentry Simulator

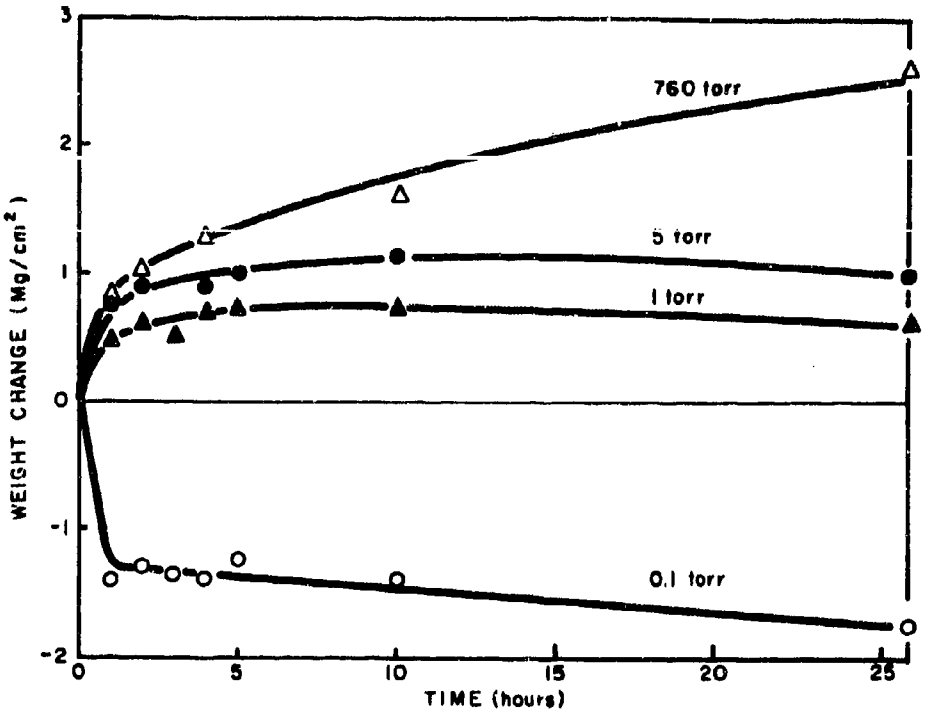

Figure 16 Weight Change Versus Time at 2500°F for Si-20Cr-5Ti on D43 at Various Air Pressures.

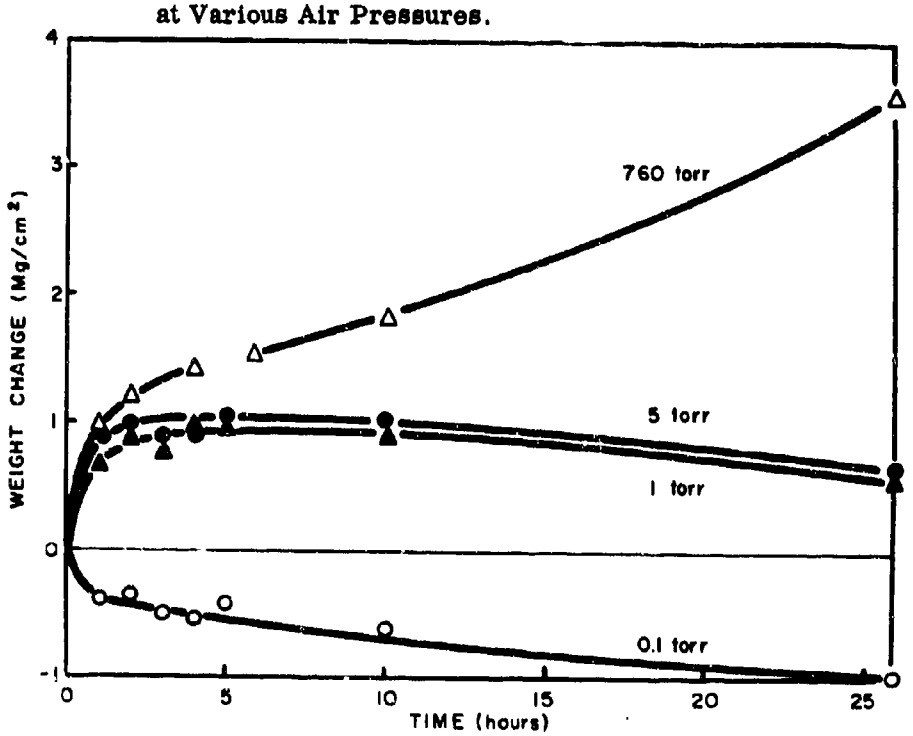

Figure 17 Weight Change Versus Time at 2500°F for Si-20Cr-5Ti on Cb752 at Various Air Pressures.

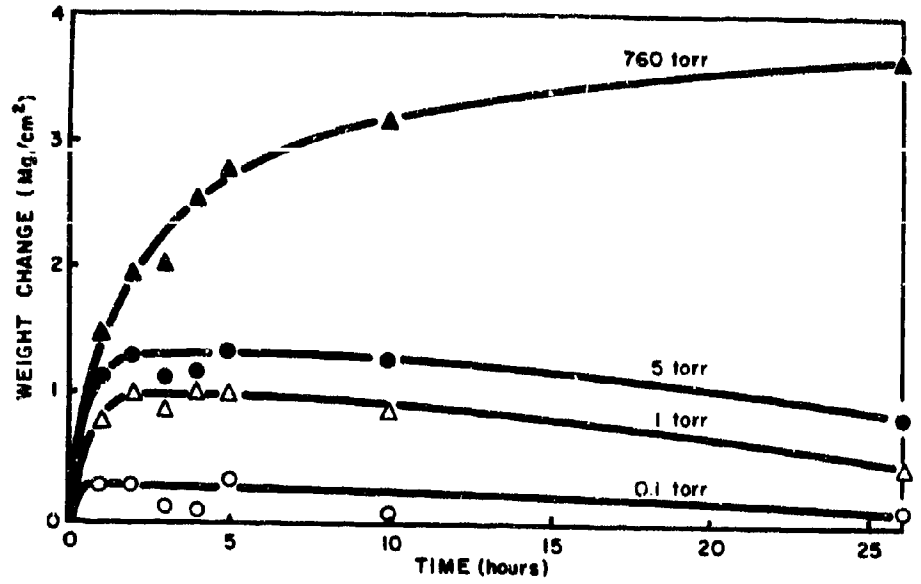

Figure 18 Weight Change Versus Time at 2500°F for Si-20Cr-20Fe on D43 at Various Air Pressures.

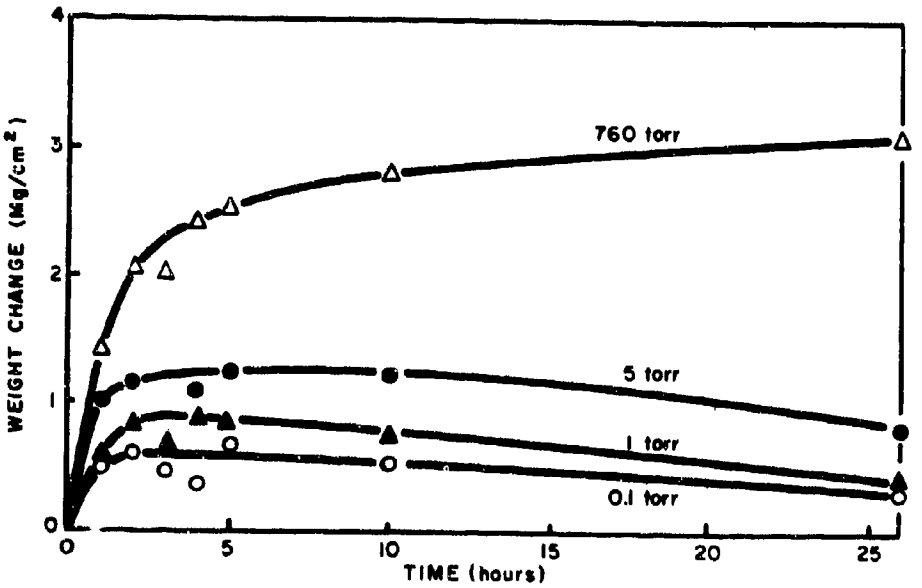

Figure 19 Weight Change Versus Time at 2500°F for Si-20Cr-20Fe on Cb752 at Various Air Pressures.

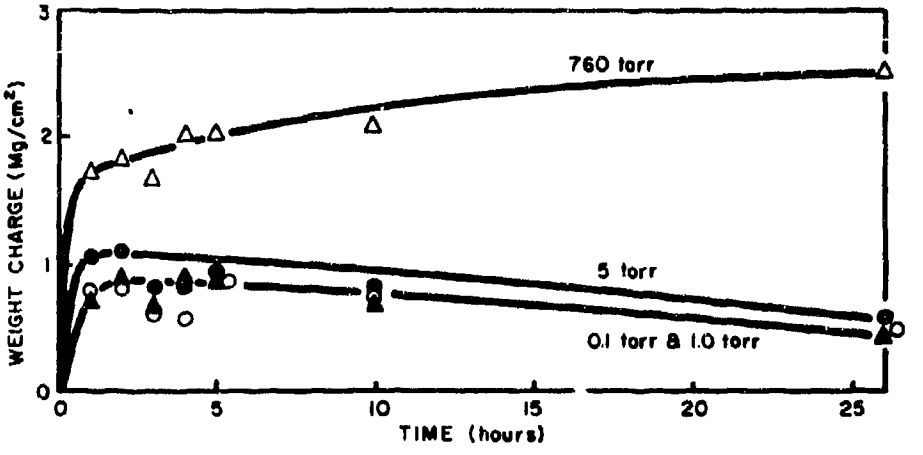

Figure 20 Weight Change Versus Time at 2500°F for Si-20Cr-20Fe-10VSi_2 on D43 at Various Air Pressures.

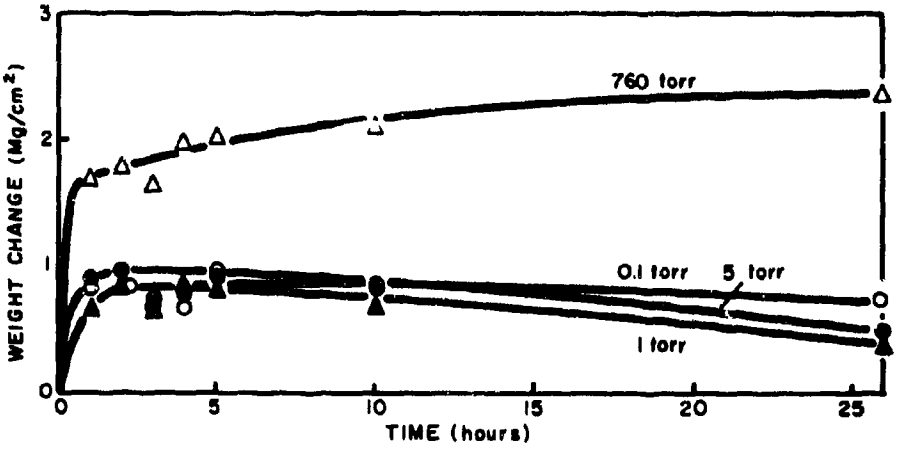

Figure 21 Weight Change Versus Time at 2500°F for Si-20Cr-20Fe-10VSi_2 on Cb752 at Various Air Pressures.

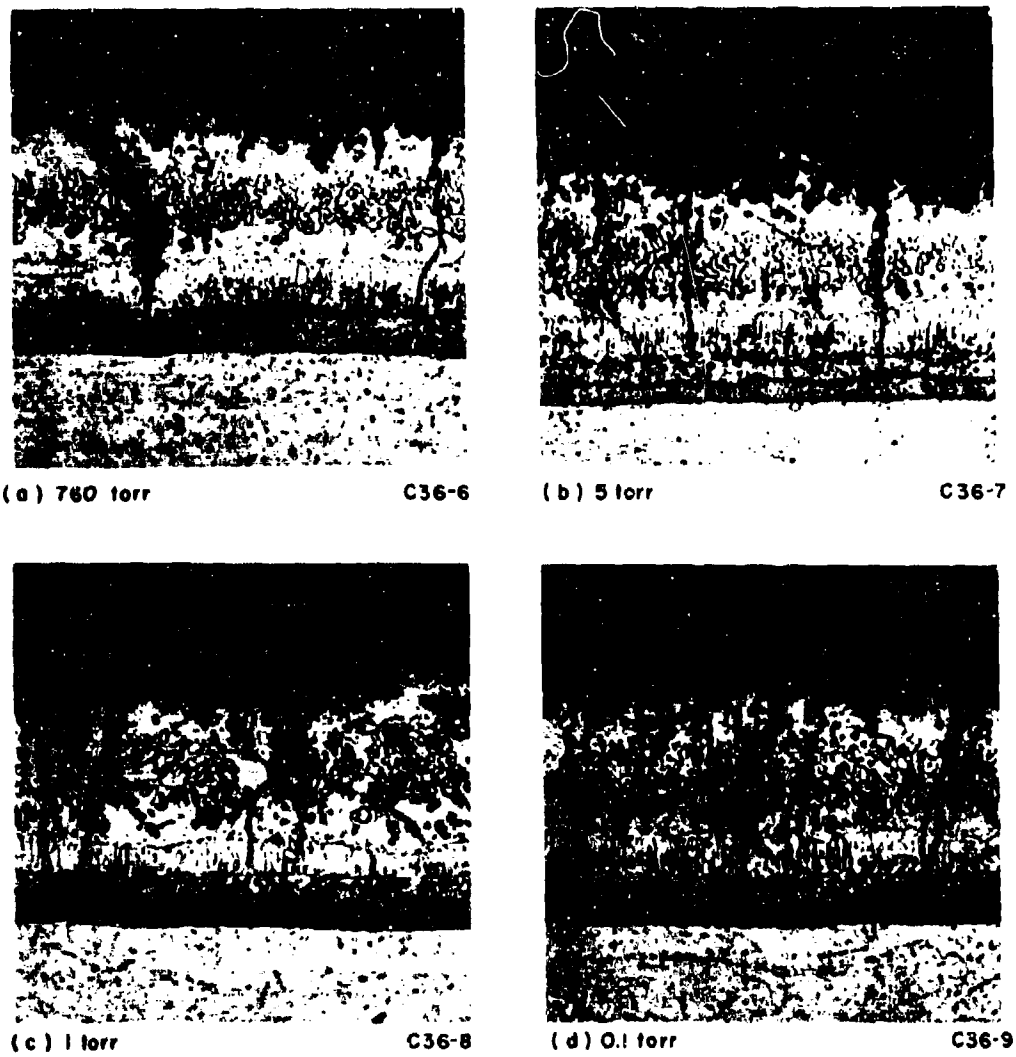

Figure 22 Photomicrographs of Si-20Cr-5Ti Coated D43 After Exposure for 26 Hours at 2500°F in Air at Pressures Indicated (300X).

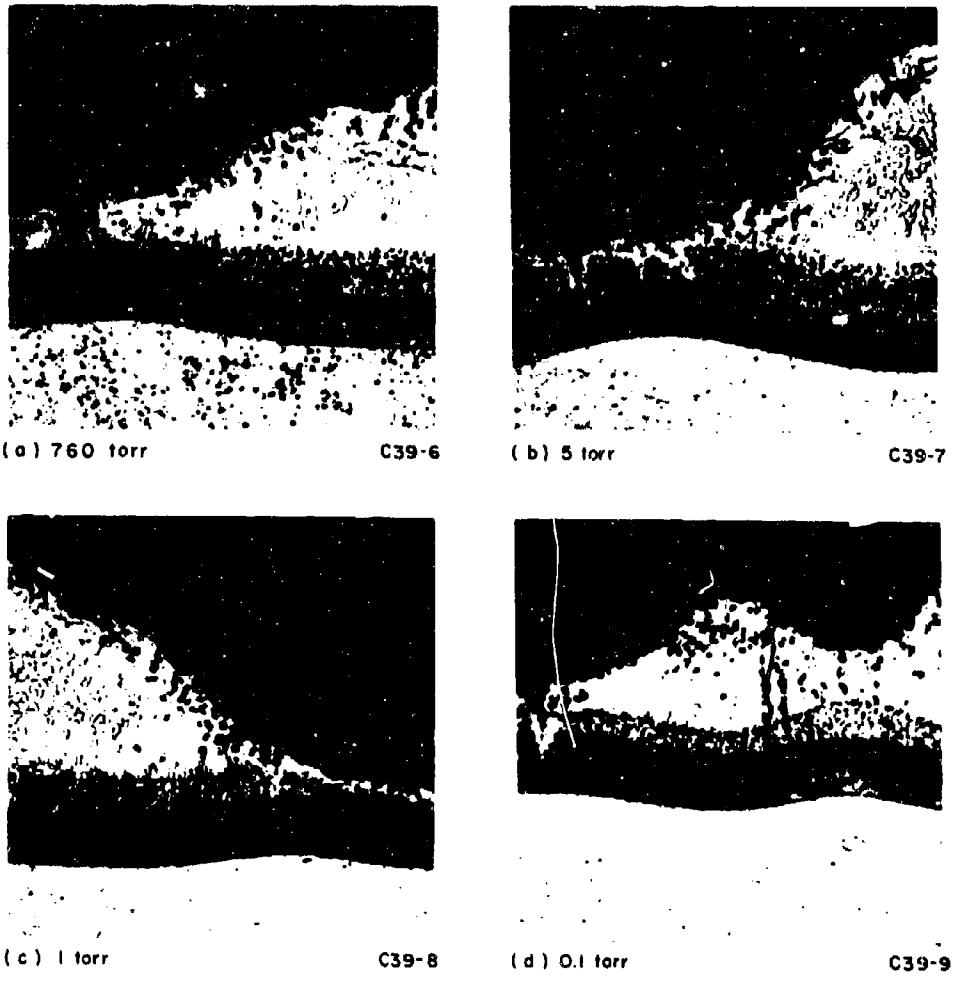

Figure 23 Photomicrographs of Si-20Cr-5Ti Coated Cb752 After Exposure for 26 Hours at 2500°F in Air at Pressures Indicated (300X).

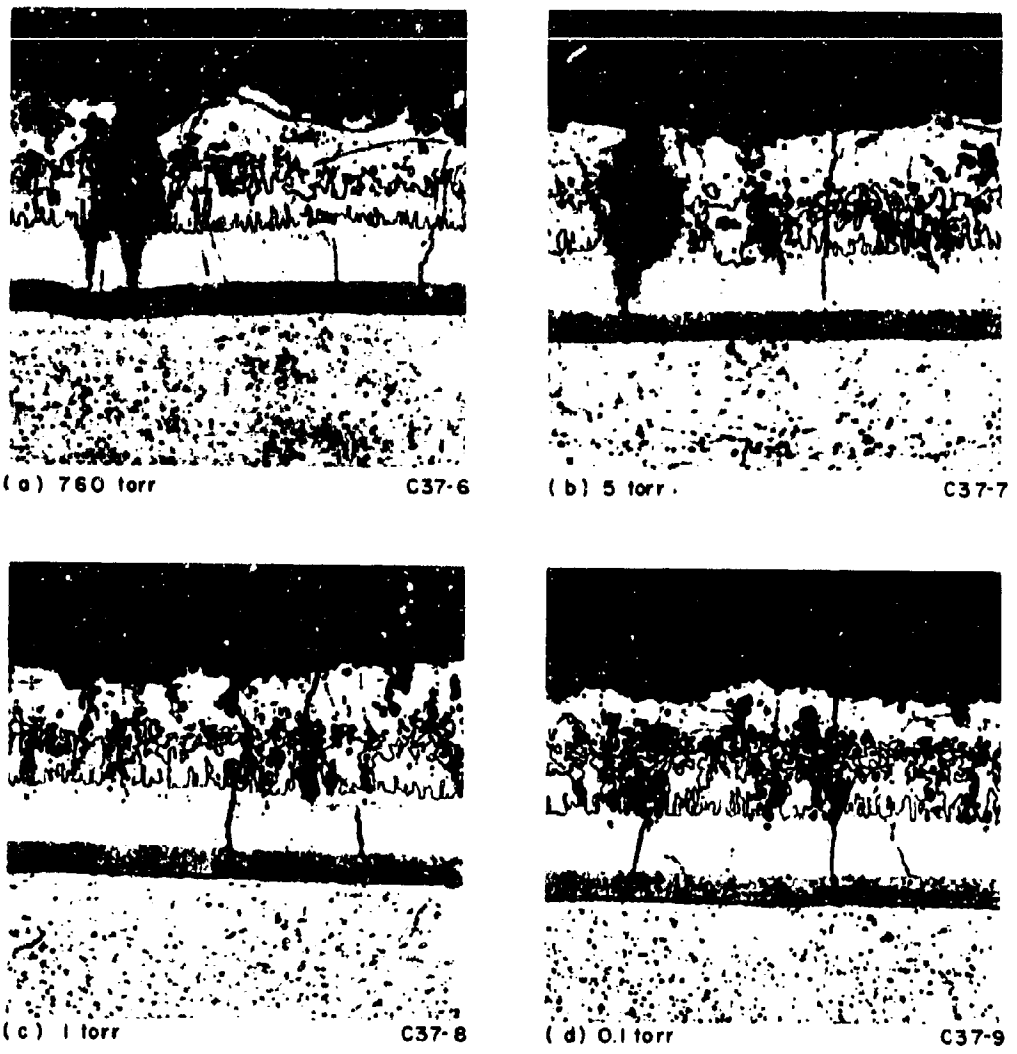

Figure 24 Photomicrographs of Si-20Cr-20Fe Coated D43 After Exposure for 26 Hours at 2500°F in Air at Pressures Indicated (300X).

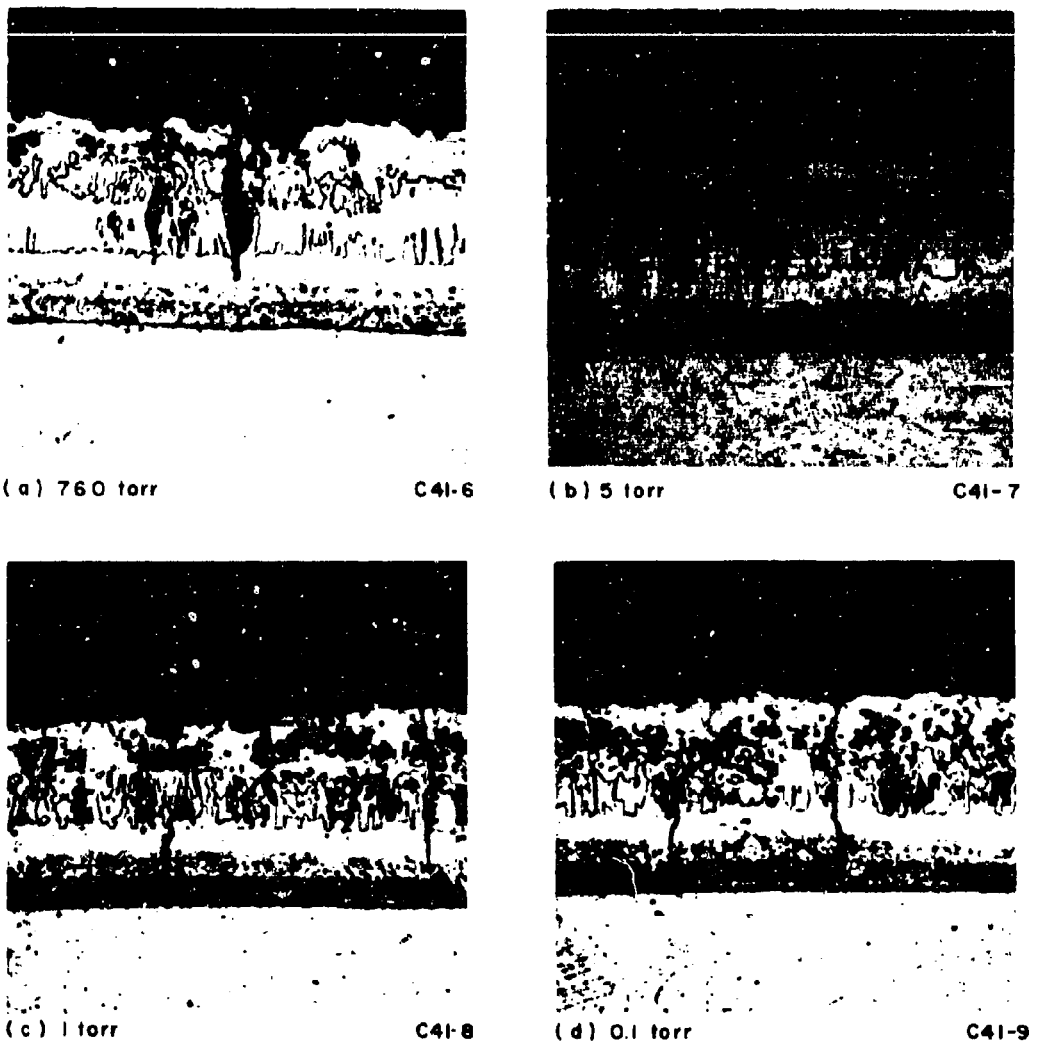

Figure 25 Photomicrographs of Si-20Cr-20Fe Coated Cb752 After Exposure for 26 Hours at 2500°F in Air at Pressures Indicated (300X).

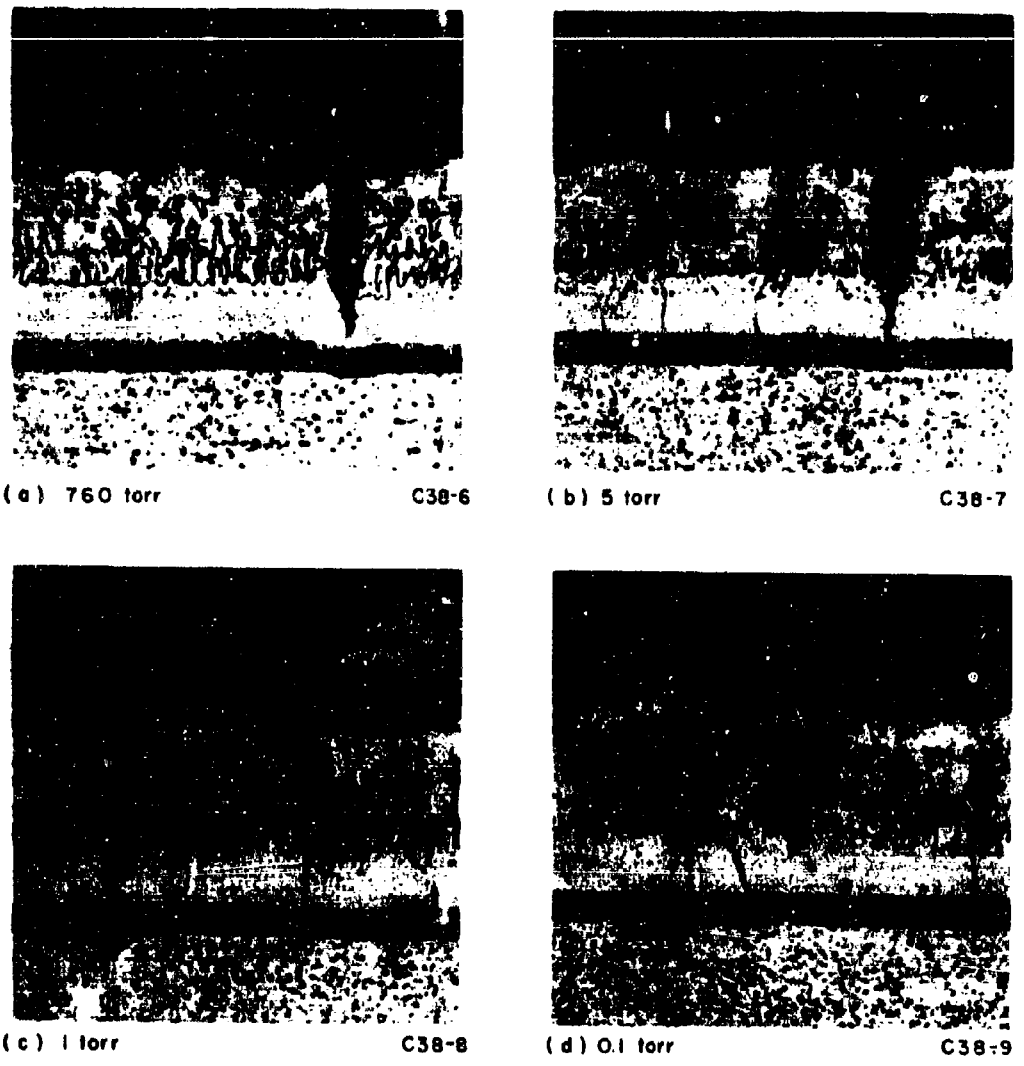

Figure 26 Photomicrographs of Si-20Cr-20Fe-10VSi_2 Coated D43 After Exposure for 26 Hours at 2500°F in Air at Pressures Indicated (300X).

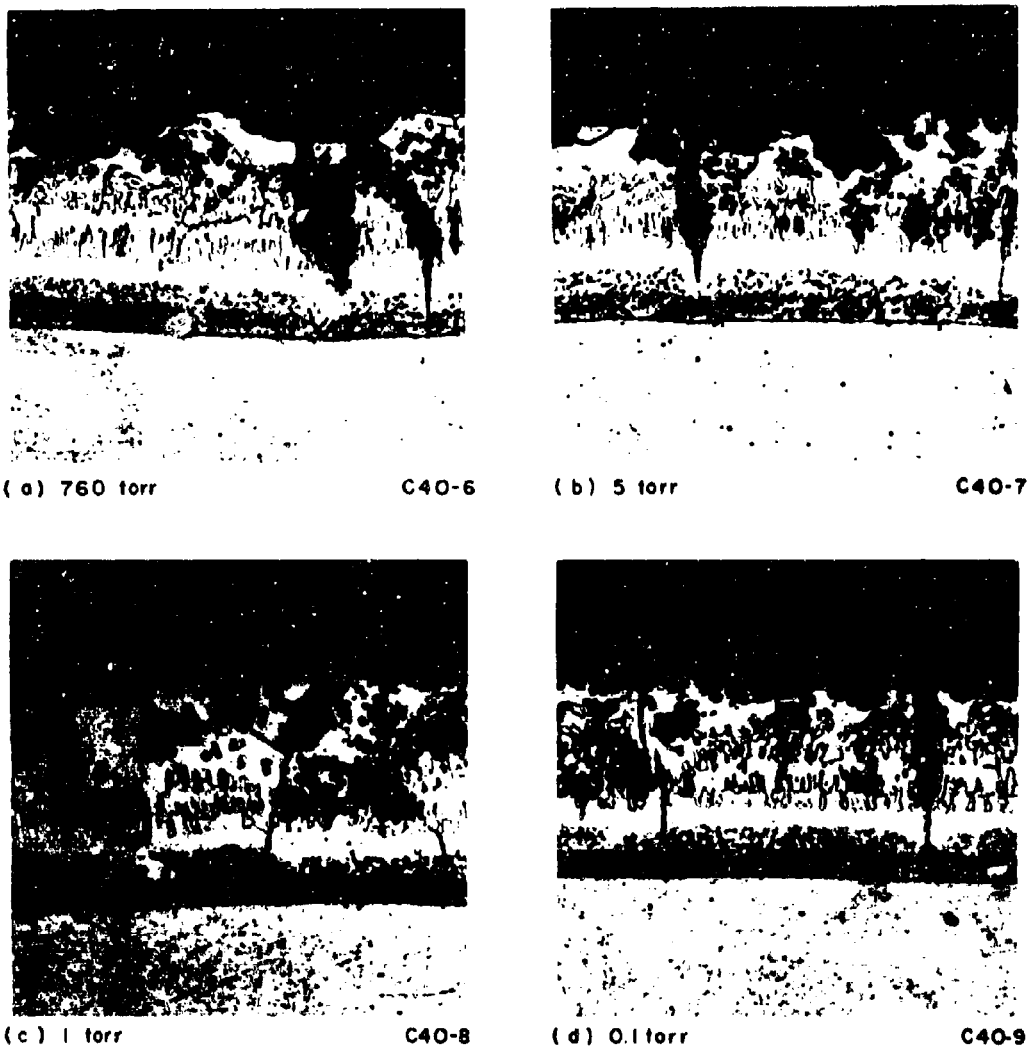

Figure 27 Photomicrographs of Si-20Cr-20Fe-10VSi_2 Coated Cb752 After Exposure for 26 Hours at 2500°F in Air at Pressures Indicated (300X).

Fused silicide coated [R512E (Si-20Cr-20Fe)] D43 and B66, pack silicide coated D43 and B66, and Ti-Cr-Si vacuum pack coated B66 constituted the five systems selected for study. The test specimens were all small, sheet-metal coupons, approximately 1/2 x 3/4 x 0.010 or 0.020 inch thick. Groups of specimens, with each group consisting of one of each type of specimen, were exposed to the environments listed in Table XII.

TABLE XII

TEST EXPOSURE CONDITIONS

Condition of Specimens Before Test Exposure	Temp. (°F)	Exposure Environment	Conditions Pressure (torr)	Time (hrs)
As coated	2700	air	760	8
As coated	2700	air	1	8
Preoxidized 2 hrs - 2700°F air - 1 atmosphere	2700	air	1	8
As coated	2700	air	5×10^{-4}	8
As coated	2700	argon	760	8
As coated	2700	argon	1	8
Preoxidized 2 hrs - 2700°F air - 1 atmosphere	2700	argon	1	8

All of the exposures were performed in the equipment shown in Figure 15. The specimens were supported in slotted quartz pads. The quartz pad and specimens were mechanically transported into the furnace hot zone after the furnace environmental pressure had been suitably stabilized. Flow rate for all tests in this furnace was 0.65 SCFH. All specimens were removed for weighing and visual inspection after 1, 2, 4, and 8 hours of exposure.

Evaporation rates in high vacuum were determined in a cold-wall, electric-resistance furnace. All specimens were examined metallographically in all of the various exposed conditions. X-ray diffraction analyses were also performed on most of the specimens.

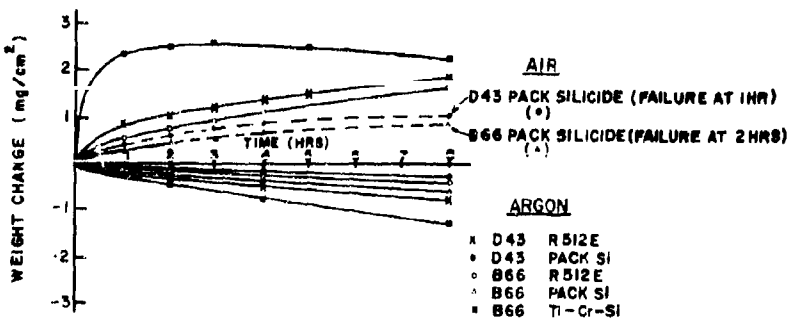

Figure 28 Weight Change vs. Time at 2700°F and 760 Torr

The weight change curves for the 2700°F, one-atmosphere tests are shown in Figure 28. The net weight change in air is positive for all systems. Both pack silicide coatings failed in the first two hours of test. The Ti-Cr-Si coating had a very high initial weight gain rate, but leveled off and finally turned down after three or four hours. The pack silicides, although short lived, had the lowest oxidation rates; the fused silicide coatings had intermediate rates.

Exposure in the one atmosphere argon environment resulted in essentially linear weight losses for all systems. The Ti-Cr-Si coated B66 had the highest evaporation rates; the pack silicides had the lowest rates, and the fused silicides exhibited intermediate rates.

Weight change curves for the 2700°F, one-torr exposures are shown in Figure 29. All systems exhibited small positive net weight gains in air. The oxidation-rate rankings are identical to the rankings in the one-atmosphere test. A fused quartz sample included in these tests showed a very small weight gain.

The weight-change curves for 2700°F, one-torr argon show very large losses for all systems. Again the Ti-Cr-Si coated B66 exhibited the highest evaporation rate, the pack silicides the lowest, and the fused silicides intermediate evaporation rates. These losses amount to 20 to 30 percent of the weight of coating initially applied. The weight loss rate observed for the fused quartz is small in comparison with that of the coatings and approximates published data for SiO_2.

The results of the 2700°F, one-torr exposure of preoxidized coatings is shown in Figure 30. The weight changes of the air-exposed specimens are small and negative except for the Ti-Cr-Si system, which is appreciably negative. The negative weight change for most of the systems can be accounted for by the fact that the continued scale growth rate is small because of the presence of the thick preoxidized scale, and is readily offset by minor evaporation from the scale or from the underlying coating. The large weight loss exhibited by the preoxidized Ti-Cr-Si coating in one-torr air cannot be similarly explained. In spite of the large weight loss,

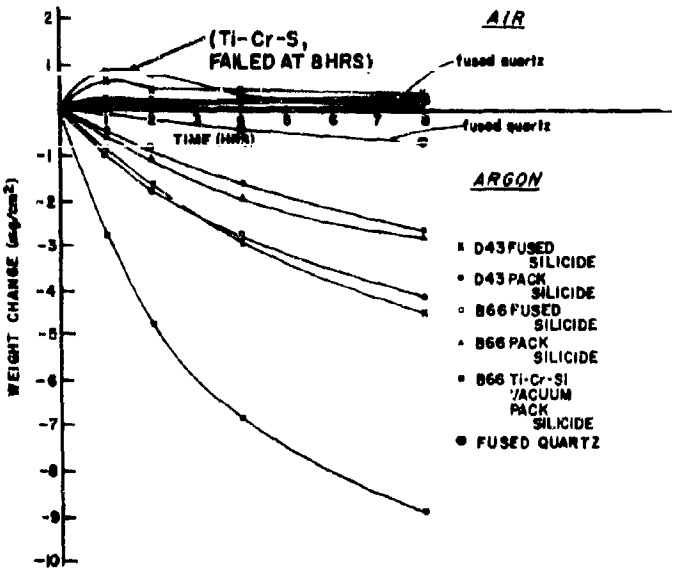

Figure 29 Weight Change vs. Time at 2700°F and 1 Torr

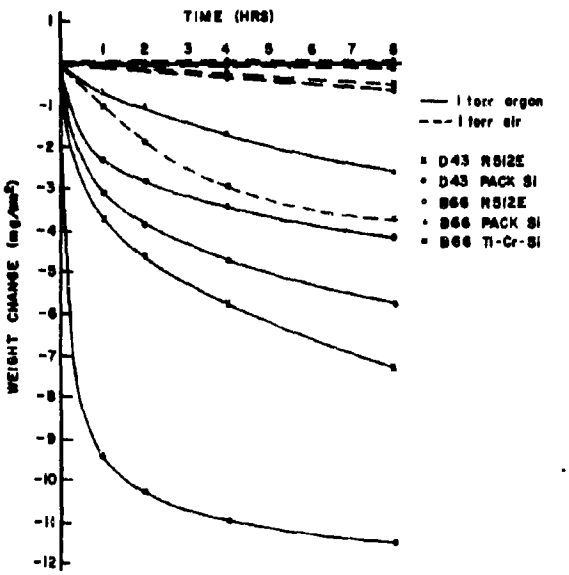

Figure 30 Weight Change vs. Time at 2700°F and 1 Torr (For Preoxidized Coatings)

however, the preoxidized Ti-Cr-Si coating remained uniformly protective to the substrate for the entire eight-hour exposure, in contrast to the as-coated specimen which failed over about 50 percent of the specimen area when similarly exposed.

The weight-change curves for preoxidized coatings in one-torr argon show losses equal to or greater than the losses exhibited by the unpreoxidized specimens. If these curves are superimposed on the corresponding curves of Figure 29, with the terminal points perfectly aligned, the pairs of curves conform very closely to each other (with the exception of the Ti-Cr-Si coating) all the way back to the one-hour points. This appears to indicate that the oxide scale evaporates completely during the first hour along with some coating, after which time the evaporation of the coating proceeds at the same rate as unpreoxidized coatings. The magnitude of the weight losses occurring during the first hour appears to be consistent with the weight gains experienced during preoxidation. From the preoxidation weight gain, the unit weight of scale can be calculated (assuming the scale to be SiO_2). If the normal weight loss observed during one hour in argon for the unpreoxidized coatings is added to this, the results are comparable to the one hour weight losses observed for the preoxidized coatings.

The Ti-Cr-Si coating is apparently affected differently by preoxidation and subsequent exposure to the inert atmosphere environment. The first hour weight losses appreciably exceed what could be expected by the mechanisms postulated above for the other systems. Also, the subsequent evaporation rate beyond the first hour is significantly lower than that observed with the same unpreoxidized coating. Since the Ti-Cr-Si coating does not oxidize to form simply a relatively dense scale, but in addition exhibits a fairly broad oxidized or contaminated zone beneath the scale, it is possible that this zone in this state is increasingly volatile.

The evaporation rates of the coatings in high vacuum (5×10^{-4} torr) are shown in Figure 31. These rates do not vary considerably from the rates evidenced in the one-torr argon tests (see Figure 29), indicating that at 2700°F and pressures below one torr, factors other than pressure govern the evaporation rate of silicide coatings.

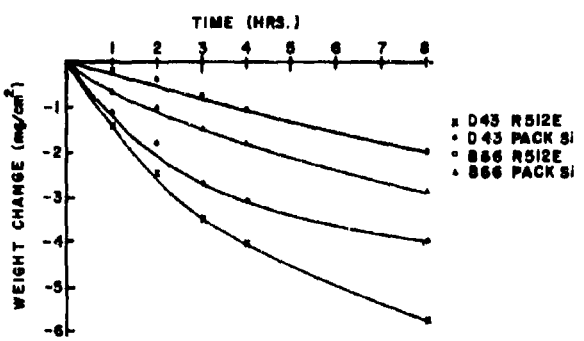

Figure 31 Weight Change vs. Time at 2700°F and 5×10^{-4} Torr.

Photomicrographs of fused silicided, Ti-Cr-Si coated, and pack silicided B66 are shown in Figures 32, 33, and 34, respectively. For each system the following six conditions are shown:

Condition	Figs. 32,33,34
As coated	a
Exposed 8 hours 2700°F - 1 torr air	b
Exposed 8 hours 2700°F - 1 torr argon	c
Preoxidized 2 hours - 2700°F 1 atm. air	d
Preoxidized 2 hours - 2700°F 1 atm. + exposed 8 hours - 2700°F - 1 torr air	e
Preoxidized 2 hours - 2700°F - 1 atm. air + exposed 8 hours - 2700°F - 1 torr argon	f

For the fused silicide coated B66 shown in Figure 32, a significantly thick oxide of nonuniform thickness has grown on the coating during exposure to 2700°F, one-torr air for eight hours (32b). A similar exposure of a previously preoxidized specimen results in appreciable further growth of the oxide (32e) even though the weight gain chart of Figure 30 shows a small weight loss. This appears to indicate that some volatile products from the coating are escaping through the scale. The preoxidized specimen exposed to the one torr argon (32f) shows no trace of an oxide scale, indicating it has been completely evaporated. In addition, both the as-coated and preoxidized specimens exposed to the one-torr argon (32c,32f) are approximately 20 percent thinner than the corresponding samples exposed to 2700°F, one-torr air for the same eight hour period (32a,32d). These results occurred even though the initial coating thicknesses and the present base metal thicknesses of all four specimens are essentially equal, as are their innermost diffusion zones.

With the Ti-Cr-Si coated B66 shown in Figure 33, the coating is completely consumed in spots as a result of the eight hour 2700°F, one-torr exposure (33b). The left half of Figure 33b, however, shows that parts of the coating are intact and covered with a protective scale. This behavior is probably the result of inhomogeneities in this coating, which have been previously reported (4). Preoxidation of the coating results in a thick oxide scale, plus a subscale, and/or a contaminated zone (33d). When the preoxidized coating is exposed to the 2700°F, one-torr, air environment for eight hours, the scale and subscale grow uniformly, and the coating remains protective (33e). Both the as-coated and preoxidized specimens exposed to the one-torr argon exhibited large decreases in thickness. Both also appear to have very thick oxidized zones.

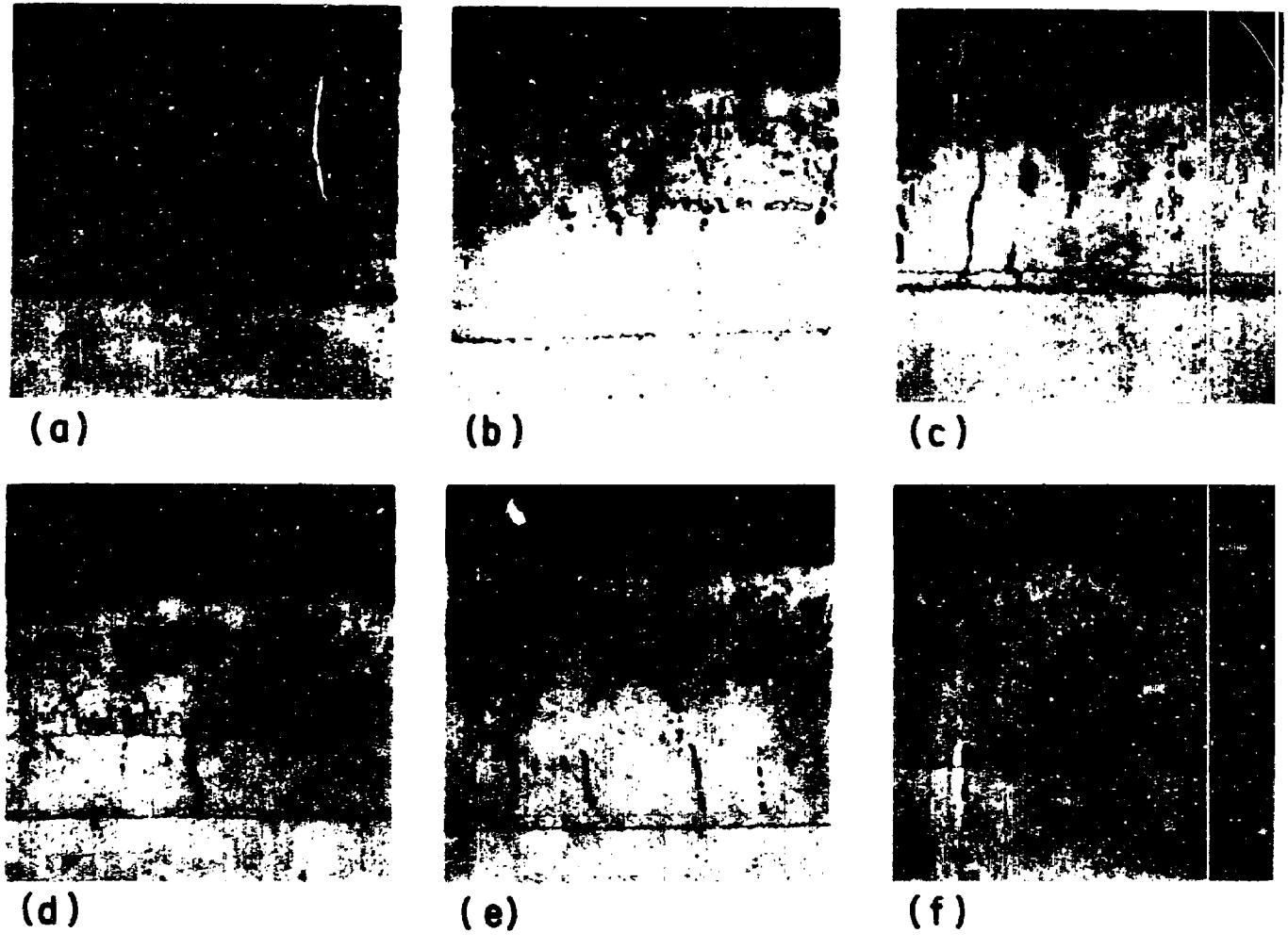

Figure 32 Microstructure of Fused Silicide Coated B66 (All 400X)
(a) As Coated, (b) 2700°F - 1 Torr Air, (c) 2700°F - 1 Torr Argon, (d) Preoxidized,
(e) Preoxidized + 2700°F - 1 Torr Air, (f) Preoxidized + 1 Torr Argon.

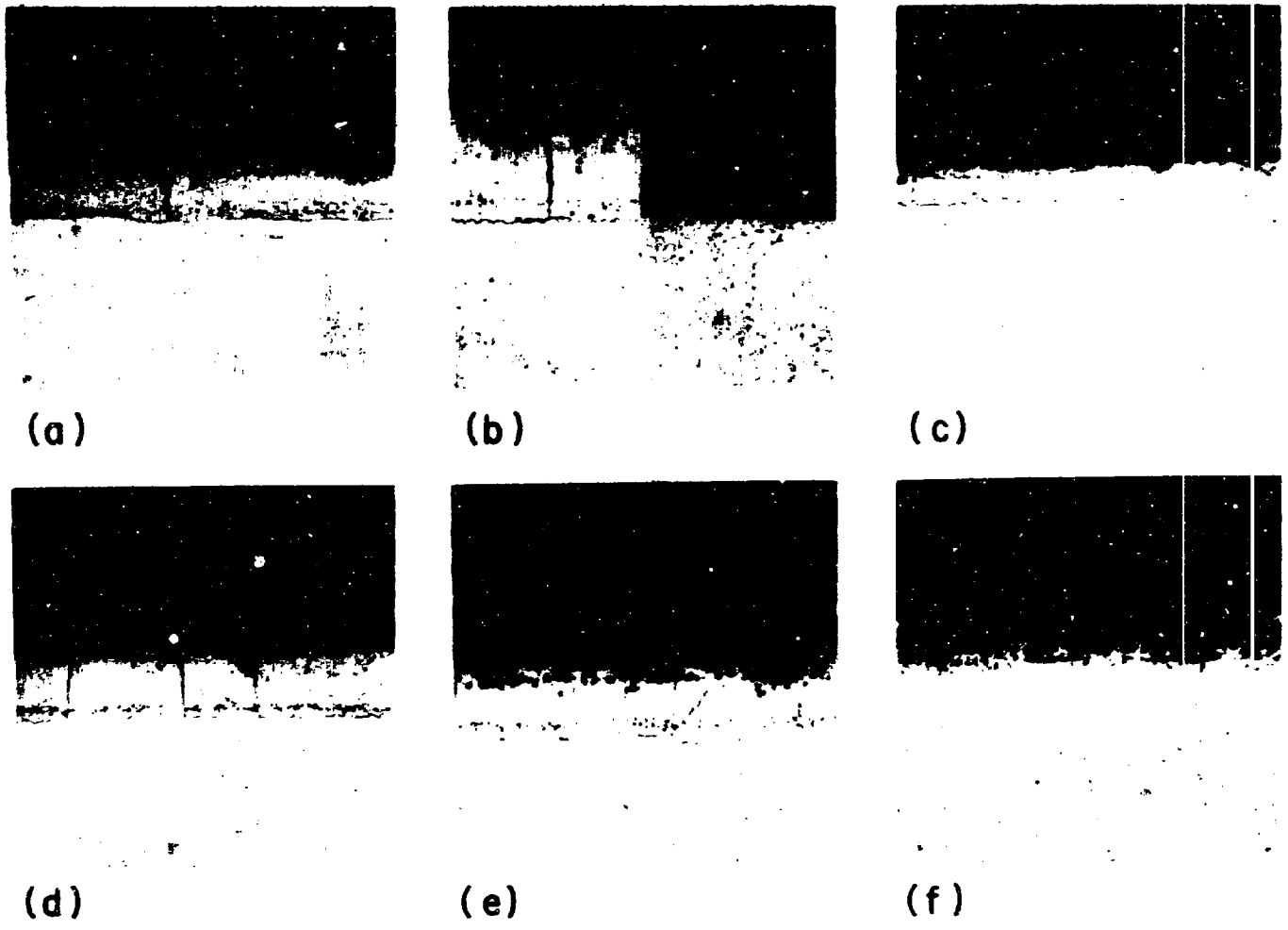

Figure 33 Microstructure of Ti-Cr-Si Coated B66 (All 400X)
(a) As Coated, (b) 2700°F - 1 Torr Air, (c) 2700°F - 1 Torr Argon, (d) Preoxidized,
(e) Preoxidized + 2700°F - 1 Torr Air, (f) Preoxidized + 2700°F - 1 Torr Argon.

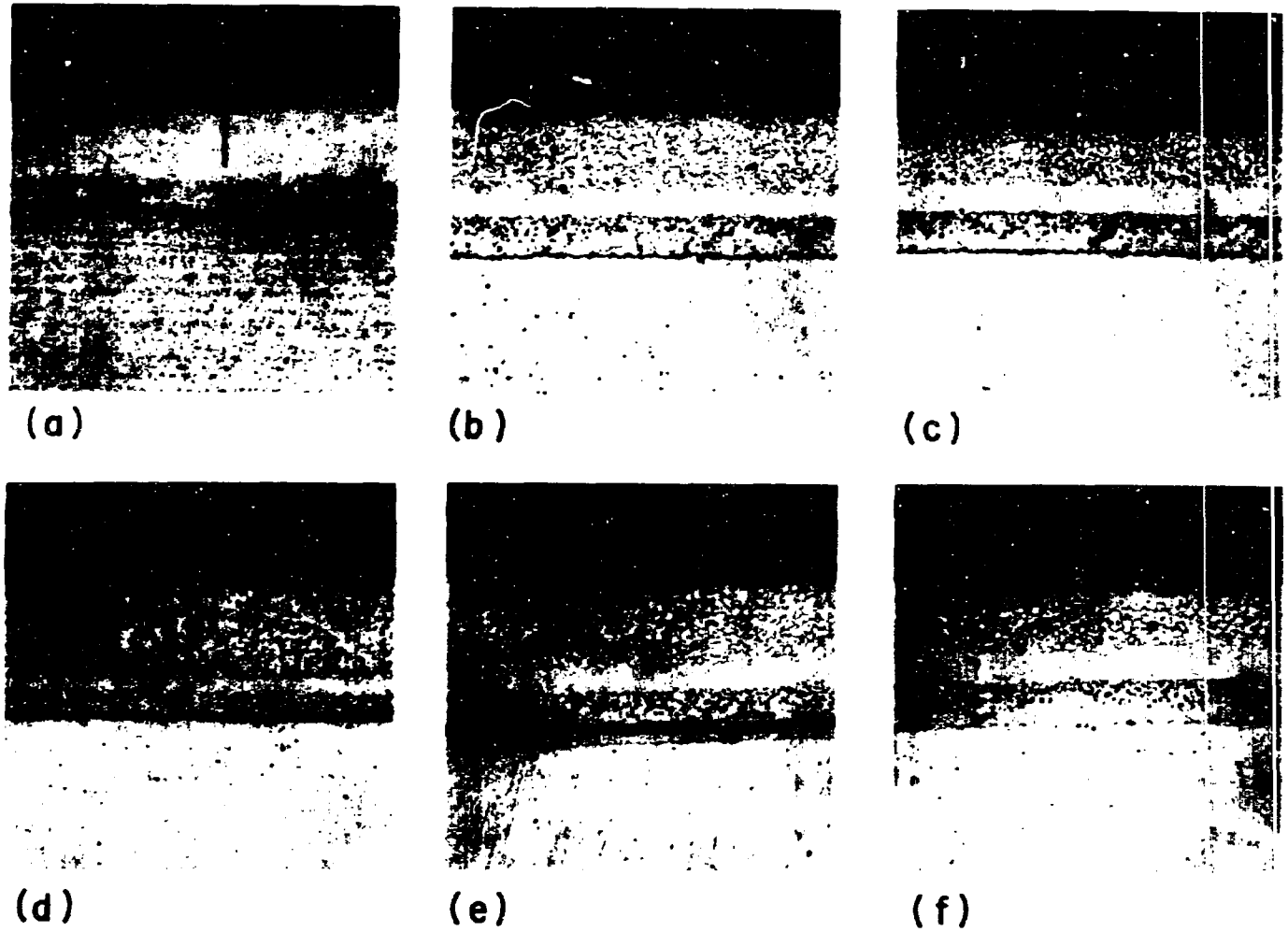

Figure 34 Microstructure of Pack Silicide Coated B66 (All 400X)
(a) As Coated, (b) 2700°F - 1 Torr Air, (c) 2700°F - 1 Torr Argon, (d) Preoxidized,
(e) Preoxidized + 2700°F - 1 Torr Air, (f) Preoxidized + 2700°F - 1 Torr Argon.

The microstructures of unalloyed pack silicide coated B66 specimens are shown in Figure 34. The lateral cracks in several of the photomicrographs should not be regarded as representative of the unmounted samples. This coating apparently has very weak planes in its lower layers, and it was difficult to mount and polish these specimens without causing such separations. The structure of the preoxidized specimen (d) becomes better defined than the as-coated specimen (a) as a result of the heat treatment imposed, and shows the main body of the coating to consist of a finely-divided, two-phased structure containing a narrow, single-phased layer near the substrate-coating interface. The oxide films on the specimens exposed to 2700°F, one-torr air environment for eight hours (b,c) are very thin, dense, and single-phased. Specimens exposed to the low pressure argon environment (c,f) are slightly thinner and are devoid of any oxide scale. The surfaces of these specimens have been converted to homogeneous layers of the precipitated phase.

Figure 35 shows a photomicrograph of a pack silicide coated B66 specimen exposed to 2700°F and 5 x 10^{-4} torr for eight hours and illustrates a phenomenon observed to be characteristic of this system in the environment as well as in the one-torr air or argon environments. The coating may delaminate in the strata shown or

Figure 35 Pack Silicide Coated B66 after Exposure to 2700°F - 5 x 10^{-4} Torr Environment for 8 Hours.

at lower levels. This results in the peeling back of the coating in such a way that makes it appear evident that it is caused by a buildup of gas pressure in the coating at that point. Similar behavior was not observed with any other system studied.

Specimens representing all five coating systems plus fused quartz specimens in six test conditions were analyzed by X-ray diffraction techniques. Only the specimen surfaces were analyzed since our primary interest was in identifying the oxide phases present. The results of these analyses which are given in Table XIII, point to the following conclusions:

Exposure of all coating systems (except the Ti-Cr-Si system) to one torr or one atmosphere air at 2700°F results in the formation of an SiO_2 (α cristobalite) film on the surface, but does not otherwise change the phases. The fact that the M_5Si_3 phases are not detected is probably attributable to the additional masking effect imposed by the scale. Exposure of as-coated or as-preoxidized specimens of the same four systems to the low pressure inert atmosphere, however, results in the disappearance of the $CbSi_2$ phase in both cases, and all the oxide phases in the case of the preoxidized specimens. With the Ti-Cr-Si system, the picture is clouded by the complexity of the systems and the number of oxide phases detected. The effect of preoxidation on the behavior of this coating in 2700°F, one-torr air appears to be related to the growth and stabilization of the TiO_2 oxide, as the major component of the scale, in lieu of SiO_2 (α cristobalite). Exposure of both the as-coated and preoxidized specimens resulted in the disappearance of the MSi_2, M_5Si_3, TiO_2, SiO_2, and $Cr_2Ti_2O_7$ phases and the appearance of Cb_5Si_3 and Ti_2O_3 phases. The appearance of Ti_2O_3, particularly in the specimen which had not previously been exposed to an oxidizing environment, may be attributable to some air leakage into the test furnace system, and to the great affinity of titanium for oxygen.

The analyses of the fused quartz show that it is readily transformed to α cristobalite which is normally the principal oxide phase grown on all silicide coatings, and that this substance is quite stable in 2700°F, one-torr air and argon environment.

To summarize the results of this low pressure mechanism study it is clear that fused silicide coated B66 and D43 and pack silicide coated B66 and D43 can withstand a 2700°F, one-torr environment without loss of protectiveness for eight hours and with small positive weight changes. Ti-Cr-Si coated B66 is not similarly protective in the same environment. Preoxidation of all coating systems for two hours at 2700°F and one atmosphere air renders the Ti-Cr-Si coated B66 protective to the 2700°F, one-torr air environment for eight hours, and has no apparent effect on the other systems. Exposure of the as-coated or preoxidized coatings (excepting Ti-Cr-Si) to a 2700°F, one-torr, air environment results in the formation and/or continued growth of a scale on its surface which contains SiO_2 (α cristobalite), with little changes taking place in the underlying phases except by way of solid state diffusion. Exposure of the as-coated or preoxidized coatings (excepting the Ti-Cr-Si coating) to a 2700°F, one-torr, argon environment for eight hours results in the loss of all oxide phases and the transformation (at least of some finite depth of surface) of the disilicide phases to lower silicides. The Ti-Cr-Si coating behaves somewhat similarly except

TABLE XIII

X-RAY DIFFRACTION ANALYSES

Coating-Substrate System	Major Phases Detected					
	As Coated	2700°F One Torr Air 8 Hours	2700°F One Torr Argon 8 Hours	Preoxidized	Preoxidized +2700°F One Torr Air 8 Hours	Preoxidized +2700°F One Torr Argon 8 Hours
R512E - D43	M_5Si_3 (hex) $CbSi_2$	SiO_2 (α crist.) $CbSi_2$	M_5Si_3 (hex) M_5Si_3 (tet. H.T. form) M_5Si_3 (tet. L.T. form)	$CbCrO_4$ SiO_2 (α crist.) $CbSi_2$	SiO_2 (α crist.) $CbSi_2$	M_5Si_3 (hex) M_5Si_3 (tet. H.T. form) M_5Si_3 (tet. L.T. form)
Pack Si - D43	$CbSi_2$	SiO_2 (α crist.) $CbSi_2$	M_5Si_3 (hex) M_5Si_3 (tet. H.T. form) M_5Si_3 (tet. L.T. form)	SiO_2 (α crist.) $CbSi_2$ Cb_5Si_3 (hex)	SiO_2 (α crist.) $CbSi_2$	M_5Si_3 (hex) M_5Si_3 (tet H.T. form) M_5Si_3 (tet. L.T. form)
R512E - B66	$CbSi_2$ M_5Si_3 (hex)	SiO_2 (α crist.) $CbSi_2$	M_5Si_3 (hex) M_5Si_3 (tet. H.T. form) M_5Si_3 (tet. L.T. form)	$CbCrO_4$ SiO_2 (α crist.) $CbSi_2$	SiO_2 (α crist.) $CbSi_2$	M_5Si_3 (hex) M_5Si_3 (tet. H.T. form) M_5Si_3 (tet. L.T. form)
Pack Si - B66	$CbSi_2$	SiO_2 (α crist.) $CbSi_2$	M_5Si_3 (hex) M_5Si_3 (tet. H.T. form) M_5Si_3 (tet. L.T. form)	SiO_2 (α crist.) $CbSi_2$	SiO_2 (α crist.) $CbSi_2$	M_5Si_3 (hex) M_5Si_3 (tet. H.T. form) M_5Si_3 (tet. L.T. form)
Ti-Cr-Si - B66	MSi_2 (close to $CrSi_2$) MS_2 (close to $CbSi_2$) M_5Si_3 (tet.)	SiO_2 (α crist.) $(Ti, Nb)O_2$ Cr_2O_3 (poss.)	Cb_5Si_3 Ti_2O_3 TiO	$(Ti, Nb)O_2$ Cr_2O_3 $Cr_2Ti_2O_7$	TiO_2 SiO_2 (α crist.) Cr_2O_3	Ti_2O_3 TiO_2
Fused Quartz	(As Received) Amporphous	SiO_2 (α crist.)	SiO_2 (α crist.)	SiO_2 (α crist.)	SiO_2 (α crist.)	SiO_2 (α crist.)

that Ti_2O_3 is observed in the argon exposed specimens. This exposure also results in the loss of thickness of coating roughly corresponding to the weight losses observed. Also, with the exception of the Ti-Cr-Si system, no oxide scale could be seen on any specimens (including preoxidized specimens) exposed to this environment. Exposure to a 2700°F, one-torr argon environment for eight hours results in appreciable weight losses by all coating systems at a nearly linear rate. The rate of weight loss is greatest for the Ti-Cr-Si system, least for the pack silicides, and intermediate for the fused silicides. Exposure to a 2700°F, 5×10^{-4} torr vacuum environment results in essentially identical weight losses to that observed in one-torr argon. Exposure of the preoxidized coatings to the 2700°F, one-torr argon environment results in even larger weight losses than observed with the as-coated specimens. With the exception of the Ti-Cr-Si system, the curves coincide with their respective as-coated curves after the first hour. This would indicate that the entire oxide is lost during the first hour of exposure. With the Ti-Cr-Si coating the rate of weight loss after the first hour is slower than for the corresponding as-coated specimen, indicating that the coating itself was converted to a more volatile state by the preoxidation treatment. SiO_2 (α cristobalite) is very stable in both inert and oxidizing environments at 2700°F and one torr. This substance exhibits very small weight changes and no phase changes as a result of such environmental exposures. In general, the coating systems studied are more stable in oxidizing than in inert one-torr, 2700°F environments. The formation of an oxide scale by preoxidation prior to exposure to the inert atmosphere is ineffective, and in the case of the Ti-Cr-Si coating, actually detrimental to its stability in that environment.

It is clear from the data that the evaporation of coating phases is inhibited by the continuing oxidation process but not merely by the presence of an oxide film. It should be emphasized that silicide coatings for columbium are not intended for use in low pressure inert environments, nor are they likely to be exposed to such environments for extended periods during processing, testing, or otherwise.

g. Reentry Simulation Tests

In earth reentry from orbital or superorbital flight, a lifting body vehicle will heat up and cool down over a one to two hour period. Also, since this heating takes place at very high altitudes, the ambient pressure will be quite low (1 to 10 torr). The specific temperature-pressure profile will depend on the vehicle design and flight mission, and will vary from point to point on the vehicle. As has been pointed out repeatedly by Perkins (4), certain combinations of high-temperature, low-pressure exposures in sequence with different combinations of values of these variables may be quite destructive to oxidation protective coatings. For example, at 2500°F chromium has a vapor pressure of about 0.10 torr. If a coating containing chromium is exposed to a 2500°F, 0.10 torr environment, the rate of evaporation of chromium will be extremely high, and the protectiveness of this coating on continued or subsequent exposure to a high-temperature oxidizing environment will surely be degraded. This problem is further aggravated by the fact that the oxides of some of the more common coating elements (silicon, chromium) may be more volatile than the elements

themselves. It is obviously difficult to determine how a coating will stand up through a real mission profile based only on oxidation testing at sea level.

In the previous program (1) it was established that the Si-20Cr-5Ti fused silicide coating on D 43 was not in any way adversely affected by exposure to 2500°F at pressure of 1.0 torr or above for periods of time up to four hours. It was also demonstrated that similar exposures at pressures in the 0.010 and 0.100 torr range are not significantly destructive to these coatings if they are sufficiently thick (3 mils). However, even though these tests may indicate that there is nothing obviously and grossly inadequate about a system, they are no substitute for tests more closely simulating actual profiles.

Figure 15 shows an automatic programmed, recycling, pressure-temperature-profile simulator. It consists of a Globar heated mullite tube furnace and controls, appropriate vacuum seals, vacuum pumping system, automatic traversing mechanism, and programmed pressure control instrumentation. Temperature variations are obtained by varying the position of the sample boat relative to the hot zone of the furnace. The temperature controller programmer permits the attainment of any shape temperature profile desired. The pressure control system consists of an absolute pressure transducer, a programmer, a pneumatic pressure controller, and a diaphragm-driven needle-bleed valve. The system is capable of controlling pressure in the range from 0.100 torr to 10 torr accurately and reproducibly. The specimen temperature is monitored by a sheathed platinum-platinum ten percent rhodium thermocouple. This thermocouple is inserted through a vacuum seal through the stoking tube; its bead is adjacent to and rides with the specimens as it is stoked in and out of the furnace hot zone.

Initially, some typical pressure temperature profiles were constructed based on some actual design profiles obtained from Lockheed, but modified to account for limitations imposed by the test equipment at the time caused by the late delivery of the temperature profiler. These profiles, which are shown in Figure 36 therefore incorporate a sinusoidal temperature program.

The external surface pressure profile was constructed by giving particular emphasis to that portion of the Lockheed flight profile where the temperatures are high and approaching maximum. In this portion of the flight, the external surface pressure will reach approximately five torr at 2500°F (max temp). The internal surface pressure profile is based on the Lockheed ambient pressure profile and particularly that portion taking place at correspondingly high temperatures. This profile appears particularly rigorous in view of the fact that it combines high temperatures with a very broad range of pressure (0.100 - 3 torr). The profiles shown in Figure 36 represent the actual recorder trace of the sample thermocouple output in the case of the temperature plot, and the McLeod Gauge readings made in the course of checking the pressure instrumentation.

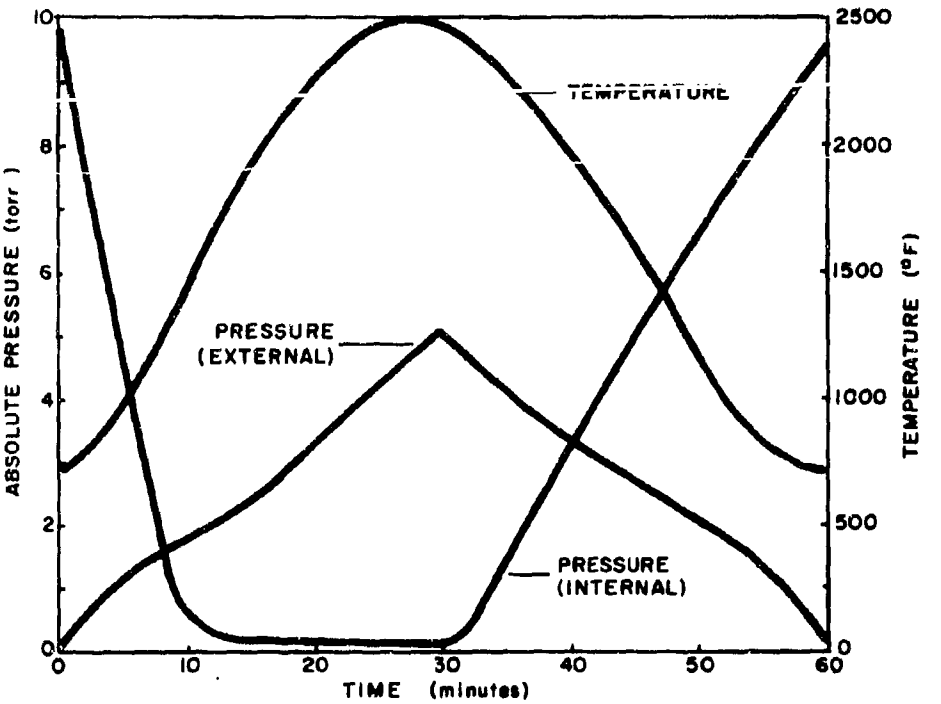

Figure 36 Temperature-Pressure Programs For Reentry Simulation Tests.

Si-20Cr-20Fe and Si-20Cr-5Ti coated D43 tabs were cycled through a number of external and internal surface profiles, as shown in Table XIV. One sample representing each type and test condition was bent 90 degrees after test to assure that no internal oxidation had occurred. Photomicrographs of some of these test specimens, Figures 37 and 38, all show a two-phased oxide scale typical of atmospheric pressure oxidation; this indicates that these oxides are not unstable under these conditions. The photomicrographs also indicate that the extent of oxidation attack is considerably less during the simulation testing than during slow cyclic oxidation at atmospheric pressure. This is more clearly evident if one examines a larger portion of the sample than that shown in the photomicrograph, and also by visual examination with the unaided eye. Metallographic measurements made of these samples also indicate that the total additional interdiffusion of coating with the base alloys is about 0.00025 inch per side after 50 to 60 slow cycles or a similar number of simulated reentry profile cycles. The amount of base metal consumed during the coating formation is about 0.001 inch for the nominal 0.003-inch-thick coatings shown.

The results of these tests, together with the general visual appearance of the samples, the post test bend ductility tests, and the microstructural examination, all indicate that the fused silicide coatings can better withstand these particular simulated profiles than the simple slow cyclic test performed at atmospheric pressure.

For example, the Si-20Cr-5Ti coating on D43 will generally fail at about 10 to 20 cycles in the slow cyclic test. (See Table II p. 14) It is believed that the longer life exhibited in the simulation tests is related to the lower oxidation rates obtained at reduced pressure. This is consistent with the hypothetical edge failure mechanism described elsewhere in this report.

TABLE XIV

RESULTS OF SIMULATED REENTRY ENVIRONMENT TESTS

Composite	Program	No. of Cycles	Remarks
Si-20Cr-20Fe on D43	Internal surface	44*	No oxidation of base metal No embrittlement of base metal
	Exterior surface	55*	No oxidation of base metal No embrittlement of base metal
Si-20Cr-5Ti on D43	Internal surface	44*	No oxidation of base metal No embrittlement of base metal
	Exterior surface	55*	No oxidation of base metal No embrittlement of base metal
Uncoated D43	Internal surface	1	Oxidized and embrittled
	Exterior surface	1	Oxidized and embrittled

*Tests arbitrarily stopped at times indicated with no evidence of failure of coated specimens.

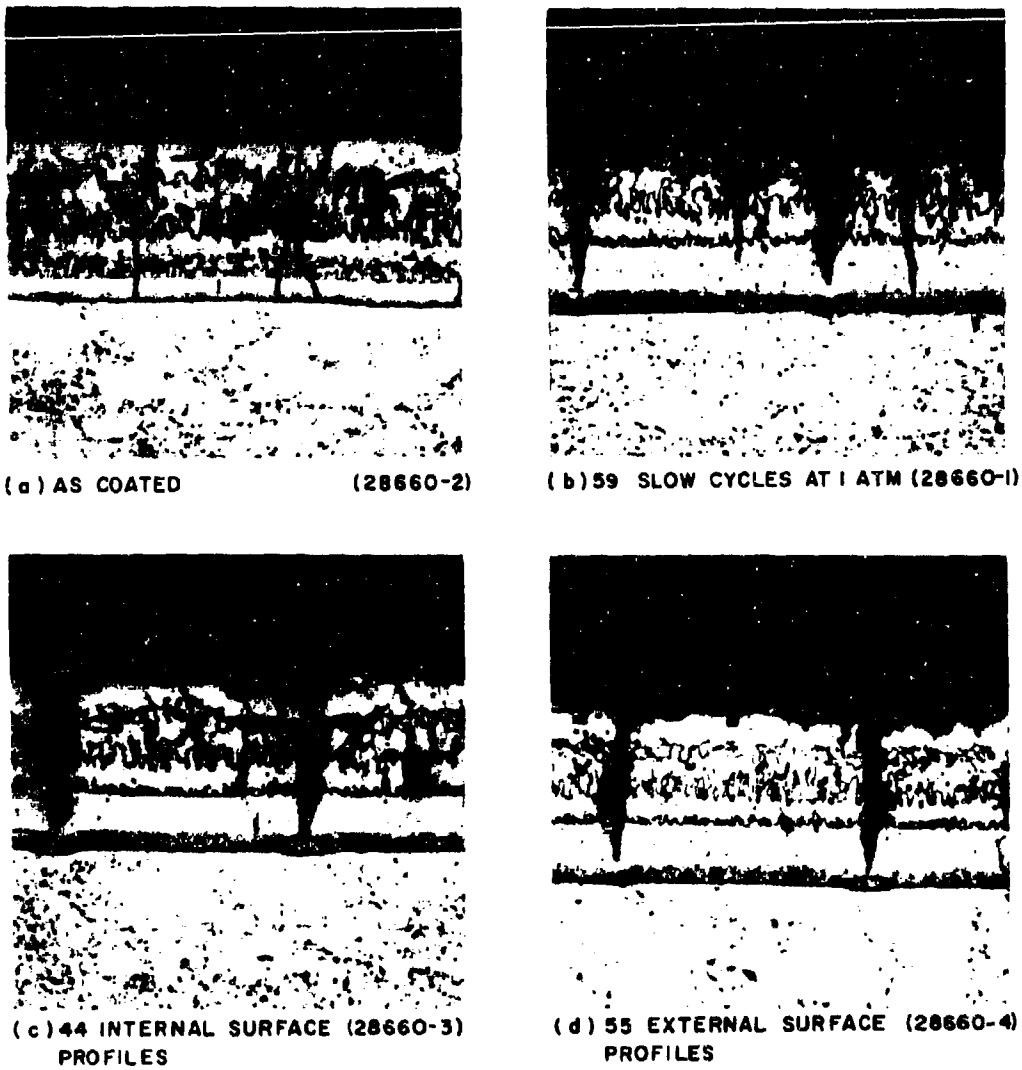

Figure 37 Microstructures of Si-20Cr-20Fe Coated D43 in As-Coated Condition and After Slow Cyclic and Reentry Simulation Tests. 300X

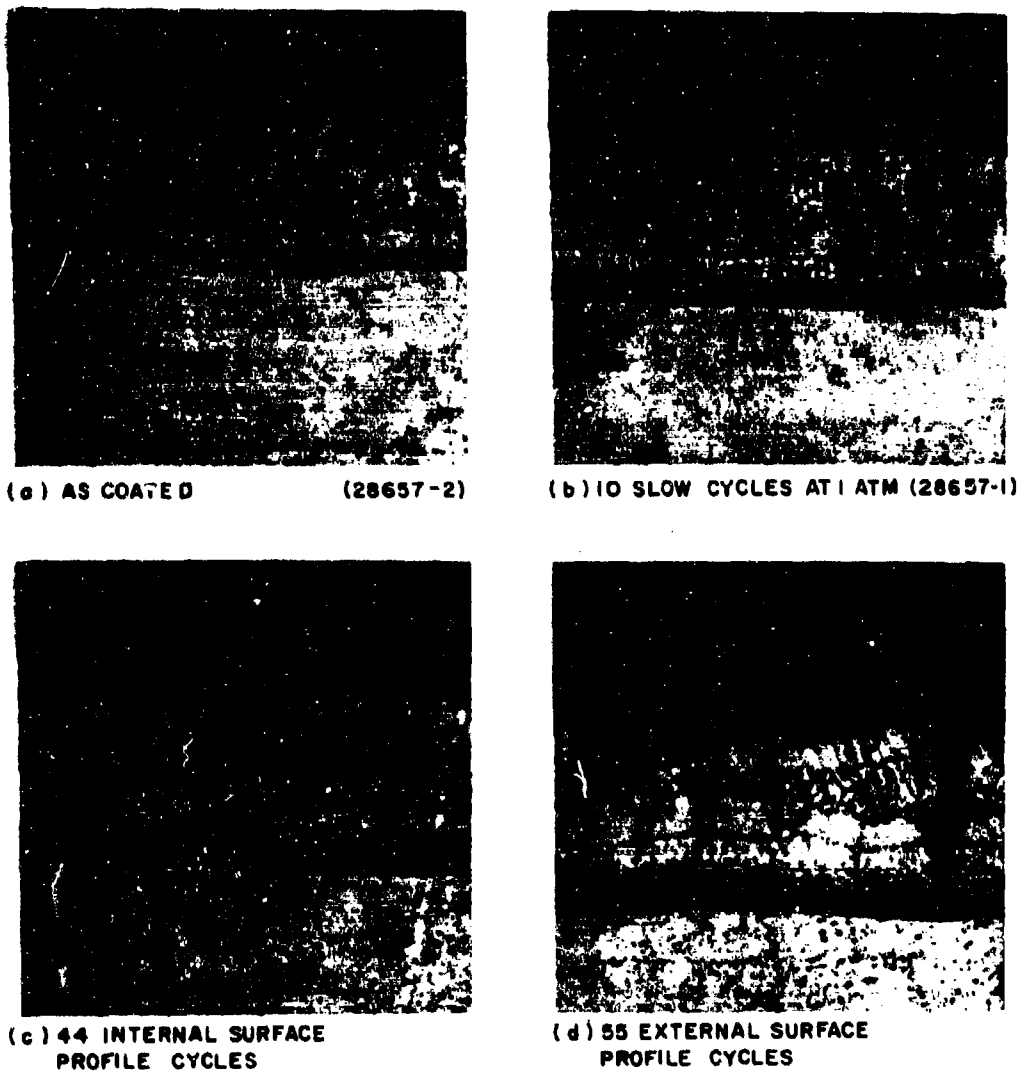

Figure 38 Microstructures of Si-20Cr-5Ti Coated D43 in As-Coated Condition and After Slow Cyclic Reentry Simulation Tests. 300X

The reentry test program next was broadened to include an evaluation of other coating composition-base alloy combinations. Two substrate alloys (D43 and Cb752) and three coating compositions (Si-20Cr-5Ti, Si-20Cr-20Fe, and Si-20Cr-20Fe-16VSi_2) were selected for this evaluation, or a total of six material system combinations. Twenty test coupons of each system were prepared with a nominal 3-mil coating thickness (20 to 25 mg/cm^2). One coupon from each system was cyclically oxidation tested at 2600°F as an indication of overshoot capability. Two coupons from each system were slow-cyclically oxidation tested to failure at atmospheric pressure.

Additional pairs of samples of each type were subjected to 40 internal and 40 external surface reentry profile cycles. The test profiles are those shown in Figure 36 and the test equipment that is shown in Figure 15. Throughout this section the temperatures cited will be the maximum temperature in the profile. Identical tests were next performed on other pairs of samples from each of the six systems, for 200 hours or to failure.

Finally, similar tests were performed for 200 hours or to failure, but with the temperature raised to 2600°F. At the conclusion of all tests, one sample from each pair was given a 90 degree bend ductility test. All of the specimens were found to be completely ductile, indicating that there had been no gross penetration of the coating by interstitial elements which might have escaped visual examination.

The results of all the above tests are shown in Table XV. Significantly, only the (Cb752) - Si-20Cr-5Ti system did not survive the 200+ simulated reentry cycles at a test temperature of 2500°F. It has been previously shown that this coating and substrate interact in a grossly nonuniform manner resulting in a coating which varies greatly in thickness. The 2600°F temperature reentry tests yielded life-times greater than 100 one-hour cycles for all systems. It was clear, however, from visual examination of the sample boat and the specimens, that as a result of contact with reaction products of the first failed sample or samples, most of the remaining samples had been contaminated. It is believed that possibly this contamination resulted in premature failure of most of the failed specimens.

Photographs of representative samples in the as-coated and reentry simulation tested conditions are shown in Figure 39. It is clear that, with the exception of the (Cb752) - Si-20Cr-5Ti system, the fused silicide coated columbium alloys are relatively unaffected by these long-term simulated reentry exposures.

Photomicrographs of the long-term 2500°F temperature reentry simulation tested specimens are shown in Figures 40 through 45 together with the as-coated and slow-cyclic oxidation test specimens. The photographs reveal that the coating is not severely attacked as a result of these long exposures in simulated reentry environments. It will be observed that all of the specimens exposed to such environments have grown an oxide scale which is similar in appearance to that grown in atmospheric pressure tests except that it is obviously thinner. It may be concluded that the fused silicide coatings are less affected by reentry simulation testing than by atmospheric pressure, slow-cyclic testing.

TABLE XV

VARIOUS OXIDATION AND REENTRY SIMULATION TEST DATA FOR SIX COATING-SUBSTRATE COMBINATIONS

Coating Composition	Base Alloy	Cyclic Oxidation Life at 2800°F (No. 1-Hour Cycles to Failure)	Slow Cyclic Oxidation Life at 1 atm. 2500°F Maximum Temperature (No. 1-Hour Cycles to Failure)	Reentry Simulation Life (No. 1-Hour Cycles to Failure)		
				2500°F Maximum Temperature Internal Surface Profiles	2500°F Maximum Temperature External Surface Profiles	2600°F Maximum Temperature Internal Surface Profiles
Si-20Cr-5Ti	D43	10^{+}	24^{e}, 24^{e}	40^{+},40^{+},200^{+},200^{+}	40^{+},40^{+},200^{+},200^{+}	200^{+},200^{+}
Si-20Cr-5Ti	Cb752	5^{e}	$15^{e,s}$,$15^{e,s}$	40^{+},40^{+},117^{e}, $161\text{-}200^{e}$	40^{+},40^{+},161^{e},200^{+}	$100\text{-}140^{*}$,$146^{e,*}$
Si-20Cr-20Fe	D43	10^{e}	63^{e},63^{e}	40^{+},40^{+},200^{+},200^{+}	40^{+},40^{+},200^{+},200^{+}	$100\text{-}140^{*}$,$100\text{-}140^{*}$
Si-20Cr-20Fe	Cb752	9^{e}	71^{e},71^{e}	40^{+},40^{+},200^{+},200^{+}	40^{+},40^{+},200^{+},200^{+}	200^{+},$169^{e,*}$
Si-20Cr-20Fe-10VSi_2	D43	10^{e}	93^{e},85^{e}	40^{+},40^{+},200^{+},200^{+}	40^{+},40^{+},200^{+},200^{+}	200^{+},$100\text{-}140^{*}$
Si-20Cr-20Fe-10VSi_2	Cb752	10^{e}	95^{e},88^{e}	40^{+},40^{+},200^{+},200^{+}	40^{+},40^{+},200^{+},200^{+}	169^{*},169^{*}

$^{+}$Test stopped. Samples not failed.
^{e}Edge failure.
^{s}Surface failure.
*Specimens contaminated by reaction products of first failed specimen.

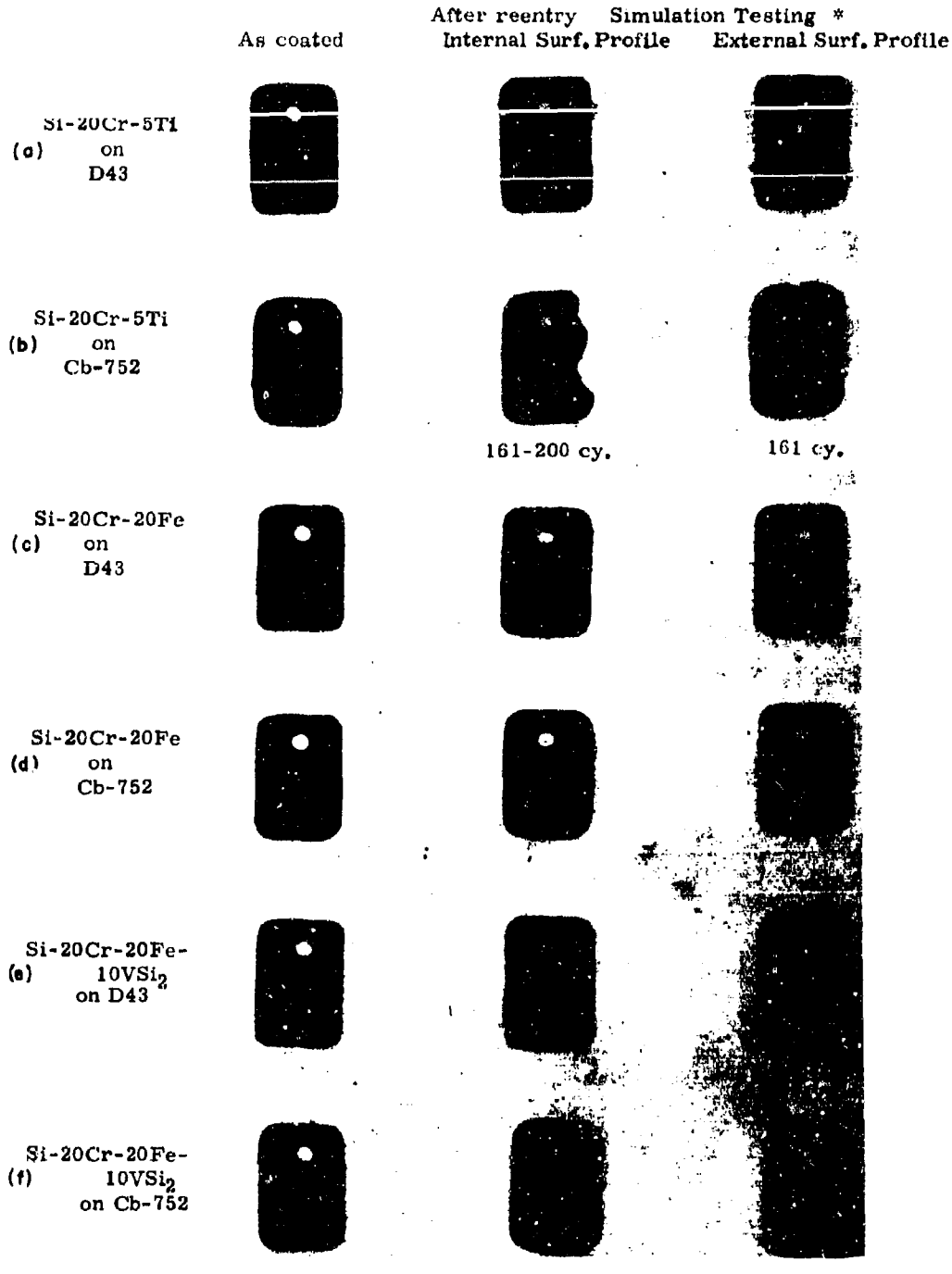

Figure 39 Specimens After Long Term Reentry Simulation Testing at 2500°F Maximum Temperature (1.3X).

*200 Cycles Unless Otherwise Noted.

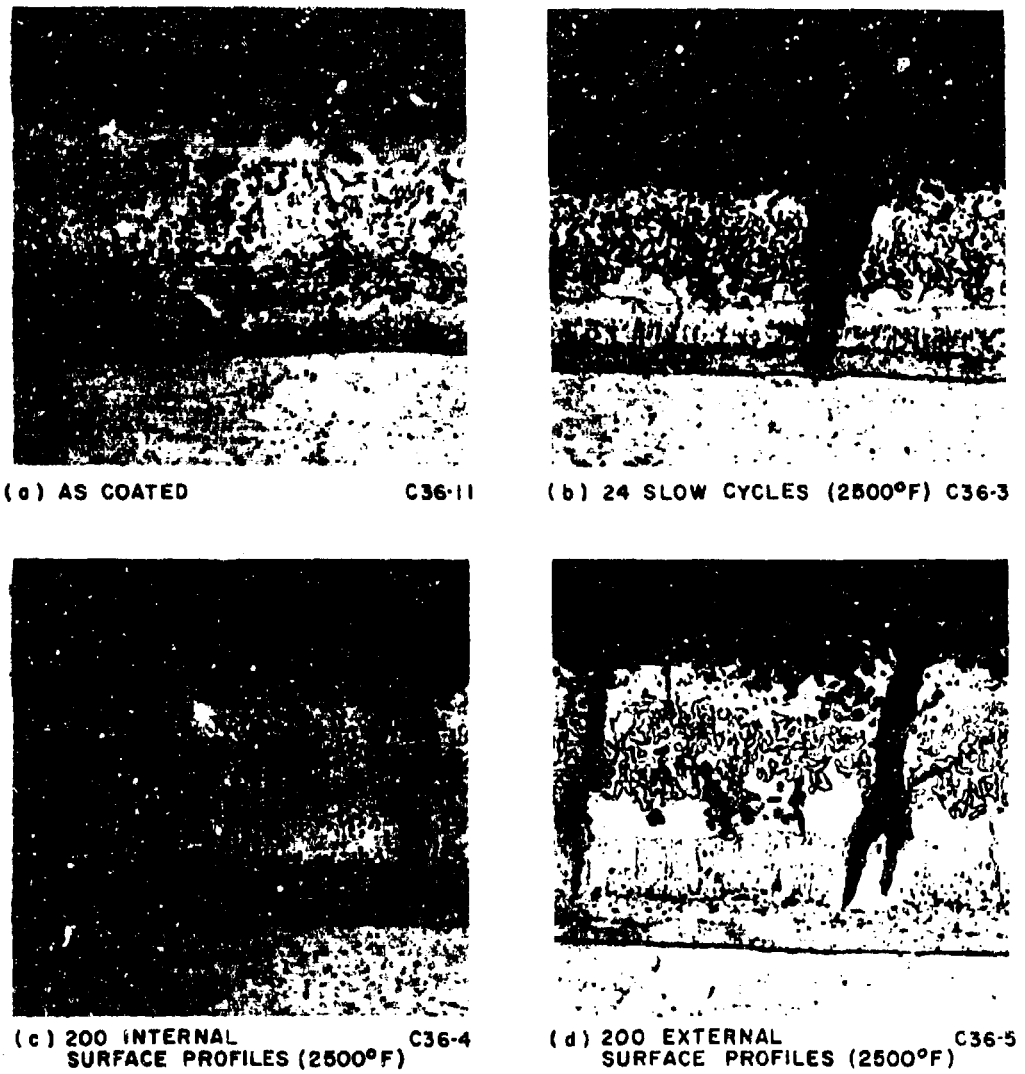

Figure 40 Photomicrographs of Si-20Cr-5Ti on D43 in As-Coated, Slow Cyclic Oxidation Tested and Reentry Simulation Tested Conditions (300X).

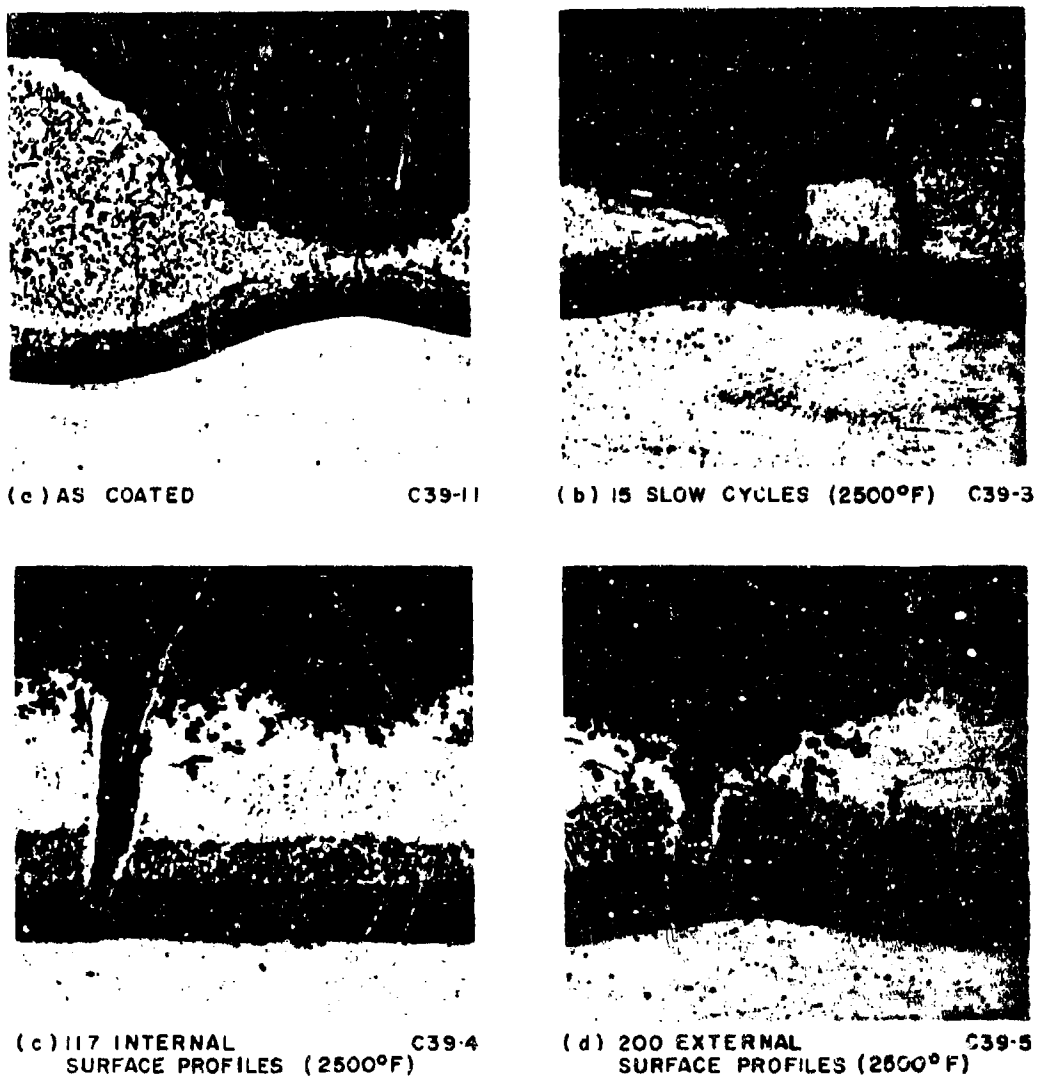

Figure 41 Photomicrographs of Si-20Cr-5Ti on Cb752 in As-Coated, Slow Cyclic Oxidation Tested and Reentry Simulation Tested Conditions (300X).

(a) AS COATED C37-1

(b) 63 SLOW CYCLES (2500°F) C37-3

(c) 200 INTERNAL SURFACE PROFILES (2500°F) C37-4

(d) 200 EXTERNAL SURFACE PROFILES (2500°F) C37-5

Figure 42 Photomicrographs of Si-20Cr-20Fe on D43 As-Coated, Slow Cyclic Oxidation Tested and Reentry Simulation Tested Conditions (300X).

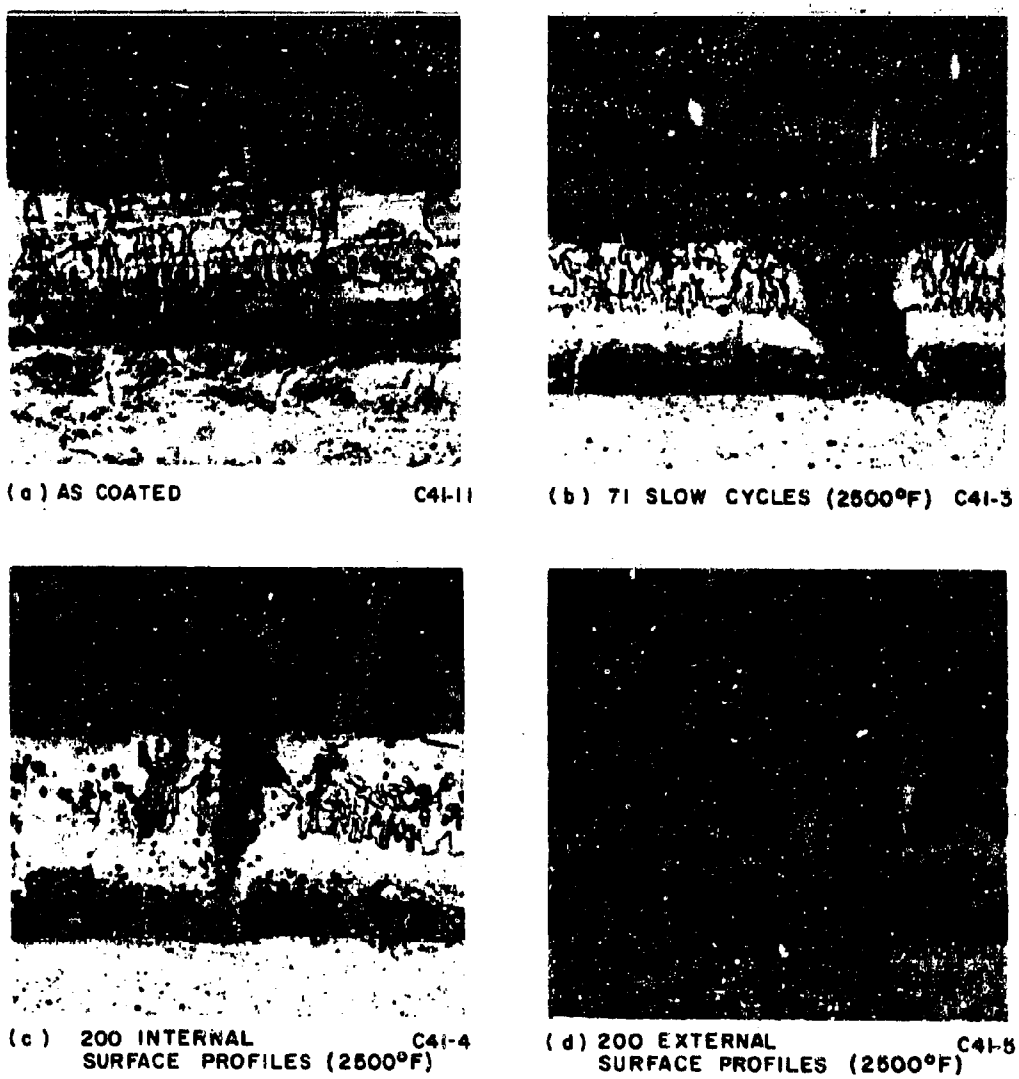

Figure 43 Photomicrographs of Si-20Cr-20Fe on Cb752 As-Coated, Slow Cyclic Oxidation Tested and Reentry Simulation Tested Conditions (300X).

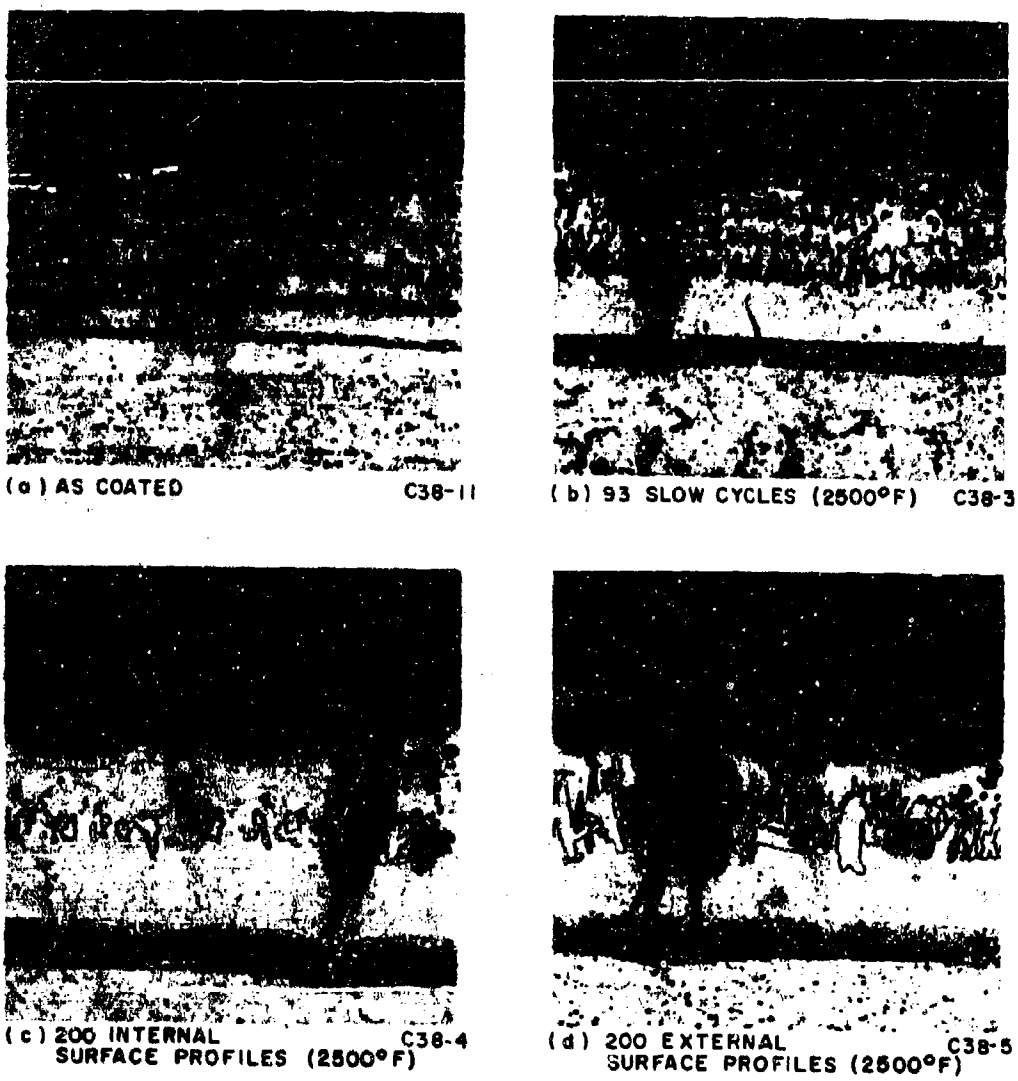

Figure 44 Photomicrographs of Si-20Cr-20Fe-10VSi_2 on D43 As-Coated, Slow Cyclic Oxidation Tested and Reentry Simulation Tested Conditions (300X).

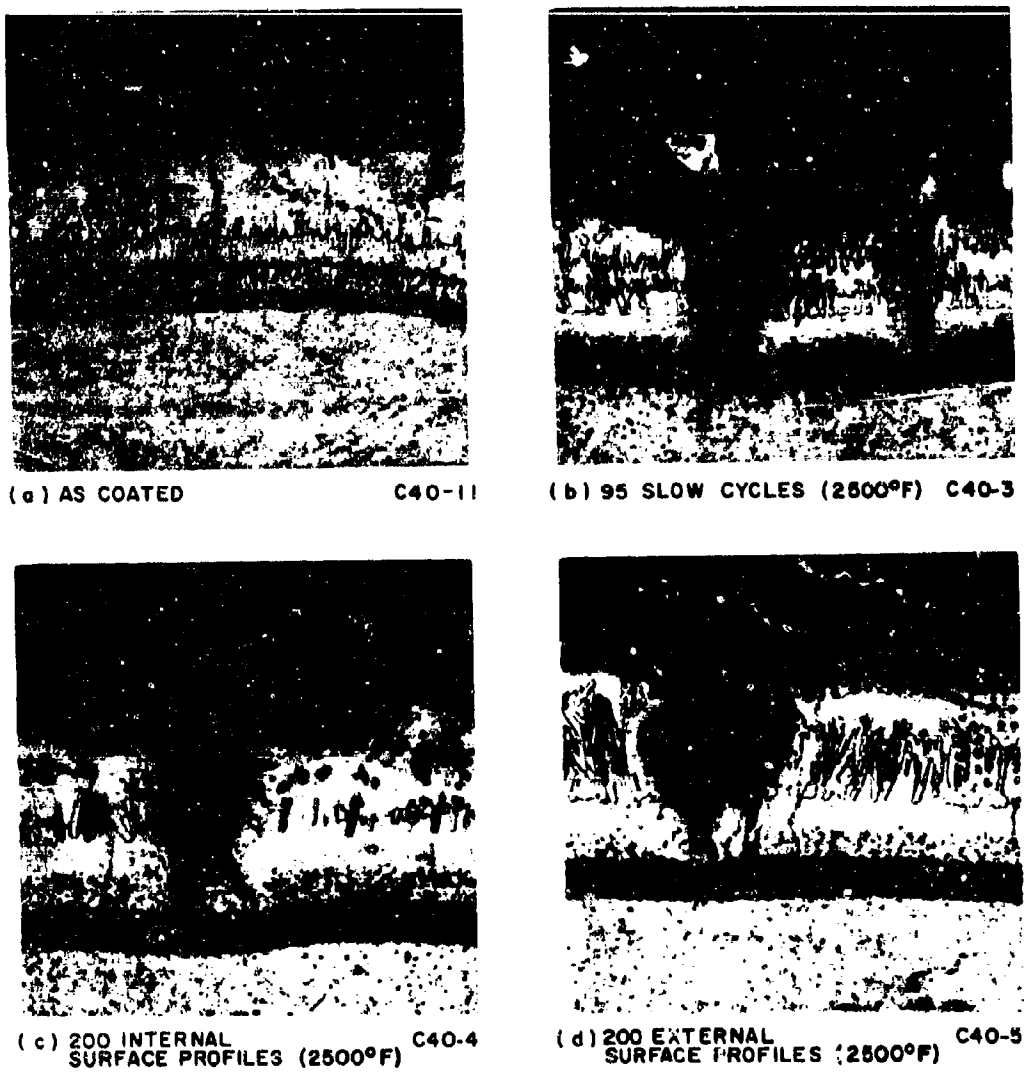

Figure 45 Photomicrographs of Si-20Cr-20Fe-10VSi_2 on Cb752 As-Coated, Slow Cyclic Oxidation Tested and Reentry Simulation Tested Conditions (300X).

The photomicrographs of Figure 41, graphically exhibit the gross nonuniformity of the Si-20Cr-5Ti coating on the Cb752 alloy. In contrast, Figures 43 and 45 show that this same alloy is uniformly coated by the Si-20Cr-20Fe and Si-20Cr-20Fe-10VSi coating.

(1) Very-High Temperature Simulated Reentry Tests

Reentry simulation tests at a peak temperature of 2900°F were performed on D43 and Cb752 specimens, coated with Si-20Cr-20Fe. The test profile used is shown in Figure 46. A description of the test samples and the number of test cycles is given in Table XVI. Samples 1 through 6 exhibited a gross roughening of their surfaces which was apparent after the first cycle, but which stabilized and did not change appreciably with continued exposure. Samples 7 and 8, which were previously tested through 40 simulated cycles to 2500°F, and had therefore reached a relatively stable condition, did not exhibit any surface roughening throughout the six-cycle exposure.

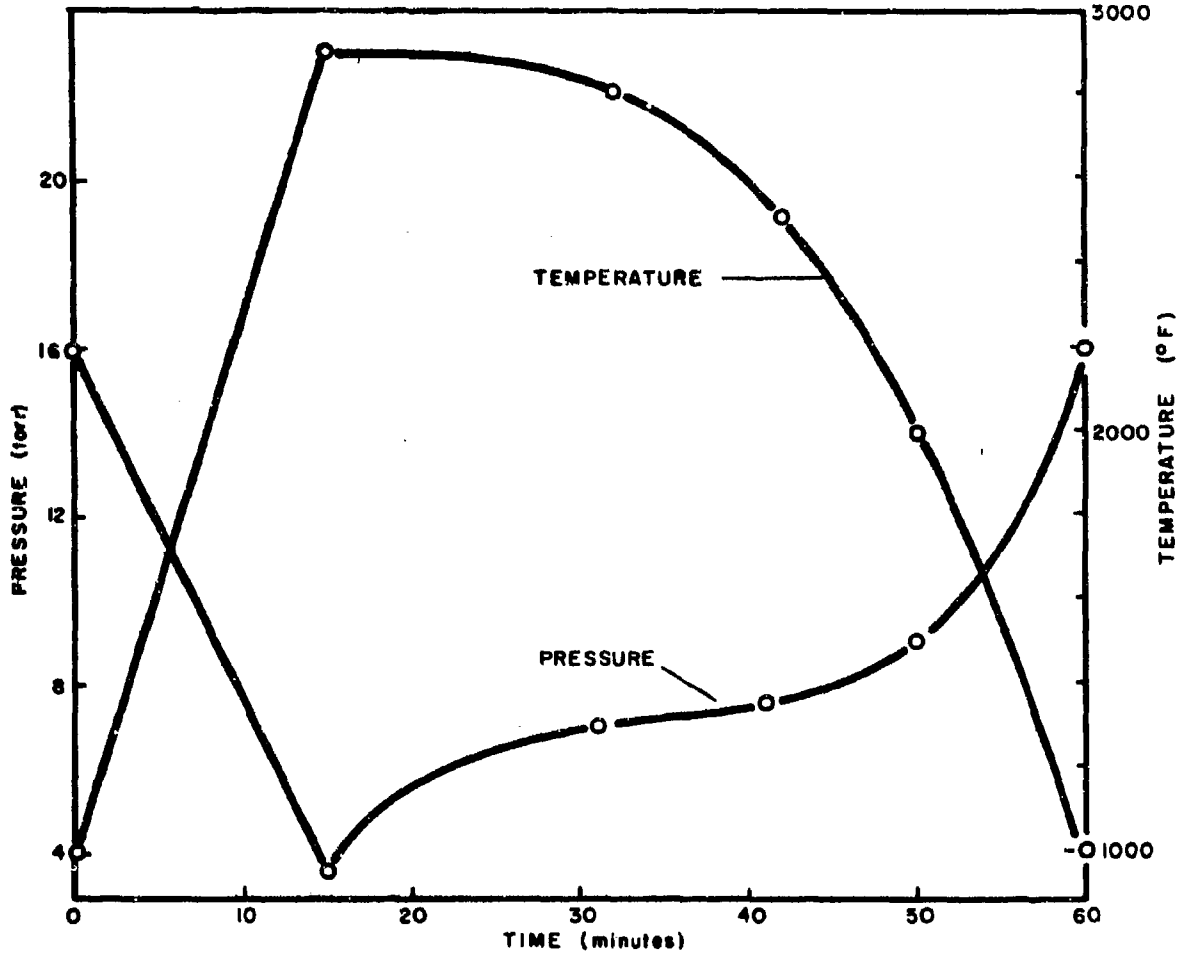

Figure 46 McDonnell High-Temperature Reentry Test Profile.

TABLE XVI

VERY-HIGH TEMPERATURE REENTRY SIMULATION TEST DATA

Sample No.	Base Alloy	Coating	Previous Exposure	No. of High Temp. Reentry Cycles	Remarks
517-74-1	D43	Si-20Cr-20Fe	None	10	Surface roughened after first cycle then stabilized
517-74-2	D43	Si-20Cr-20Fe	None	10	Surface roughened after first cycle then stabilized
517-74-3	D43	Si-20Cr-20Fe	None	10	Surface roughened after first cycle then stabilized
517-74-4	Cb752	Si-20Cr-20Fe	None	10	Surface roughened after first cycle then stabilized
517-74-5*	D43	Si-20Cr-20Fe	None	10	Surface roughened after first cycle then stabilized
517-74-6*	D43	Si-20Cr-20Fe	None	10	Surface roughened after first cycle then stabilized
517-74-7	D43	Si-20Cr-20Fe	40 internal surface profiles - 2500°F max. temp.	6	No change in surface appearance
517-74-8	Cb752	Si-20Cr-20Fe	40 internal surface profiles - 2500°F max. temp.	6	No change in surface appearance
517-77-1	Cb752	Si-20Cr-20Fe	None	5	Rough edges
517-77-2	Cb752	Si-20Cr-20Fe	None	5[e]	Rough edges (bend tested - O.K.)
517-77-3	Cb752	Si-20Cr-20Fe	None	5	Rough edges (bend tested - O.K.)
517-77-4	Cb752	Si-20Cr-20Fe	None	5	Rough edges (bend tested - O.K.)
517-77-6	Cb752	Si-20Cr-20Fe	Preox 2 hrs 2500°F	8[e]	Rough edges (bend tested - O.K.)
517-77-7	Cb752	Si-20Cr-20Fe	Preox 2 hrs 2500°F	8	Rough edges (bend tested - O.K.)
517-77-8	Cb752	Si-20Cr-20Fe	Preox 2 hrs 2500°F	5	Rough edges (bend tested - O.K.)
517-77-9	Cb752	Si-20Cr-20Fe	Preox 2 hrs 2500°F	5	Rough edges (bend tested - O.K.)

*Spotwelded lap joint specimens.

Photomicrographs of several samples from these tests are shown in Figure 47. There was no significant difference either visually or microstructurally between the preoxidized and unpreoxidized specimens after exposure. After five cycles, the coating is obviously intact and an oxide scale can be seen on the surface. There is, however, an intermediate zone that appears to have been severely attacked and now contains large voids. This zone appears to coincide with an as-coated subsurface phase that was shown to be M_5Si_3 quite rich in chromium. Continued exposure for eight cycles results in further attack in this same intermediate zone. The observed edge roughness is possibly due to the existence of larger proportions of this chromium-rich phase in these areas which have been observed.

(2) Statistical Simulated Reentry Life Tests

Statistical simulated reentry life tests were performed on a group of 12 Si-20Cr-20Fe coated D43 coupons. The test profile employed was the interior surface profile shown in Figure 46. After 553 cycles, none of the samples had developed oxidation failures and the test was terminated. For a 24-hour period during the last 50 hours of testing, the furnace temperature at the hot zone was 2600°F rather than 2500°F due to improper operation of the furnace control system.

After testing, one specimen was bent 90 degrees and was completely ductile, indicating that no significant contamination of the D43 alloy had occurred. For comparison, uncoated coupons of unalloyed Cb, D43, and Cb752 were cycled through a single profile and similarly bent. The uncoated specimens all fractured when attempts were made to bend them. Although all three uncoated materials were completely and equally embrittled by the single reentry cycle, it was apparent that the unalloyed Cb752 had essentially no strength in this condition in comparison with the unalloyed columbium and the D43 alloy. Figure 48 illustrates the results of these post-simulation bend tests.

Photomicrographs of the as-coated and simulation-tested coated D43 specimens are shown in Figure 49. Although there obviously has been extensive oxidation of the coating in the thermal stress cracks, none of them extends beyond the coating's inner layer even after such an extremely long exposure. The incremental base metal consumption during this exposure is equal to approximately 1.1 mils per side.

Figure 50 shows photomicrographs of the uncoated columbium and its alloys after exposure to a single reentry cycle, and the extent of contamination is evident. The unalloyed columbium appears to have a more adherent scale and correspondingly less internal oxidation. The D43 has apparently been more heavily contaminated than the Cb752, but the latter appears to have oxidized more rapidly at the grain boundaries, which may account for its complete lack of strength in this condition.

(3) Reentry Simulation Testing of Simple Coated Joints

Ten simple spotwelded lap joint specimens, consisting of two 1/2 x 1/2 x 0.010 inch-thick D43 coupons overlapped 1/4 inch and joined with a single spotweld, were

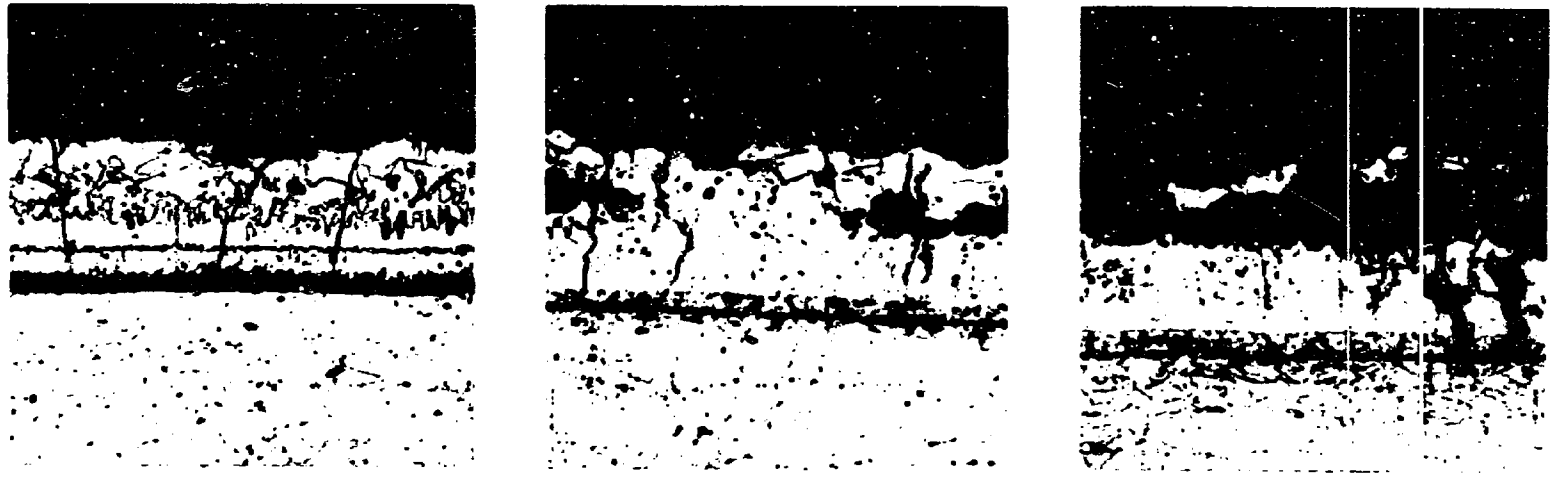

Figure 47 Photomicrographs of Si-20Cr-20Fe Coated Cb752 After Exposure to 2900°F Simulated Reentry Test (300X).

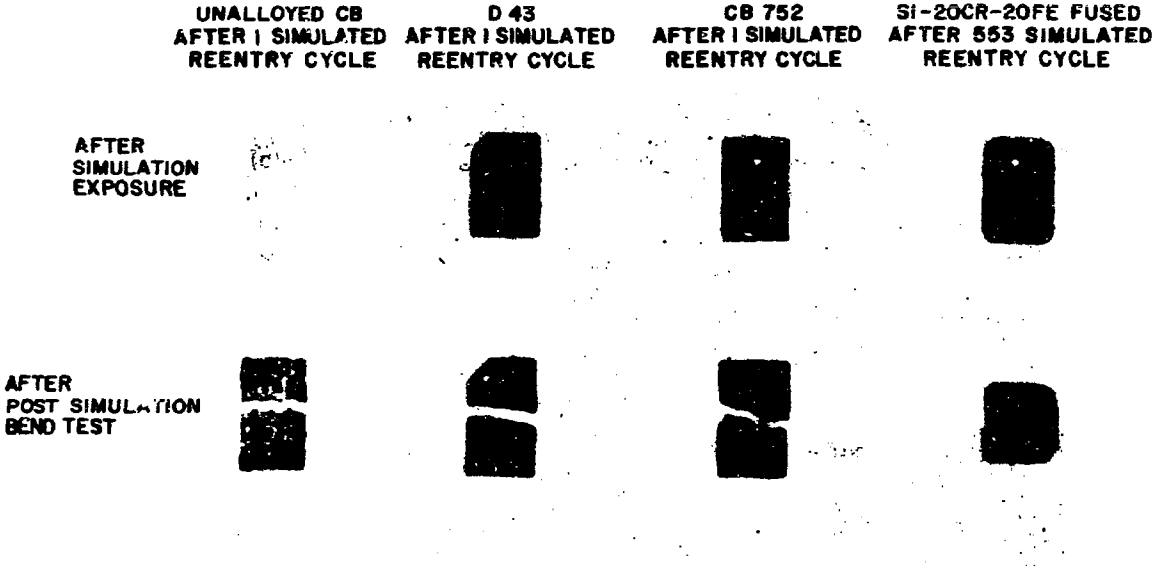

Figure 48 Coated and Uncoated Columbium Alloys After Exposure to Simulated Reentry Environment.

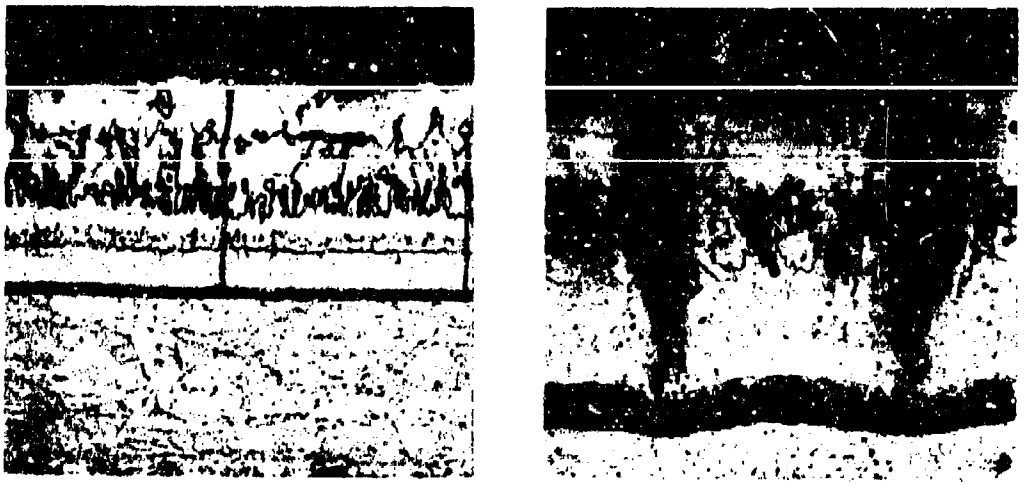

(a) AS COATED (C73-3) (b) AFTER 553 SIMULATED REENTRY CYCLES (C73-1)

Figure 49 Photomicrographs of Si-20Cr-20Fe Coated D43 in As-Coated and Reentry Simulation Tested Conditions.

fabricated and coated with the Si-20Cr-20Fe coating. The coating was applied by spraying, and no effort was made to penetrate the joint with the slurry. The coatings were given the usual fusion-diffusion heat treatment of one hour at 2580°F in vacuum.

The specimens were tested in the reentry simulator using the internal surface profile shown in Figure 46. Two samples were withdrawn after 285 cycles, two were withdrawn after 332 cycles, and the remaining six were tested for 500 hours. There were no failures evident in any of the ten specimens.

Photographs and photomicrographs of the joint samples in the uncoated, coated, and reentry simulation tested conditions are shown in Figure 51. The clearly excellent penetration of the extremely tight joint by the fused silicide coating is noteworthy. It is doubtful if such a tight joint could be penetrated and/or protected by any other type of coating process.

The complete protectiveness afforded to the joint faying surfaces by the coating is also quite apparent. It is significant to note that the Si-20Cr-20Fe coating has a greater tendency to form a fillet than the Si-20Cr-5Ti composition, and that there appears to be no tendency for the sheets to separate in the fillet area during exposure.

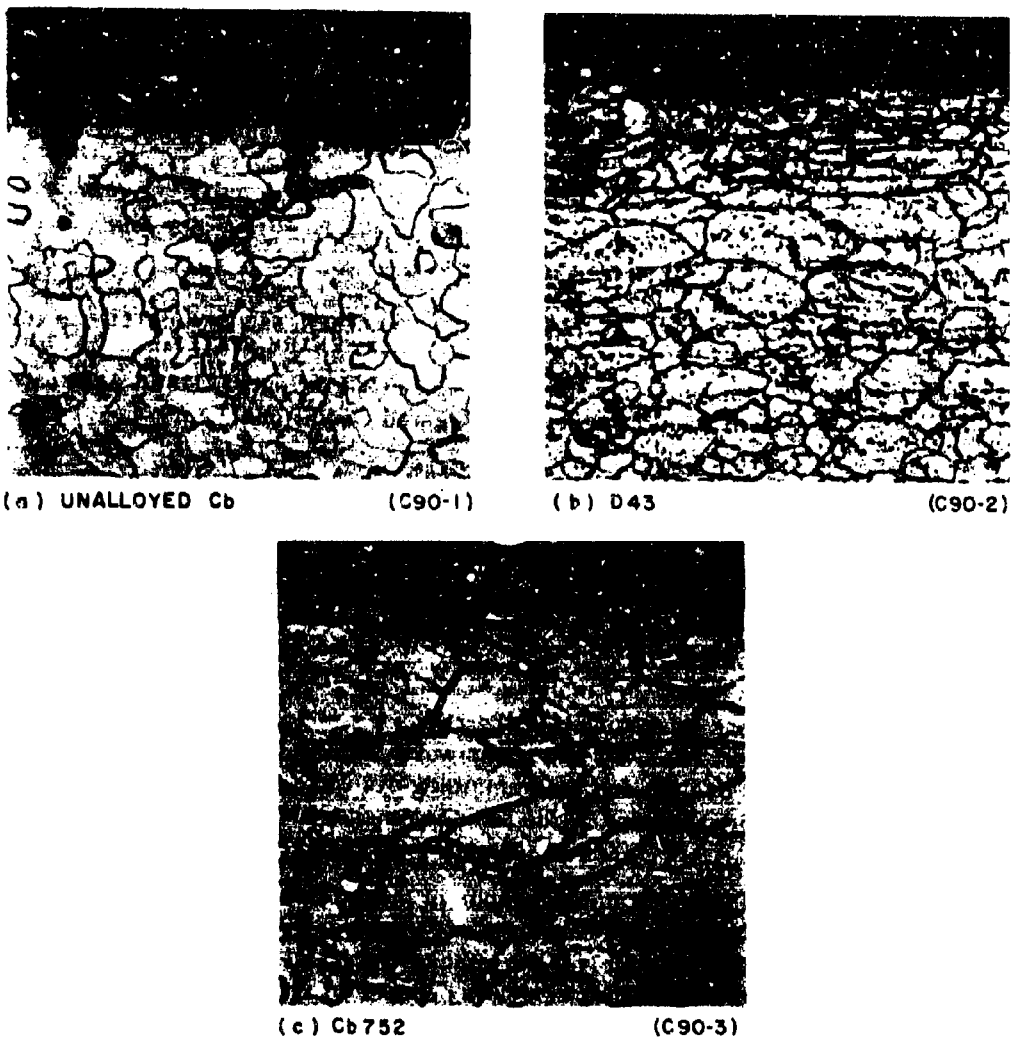

Figure 50 Photomicrographs of Uncoated Columbium Alloys After a Single Simulated Reentry Cycle (300X).

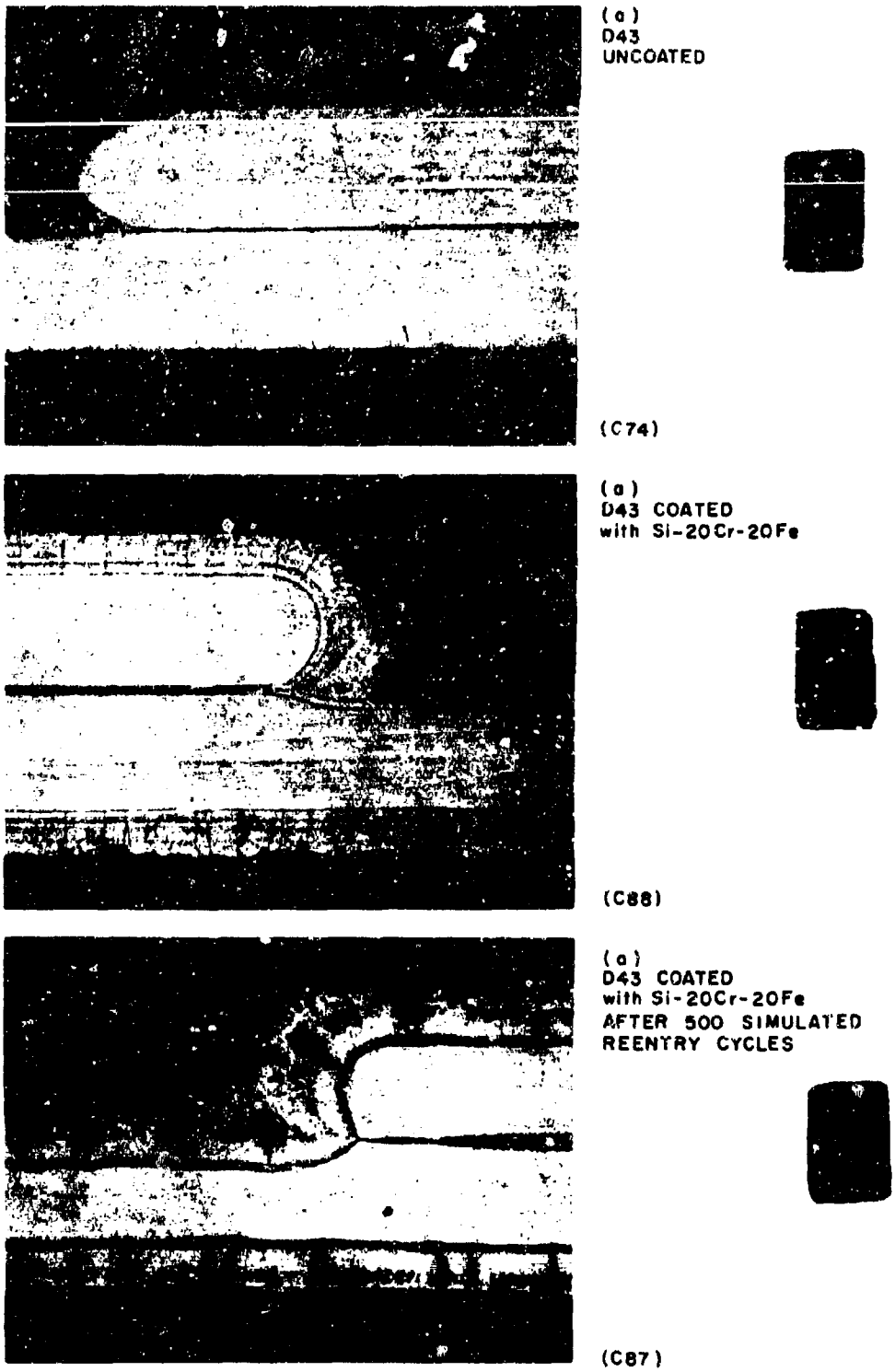

Figure 51 Photomicrographs (70X) and Photographs (1X) of Uncoated, Coated, and Reentry Simulation Tested Joint Specimens.

(4) Tests of Artificially Defected Coated Specimens

Artificially defected Si-20Cr-20Fe coated D43 coupons were tested in the reentry simulator for up to ten hours duration. The defects consisted of 0.0175, 0.0225, and 0.032 inch diameter holes drilled completely through the coated coupons. The exposure conformed to the 2500°F peak temperature internal surface profile shown in Figure 46. One sample having each size defect was tested for 1, 3, and 10 hours. Macrophotographs of defected and exposed coupons are shown in Figure 52. Although it is clear that the columbium alloy substrate is exposed and yellow columbium oxide is formed, the hole does not seem to have been appreciably enlarged and, significantly, the coating does not appear to have been undermined by lateral oxidation of coating sublayers. Photomicrographs of sections through the defects are shown in Figure 53. The extent of oxygen contamination is quite evident.

The 'contamination front" appears to be quite discrete and correlates with a sharp change in microhardness. A plot of the radial extent of this front versus the number of exposure cycles is shown in Figure 54. These data are extremely significant since they roughly define the consequences of casual or random coating failures, and indicate that the consequences are far from catastrophic. After ten reentry cycles the defect has resulted in the contamination of an area less than 3/16 inch in diameter. It is doubtful if a flight vehicle would be seriously weakened by the existence of such contaminated areas unless they occurred in large numbers.

h. Furnace and Torch Tests

Since most oxidation test data relating to coatings consists of isothermal or rapid cycling tests between two temperature levels, there is a certain amount of need for directly comparable data for the fused silicide coatings. Table XVII below gives furnace oxidation test data for the Si-20Cr-20Fe (.0035 inch thick) coated Cb752 system.

TABLE XVII

FURNACE OXIDATION LIFE OF Si-20Cr-20Fe COATED Cb752

Test Condition	Oxidation Life (Hours)
1600°F isothermal	1300+ (6 specimens)
2000°F to R.T.	560+ (14 cycles) (4 specimens)
2500°F to R.T. (1 hr. at temp.; 5 min. at R.T.)	97, 97
2600°F to R.T. (1 hr. at temp.; 5 min. at R.T.)	33, 44
2700°F to R.T. (1 hr. at temp.; 5 min. at R.T.)	19, 19
2800°F to R.T. (1 hr. at temp.; 5 min. at R.T.)	15, 14

+ Indicates test stopped with samples unfailed

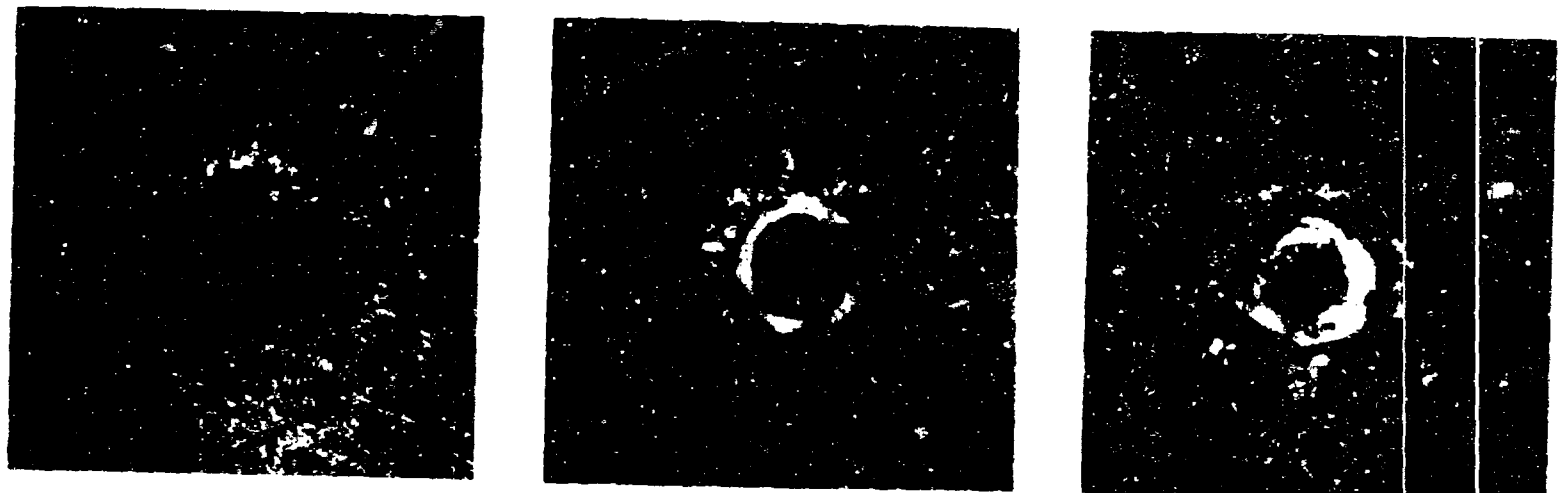

(a) COATED SPECIMEN WITH 0.032" HOLE DRILLED THROUGH

(b) AFTER EXPOSURE TO 3 SIMULATED REENTRY CYCLES

(c) AFTER EXPOSURE TO 10 SIMULATED REENTRY CYCLES

Figure 52 Photographs of Surfaces Artificially Defected and Reentry Simulation Tested Coated Specimens (22-1/2X).

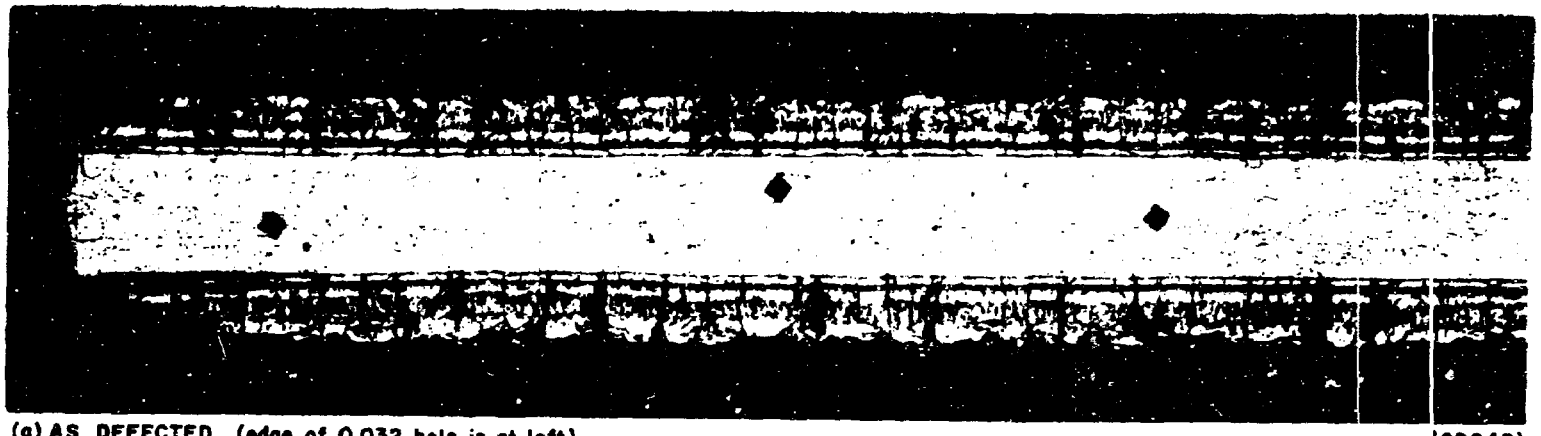

(a) AS DEFECTED (edge of 0.032 hole is at left) (29048)

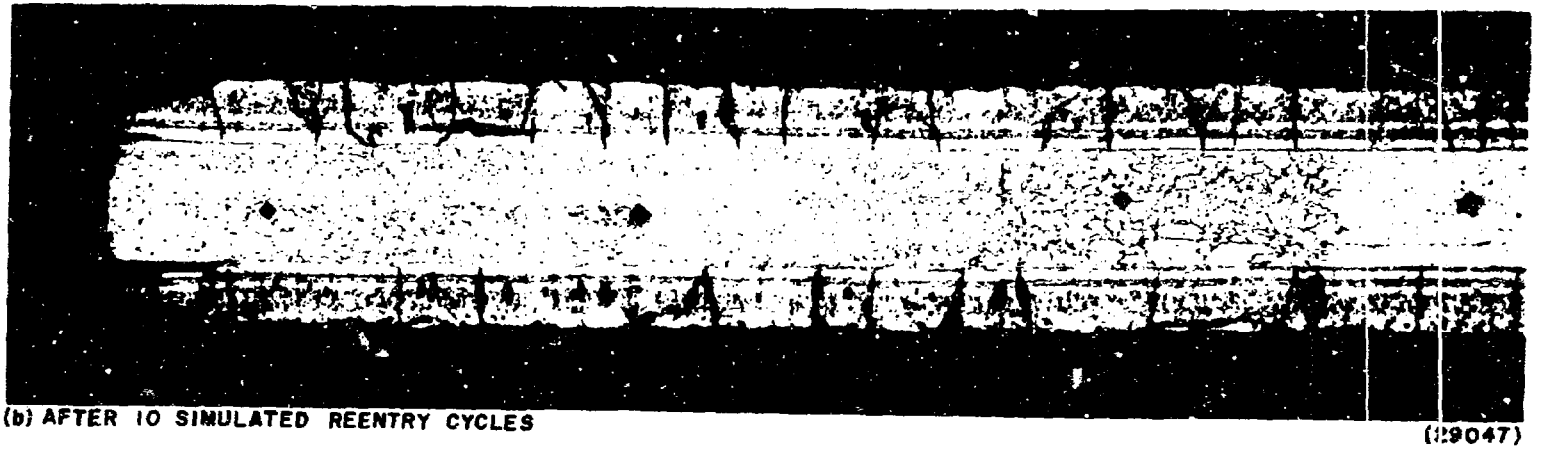

(b) AFTER 10 SIMULATED REENTRY CYCLES (29047)

Figure 53 Sections Through Reentry Simulation Exposed Defected Coated Specimens (100X). (Reduced 10 Percent in Reproduction)

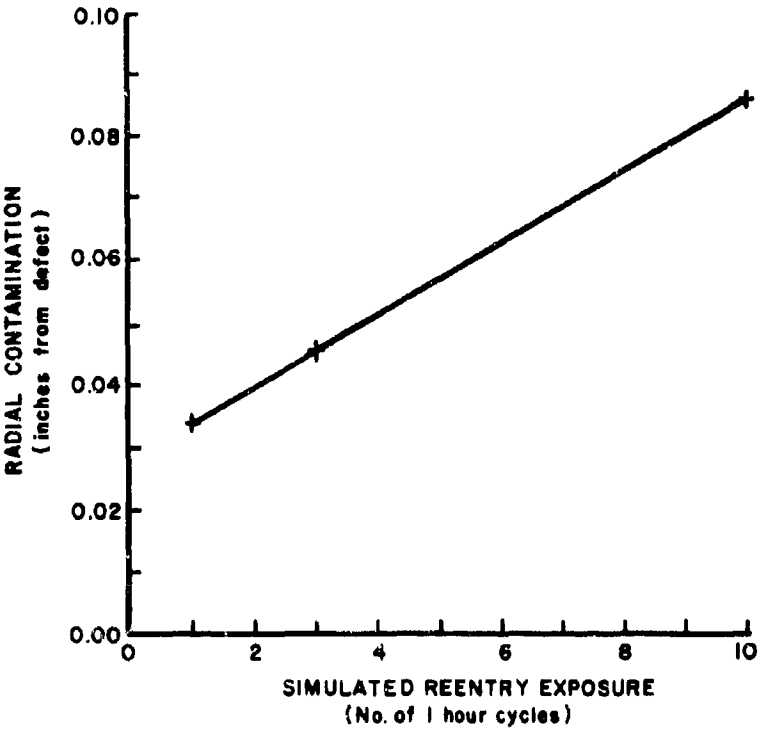

Figure 54 Radial Contamination Through a Defect vs. Simulated Reentry Exposure

These data are also plotted in Figure 55 and Figure 56, which is an expanded scale plot of the higher temperature portion of the curve. These curves indicate that the fused silicide coatings are not susceptible to any type of "pest" reactions but rather have characteristic lifetimes which are an inverse function of the exposure temperature. Of course this has been previously demonstrated far more convincingly by the slow cyclic oxidation testing which has been used extensively in this program.

Oxyacetylene torch tests of Si-20Cr-20Fe coated Cb752 were performed at temperatures of 2900, 2950, and 3000°F. These results are given in Table XVIII. Included in this table are similar results for the Si-20Cr-5Ti coating on D43 which shows this latter system to have somewhat better protectiveness in this temperature range.

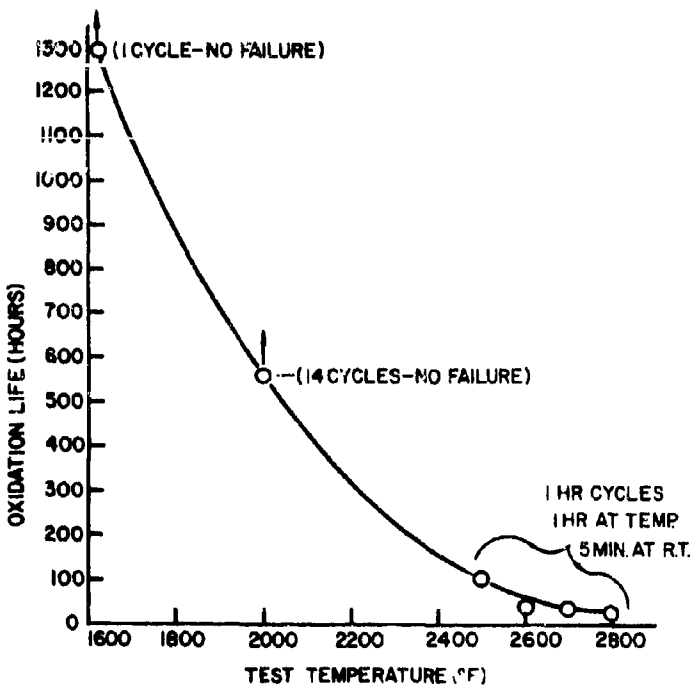

Figure 55 Furnace Oxidation Life vs. Test Temperature (Si-20Cr-20Fe Coated Cb752).

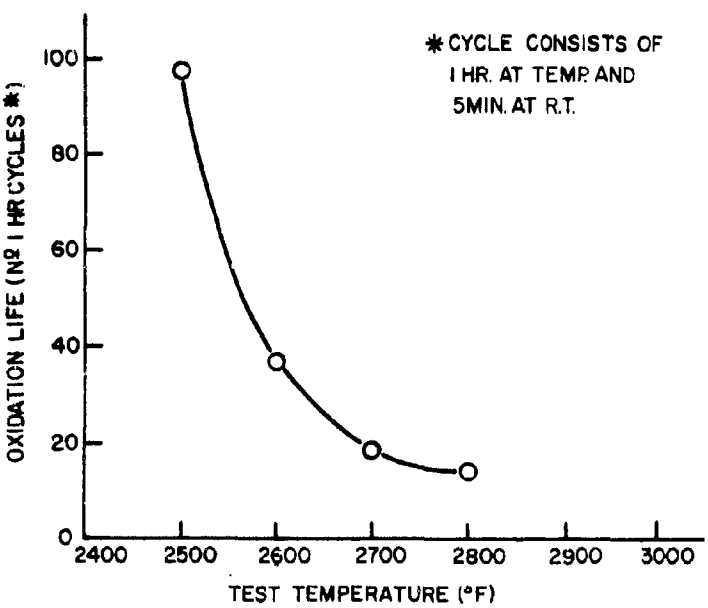

Figure 56 Furnace Oxidation Life vs. Test Temperature (Si-20Cr-20Fe Coated Cb752).

TABLE XVIII

TORCH TESTS OF FUSED SILICIDE COATED Cb752 AND D43

Base Alloy	Coating Comp.	Temp. (°F)*	Time (hrs)	Cycles	Remarks
D43	Si-20Cr-5Ti	3000	1.0	4	No failure
D43	Si-20Cr-5Ti	3100	1.5	6	No failure
D43	Si-20Cr-5Ti	3200	0.1	1	Burn thru
Cb752	Si-20Cr-20Fe	2900	1.25	5	Burn thru
Cb752	Si-20Cr-20Fe	2950	1.00	4	Burn thru
Cb752	Si-20Cr-20Fe	3000	0.50	2	Burn thru

*True brightness temperature.

Some slow cycle oxidation test results cited in an earlier paragraph which indicated that fused silicide coating fired in a one atmosphere inert argon had superior protectiveness to identical coatings fired in vacuum.

A comparison of the oxidation protectiveness of argon-fired and vacuum-fired Si-20Cr-20Fe coatings on D43 alloy was therefore undertaken. Oxidation test evaluation consisted of cyclic furnace tests at 1600, 1800, 2000, 2300, 2400, and 2500°F plus slow cyclic oxidation. The specimens were weighed after 1, 2, 4, 8, 24, 50 and 100 hours. The tests were continued for 595 hours or to failure with the results as shown in Table XIX.

TABLE XIX

FURNACE OXIDATION LIFE OF VACUUM AND ARGON FIRED Si-20Cr-20Fe COATED D43

Test Temp. (°F)	Oxidation Life (Hours)	
	Vacuum Fired	Argon Fired
1600	595^{+} (16)*	595^{+} (16)
1800	595^{+} (16)	595^{+} (16)
2000	595^{+} (16)	595^{+} (16)
2300	189^{e} (8)	189^{e} (8)
2400	100^{e} (7)	189^{e} (8)
2500	120^{e} (8)	189^{s} (8)
800-2500-800 (slow cyclic)	96^{e}	120^{e}

* No. of cycles given in parentheses.
+ Indicates test still in progress.
e Edge Failure.
s Spot Failure.

At the three lower temperatures there were no specimen failures and the tests were discontinued after 595 hours. The argon fired samples did exhibit longer lives at 2400, 2500, and in the slow cyclic test. The argon fired specimens also exhibited lower weight gains at all temperatures. They also did not exhibit the yellow dusting oxide that is characteristic of the vacuum fired coating of this composition.

i. Arc Plasma Tests

The simulated, leading-edge, test specimens fabricated of Cb-752 were furnished by the Air Force. These specimens were fused-silicide coated and sent to Space General Corporation for arc plasma tests under their contract AF 33(615)-5235 with AFML.

In view of past difficulties encountered with the Si-20Cr-5Ti composition on Cb-752 alloy, it was decided to apply this composition to five of the specimens, and the Si-20Cr-20Fe composition to the remainder, since it had been demonstrated that this latter composition reacts normally with this alloy. Figure 57 shows a three-quarter view of a Si-20Cr-20Fe coated specimen. Figures 58 and 59, respectively, show enlarged views of the surfaces of Si-20Cr-20Fe and Si-20Cr-5Ti coated specimens. Although it had previously been observed on several occasions that the Si-20Cr-5Ti coating reacts nonuniformly with Cb752, the pattern of nonuniformity shown in Figure 59 had not been observed before. Invariably the specimen or part had reacted in a "uniformly" nonuniform manner. Since it had been determined than chemical removal of a thin layer of surface alloy appeared to ameliorate this abnormal reaction, the ten specimens were acid-pickled to remove approximately 0.0005 inch of surface material. It is possible that removal of a somewhat thicker layer of material might have yielded more desirable results. One sample of each coating was tested at Space General at surface temperatures of 2600, 2700, and 2800°F (true brightness temperature) for four 15-minute cycles or to failure. These results compare favorably with all other coated columbium alloys similarly tested. The remaining samples were used to determine maximum temperature capabilities in the arc plasma. The test data and results are summarized in Table XX. Photographs of all the specimens, except those used for melting point determinations, are shown in Figure 60 and 61. A more detailed description of the test will be found in the appropriate progress reports from Space General covering their above-referenced contract.

j. Base Alloy Effects.

It was observed that the Si-20Cr-5Ti coating did not coat the Cb752 alloy as uniformly as it did the D43 alloy which it so closely resembles chemically. On Cb-752, the surfaces of this coating are not as smooth and the edge coverage is not as good as that obtained with the same coating on D-43. Also, it was observed microscopically that the coating-substrate interface is very irregular, whereas on most other alloys it is quite planar. This behavior is apparently characteristics of the alloy since it has been observed on several heats from two sources (Union Carbide and Fansteel). Faster heating and higher diffusion temperatures improve these conditions to some extent, but do not completely correct the situation.

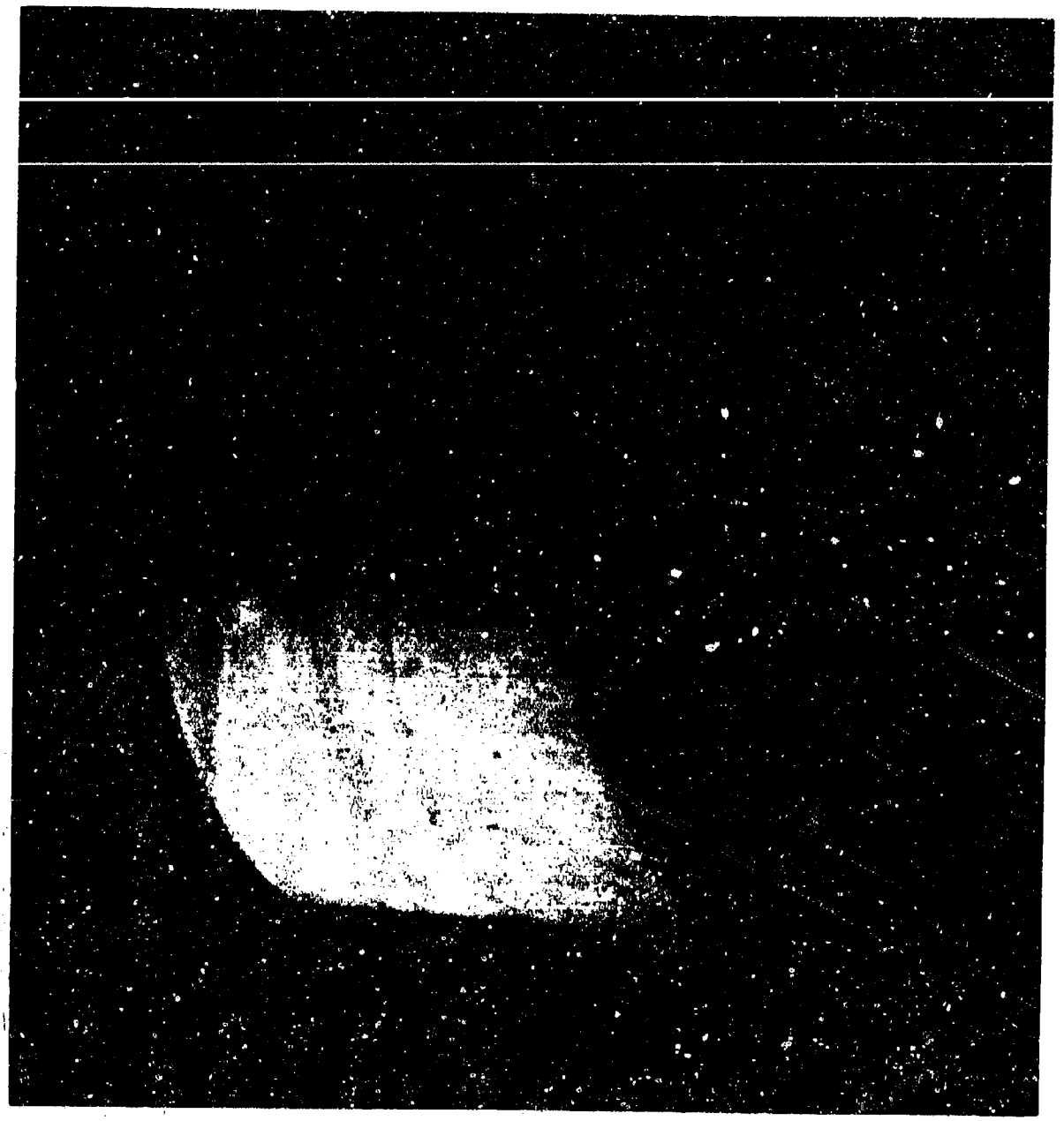

Figure 57 Simulated Leading Edge Specimen for Arc Plasma Test. Cb752 Alloy With Si-20Cr-20Fe Fused Silicide Coating.

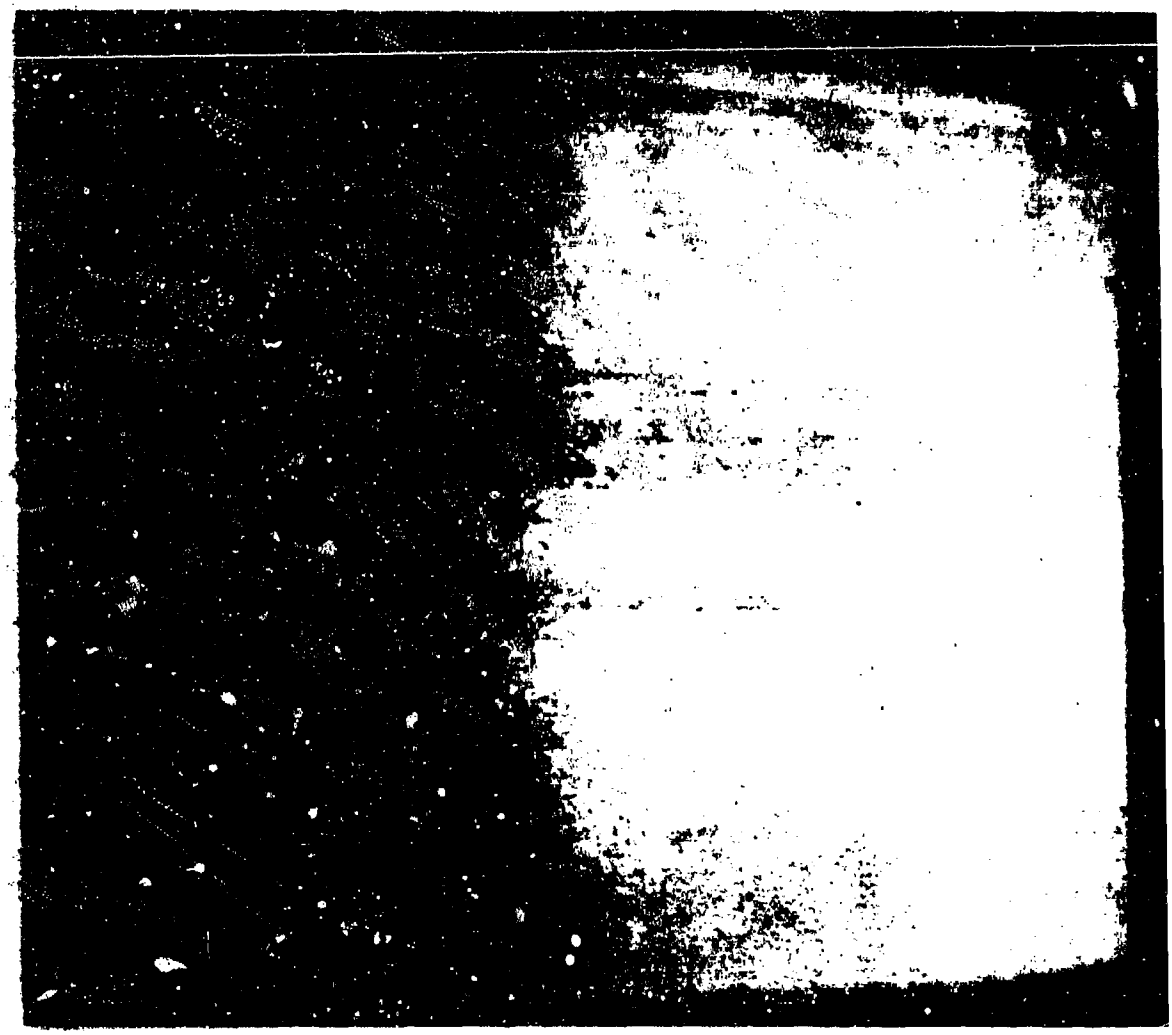

Figure 58 Close-up of Surface of Si-20Cr-20Fe Coated Cb752 Leading Edge Specimens.

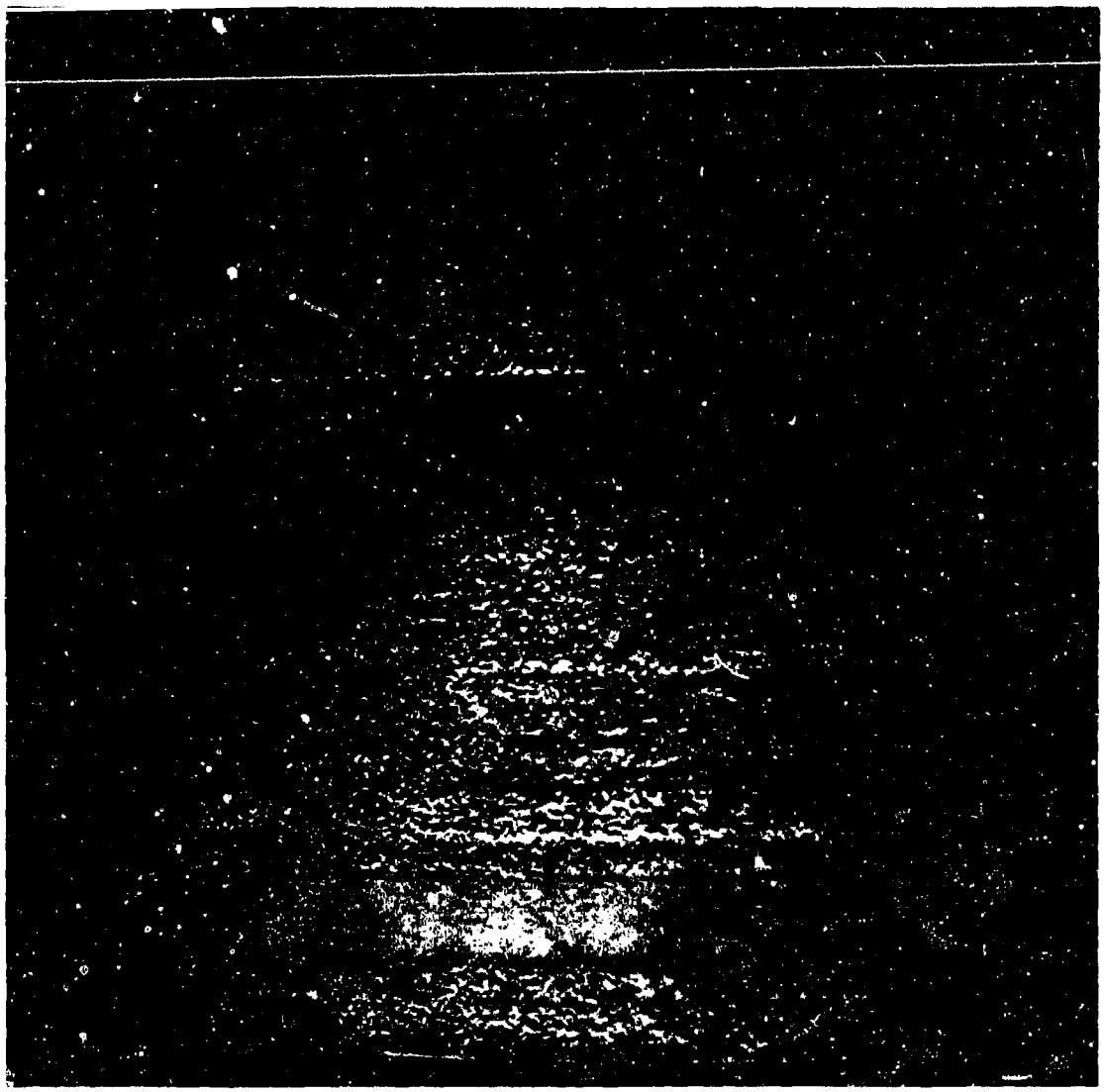

Figure 59 Close-Up of Surface of Si-20Cr-5Ti Coated Cb752 Leading Edge Specimen.

TABLE XX

TEST DATA AND RESULTS OF ARC PLASMA TESTS AT SPACE GENERAL

Model No.	Coating Composition	Temp. (°F)	Gas Enthalpy (Btu/lb)	Model Stagnation Pressure (torr)	Btu/ft^2/sec	Static Pressure (torr)	Test Duration and Comments
3-3	Si-20Cr-20Fe	Increased to 3210	8695	8.0	70.8	0.70	Melting occurred when surface temp. reached 3210°F
3-4	Si-20Cr-20Fe	Increased to 3210	9025	8.0	71.2	0.70	Melting occurred when surface temp. reached 3210°F
3-5	Si-20Cr-20Fe	Increased to 2600	6485	5.8	34.9	0.57	Model withstood four 15-min. cycles at 2600°F
3-6	Si-20Cr-20Fe	Increased to 2700	7510	6.1	41.2	0.60	Model withstood four 15-min. cycles at 2700°F
3-7	Si-20Cr-20Fe	Increased to 2800	8155	7.0	46.1	0.69	Model withstood three 15-min. cycles at 2800°F melting at 540 secs in 4th cycle
3-8	Si-20Cr-5Ti	Increased to 3100	8720	7.7	64.5	0.76	Melting occurred when surface temp. reached 3100°F
3-9	Si-20Cr-5Ti	Increased to 2600	6685	5.8	35.1	0.57	Model withstood four 15-min. cycles at 2600°F
3-10	Si-20Cr-5Ti	Increased to 2700	7565	6.0	40.9	0.59	Model withstood four 15-min. cycles at 2700°F
3-11	Si-20Cr-5Ti	Increased to 2800	6285	7.0	45.8	0.69	Model withstood two 15-min. cycles at 2800°F, melting at 840 secs in third cycle
3-12	Si-20Cr-5Ti	Increased to 3000	8655	7.7	58.7	0.75	Melting at 3000°F

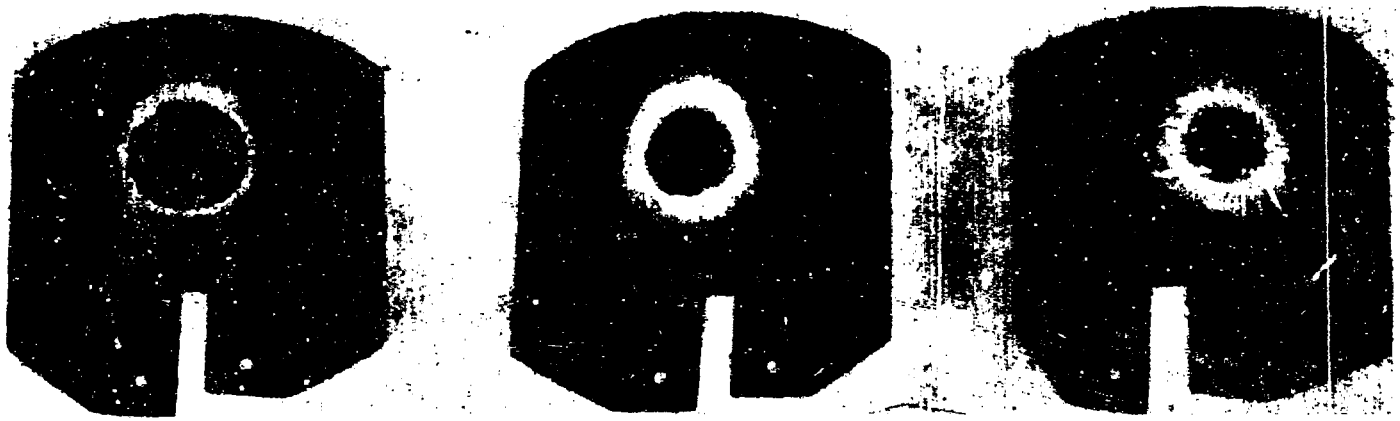

MODEL 3-11	MODEL 3-10	MODEL 3-9
Cb752 - R512A (Si-20Cr-5Ti)	Cb752 - R512A (Si-20Cr-5Ti)	Cb752 - R512A (Si-20Cr-5Ti)
SURFACE TEMP - 2800°F (true brightness temp)	SURFACE TEMP - 2700°F (true brightness temp)	SURFACE TEMP - 2600°F (true brightness temp)
NOZZLE STATIC PRESSURE - 0.7 torr	NOZZLE STATIC PRESSURE - 0.6 torr	NOZZLE STATIC PRESSURE - 0.6 torr
MODEL STAG. PRESSURE - 7.0 torr	MODEL STAG. PRESSURE - 6.0 torr	MODEL STAG. PRESSURE - 5.8 torr
HEAT FLUX (Btu/ft^2-sec) - 45.8	HEAT FLUX (Btu/ft^2-sec) - 40.9	HEAT FLUX (Btu/ft^2-sec) - 35.1
TEST DURATION - 2-15 min cycles + 14 min	TEST DURATION - 4-15 min cycles	TEST DURATION - 4-15 min cycles

Figure 60 Photograph of Si-20Cr-5Ti Coated Cb752 Leading Edge Specimens After Arc Plasma Testing.

MODEL 3-5	MODEL 3-6	MODEL 3-7
Cb752 - R512E (Si-20Cr-20Fe)	Cb752 - R512E (Si-20Cr-20Fe)	Cb752 - R512E (Si-20Cr-20Fe)
SURFACE TEMP - 2600°F (true brightness temp)	SURFACE TEMP - 2700°F (true brightness temp)	SURFACE TEMP - 2800°F (true brightness temp)
NOZZLE STATIC PRESSURE - 0.6 torr	NOZZLE STATIC PRESSURE - 0.6 torr	NOZZLE STATIC PRESSURE - 0.7 torr
MODEL STAG. PRESSURE - 5.8 torr	MODEL STAG. PRESSURE - 6.1 torr	MODEL STAG. PRESSURE - 7.0 torr
HEAT FLUX (Btu/ft^2-sec) - 34.9	HEAT FLUX (Btu/ft^2-sec) - 41.2	HEAT FLUX (Btu/ft^2-sec) - 46.1
TEST DURATION - 4-15 min cycles	TEST DURATION - 4-15 min cycles	TEST DURATION - 3-15 min cycles + 9 min

Figure 61 Photograph of Si-20Cr-20Fe Coated Cb752 Leading Edge Specimens After Arc Plasma Testing.

It is not known to what extent, if any, the protectiveness of the Si-20Cr-5Ti coating on Cb-752 is adversely affected by these nonuniformities. However, since tests performed by Lockheed (4) yielded more than satisfactory results, with the fused silicide coating clearly superior to other coatings applied to this material, the problem is not as serious as it might appear. Nonetheless, since Cb-752 is one of the more popular present-day columbium alloys, it was concluded that some effort should be directed toward determining the cause of this unusual behavior, and toward the development of corrective procedures, if possible.

Slight modifications in coating composition (Si-20Cr, Si-25Cr, Si-30Cr) and several diffusion temperatures from 2400 to 2620°F were studied, as were variations in heating rates. No significant differences were noted as a result of the compositional modifications. Marginal improvement resulted from faster heating rates and higher diffusion temperatures.

Electron microprobe analyses of Si-20Cr-5Ti coated Cb-752 were also negative. Tungsten and zirconium x-ray scans were made of Cb-752 and D-43 and showed both alloys to be chemically homogeneous. Tungsten, zirconium, and silicon x-ray scans of Si-20Cr-5Ti coated Cb-752 were made in several abnormal areas in and below the coating; no gross chemical inhomogeneities were revealed.

X-ray diffraction analyses of both alloys showed the grains of Cb-752 to be strongly oriented in the (200) and (211) directions, while the grain structure of D-43 alloy was randomly oriented. In addition, it was noted metallographically that the Cb-752 has a highly textured structure indicative of a highly cold-worked metal.

Removal of surface metal from Cb-752 by chemical dissolution appreciably improved the uniformity of subsequently applied Si-20Cr-5Ti fused silicides. Removal of one mil appears to be sufficient to achieve this improvement. Removal of more material did not effect any further improvement.

The Si-20Cr-20Fe and Si-20Cr-20Fe-10VSi_2 coatings were also applied to Cb-752, and microstructurally, it was observed that both result in much more uniform coatings on this alloy than the Si-20Cr-5Ti composition. The Si-20Cr-20Fe coating in particular appears to result in a smooth interface as well as a relatively smooth surface.

Figure 62 shows the microstructures of the Si-20Cr-5Ti coating on both D-43 and Cb-752. This coating is quite uniform on D-43 alloy but very irregular on Cb-752. The degree of irregularity varies to a great extent from sample to sample and batch to batch as evidenced by the two examples shown, but is always manifestly present. It will also be noticed that the inner zone of this coating on Cb-752 etches much darker than the corresponding area of this coating on the D-43. The significance of this observation, if any, is not known.

Figure 63 shows the microstructure of the Si-20Cr-20Fe coating on the same two alloys. Clearly this coating reacts very uniformly with both alloys.

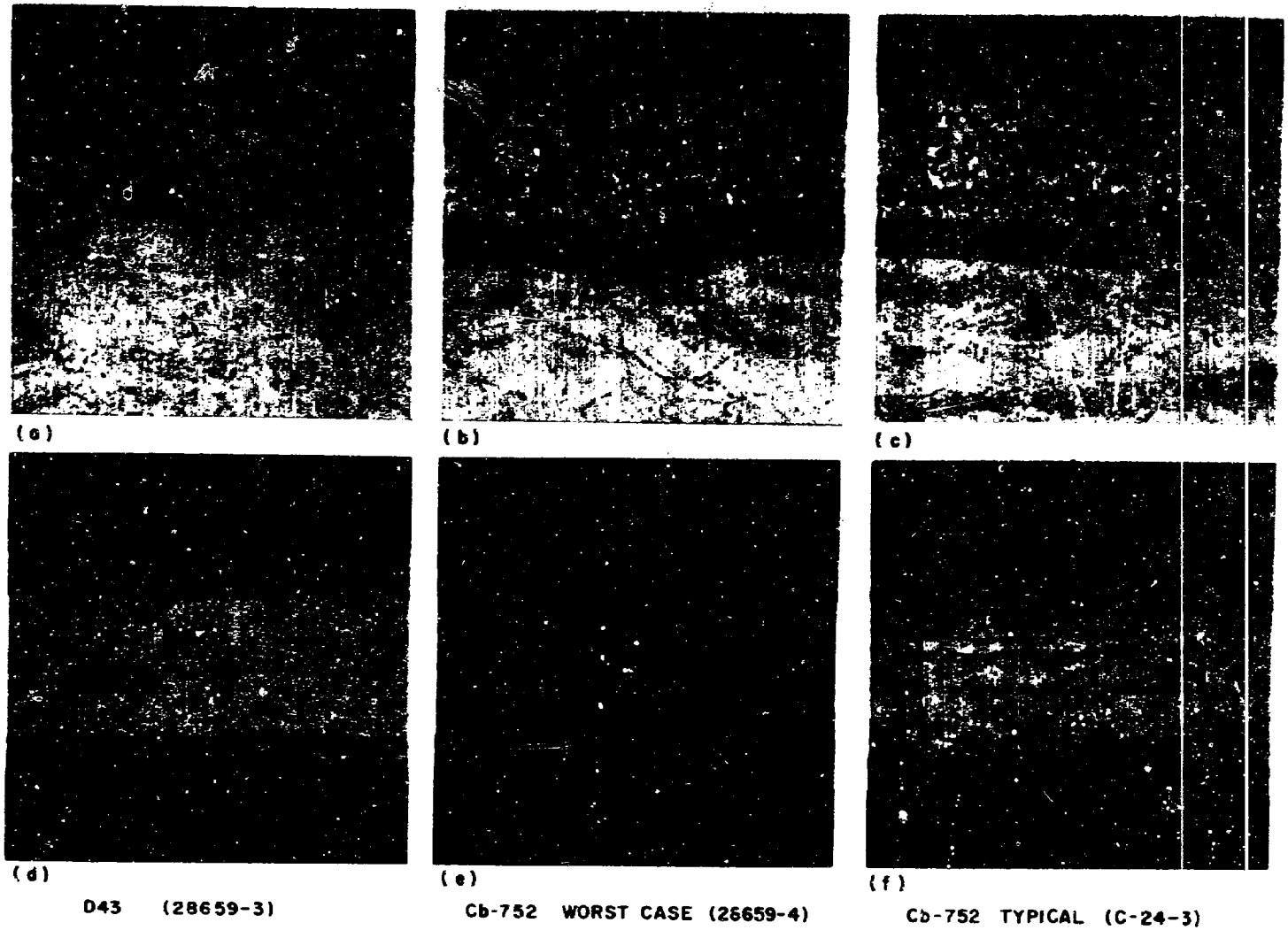

Figure 62 Microstructures of Si-20Cr-5Ti Coating on Cb752 and D43. Top Row 300X. Bottom Row 100X.

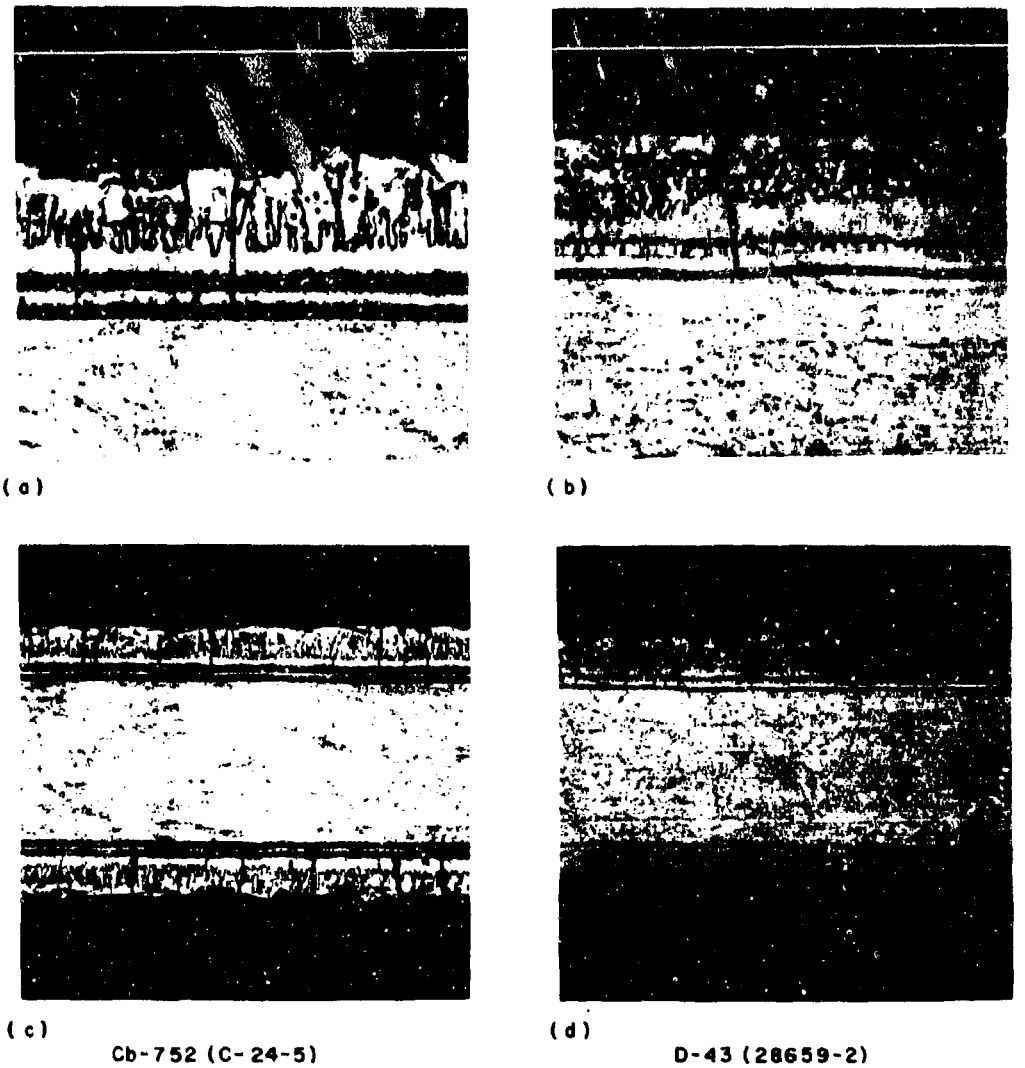

Figure 63 Microstructures of Si-20Cr-20Fe Coatings on Cb752 and D43. Top Row 300X. Bottom Row 100X.

The protectiveness of the fused silicide coatings to a selected group of alloys not previously investigated was determined by means of several screening tests. A nominal three-mil-thick coating (20 to 25 mg/cm^2) was applied in each case. The alloys and coating compositions investigated and the test results are given in Table XXI. The B66 and SU-16 are sheet alloys and were given screening tests believed to be more indicative of their merit for reentry applications. Both alloys developed somewhat better protectiveness in combination with the Si-20Cr-5Ti coating than the D43 and Cb-752 alloys which have been the standard alloys used in this program to date.

The XB88 and Cb-132M are very high strength alloys which are candidates for turbine blade applications. Consequently these coated alloys were given slightly different screening tests. The protectiveness of these coatings is quite good, particularly with respect to slow-cyclic oxidation resistance.

Photomicrographs of the selected columbium alloy-fused silicide systems in the as-coated and tested conditions are shown in Figures 64 through 67.

TABLE XXI

OXIDATION TEST DATA OF FUSED SILICIDE COATINGS APPLIED TO VARIOUS ALLOYS

Substrate Alloy	Coating Composition	Slow-Cyclic Oxidation Life (No. 1-Hour Cycles to Failure)	High-Temperature Cyclic Life (No. of 1-Hour Cycles From Temperature Indicated to Room Temperature)			
			2400	2600	2700	2800
B66	Si-20Cr-5Ti	29^e, 29^e	--	10$^+$, 10$^+$	10$^+$, 10$^+$	10$^+$, 10$^+$
SU16	Si-20Cr-5Ti	45^e, 45^e	--	10$^+$, 10$^+$	--	--
XB88	Si-20Cr-5Ti	10^e	80^e	--	--	--
XB88	Si-20Cr-5V	79^e, 83^e	118^e, 84^e	--	--	--
Cb132M	Si-20Cr-5Ti	112^e, 175^e	80^e, 90^e	--	--	--
Cb132M	Si-20Cr-5V	177^s, 177^s	113^e, 94^e	--	--	--

$^+$ Test stopped, sample not failed.

^{e} Edge failure.

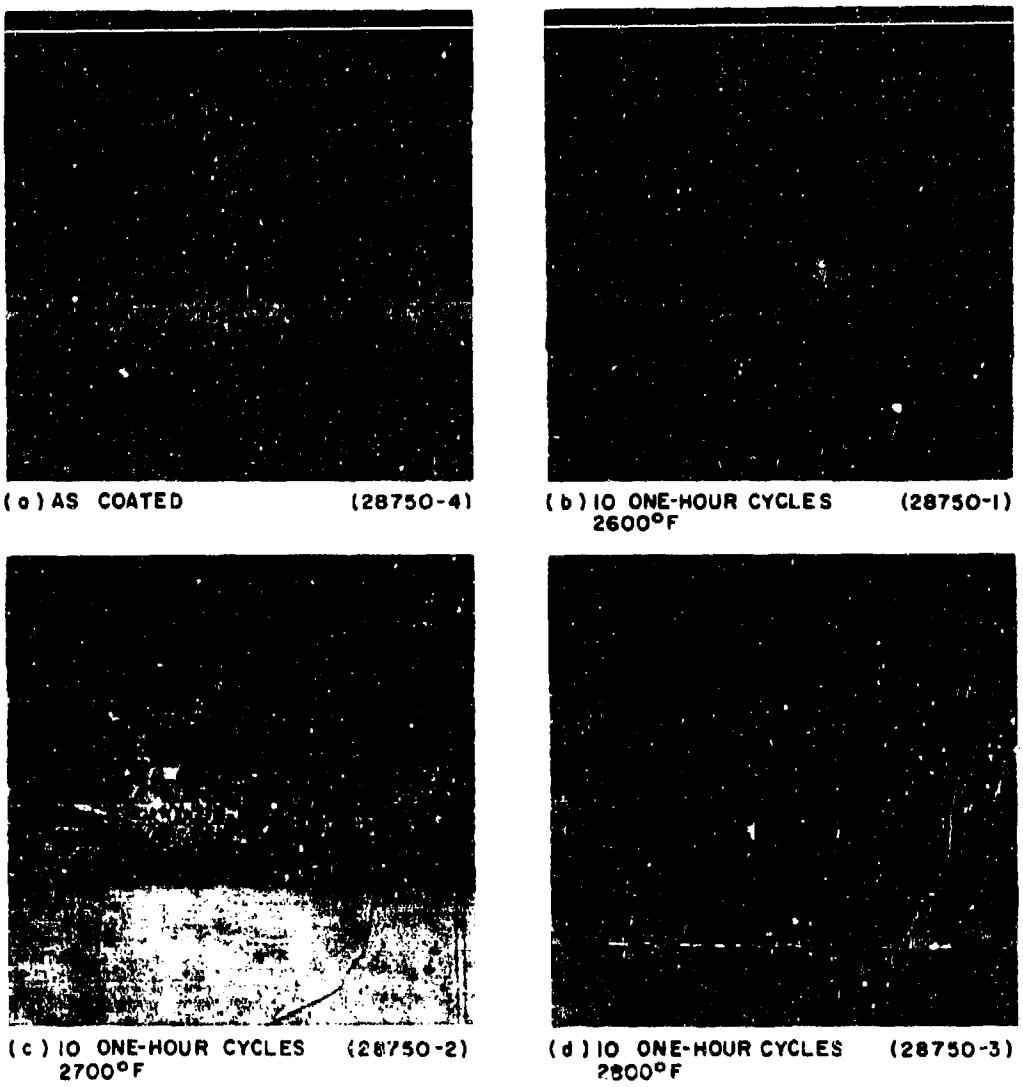

Figure 64 Photomicrographs of Si-20Cr-5Ti Coated B66 Alloy in Various Conditions (300X).

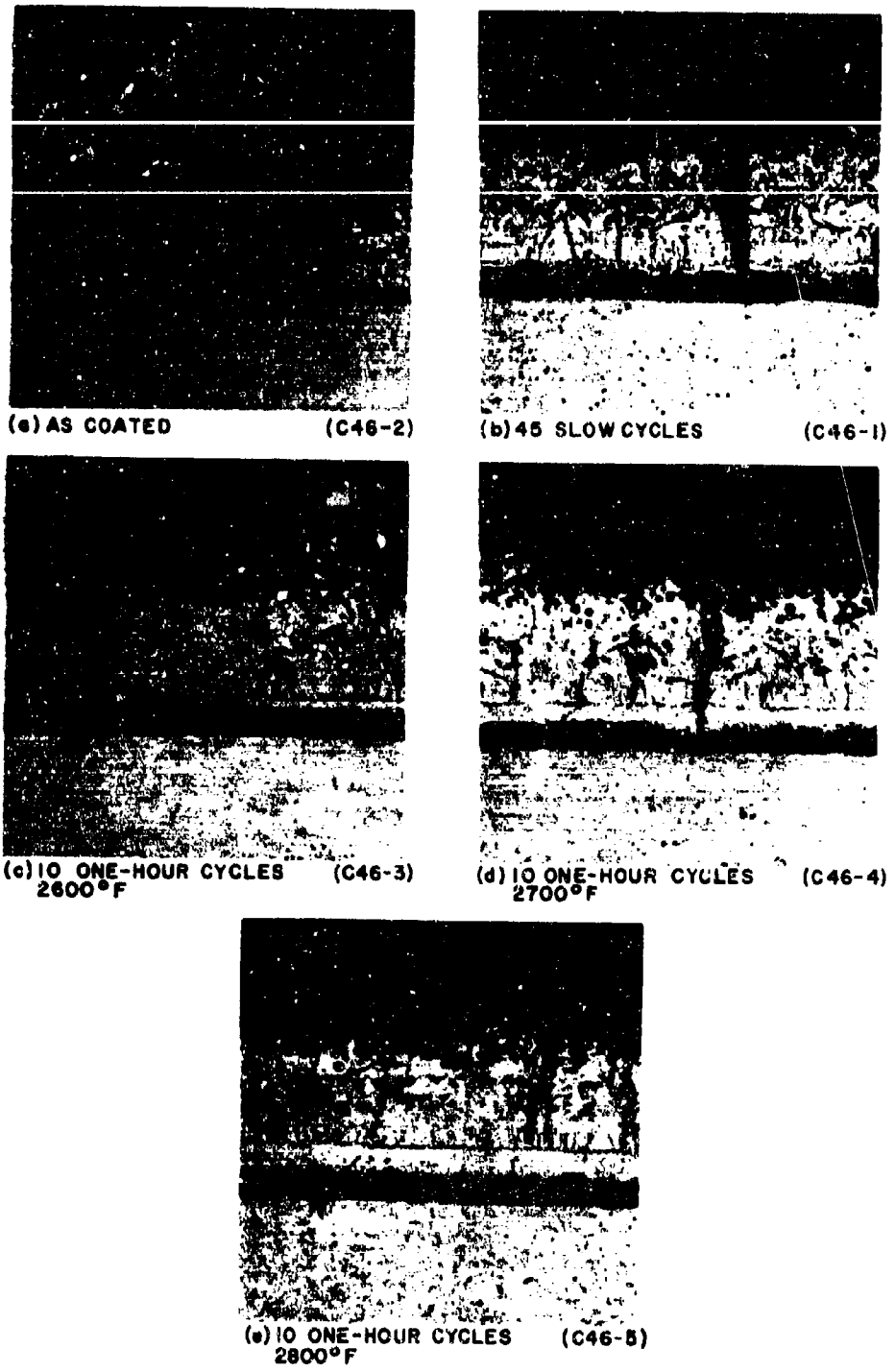

Figure 65 Photomicrographs of Si-20Cr-5Ti Coated Su-16 Alloy in Various Conditions (300X).

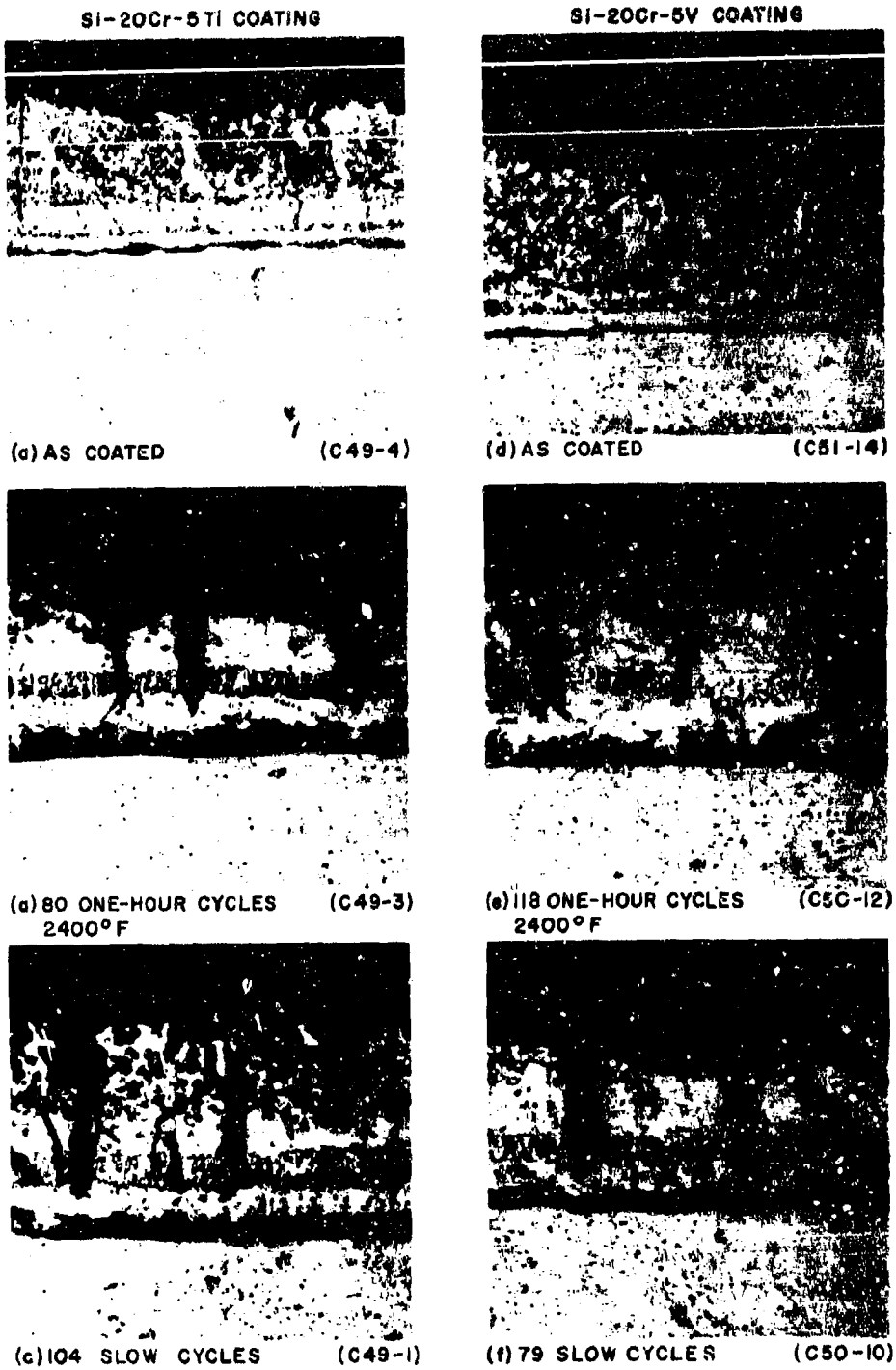

Figure 66 Photomicrographs of Fused Silicide Coated XB88 in Various Conditions (300X).

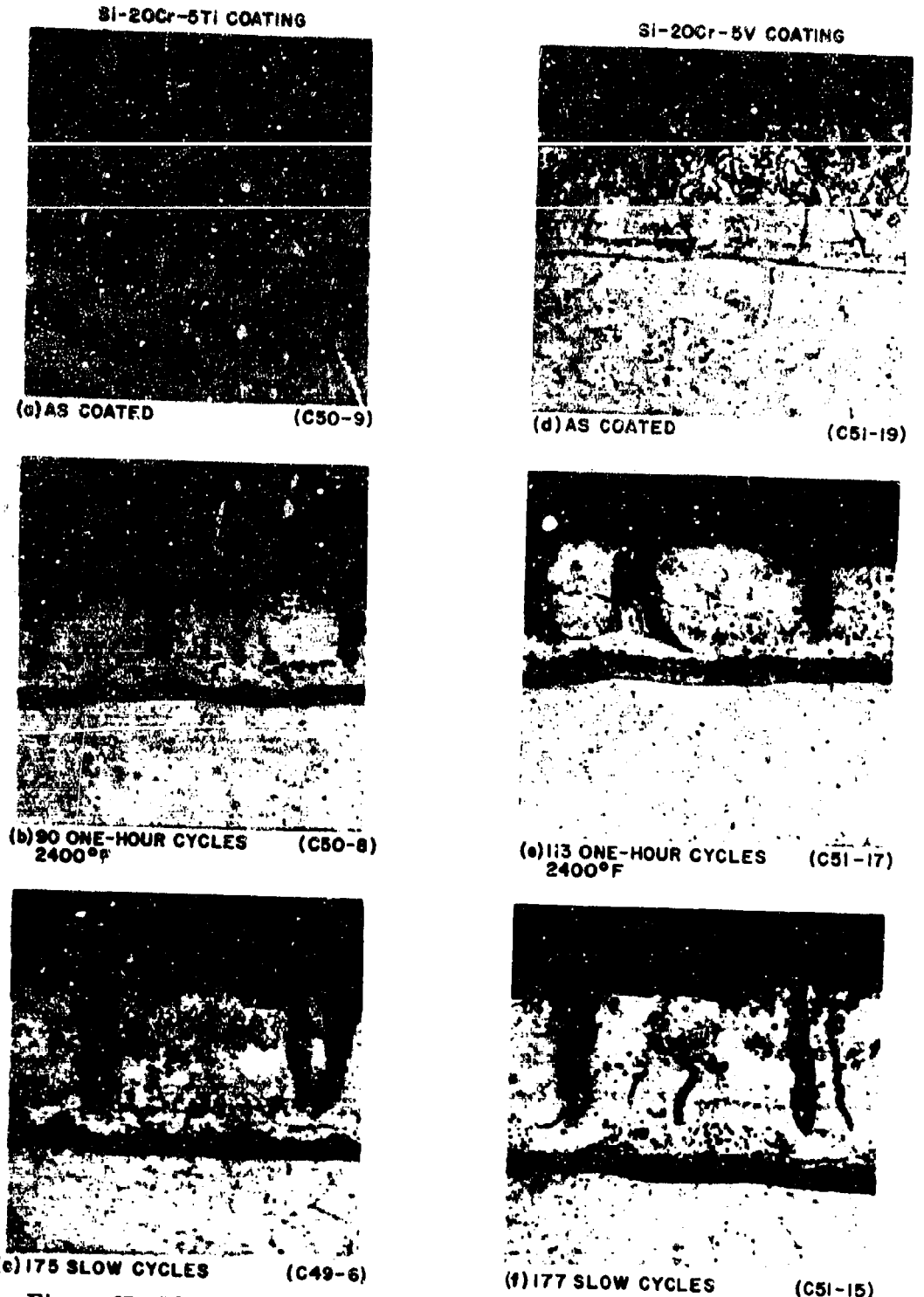

Figure 67 Photomicrographs of Fused Silicide Coated Cb132M in Various Conditions (300X).

k. Analysis of Coating Formation

An analysis of the mechanism of formation of the fused silicide coating was undertaken in an effort to determine the sequence of events involved, as an aid to further development efforts. For this study the Si-20Cr-5Ti slurry composition was applied to D-43 alloys, and the samples were given various diffusion heat treatments from five minutes to four hours, and from 2300 to 2620°F. Photomicrographs of these samples are shown in Figure 68.

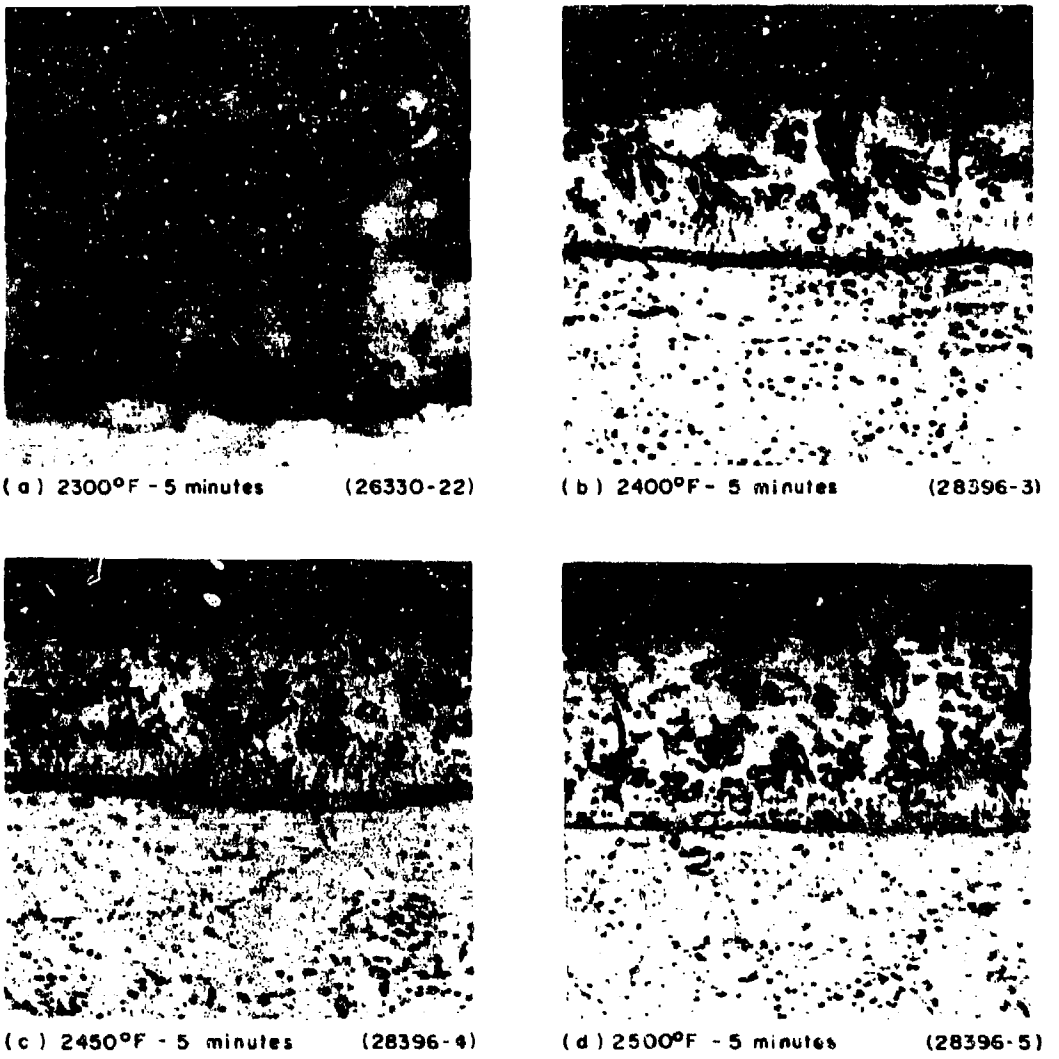

Figure 68 Formation of Si-20Cr-5Ti Fused Silicide Coating on D43 Showing Effect of Time and Temperature (500X).

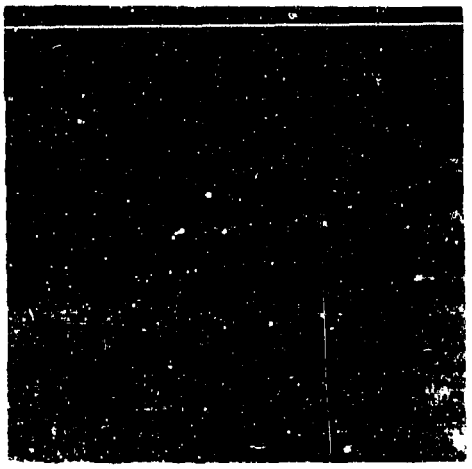

(e) 2580°F - 5 minutes (28396-6)

(f) 2620°F - 1 hour (28396-11)

(g) 2500°F - 1 hour (28396-7)

(h) 2500°F - 4 hours (28396-8)

Figure 68----Continued

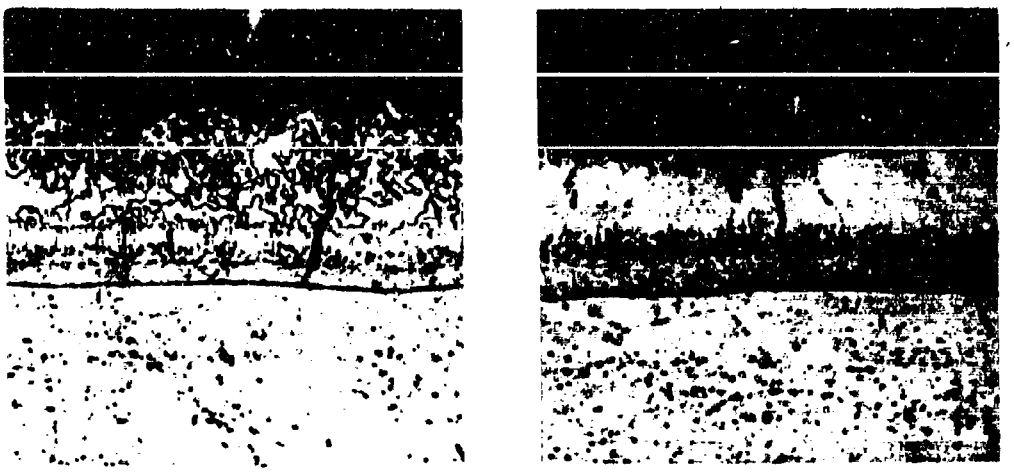

(i) 2580°F - 1 hour (28396-9) (j) 2580°F - 4 hours (28396-10)

Figure 68---Concluded

At 2300°F, fusion of the coating had not yet occurred, but a slight reaction is evident between the coating components themselves as well as between the coating and the columbium alloy substrate. All of the other heat treatments resulted in complete fusion of the coating and reaction with the base to form solid intermetallic coatings. As the temperature and/or time are increased, the amount of second phase in the outer coating layer also increases. The thickness of the inner subsilicide layer is proportional to the diffusion temperature and time, as would be expected. At the longer times and higher temperatures the "second phase" appears to have become the major phase.

The results of x-ray diffraction analyses performed on these samples are given in Table XXII. In the coatings heat treated for five minutes the main and only phase detected was MSi_2. The concentration of the second phase close to the surface was apparently not sufficient to be detected in these samples. In the coatings heat treated for one and four hours, both MSi_2 and M_5Si_3 were detected, and in the four-hour samples, M_5Si_3 was the major phase. The four-hour, 2500°F heat treatment coating is primarily M_5Si_3. No MSi_2 was detected in this sample, and the structure appears single-phased. After approximately one mil of the coating was ground from the four-hour samples, MSi_2 was analyzed as the major phase and tetragonal M_5Si_3 as the second phase.

A study of the fusion-diffusion temperature requirements of the Si-20Cr-20Fe coating was also undertaken. The initial goals were to determine the fusion temperature and to observe the variations in structure resulting from different firing temperatures. Coated specimens were fired at 2200, 2300, 2400, 2500, and 2650°F for 15 minutes. The microstructures of these specimens are shown in Figure 69. The 2200°F specimen does not appear to have fused completely. At 2300 and 2400°F,

although complete fusion has obviously taken place, the structure has not formed to the normal extent, and the coating surface is not as smooth as usual. This may be the result of more rapid freezing at these lower treatment temperatures. At the higher temperatures the structure is better defined, and the surfaces are considerably smoother. On the basis of these observations alone it appears that firing temperatures above 2500°F are desirable.

TABLE XXII

SUMMARY OF X-RAY DIFFRACTION ANALYSIS OF Si-20Cr-5Ti FUSED SILICIDE COATING ON D43 SHOWING EFFECT OF VARIATIONS IN DIFFUSION TREATMENT

Fig. No.	Diffusion Treatment	MSi_2	M_5Si_3 (hex)	M_5Si_3 (tetragonal)
24a	2300°F - 5 min		Not Analyzed	---
b	2400°F - 5 min	X	---	---
c	2450°F - 5 min	X	---	---
d	2500°F - 5 min	X	---	---
e	2580°F - 5 min	X	---	---
f	2620°F - 1 hr	X	x	---
g	2500°F - 1 hr	X	x	---
h	2500°F - 4 hr	x	X	---
h*	2500°F - 4 hr	X	---	x
i	2580°F - 1 hr	X	x	---
j	2580°F - 4 hr	---	X	---
j*	2580°F - 4 hr	X	---	x

* 1 mil removed from surface
X strongest phase
x secondary phase
--- not detected

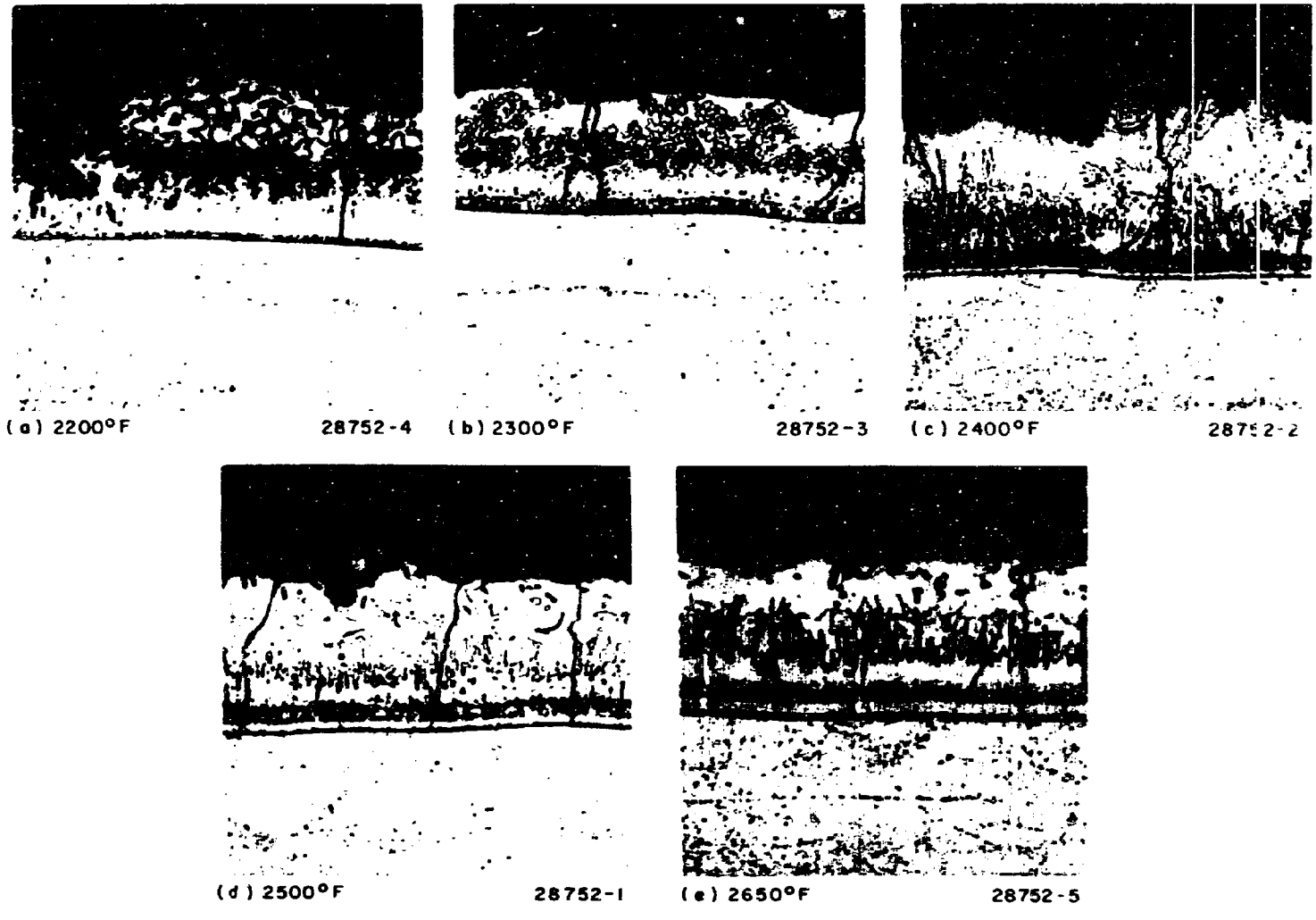

Figure 69 Photomicrographs of Si-20Cr-20Fe Coatings on D43 Fired at Temperatures Indicated for 15 Minutes (300X).

In paragraph 1 which follows, it is reported that as-coated Si-20Cr-5Ti-10Fe-10VSi_2 coatings on D-43 analyzed by x-ray diffraction yielded M_5Si_3 as the principal phase of the outer coating layer. However, from metallographic observations, it is obvious that this outer layer is still two-phased. Electron microprobe analyses identified the minor (matrix) phase as $CbSi_2$.

The incentive to produce M_5Si_3 type of coatings lies in the lower thermal expansion coefficient of this compound and the increased stability of this coating both with columbium substrates and in low-pressure environments. Although most coatings having basically this structure are not oxidation resistant in the intermediate to low-temperature range, the basic protectiveness of the complex fused silicide and its essentially M_5Si_3 makeup was sufficiently promising to warrant a minor effort directed at the production of single-phased M_5Si_3 coatings in this system. The Si-20Cr-20Fe-10VSi_2 composition was used for these experiments. Work to date has consisted primarily of a heat treatment and metallographic study. Coatings of this composition were vacuum-diffusion heat treated under six different conditions. Photomicrographs of each specimen, shown in Figure 70, indicate that only the 2580°F, four-hour diffusion treatment resulted in a coating with a single-phased outer layer.

1. X-Ray Diffraction and Electron Microbeam Probe Analyses

(1) Analysis of Coatings in the Si-Cr-Ti-Fe-V System

Some of the early work on the program had indicated that the highly complex Si-20Cr-5Ti-10Fe-10VSi_2 fused silicide coating system offered improved all-around oxidation protectiveness. An analytical study was therefore undertaken with the aim of characterizing this coating and shedding some light on the reasons for the improved protectiveness of this system.

A number of D-43 alloy coupons were coated and exposed in air according to the following schedule:

Temp. (°F)	Time (hours)
1000	100
1600	100
2000	100
2500	50
2800	10
3000	10 min
800-2500-800 (slow cycle)	10

All coupons were heat treated in furnaces except for the one at 3000°F which was torch heated.

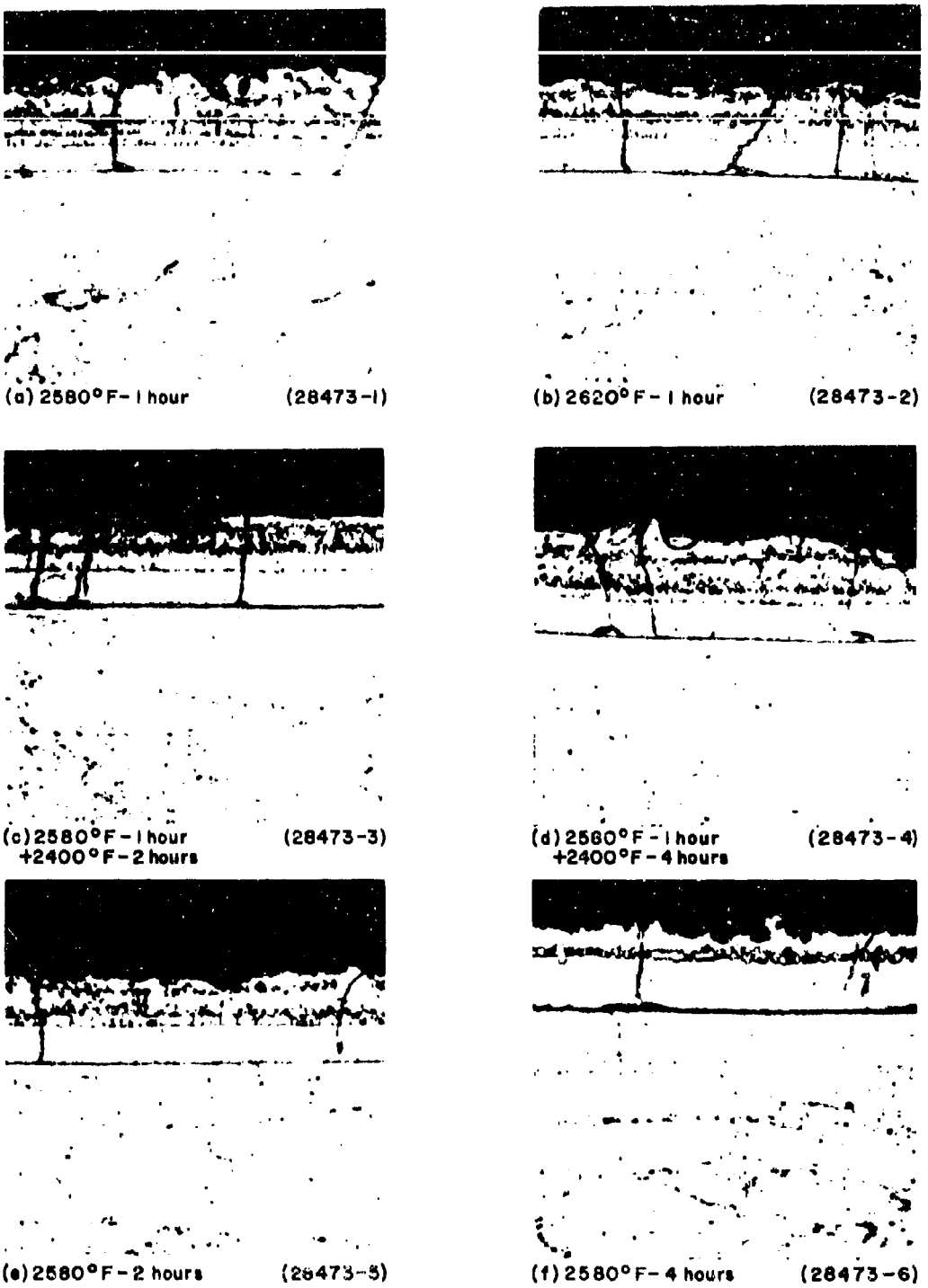

Figure 70 Photomicrographs (300X) of Si-20Cr-20Fe-10VSi_2 Coating on D43 Given Various Vacuum-Diffusion Heat Treatments.

Photomicrographs of these samples are given in Figure 71. The as-coated sample displays the porous surface typical of this system. The "second phase" component is larger and more plentiful in this system than in the Si-20Cr-5Ti coating. The main outer coating layer appears to retain two phases through most of the exposures, although after ten hours at 2800°F, this layer appears to be single phased. There are three distinct sublayers in most of the samples. The scale in every case is two-phased, and in particular samples, shows a tendency to form in layers. The scale is moderately thick, as has been previously observed, but there does not appear to be any anomalous "pest-type" tendencies. Oxide thickness appears to increase with temperature and time.

The results of x-ray diffraction analysis of the surface of each of these samples are summarized in Table XXIII.

TABLE XXIII

SUMMARY OF RESULTS OF X-RAY DIFFRACTION ANALYSES OF Si-20Cr-5Ti-10Fe-10VSi_2 COATINGS ON D43

Fig. No.	Condition	M_5Si_3 hex	$CrCbO_4$	SiO_2 (α cristobalite)
25a	As Coated	X	---	---
b	1000°F - 100 hrs	X	poss.	---
c	1600°F - 100 hrs	---	X	x
d	2000°F - 100 hrs	---	X	x
e	2500°F - 50 hrs	---	X	x
f	2800°F - 10 hrs	---	X	x
g	3000°F - 10 min	---	X	x

X major phase

x secondary phase

poss possibly present

--- not detected

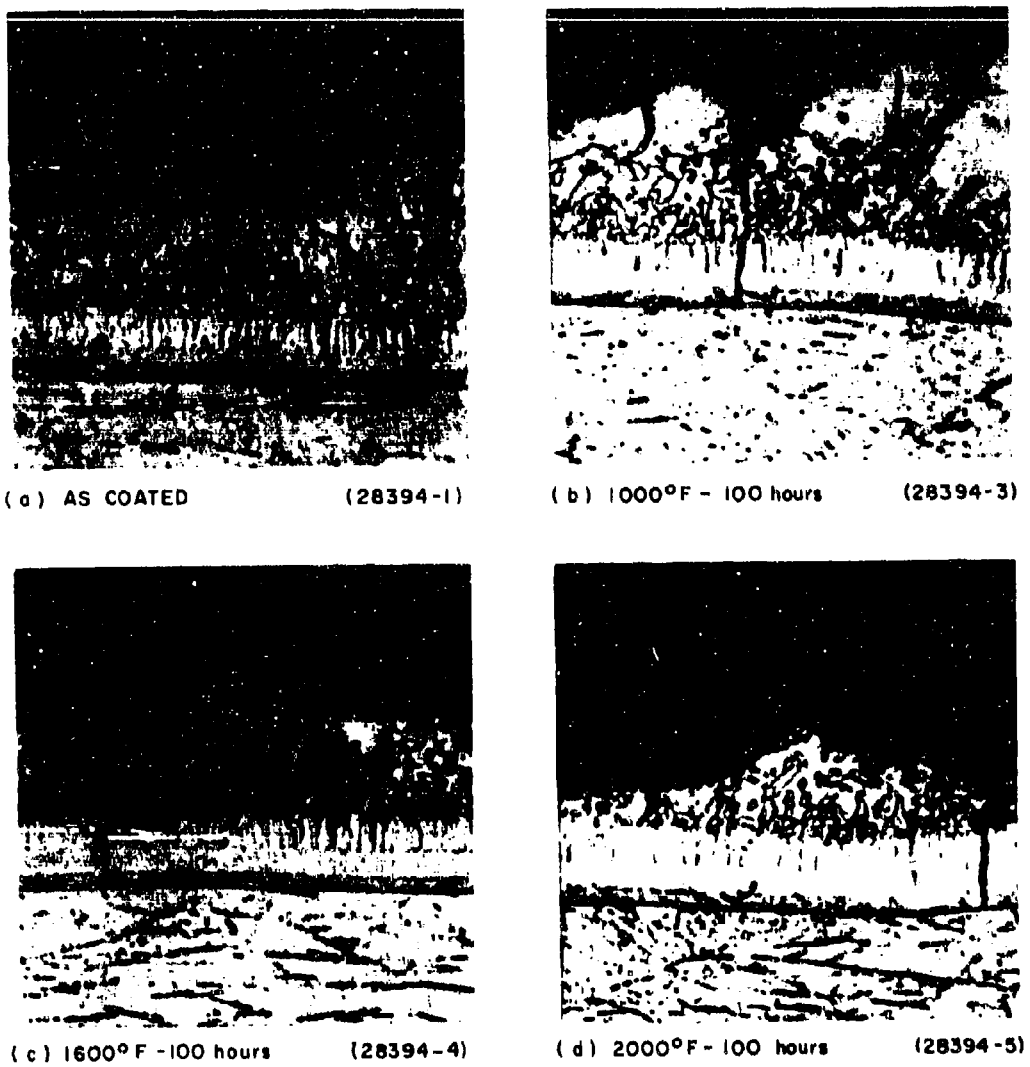

Figure 71 Photomicrographs of Si-20Cr-5Ti-10Fe-10VSi_2 Coating on D43 After Various Oxidation Exposures (500X).

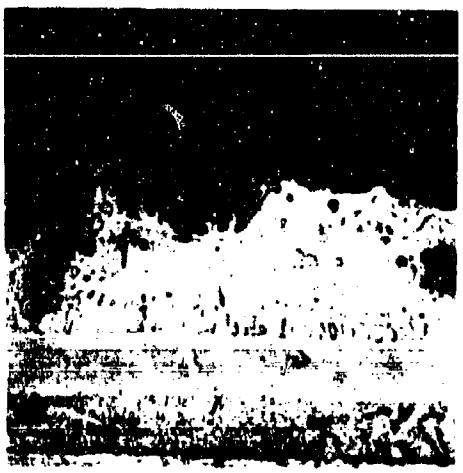

(e) 2500°F - 50 hours (28394-6)

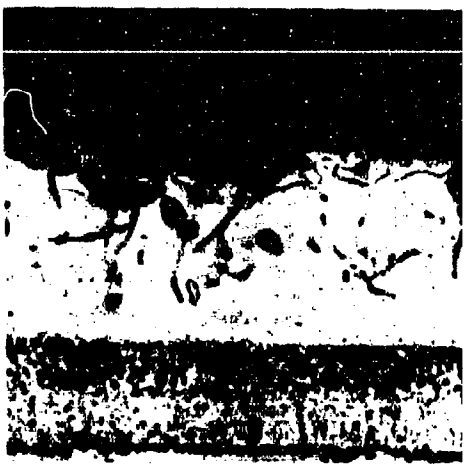

(f) 2800°F - 10 hours (28394-7)

(g) 3000°F - 10 minutes (28394-8)

(h) SLOW CYCLES - 10 hours (28394-2)

Figure 71---Concluded

The major phase present in the coating in the as-coated condition is hexagonal M_5Si_3. The significant point here is that there is apparently a silicide lower than MSi_2 which is oxidation resistant over the whole temperature spectrum. Until now, it had been demonstrated that M_5Si_3 coatings can be very protective at elevated temperatures, but undergo an active-passive oxidation transformation as the temperature is reduced (6). According to the definitions of "active" and "passive" oxidation presented in Reference 6, this coating fits in neither category. In their view, a silicide oxidizes "passively" and protectively if only silica is formed by selective oxidation of the silicon in the compound, and "actively" and nonprotectively if both silica and an oxide of the base metal are formed. However, for the coating under study the oxidation is "passive" in the sense that it is protective, and "active" in the sense that a complex oxide of the substrate metal is formed along with silica. It is significant that no transformation of oxidation modes appears to occur over the 1000 to 3000°F temperature range studied.

It has been reported (5) that Cb_5Si_3 has an expansion coefficient that comes closer to matching that of columbium than does $CbSi_2$, and that both silicide compounds have higher thermal expansions than columbium. Others (7), however, have stated that although Cb_5Si_3 has a lower expansion coefficient than $CbSi_2$, both compounds have lower expansion coefficients than columbium. Therefore Cb_5Si_3 coatings will have lower room-temperature stresses (in tension) than $CbSi_2$ coatings according to Reference 5 or higher room-temperature stresses (in compression) according to Reference 7. Clearly, the data and conclusions of Reference 7 are inconsistent with some generally observed and acknowledged facts. First, it has been observed that every MSi_2 coating in the as-formed condition contains regularly spaced transverse cracks. These cracks could only have resulted from tensile stresses due to the higher expansion coefficient of the coating, and from a compressive stress in the coating. Secondly, if the coating contained transverse cracks, and if the expansion of the substrate were greater than that of the MSi_2 coating, then the cracks would tend to open as the temperature raised; oxidation would then proceed rapidly at the base of these cracks, the cracks would tend to propagate through the substrate, and catastrophic oxidation would soon result. In most actual cases, however, there has been no evidence of oxidation occurring even on the surfaces of the cracks, which would indicate that at elevated temperatures the cracks tend to be closed by the higher expansion of the coating.

A tentative conclusion would be that M_5Si_3 coatings probably have an expansion coefficient between those of MSi_2 and columbium, and M_5Si_3 coatings might therefore be relatively more crack-free and better able to withstand thermal cycling.

After oxidation, with the exception of the 100-hour, 1000°F exposure, the scale is too thick to penetrate and only the oxide phases are detected. At all temperatures both $CrCbO_4$ and SiO_2 (α cristobalite) are detected, with the former yielding the strongest lines.

Selected samples of this group were subsequently analyzed by the electron microbeam probe (EMP) x-ray analyzer in an effort to correlate metallographic

phases with x-ray diffraction results, and to identify deep sublayers probably not reached by the x-ray diffraction beam.

Qualitative EMP x-ray scanning images were first obtained for the as-coated and the 2800°F, ten-hour oxidized sample; the micrographs are shown in Figures 72 and 73. In Figure 72 it can be seen that the Cr and Fe distributions coincide. Also, these elements are found concentrated in the innermost layer, and in the second phase particles in the outer layer. Where the Cr and Fe concentrations are greatest, the silicon concentration is lower. It is significant that the silicon concentration is greatest in the second innermost layer directly above the thin Cr and Fe rich layer.

The x-ray and sample current scans of Figure 73 show that the Cr distribution in the scale coincides with the Cb distribution in the scale, both of which coincide with the islands shown as light areas in the sample current scan or in bright field photomicrographs. This clearly establishes these areas as the $CrCbO_4$ identified by x-ray diffraction. The matrix phase of the scale which shows up dark in current scans and photomicrographs must therefore be the SiO_2 (α cristobalite), the other phase identified by x-ray diffraction techniques.

Quantitative EMP analyses were performed on both the as-coated and the 2800°F, ten-hour oxidized sample. Results are given in Figure 74. The matrix phase in the outer layer appears to be essentially $CbSi_2$ with small amounts of Fe, V, and Ti and about five percent Cr. Since the matrix phase is quite sparse in this coating ($CbSi_2$ was not detected by x-ray diffraction), it is possible that the beam is striking some of the island-like second phase, and this may account for some error in analysis. The islands appear to be what was identified by x-ray diffraction as M_5Si_3 (hex).

The composition is quite far off stoichiometry, but with the appreciable degree of alloying added, the structure could be stable over a wide range of compositions. Layer C is obviously $CbSi_2$ with little if any alloying present, and Layer D is probably Cb_5Si_3 with some Fe and Cr substituted for Cb.

In the oxidized specimen the coating remaining is divided into two layers, both of which appear to be approximately M_5Si_3. The outer layer, however, contains about 13 percent alloying, while the inner is essentially Cb_5Si_3.

(2) Analysis of the Si-20Cr-20Fe Fused Silicide Coating on D43 Alloy

The Si-20Cr-20Fe fused silicide coating has demonstrated excellent protectiveness with high reliability in the slow-cyclic test and in reentry simulation tests. Its coatability properties are also excellent in that it wets out very well. Consequently, this coating exhibits uniform thickness and smooth planar surfaces and interfaces, even when it is applied to the Cb-752 alloy.

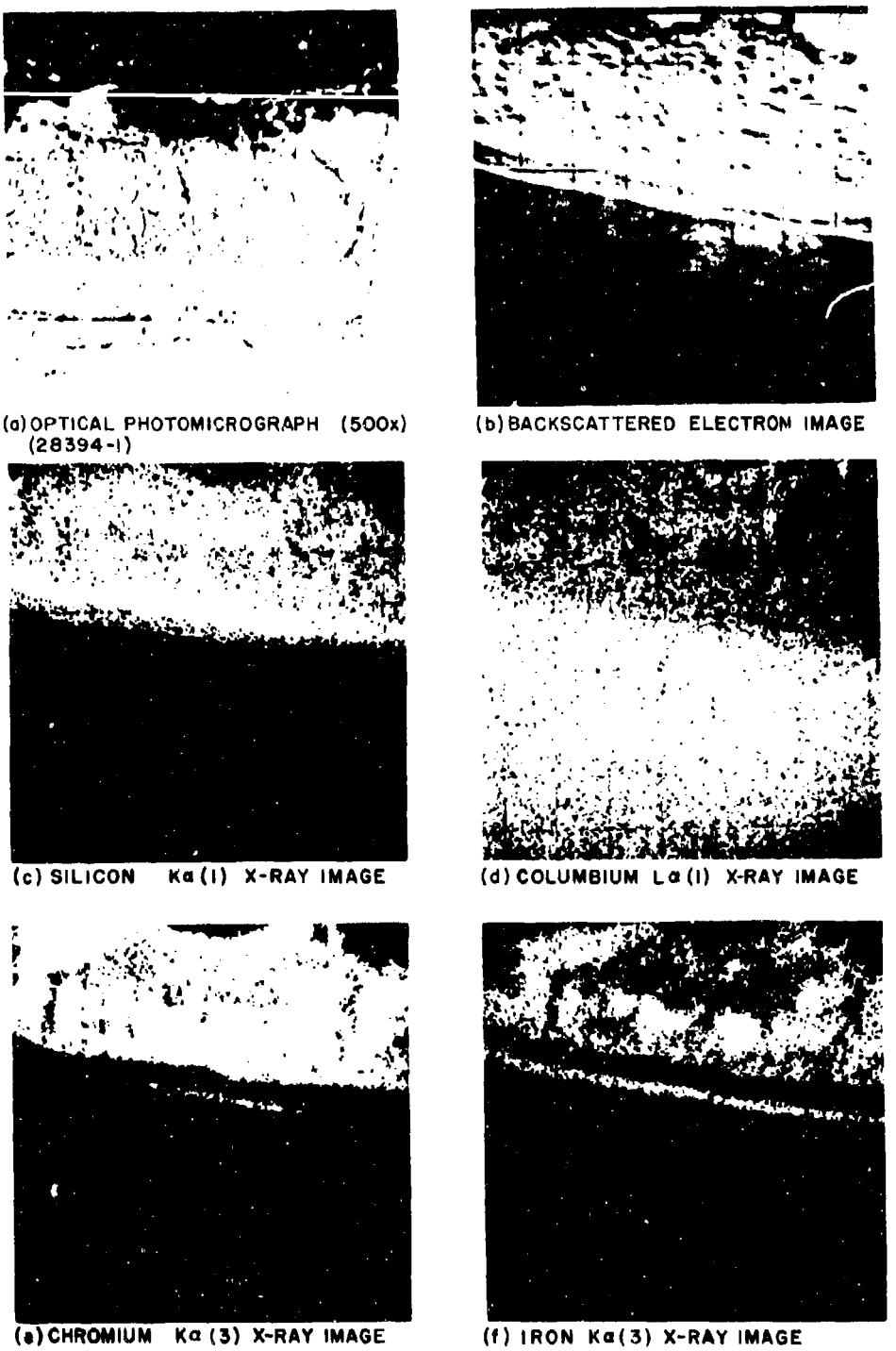

Figure 72 Electron Microprobe X-Ray Scanning Images (400X) of Si-20Cr-5Ti-10Fe-10VSi_2 Coated D43 Alloy in As-Coated Condition.

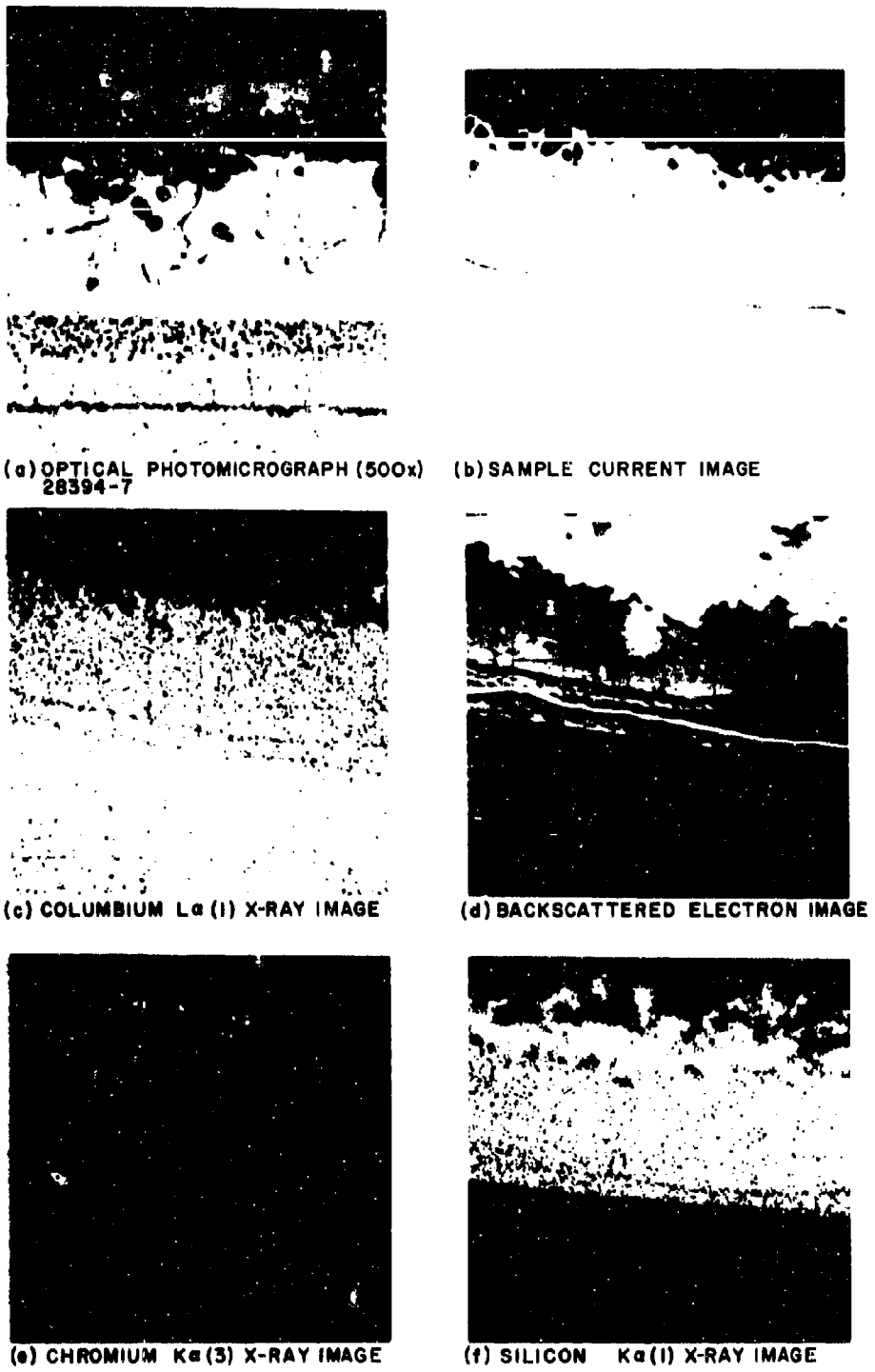

Figure 73 Electron Microprobe X-Ray Scanning Images (400X) of Si-20Cr-5Ti-10Fe-10VSi_2 Coated D43 Alloy After 10 Hours at 2800°F.

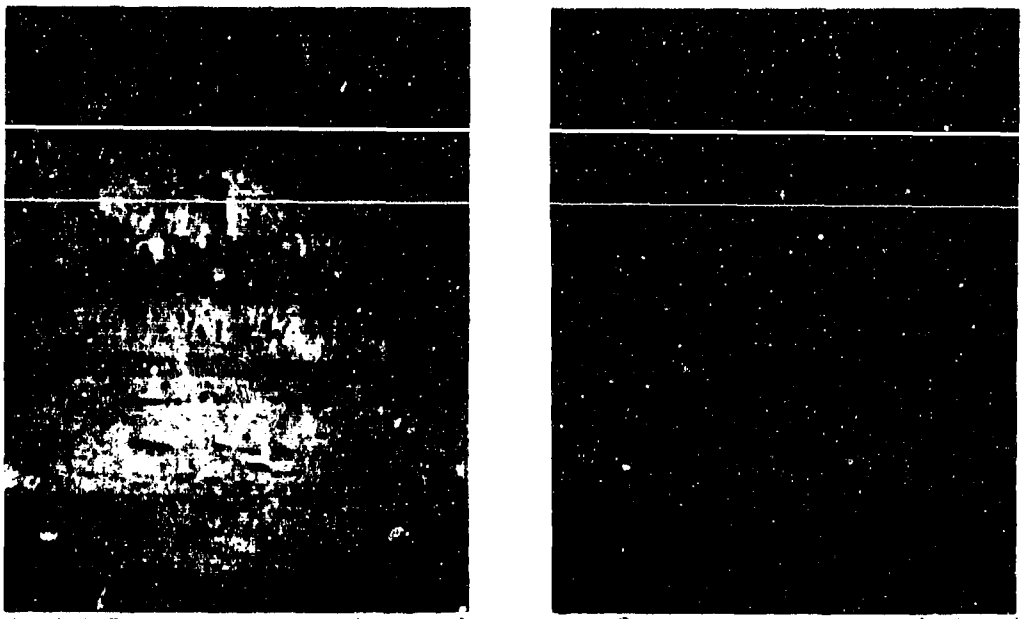

AS COATED 500x (28394-1) 2800°F - 10 hours 500x (28394-7)

Sample	Location	Element Concentration (a/o)					
		Fe	Cr	V	Ti	Cb	Si
As coated	A	0.1	5.1	1.7	0.2	24.6	68.3
	B	11.1	26.4	3.8	0.4	12.8	45.5
	C	0.2	0.8	0	0	31.0	68.0
	D	2.2	6.2	0	0	50.2	41.3
2800°F 10 hours	A	7.0	2.9	2.4	0.3	45.0	42.5
	B	0.7	0.5	0	0	58.1	40.7

Figure 74 Quantitative EMP Analyses of Si-20Cr-5Ti-10Fe-10VSi_2 Coatings on D43

During the course of slow-cyclic oxidation testing or high-temperature atmospheric pressure oxidation testing, the scale that grows on this coating tends to powder and spall. It should be emphasized that notwithstanding this behavior, this coating retains its excellent protective properties. Furthermore, the coating does not behave similarly in reduced pressure environments; the 500-hour + reentry test specimens, for example, did not exhibit any spalling of the oxide scale.

A group of D43 coupons were coated with the Si-20Cr-20Fe composition and were subjected to the slow-cyclic oxidation test with pairs of samples being withdrawn after 1, 2, 3, 4, 5, 6, 10, and 50 cycles. In addition, two coupons were oxidized at 2800°F for 10 one-hour cycles.

The photomicrograph of Figure 75 shows the rather rapid progression of oxidation of the outer layer of the coating, during the slow cyclic exposure, to form a nonadherent layered scale. After 50 cycles, the outer layer had been consumed and most of the scale had flaked away. The new scale formed on the coating is now dense, adherent and protective.

The x-ray diffraction analyses of these samples is summarized in Table XXIV. The x-ray results reveal a complex three-component (SiO_2, $CrCbO_4$, and Cb_2O_5) scale existing in most specimens. Depending on the time and temperature of exposure, the relative concentrations of these components varied. Either SiO_2 or $CrCbO_4$ was always the major oxide phase. There seems to be correlation between the existence of Cb_2O_5 as the secondary phase and the appearance of the powdery scale. For the sample oxidized through 50 slow cycles and the sample oxidized for ten hours at 2800°F, Cb_2O_5 is present as a minor phase or in undetectable quantities respectively. In neither case do these samples exhibit a powdery scale at the conclusion of these exposures.

Qualitative and quantitative electron microprobe analyses were performed on the as-coated, 10- and 50-hour slow cycled, and 10-hour, 2800°F exposed samples. The qualitative x-ray scanning images, and the quantitative point analyses of each discrete phase and layer of each sample are given in Figures 76 through 83.

In the as-coated condition (Figures 76 and 77), the points analyzed appear essentially, as single-phased. There could, however, be a fine $CbSi_2$ second phase throughout the B and C planes. Plane A is obviously $CbSi_2$ with very little modification. Plane B is apparently M_5Si_3 hex since this was the secondary phase detected by x-ray diffraction of the surface. It is surprising that the pattern was reported to be close to Cb_5Si_3 in view of the considerable variation in chemistry of this phase from Cb_5Si_3. Planes C and E are probably the same phase as B although the chemistries are quite different.

Plane G is the base metal D43 and it is seen that a small amount of Fe is in solution, while neither Cr nor Si is present in detectable quantities. Between planes C and E there is another layer which can be seen to be essentially free of Cr and Fe and rich in columbium and silicon. This layer was too narrow to analyze. In an analogous situation with a similar coating (Figure 74), a corresponding layer was analyzed as $CbSi_2$ containing 0.2 a/o Fe and 0.8 a/o Cr.

After exposure to ten slow-oxidation cycles (Figures 78 and 79), there are now two additional layers of sufficient width to be analyzed. Plane F is a slightly modified Cb_5Si_3 layer formed by the inward diffusion of silicon. The inner zone in the as-coated condition (Figure 77, plane E), corresponds very closely to the next-to-the-inner zone in the 10 slow-cycle condition (Figure 79, plane E). The other "new" layer is plane D. This is the layer that was too narrow to analyze in the as-coated condition and which was inferred to be $CbSi_2$, based on the x-ray scans and previous analyses (see Figure 74.) This layer has grown and stabilized, chemically, with the adjacent layers by diffusion.

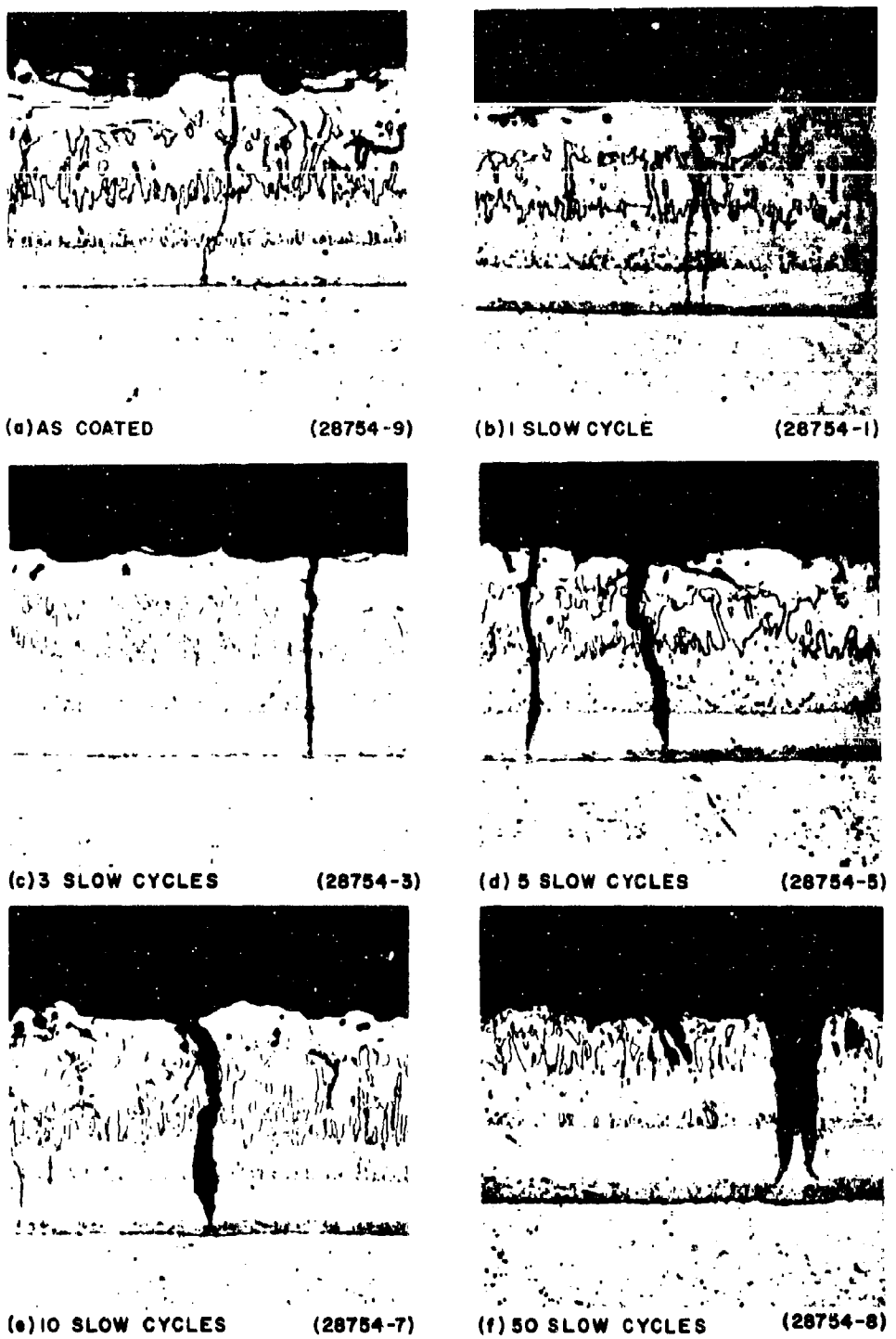

Figure 75 Photomicrographs of Si-20Cr-20Fe Coated D43 Showing Effect of Exposure to Slow Cyclic Oxidation Environment (400X).

TABLE XXIV

X-RAY DIFFRACTION ANALYSIS OF Si-20Cr-20Fe COATED D43 IN VARIOUS CONDITIONS

Condition	Major Phase	Secondary Phase	Other Phases Detected
As coated	MSi_2 (close to $CbSi_2$)	M_5Si_3 hex (close to Cb_5Si_3)	
After 1 slow cycle	MSi_2 (close to $CbSi_2$)	$CrCbO_4$ (shift to higher d spacing)	Cb_2O_5 (high temperature form) SiO_2 (α cristobalite)
After 2 slow cycles			
After 3 slow cycles	With increasing test exposure MSi_2 and $CrCbO_4$ decrease while SiO_2 and Cb_2O_5 show up as stronger phases.		
After 4 slow cycles			
After 5 slow cycles			
After 6 slow cycles			
After 10 slow cycles	SiO_2 (α cristobalite)	Cb_2O_5 (high temperature form)	MSi_2 (close to $CbSi_2$) $CrCbO_4$ (shift to higher d spacing)
After 50 cycles	$CrCbO_4$ (shift to higher d spacing)	SiO_2 (α cristobalite)	Cb_2O_5 (high temperature form)
Oxidized 2800°F 10 hours	SiO_2 (α cristobalite)	MSi_2 (close to $CbSi_2$)	$CrCbO_4$ (shift to higher d spacing) M_5Si_3 hex (very weak) $FeCbO_4$ (possible)

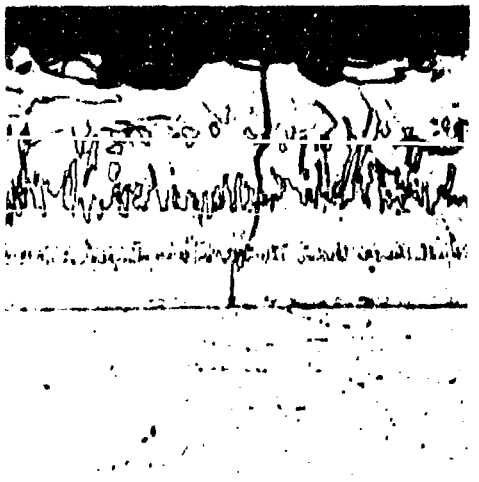

(a) OPTICAL PHOTOMICROGRAPH

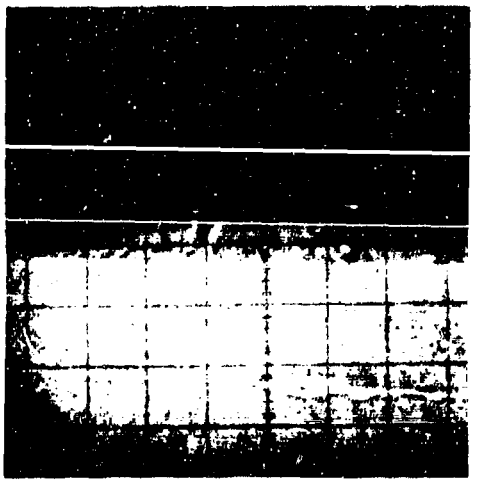

(b) SAMPLE CURRENT IMAGE

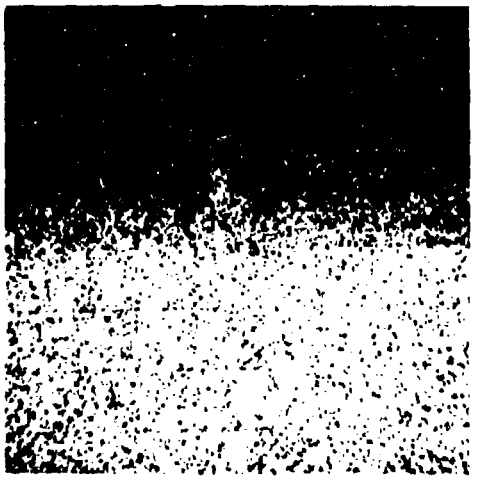

(c) COLUMBIUM Lα (1) X-RAY IMAGE

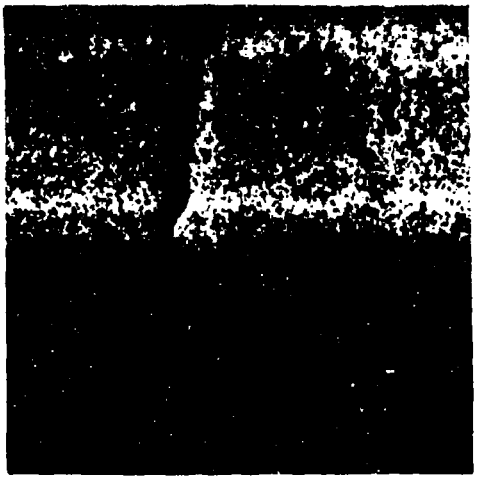

(d) SILICON Kα (1) X-RAY IMAGE

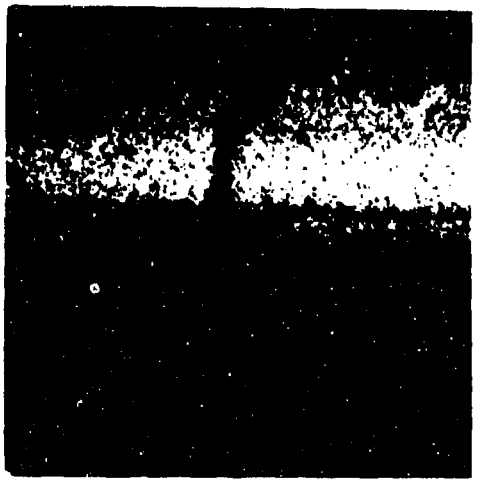

(e) CHROMIUM Kα (3) X-RAY IMAGE

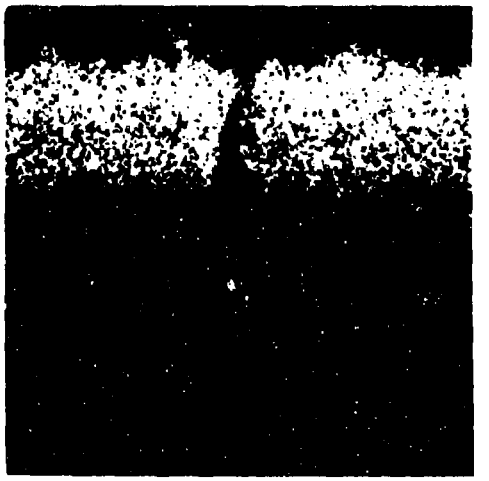

(f) IRON Kα (3) X-RAY IMAGE

Figure 76 Electron Microprobe X-Ray Scanning Images of Si-20Cr-20Fe Coated D43 in As-Coated Condition (400X).

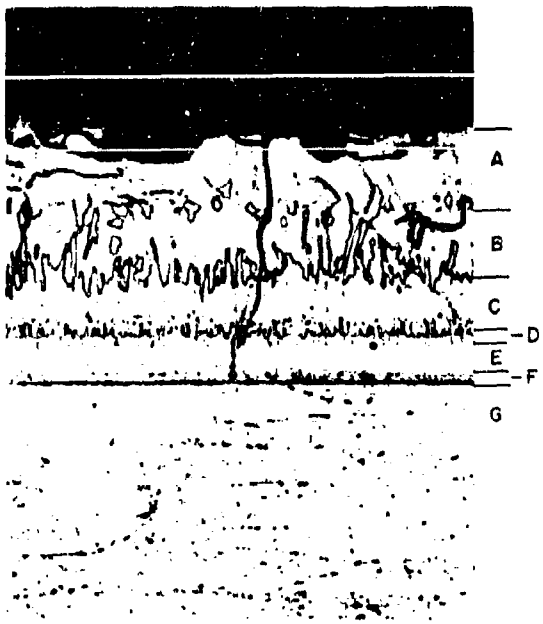

Plane	Element Concentration (a/o)				
	W	Fe	Cr	Cb	Si
A	1.0	0.2	0.8	30.3	67.3
B	0.9	13.4	19.4	20.6	45.7
C	0.6	18.3	9.8	27.4	43.9
D	too narrow to analyze				
E	1.9	8.0	4.1	45.3	40.7
F	too narrow to analyze				
G	4.6	0.2	0.0	95.2	0.0

Figure 77 Quantitative Electron Microprobe Analysis of Si-20Cr-20Fe Coated D43 in As-Coated Condition.

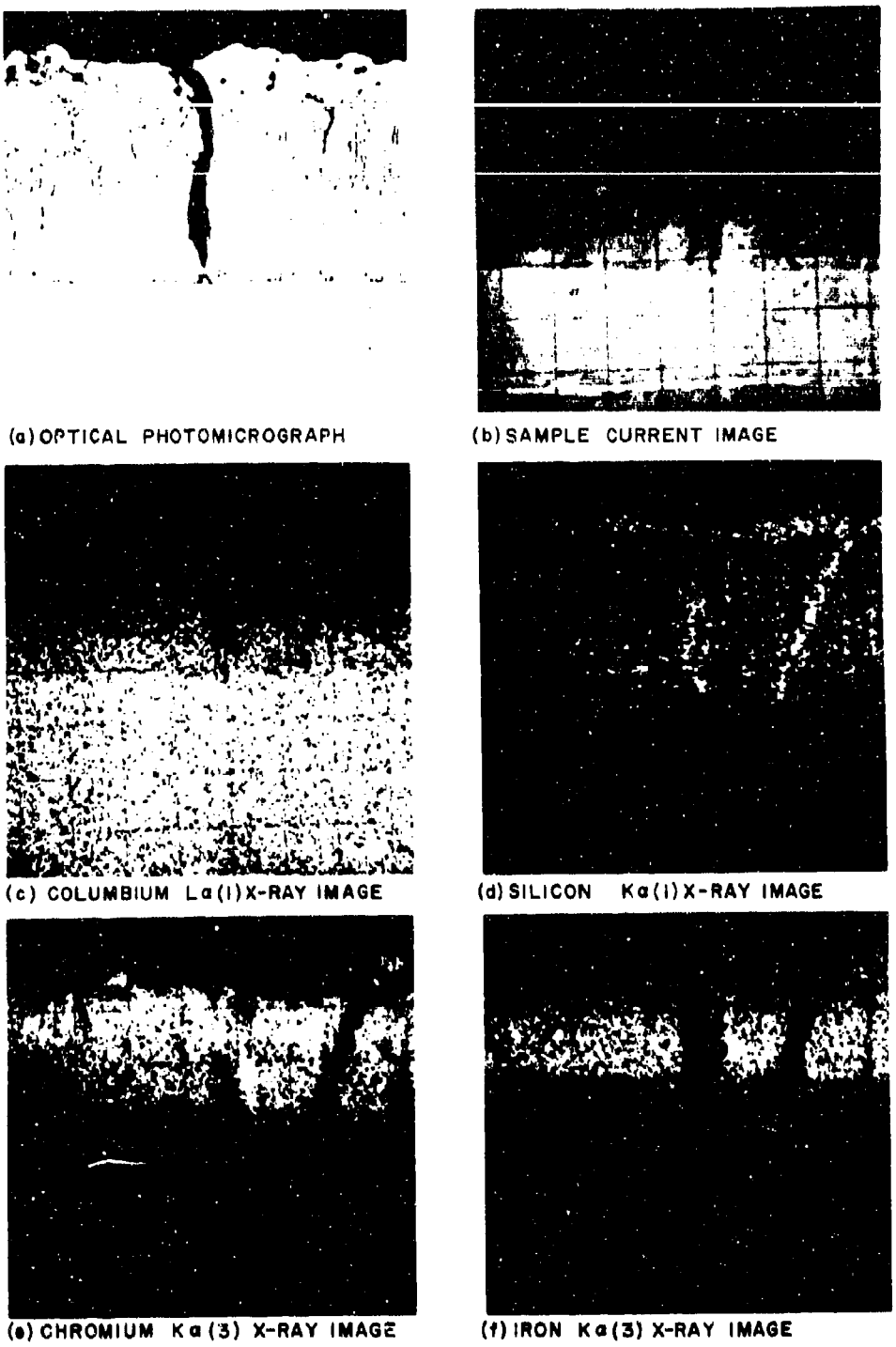

Figure 78 Electron Microprobe X-Ray Scanning Images of Si-20Cr-20Fe Coated D43 After Oxidation Exposure of Ten Slow Cycles (400X).

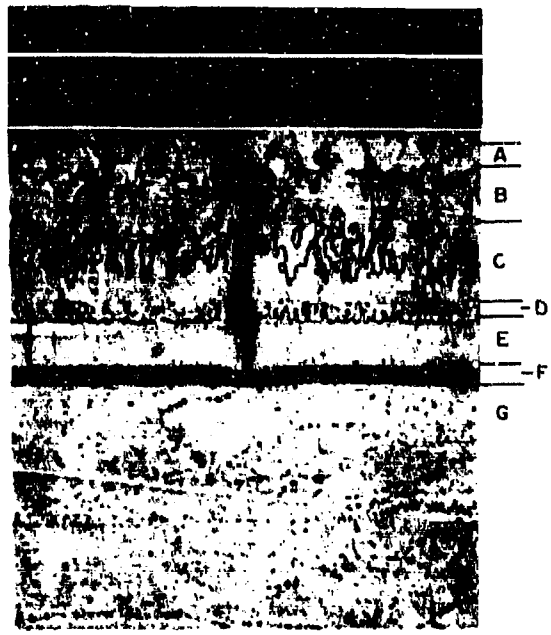

Plane	Element Concentration (a/o)				
	W	Fe	Cr	Cb	Si
A	1.1	0.1	0.6	28.9	69.2
B	1.1	11.7	19.0	23.0	45.2
C	0.5	18.6	7.5	27.3	46.1
D	0.5	15.0	6.4	32.0	46.1
E	2.0	6.9	2.2	46.0	42.9
F	2.3	0.4	0.0	57.8	39.5
G	4.9	0.2	0.0	94.9	0.0

Figure 79 Quantitative Electron Microprobe Analysis of Si-20Cr-20Fe Coated D43 After Oxidation Exposure of Ten Slow Cycles.

It is believed that planes B, C, D, and E are all of the $(Cr, Fe, Cb)_5Si_3$ (hex) structure, possibly mixed with a minor fine phase of $CbSi_2$. An outer layer of $CbSi_2$ (plane A) is still present.

After 50 slow-oxidation cycles (Figures 80 and 81) the analysis indicates a close correspondence to the 10-cycle sample, except that the outer $CbSi_2$ layer (plane A) appears to have been completely consumed by oxidation.

In the sample exposed for ten hours at 2800°F (Figures 82 and 83), the coating now consists of only two layers. The outer layer consists of A, B, C, D, and E of the original coating. This layer appears to be homogeneous and single-phased with a M_5Si_3 (hex) structure (see x-ray diffraction results, Table XXIV). The appreciable concentration gradients evident in the analyses of the other samples have been significantly reduced by diffusion as a result of the substantial ten-hour 2800°F heat treatment.

The other layer (plane F) is the Cb_5Si_3 phase formed by inward diffusion of silicon. This layer has grown somewhat, but chemically conforms to the corresponding F plane in the other samples analyzed.

There probably also exists a thin remnant of layer A in the $CbSi_2$ structure, since this phase was detected by x-ray diffraction as the secondary phase in this sample while shooting through the surface scale.

Quantitative EMP analyses were performed on the oxide phases present in this specimen. The dark colored phase, which had been tentatively identified as SiO_2 (α cristobalite) by x-ray diffraction and the EMP scanning pictures, is apparently pure SiO_2. No significant amounts of Cb, Cr, or Fe were found in this phase. However, the exact chemical composition could not be determined because of the unavailability of mass absorption coefficient data of oxygen Kα radiation for elements beyond the L_3 edge (titanium and elements of higher atomic number).

For the same reasons the exact composition of the light-colored oxide phase could not be determined. Based on the x-ray diffraction analyses and EMP scanning pictures, this phase was previously identified tentatively as $CbCrO_4$. The present analysis indicates, however, that in addition to Cb, Cr, and O, appreciable quantities of Fe and Si are also present. Of course it is quite possible that this light-colored substance is not single-phased material. A close examination of the photomicrograph (Figure 83) does appear to show this material to be two-phased. Additionally, the x-ray diffraction analysis of this sample indicated the presence of another oxide in the scale (possibly $FeCbO_4$).

An effort was made to determine if the sublayers in the Si-20Cr-20Fe coating on D43 are single-phased M_5Si_3 or if they contain some fine dispersion of $CbSi_2$ or some other phases. Specimens identical to those represented in Figures 76 through 83 were ground down in increments of 0.0005 inch and were analyzed by x-ray diffraction after each layer was removed. The data indicates that $CbSi_2$ is generally present

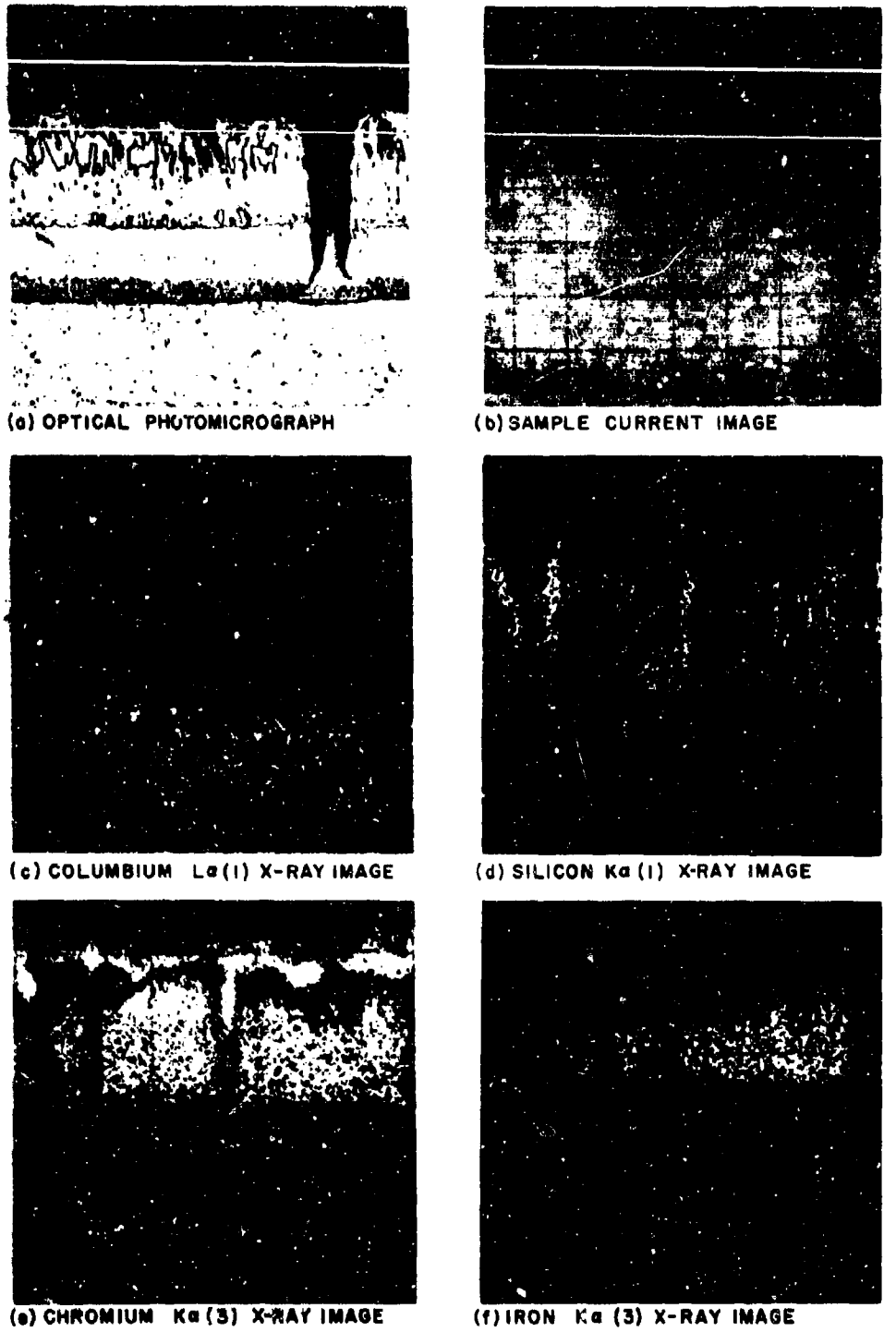

Figure 80 Electron Microprobe X-Ray Scanning Images of Si-20Cr-20Fe Coated D43 After Oxidation Exposure of 50 Slow Cycles (400X).

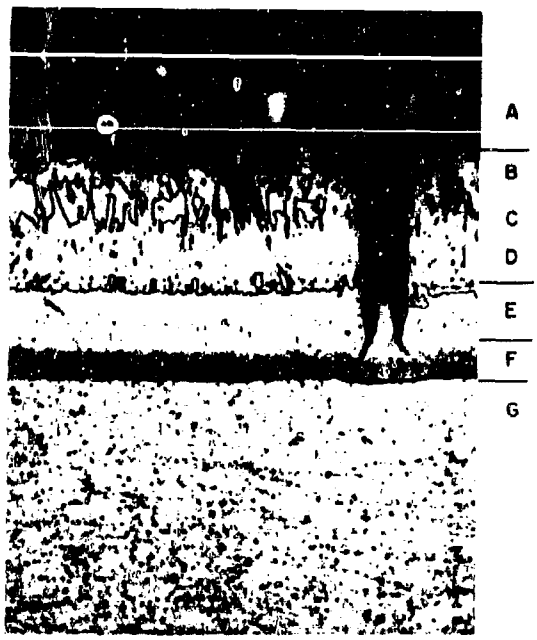

Plane	Element Concentration (a/o)				
	W	Fe	Cr	Cb	Si
A	consumed by oxidation				
B	0.8	12.3	14.9	25.8	46.2
C	0.4	19.2	8.7	25.9	45.8
D	1.8	9.1	7.1	39.9	42.1
E	2.0	8.1	0.3	46.8	42.8
F	2.0	0.6	0.0	59.1	38.3
G	4.3	0.2	0.0	95.5	0.0

Figure 81 Quantitative Electron Microprobe Analysis of Si-20Cr-20Fe Coated D43 After Oxidation Exposure of 50 Slow Cycles.

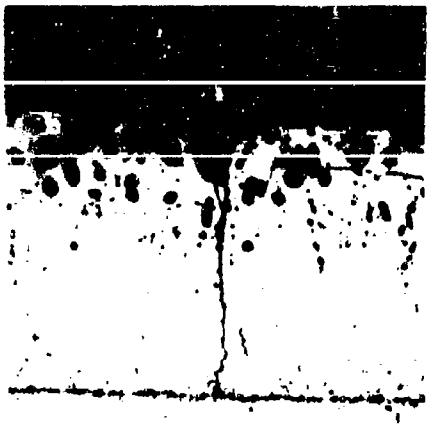

(a) OPTICAL PHOTOMICROGRAPH

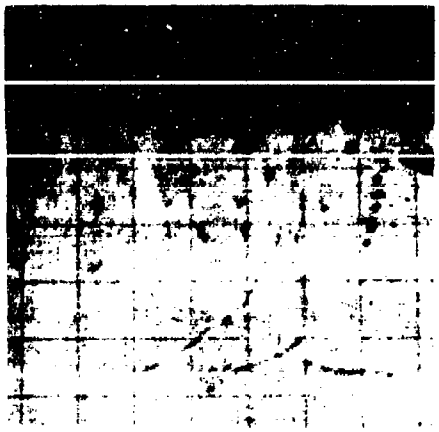

(b) SAMPLE CURRENT IMAGE

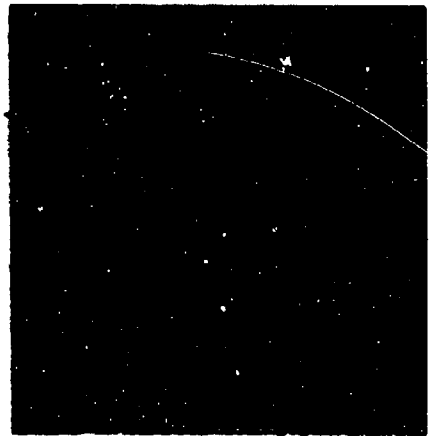

(c) COLUMBIUM Lα(1) X-RAY IMAGE

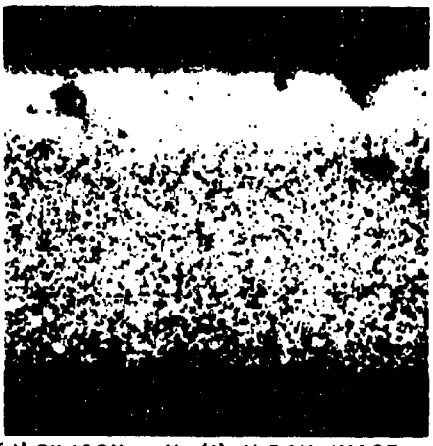

(d) SILICON Kα(1) X-RAY IMAGE

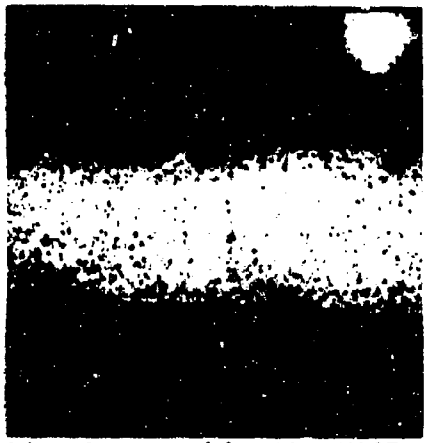

(e) CHROMIUM Kα(3) X-RAY IMAGE

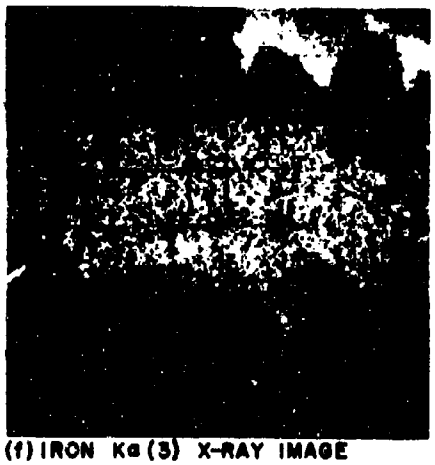

(f) IRON Kα(3) X-RAY IMAGE

Figure 82 Electron Microprobe X-Ray Scanning Images of Si-20Cr-20Fe Coated D43 After Oxidation Exposure of Ten One-Hour Cycles at 2800 °F (400X).

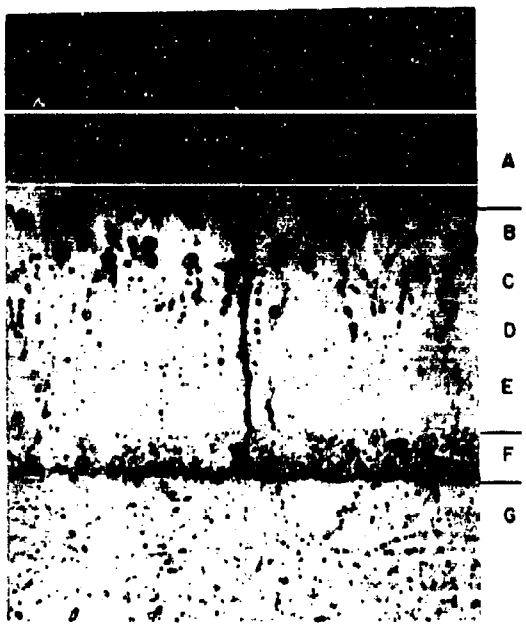

Plane	Element Concentration (a/o)				
	W	Fe	Cr	Cb	Si
A	2.0	8.9	4.5	41.8	42.8
B	1.7	8.8	7.2	40.8	41.5
C	2.1	8.5	6.2	41.8	41.4
D	1.9	7.9	4.3	44.9	41.0
E	1.9	6.5	2.8	46.7	42.0
F	2.3	0.5	0.2	57.8	39.2

Figure 83 Quantitative Electron Microprobe Analysis of Si-20Cr-20Fe Coated D43 After Oxidation Exposure of Ten One-Hour Cycles at 2800°F.

in small quantities in those layers tentatively identified on the basis of EMP quantitative analyses as M_5Si_3. The innermost layer adjacent to the substrate, however, was analyzed as M_5Si_3 and no other phases were detected.

Optical and scanning electron micrographs of the 2800°F - 10 hour oxidized specimen are shown on Figure 84. The scanning electron micrograph is a secondary electron image and was produced with a JELCO instrument. This picture is centered on the coating-substrate interface, but shows portions of the inner and main coating layers as well as a portion of the substrate.

It is interesting to note that the inner coating zone which appears to be two-phased in both pictures was identified by x-ray diffraction of a sequentially ground sample as single-phased M_5Si_3 (tetragonal), while the main coating layer above this which appears to be single-phased was identified by similar means as a mixture of MSi_2 and M_5Si_3 (tetragonal) and M_5Si_3 (hexagonal).

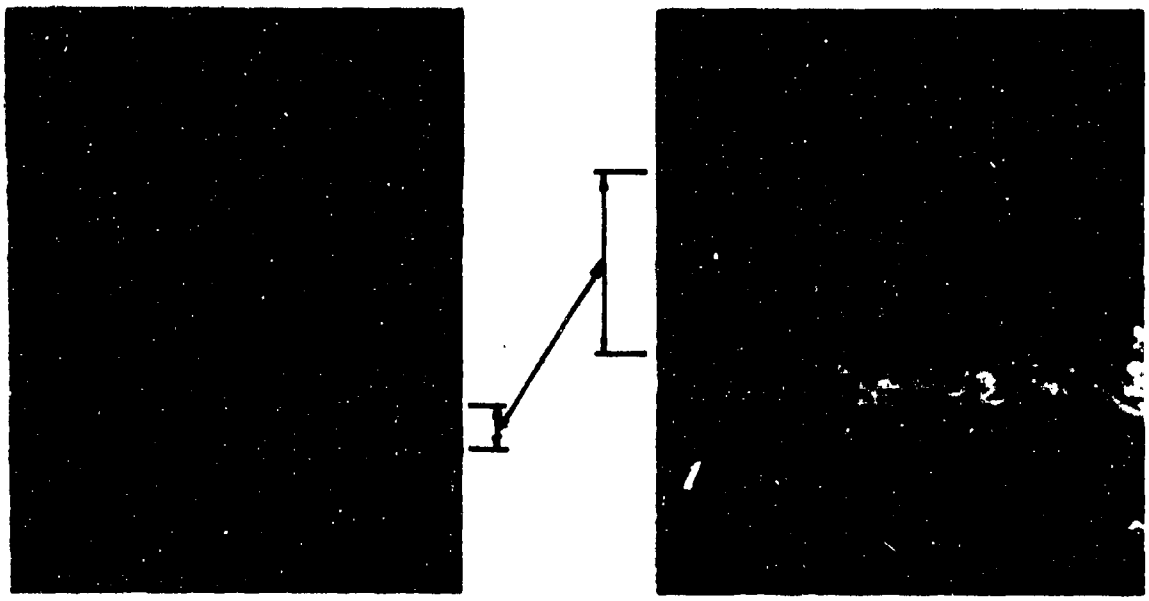

(a) OPTICAL MICROGRAPH 400X

(b) SCANNING ELECTRON MICROGRAPH 2000X

Figure 84 Photomicrographs of Si-20Cr-20Fe Coated D43 After 10 Hours - 2800°F Oxidation Exposure.

Additional x-ray diffraction analyses were performed on Si-20Cr-20Fe coated D43 specimens exposed to various low-pressure, high-temperature, and simulated reentry environments. The results are given in Table XXV. The analyses of all samples were quite similar in that they all had $CrCbO_4$ as the major phase and SiO_2 and MSi_2 as the next stronger phases. It is significant to note that these phases are the same as those present in the surfaces of samples exposed to the atmospheric pressure slow cycling test (see Table XXIV), with the important exception that Cb_2O_5 is not present in the former.

The bar graphs in Table XXV, which indicate the intensities of each phase relative to the other samples, show that $CrCbO_4$ is formed in preference to SiO_2 at higher pressures. As the pressure level is reduced, the $CrCbO_4$ to SiO_2 ratio decreases, although $CrCbO_4$ remains as the major phase. The increase in the MSi_2 intensity as the pressure is reduced is probably attributable to the decrease in overall oxidation rate with pressure, which serves to reduce the rate of consumption of this phase, and also to reduce the masking effect of the resulting thinner scale.

m. Wettability and Flowability

The experiments described in the following paragraphs were devised in an effort to demonstrate semi-quantitatively some of the more practical attributes of the fused silicide coatings.

Four coating-base alloy systems were evaluated for these properties. They were Si-20Cr-5Ti(D43), Si-20Cr-5Ti(Cb752), Si-20Cr-20Fe(D43), and Si-20Cr-20Fe (Cb752).

The term wettability, as used here, refers to the ability of the fused slurry to react with the surface of the part to be coated, and to what degree this property is affected by surface conditions such as cleanliness, surface oxidation, dissolved oxygen, or surface preparation method.

It is not always practical or possible to have 100 percent of the surface of a complex structure perfectly clean, uncontaminated, or prepared by some single preferred method. For example, if two sheet metal parts are spot-welded together, the faying surface formed can not be readily cleaned by grit blasting, or even by pickling, if the joint is a tight one. Also the areas in the faying surface immediately adjacent to the spot welds may be slightly contaminated, as well as oxidized, and are obviously difficult to clean short of solutioning the oxygen with a high-temperature vacuum anneal.

The different surface conditions of both alloys to which the fused silicides of both compositions were applied and evaluated for wettability are as follows:

(1) As received and degreased
(2) Grit blasted (40 psi - iron grit)
(3) Acid etched (equal parts HNO_3-HF-H_2O for 2 minutes)
(4) Tumbled and degreased
(5) Oxidized 1 hour at 800°F.

TABLE XXV

X-RAY DIFFRACTION ANALYSIS OF Si-20Cr-20Fe COATED D43 AFTER VARIOUS REDUCED PRESSURE OXIDATION EXPOSURES

Sample No.	Sample Exposure	Major Phase $CrCbO_4$	Secondary Phase SiO_2 (a crist)	MSi_2 (close to $CbSi_2$	Other Phases Detected	
					M_5Si_3	Cr_2O_3
7	Reentry simulation tested 200 cycles internal surface profile, 2500° max. temp.	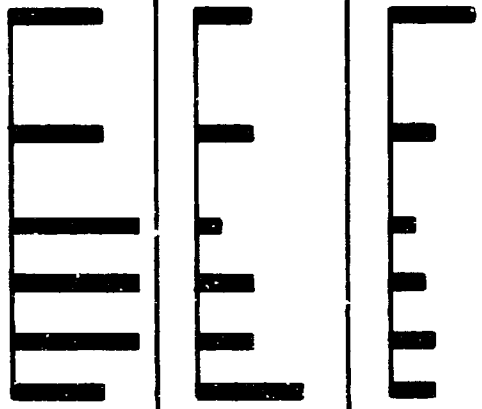			Very weak	---
9	Same, but external surface profile				Very weak	---
11	2500°F, 1 atm, 24 hr				---	---
12	2500°F, 5 torr, 24 hr				Very weak	---
13	2500°F, 1.0 torr, 24 hr				Very weak	---
14	2500°F, 0.1 torr, 24 hr				Very weak	Cr_2O_3 detected in this sample only

Relative intensities of these three phases shown in charts above with increasing intensity in this direction

Photographs of one group of wettability specimens [(Si-20Cr-5Ti)-D43] are shown in Figure 85 and indicate that all of the specimens are coated. The other groups of specimens were similar in appearance.

Metallographic examination indicated that all specimens were completely wetted and a coating with a normal microstructure had formed on all surfaces. There was evidence of grain boundary oxidation of the D43 substrate in the as-tumbled specimen after coating. There was no apparent contamination or oxidation of the substrates of any of the other specimens.

Slow-cycling oxidation tests of these coatings indicated that the resultant coatings were equal in protectiveness whether applied to very clean prepared surfaces or to dirty, contaminated, or oxidized surfaces.

The ability of the fused silicide coating to flow, wet, and protect areas to which the slurry may not have been directly applied or from which it may have been accidentally removed is illustrated in Figure 86. This photograph shows a number of test coupons which were variously masked during application of slurry, and an identically masked similar set of specimens after fusion of the slurry. The specimens shown are D43 alloy coated with the Si-20Cr-5Ti composition. The coating appears to have completely wet those areas which were masked off. Photomicrographs of sections through the masked-off areas, Figures 87 and 88, show that the masked areas are fully coated. The sample which is coated on one side has a coating on that side whose thickness is only slightly greater than that on the other side. The edge coverage on samples with the edges masked is just as good as that on samples not masked.

The other three systems showed markedly different flowability properties and indicate both coating and base metal effects. The (Si-20Cr-20Fe) - Cb752 system displayed the poorest flow characteristics with the coating interface moving only about 1/32 inch. The (Si-20Cr-20Fe) - D43 flowed about 1/16 inch and the (Si-20Cr-5Ti) - Cb752 about 1/8 - 3/16 inch.

The ability of the fused silicide coating to protect faying surfaces adequately is demonstrated in Figure 89, which shows a section through two sheets formed with a spot weld and subsequently coated. The system shown is D43 - Si-20Cr-5Ti. No coating was applied to the faying surfaces either before or after spot welding, but extra slurry was applied to the fillet area. It can be seen, however, that during the vacuum fusion process, the coating alloy was drawn into the joint and complete penetration was effected. A similar joint coated by the pack silicide process is shown in Figure 89 for comparison. This latter process results in essentially no penetration of the joint, although these surfaces in use will be easily accessible to the oxidizing environment. The coating of faying surfaces as shown is also characteristic of the other three systems even though those systems have shown less flowability on flat surfaces. An example of faying surfacing penetration by the Si-20Cr-20Fe coating can be seen in Fig. 51, p. 85.

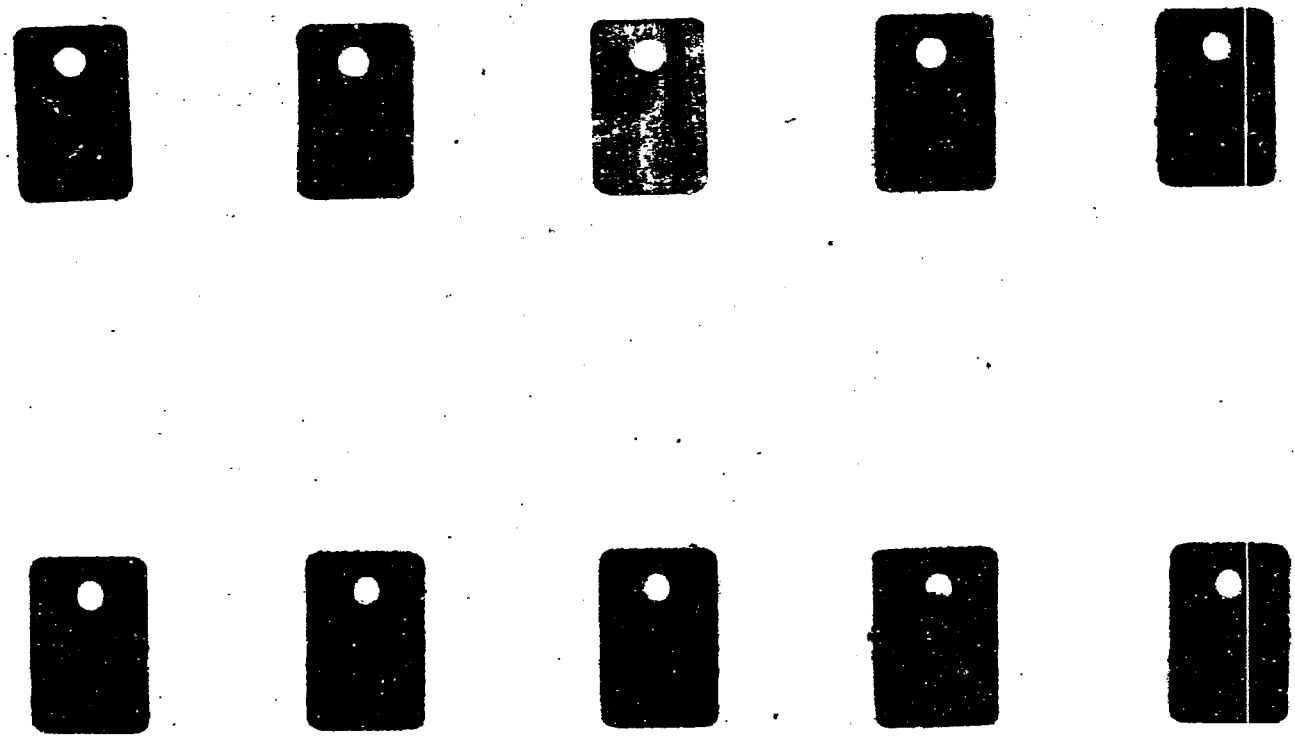

Figure 85 Effect of Surface Condition on Wettability of Fused Silicides. Top Row Uncoated D43 Samples From Left to Right, Degreased, Grit Blasted, Acid Etched, Tumbled, Oxidized. Bottom Row Same Samples After Coating With Fused Silicide. Si-20Cr-5Ti Coating on D43 Alloy.

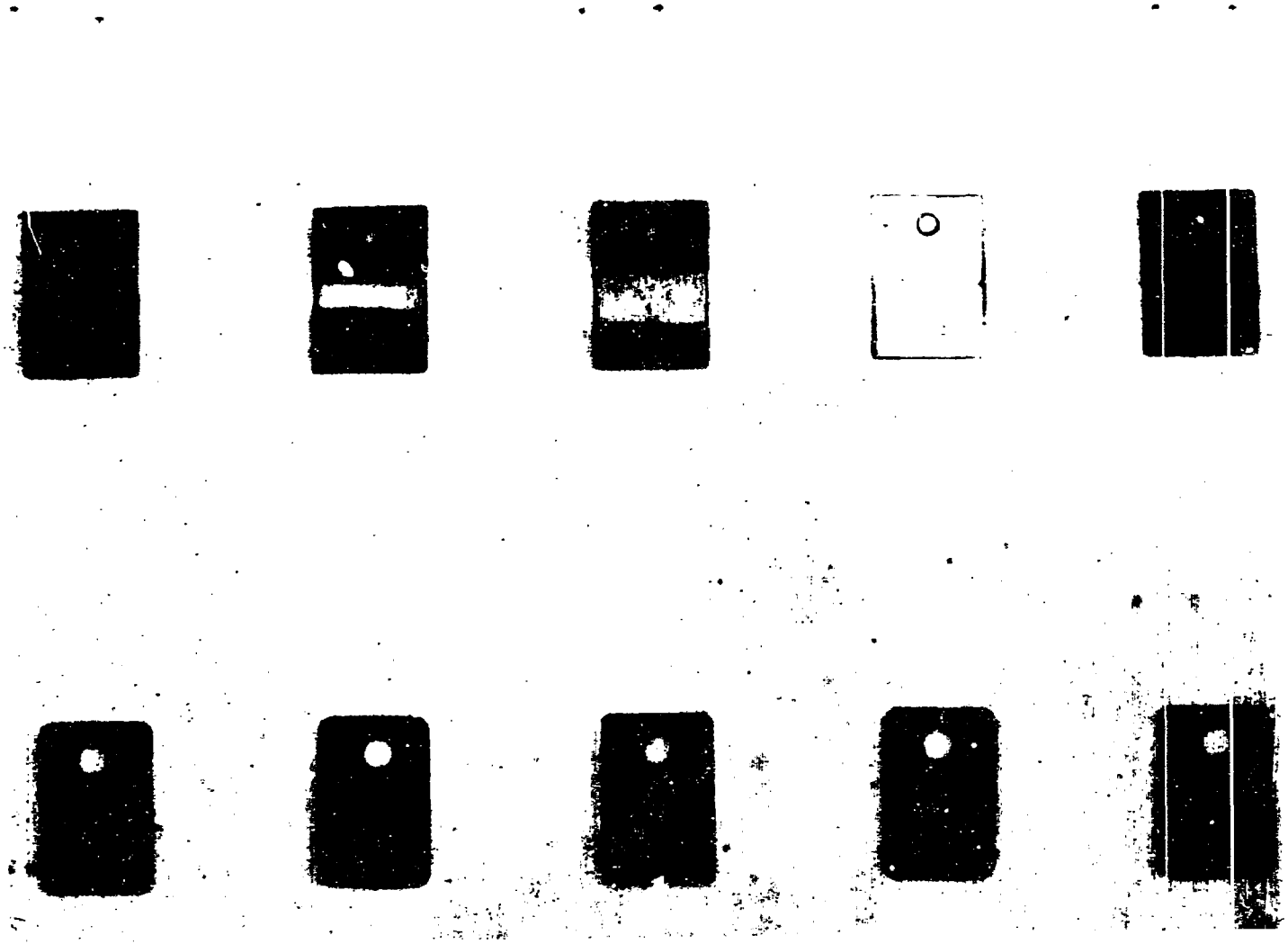

Figure 86 Flowability and Wettability of Fused Silicide Coatings. Top Row Samples as Spray Coated: (From Left to Right) Coated All Over, 1/8-Inch Masked Stripe, 1/4-Inch Masked Stripe, Coated One Side Only, Edges Masked. Bottom Row Shows Similar Set of Samples After Vacuum Fusion Firing. Si-20Cr-5Ti Coating on D43 Alloy.

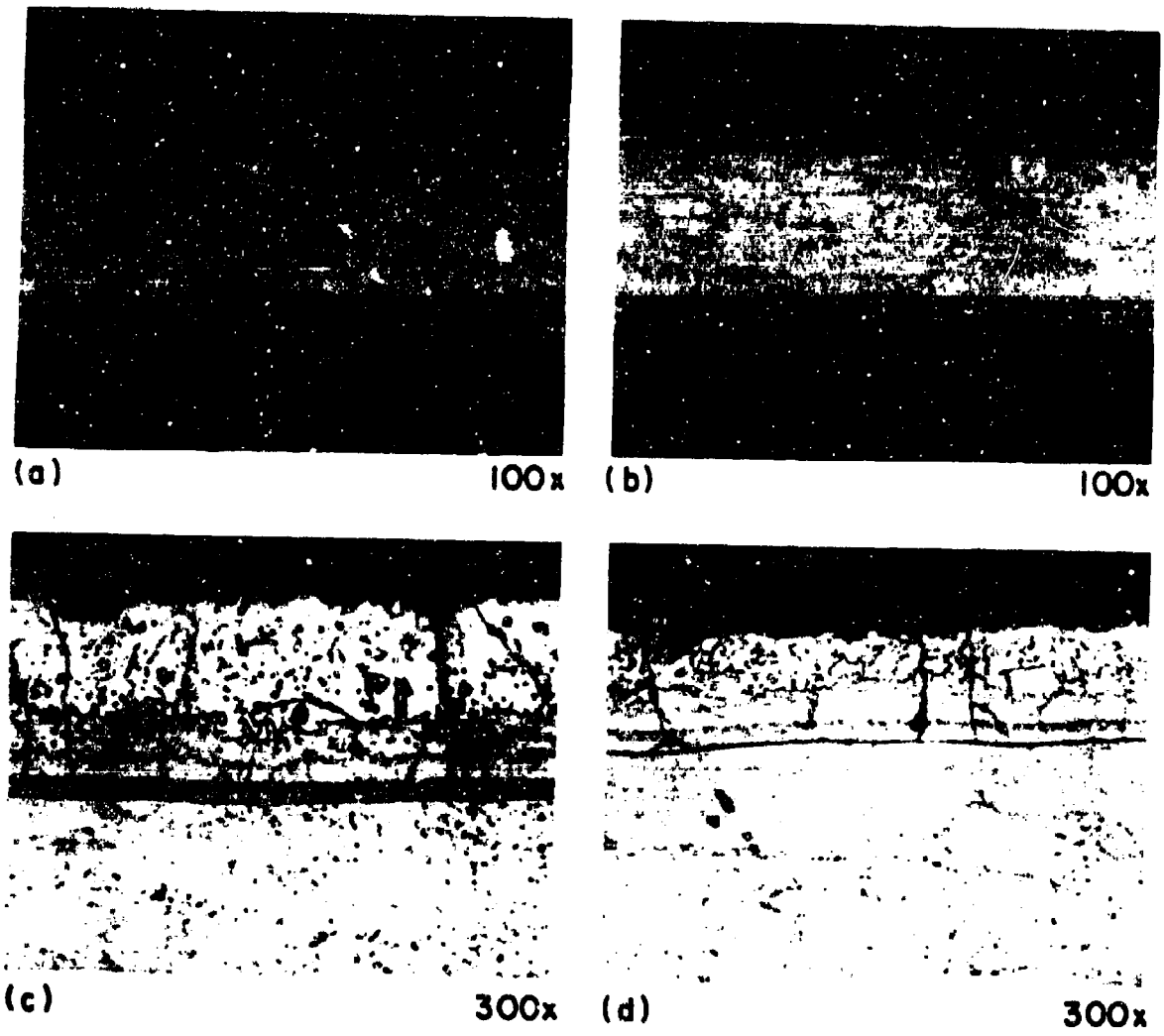

Figure 87 Microstructures of Flowability Specimens (a) (c) Coated All Over, (b) (d) Coated on Bottom Surface Only.

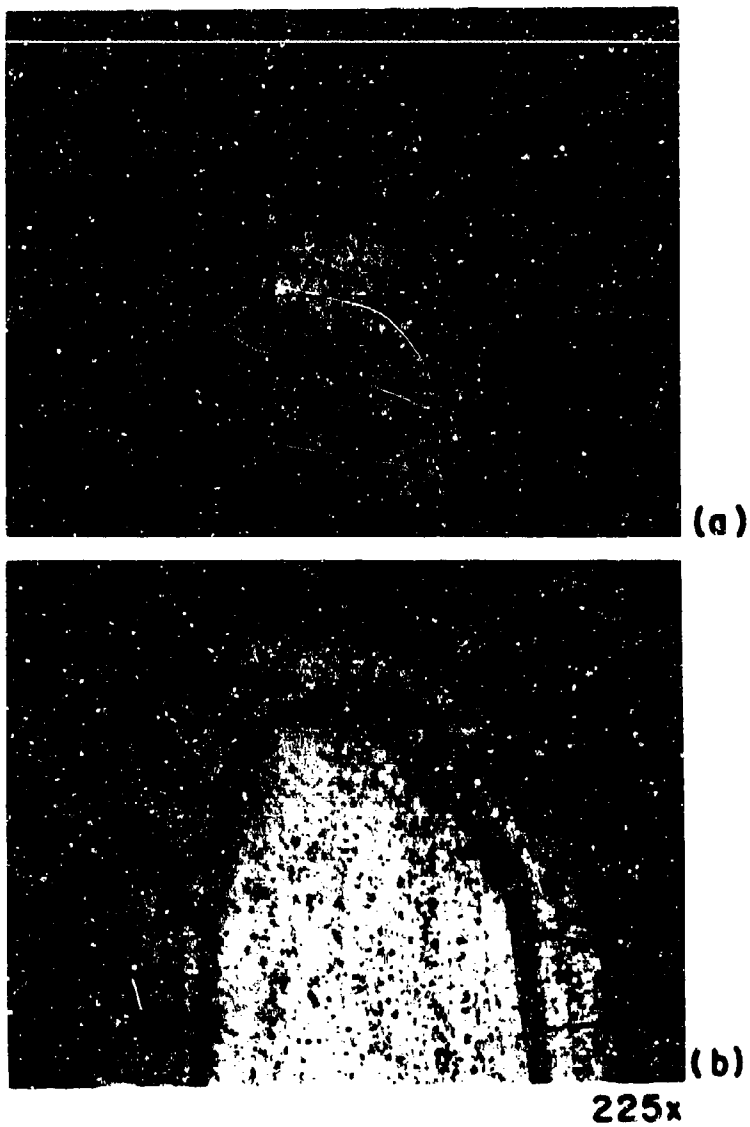

Figure 88 Flowability Test Specimens (a) Edge of Sample Coated All Over, (b) Edge of Sample in Which Edges Were Masked During Coating Application.

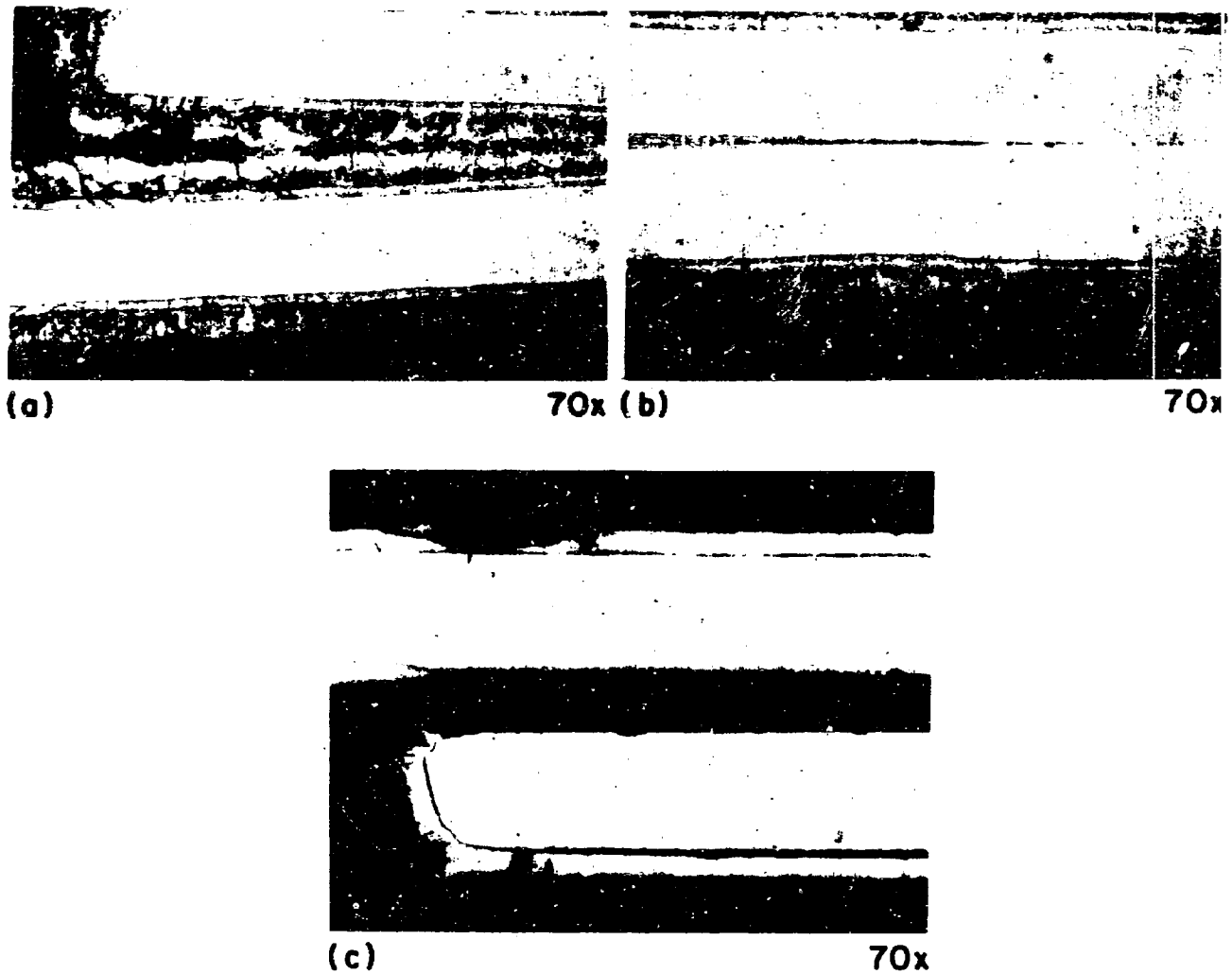

Figure 89 (a) Fused Silicide Coating of Faying Surfaces Formed by Spot Welded Sheet Joint, (b) Same Joint Showing Penetration Right Up to Weld, (c) Similar Joint Coated by Pack Silicide Process.

n. Coating Repair

It is obviously desirable, if not mandatory, that methods be available to reprocess (strip and recoat) and/or repair locally damaged or prematurely failed localized areas in coated refractory metal structures, if such structures are to be economically feasible. Since the fused silicide coating process is essentially a brazing process, it appeared logical to examine self repair techniques first. There were two general objectives. One was to determine generally the effectiveness of such self repair procedures by using metallographic examination and oxidation testing, and the optimum processing parameters for such procedures using conventional furnace heat treating, where the whole part was placed in the furnace. The other task was to design, build, and demonstrate the effectiveness of a small portable unit capable of making small repairs locally on coated refractory metal structures in place. Since, for field repair, it would be simpler to provide an inert gas cover than a vacuum environment for the areas to be repaired, this aspect of the problem was investigated, first.

Two groups of ten D-43 coupons each were spray coated with the Si-20Cr-20Fe-10VSi_2 composition, and were fired in vacuum and in argon respectively for one hour at 2580°F. Six samples from each group then had a 1/8-inch hole drilled completely through the coated pieces. Additional slurry of the same composition was painted around the edges of the drilled holes and the samples were refired in argon for 15 minutes at 2580°F. The repair slurry wet very well, and visual examination indicated that the drilled holes were repaired.

The results of the slow cyclic oxidation testing of the various types of specimens that comprise this experiment are given in Table XXVI. These results may be quite significant. For material coated in the normal vacuum firing process, the repair procedure is completely effective; the repaired coupons display lives in excess of that of the as-coated coupons. The samples coated in argon did not develop the characteristic properties of this coating. After defecting and repairing, however, the slow cyclic life is substantially improved, although still less than that for comparable samples initially coated in vacuum. It appears that the firing cycle for argon processing could be studied to some advantage if there were real interest in inert gas diffusion treatments. However, in general, it is in every sense simpler, better, and more economical to process parts in vacuum initially.

Typical microstructures of as-coated and repaired coatings, shown in Figure 90, exhibit a general similarity between the vacuum-fired and argon-fused coatings. The second phase islands in the vacuum-fired, as-coated structure are not as prominent, however, due to insufficient etching of this particular sample.

Photomicrographs of the edge of the drilled hole defects are shown in Figure 91. These show quite clearly how a defect of this type may be completely and effectively repaired by fusing on the original slurry in an argon atmosphere.

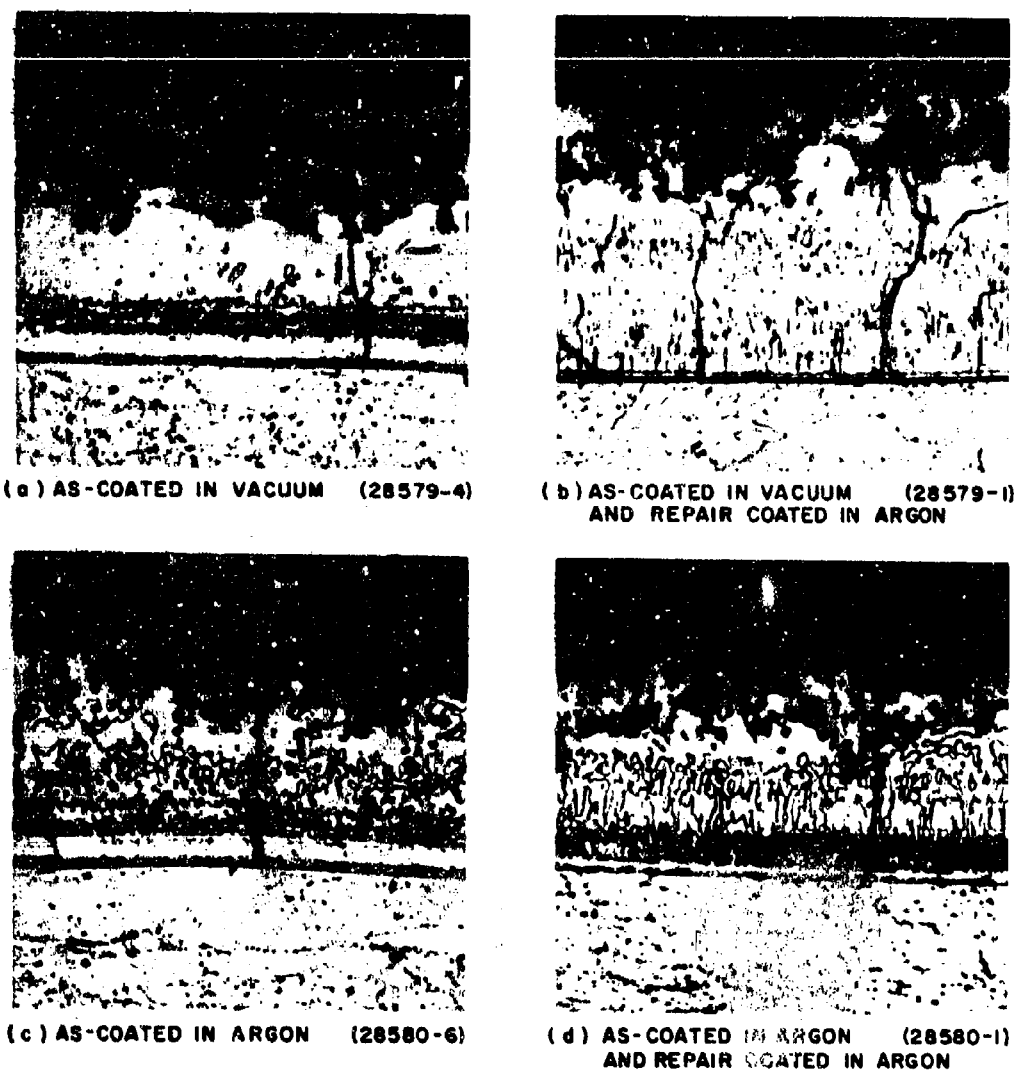

Figure 90 Structures of Si-20Cr-20Fe-10VSi_2 Fused Coatings on D43 Resulting From Repair Procedures (300X).

Figure 91 Photomicrographs of Edge of Drilled Hole "Defect" in Si-20Cr-20Fe-10VSi_2 Coated D43 Tabs. Initial Coating Fired in Vacuum. Repair Coating Fired in Argon (100X).

TABLE XXVI

SLOW CYCLIC OXIDATION TESTS OF REPAIRED COATINGS

Initial Coating Procedure	As-Coated	Slow Cyclic Oxidation Life (No. of 1-hour Cycles to Failure)	
		Coated and Defected (1/8 inch Hole Drilled Through Coupon)	Coated, Defected and Repaired ($Si-20Cr-20Fe-10VSi_2$) 2580°F, 15 Minutes
$Si-20Cr-20Fe-10VSi_2$ Fire 1 hr, 2580°F, vac	43	3	78, 49, 49
$Si-20Cr-20Fe-10VSi_2$ Fire 1 hr, 2580°F, argon	6, 8	2	30, 46

Additional repair processing studies were conducted with Si-20Cr-20Fe coated D43 coupons which were defected by drilling 0.040 inch diameter holes completely through the as-coated specimens. These holes were subsequently repaired in a conventional vacuum furnace using the same slurry and firing schedules of 2500°F - 15 minutes, 2400°F - 15 minutes, 2300°F - 15 minutes, and 2300°F - 1 hour. With the lower temperature repair cycles there appeared to be a residue from the repair slurry that did not melt and wet. Photomicrographs of several typical repaired specimens are shown in Figure 92. These pictures show the edges of the repaired holes, and in each case the repair coating appears to have completely covered the base material and blended in with the existing coating very well.

Slow cyclic oxidation tests were performed on the repaired specimens with the results given in Table XXVII. Based on those limited results it would appear that all of these repair cycles are satisfactory but that the higher temperature or longer time cycles are preferred.

The structure of a repaired surface area is shown in Figure 93. This shows a Si-20Cr-20Fe coated Cb752 sheet in which a 1/16-inch strip of coating was removed by grit blasting, following which this area was repaired using the Si-20Cr-20Fe slurry and a 2500°F - 15 minute furnace cycle in vacuum. It would be difficult to discern the repaired area by examination of the coating structure itself. However, the additional consumption of substrate in the repaired area makes it possible to determine the repair boundaries.

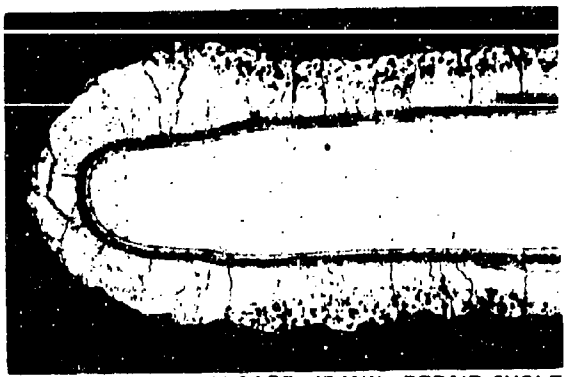

29235-1 2500°F - 15 MIN. REPAIR CYCLE

29235-4 2400°F - 15 MIN. REPAIR CYCLE

29235-6 2300°F - 15 MIN. REPAIR CYCLE

Figure 92 Photomicrographs of Repaired Hole Defects in Si-20Cr-20Fe Coated 0.101 Inch Thick D43 Sheet Using Si-20Cr-20Fe Repair Slurry (100X).

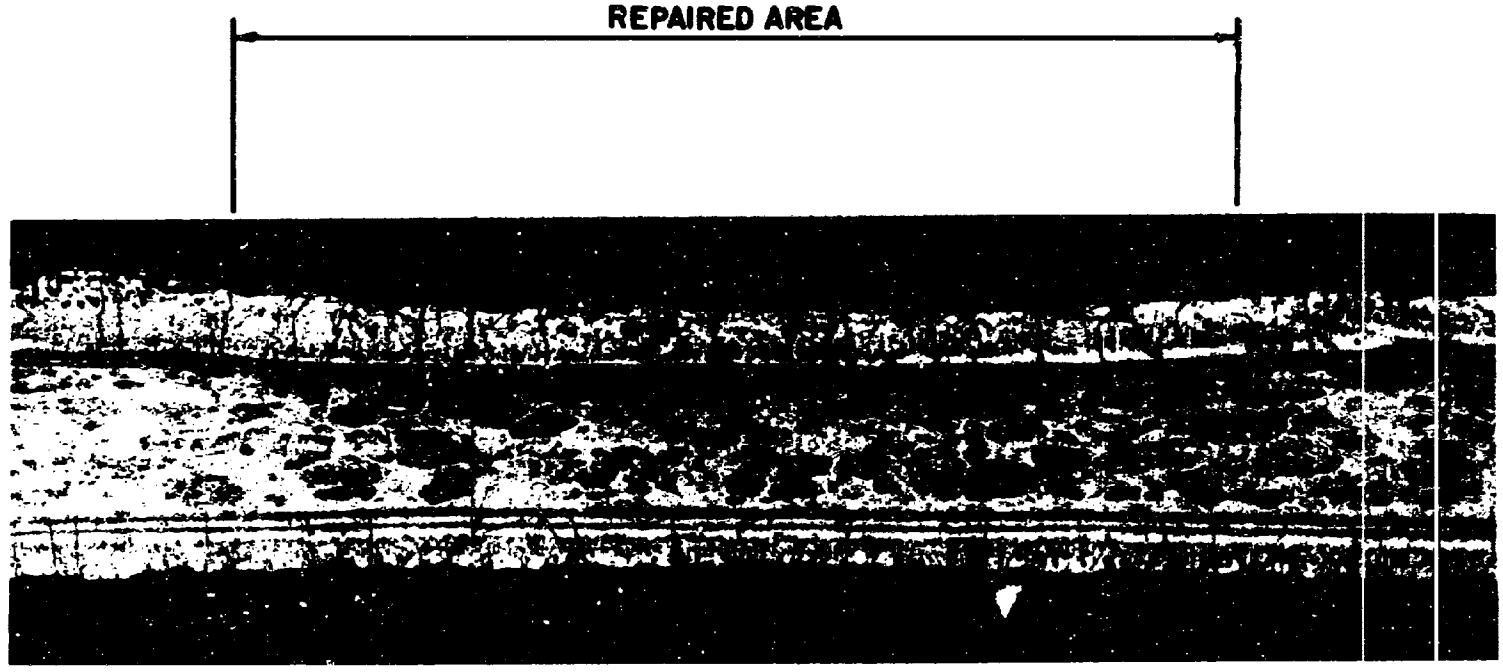

Figure 93 Repair Coated Surface Area of Si-20Cr-10Fe Coated Cb752 (100X).

TABLE XXVII

SLOW CYCLIC OXIDATION TESTS OF DEFECTED AND REPAIRED SPECIMENS

Repair Cycle	No. 1-hr Slow Cycles to Failure	Remarks
2500°F - 15 min.	54	Failed at edge; repaired hole O.K.
2400°F - 15 min.	80	Failed at edge; repaired hole O.K.
2300°F - 1 hour	80	Failed at repaired hole
2300°F - 15 min.	54	Failed at repaired hole

A small portable field repair coating unit was designed and constructed and is shown in Figures 94 and 95. It consists of a small water-cooled vacuum shell and a one-inch O.D. pancake induction coil which can be precisely positioned vertically. The bottom of the bell chamber is fitted with an "O" ring for sealing to the work surface and either a vacuum or inert atmosphere may be provided as the coating repair environment.

An 8 x 8-inch section of an ASCEP honeycomb panel was obtained from the Martin Company and was coated with the Si-20Cr-20Fe composition. This panel was locally heated with the repair unit to above the coating temperature. However, there was overheating of the shell and "O" ring necessitating some design modifications. The unit was redesigned and rebuilt to provide for more efficient electrical coupling and to eliminate overheating of the "O" ring. Both objectives were met enabling the unit to readily heat the surface of a panel to the coating temperature or higher without any undesirable overheating.

Si-20Cr-20Fe coated 0.010-inch thick D43 sheet specimens were defected by drilling 3/32-inch diameter holes completely through the specimens. The holes were repaired in the portable unit using the same slurry and a 2500°F - 8 minute vacuum heating cycle. One specimen was then slow cyclically oxidation tested for 25 one-hour cycles when a spot failure occurred at the repaired hole site. The other specimen was similarly tested for 21 cycles at which time a spot failure developed at the repaired hole site. This specimen was repaired again and was tested for six additional cycles at which time a spot failure was detected on the surface of the specimen, while the coating at the repaired hole was still protective.

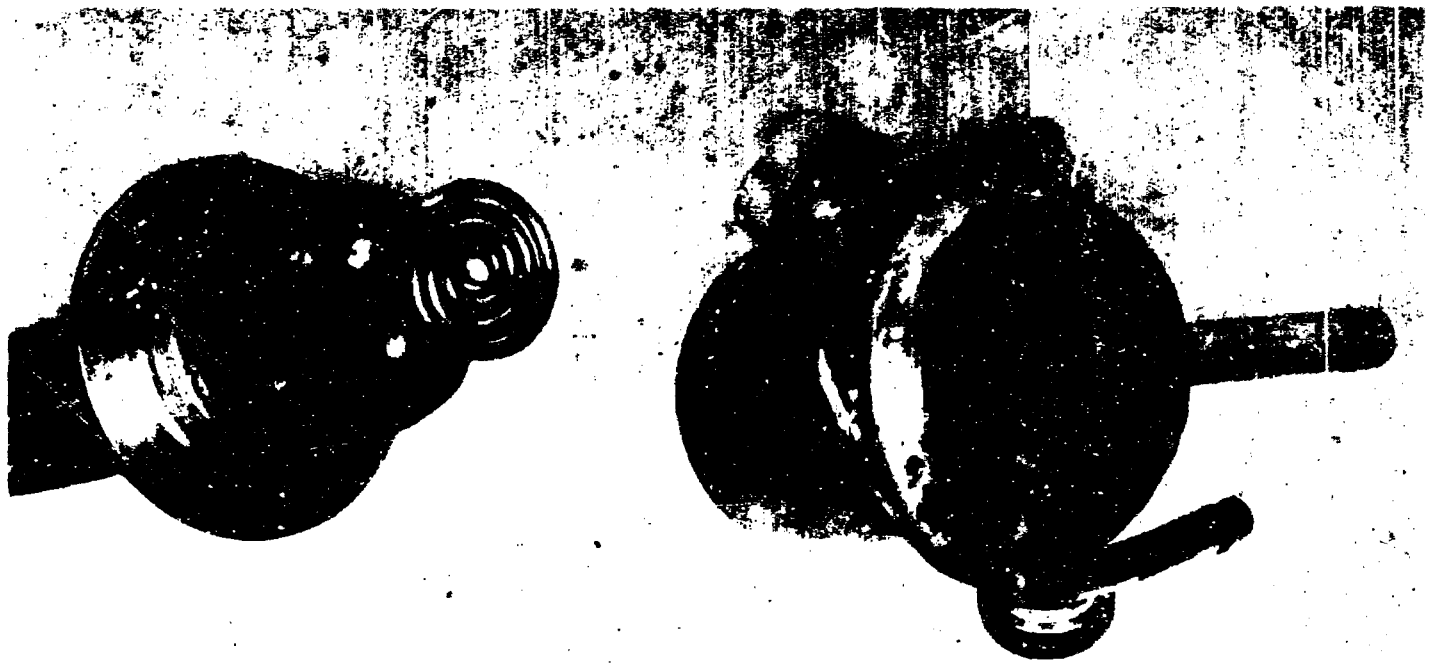

Figure 94 Disassembled View of Coating Repair Unit

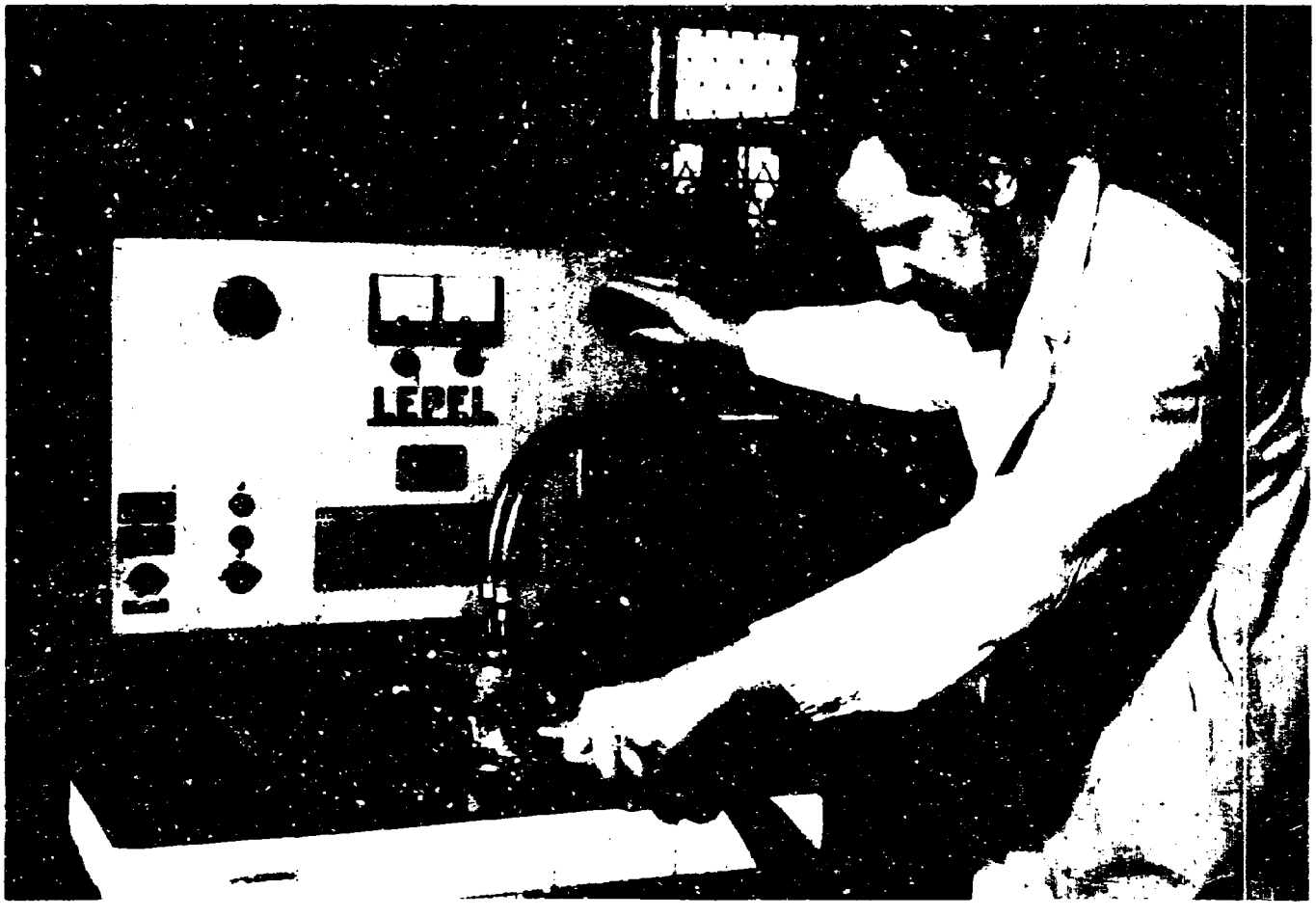

Figure 95 Portable Coating Repair Unit

These results indicate that quite good protectiveness can be expected of field repaired coatings, although the lifetimes demonstrated are not equivalent to that of as-coated or furnace repaired coatings. However, it is expected that further equipment refinement and repair processing parameter studies will result in additional improvement in the lifetimes of coatings repaired with this or similar units.

o. Coating of Mechanical Fasteners

If large coated structures are to be used, it will probably be necessary to join coated subassemblies with mechanical fasteners. At least two options are available. In one case the nuts and bolts or rivets may be coated as individual parts, then assembled, and finally repair coated (with nuts and bolts, repair coating may not be necessary). Another choice would be to assemble the coated subassemblies with uncoated fasteners, and then locally coat the assembled fastener. There are a number of advantages and disadvantages with either scheme.

Several, small, simulated, mechanically-fastened joints were furnished by the Standard Pressed Steel Company for coating studies. One joint consisted of two sheets and a thick washer fastened with a 1/8-inch rivet. Another consisted of two sheets, two thick washers (one of which was countersunk), and a flush-head 10-24 bolt and hex nut. The third joint was similar to the second except that a hex-head bolt was used in place of the flush-head bolt. All components were made of Cb-752 alloy.

One flush-head and one hex-head bolt assembly were coated with the Si-20Cr-20Fe-10VSi_2 composition. Slurry was applied to the bolt holes in the sheet and washers, and to the shank of the bolt. The joints were then assembled, tightened to a torque of 25 in-lb and spray-coated with slurry. Additional slurry was painted at the intersections of all mating parts. After the assemblies were fired, they were tested by slow cycling. The assembly with the hex-head bolt developed two spot failures on the washers at the end of four cycles. The flush-head bolt assembly developed two spot failures on the side on one washer and the end of the nut after nine cycles. No failures were noted in any of the faying surfaces or on the threads. Attempts to unfasten the nut from the hex-head bolt resulted only in shearing of the bolt with no loosening of the threads.

The flush-head joint was sectioned for metallographic examination after the nine-hour slow cyclic exposure; the results are shown in Figure 96. All surfaces of the components are coated, and where parts mate, the coating formed a brazed joint. The thinness of the coating in the threaded area results in excessive clearance since these fasteners were provided with allowance for a 3-mil-thick coating. When it is desired to coat a threaded fastener after assembly with a fused silicide-type coating, it may be preferable to make fasteners with normal clearances (no allowance for coating buildup). This procedure would provide a stronger joint due to the increased bearing area, as well as improved capillary action which would cause the small void spaces to be completely filled.

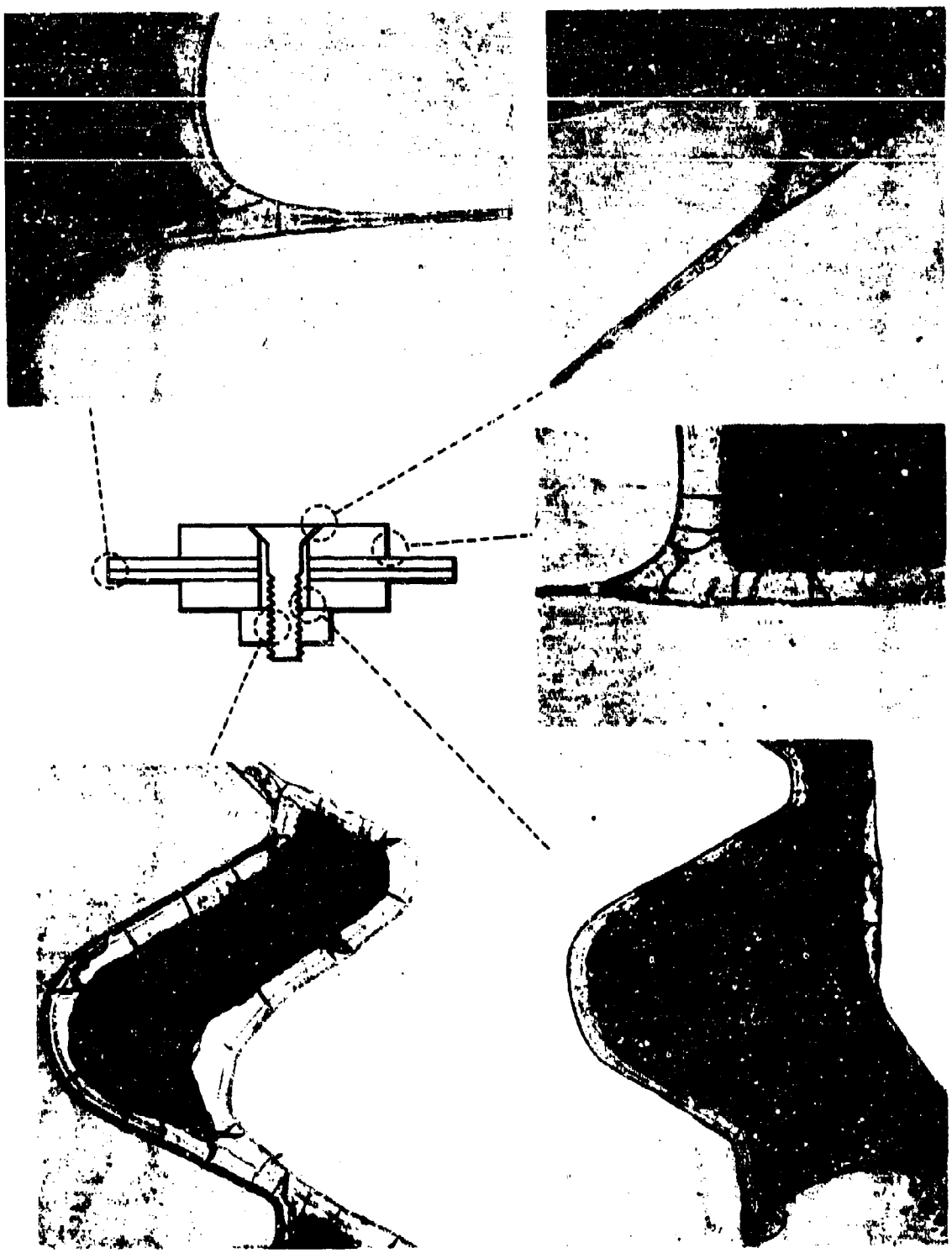

Figure 96 Coated and Oxidized Cb752 Flush-Head Bolted Joint (70X).

In preparing the flush-head joint for photomicrographs, the opposing coated surfaces made it impossible to polish in the preferred direction (toward the edge) for both surfaces. Therefore considerable chipping of the coating occurred in certain areas, such as where the threads of nut and bolt engaged. The pictures are therefore not completely representative of the actual case.

A 1/4-20 Cb752 bolt was coated with Si-20Cr-20Fe slurry by spraying while the bolt was rotated about its axis. This resulted in a relatively uniform green coating. After vacuum firing in the normal manner the bolt was found to be very uniformly coated as shown in Figure 97.

A 10-24 nut and bolt were subsequently coated using the same coating but in this case the slurry was applied with a brush in a deliberately nonuniform manner. The object here was to determine if a uniform coating would result from the wetting action of the coating during the fusion operation. Metallographic inspection of the coated nut and bolt after fusion shows that this is exactly what has happened. This is shown in Figure 98. Before sectioning of the nut and bolt they were readily assembled and disassembled with no difficulty.

Several additional Cb752 10-24 nuts and bolts were coated with the Si-20Cr-20Fe composition for the purpose of demonstrating the wettability and flowability of this system. The slurry was applied by brush in a deliberately nonuniform manner. However the coating thickness was controlled by applying a known total weight of slurry to each part, which, when apportioned on a unit area basis, resulted in the desired thickness. After firing, the coating appeared to be uniform and the fasteners could be readily assembled and disassembled. Photographs of the green coated, fused, and assembled fasteners are shown in Figure 99.

p. Improvement of Coating Protectiveness at Sheet Edges

Experiments were initiated in an attempt to improve the protectiveness of the fused silicide type coating at sheet edges. The first approach tried was the most direct and consists of double-coating the edges in an effort to build up the coating thickness at these points, since it has been demonstrated that oxidation life is directly related to coating thickness. A group of D43 coupons were coated with the Si-20Cr-20Fe composition. After vacuum firing, the edges of individual coupons were brush coated with slurries of Si-20Cr-20Fe, Si-20Cr-5Ti, Si-20Cr-20Fe-10Ta, and Si-20Cr-20Fe-10Mo, and refired. Photomicrographs of these specimens, shown in Figure 100, indicate that the desired result was generally achieved.

The effect of double coating sheet edges with the Si-20Cr-20Fe coating on the slow cyclic oxidation life was determined for three initial coating thicknesses (10, 20, and 30 mg/cm^2). The results, given in Table XXVIII, indicated no significant change in oxidation life as a result of the double coating procedure.

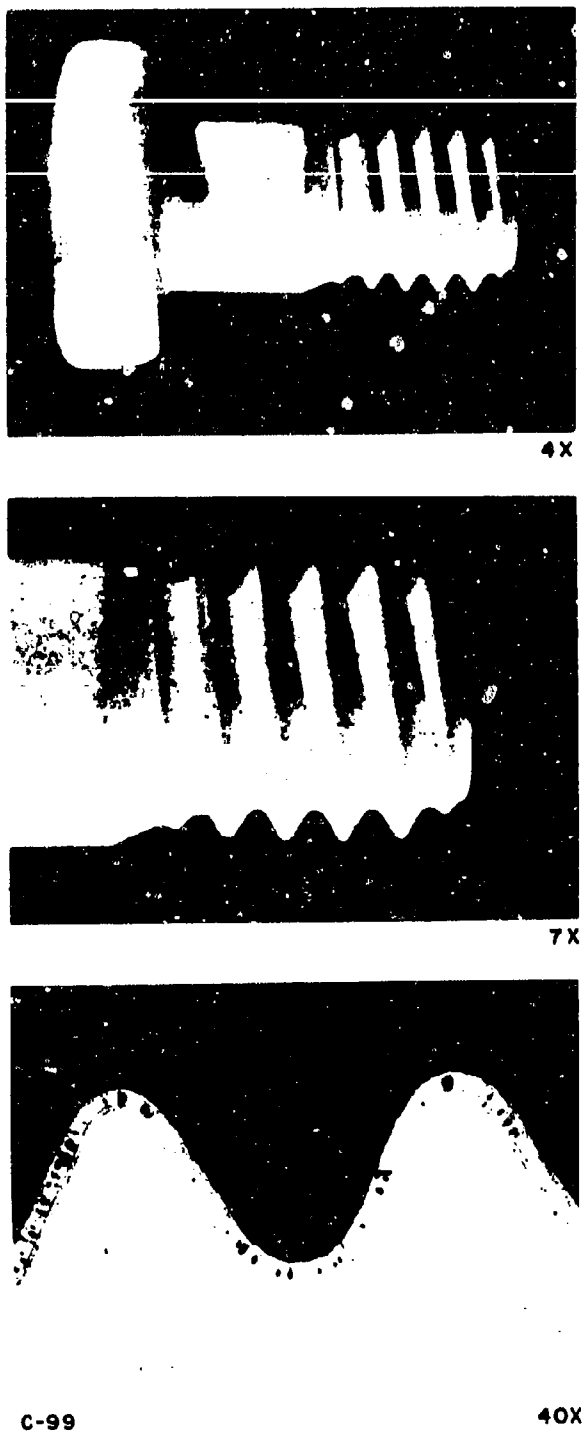

Figure 97 Cb752 Bolt (1/4-20) Spray Coated With Si-20Cr-20Fe and Fused in Vacuum

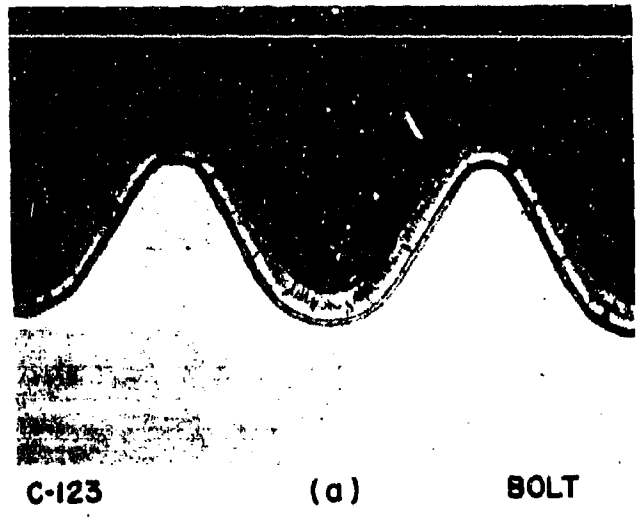

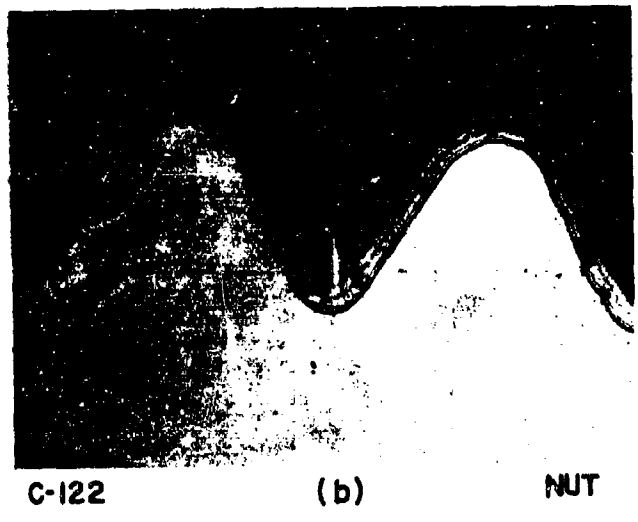

Figure 98 Photomicrographs of Sections Through Cb752 Nut and Bolt (10-24) Brush Coated With Si-20Cr-20Fe and Fused in Vacuum (40X).

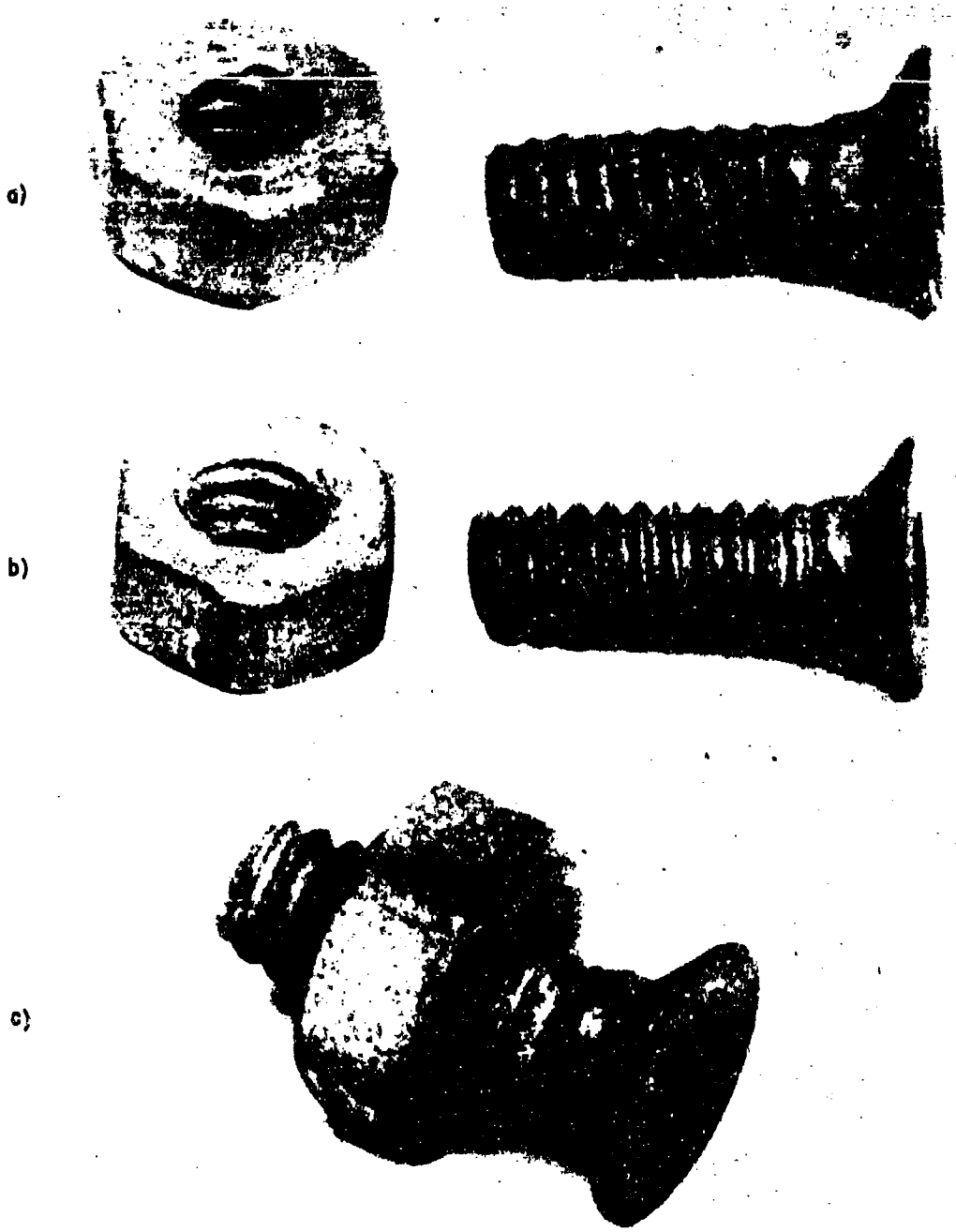

Figure 99 Cb752 - 10-24 Nut and Bolt Coated With Si-20Cr-20Fe Fused Silicide. (a) Brush Coated With Slurry, (b) After Fusion (c) Nut and Bolt assembled. All Photographs Approximately 6X.

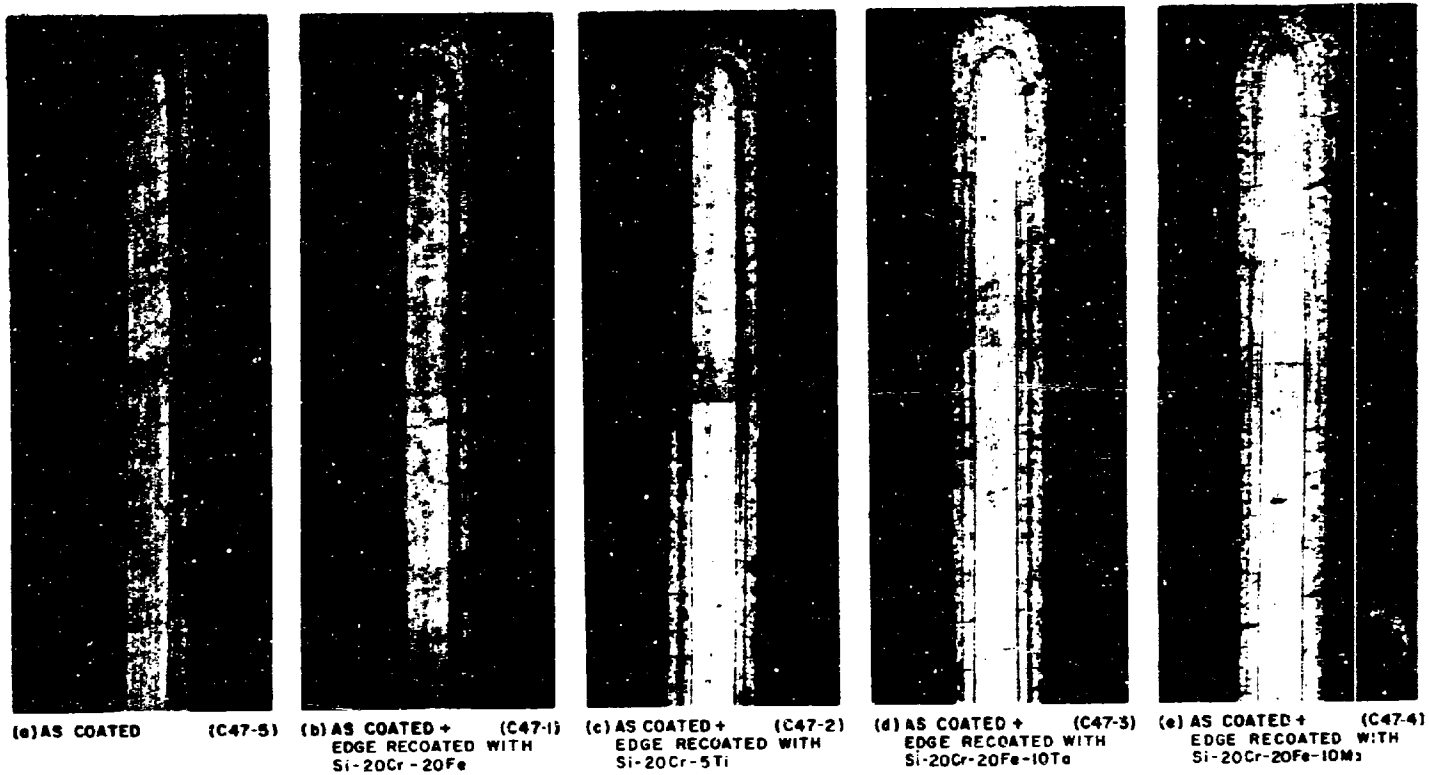

Figure 100 Photomicrographs of Si-20Cr-20Fe Coated D43 With Edges Recoated With Various Fused Silicides (40X). (Reduced 35% in Reproduction)

TABLE XXVIII

EFFECT OF DOUBLE COATING SHEET EDGES ON SLOW CYCLIC OXIDATION LIFE OF Si-20Cr-20Fe COATING ON D43 ALLOY

Coating Thickness (mg/cm^2)	Slow Cyclic Oxidation Life No. of 1 Hour Cycles to Failure	
	As Coated	Edges Recoated
10	33, 33	30, 33
20	92, 97	86, 86
30	57, 57	57, 57

q. Sealing of Coating Cracks

Preliminary experiments were performed which aimed at sealing coating thermal expansion cracks by the deposition of silicon from low melting silicon alloys. D43 specimens coated with both Si-20Cr-20Fe and Si-20Cr-5Ti were subsequently overcoated with Al-11Si, Sn-5Si, Ag-4Si or Cu-10Si and refired at 1200, 1400, 1550, and 1750°F respectively. These specimens were examined metallographically, and it does appear as if crack sealing is being effected with the Cu-Si alloy. This is shown in Figure 101. The top photomicrograph shows a normal, as-fired, fused silicide coating in which the crack spacing is approximately equal to the coating thickness. The bottom photomicrograph shows an identical coating which was subsequently overcoated with the Cu-10Si and refired at 1750°F for ten minutes. It is obvious that the latter coating has substantially fewer cracks.

Subsequent efforts to perfect this crack-sealing procedure by variation of the processing parameters were not successful in that complete crack elimination was not achieved and this study was therefore not pursued any further. No oxidation tests of crack sealed specimens were performed.

r. Braze-Coating Studies

Brazing and coating a columbium alloy structure by means of conventional brazing and pack cementation coating procedures requires at least two high-temperature processing cycles. To keep the number of cycles to this minimum value, it would be necessary to employ a single-cycle pack coating, none of which has been shown to be exceptionally protective or reliable to columbium. If a two-cycle pack coating such as the Ti-Cr-Si vacuum pack coating is selected, then a three-cycle process results. In general, with pack coatings there are also potential problems in compatibility between the braze and the coating, and problems of coating in faying surfaces.

C-124-1 Si-20Cr-5Ti COATING ON D43 AS COATED 300X

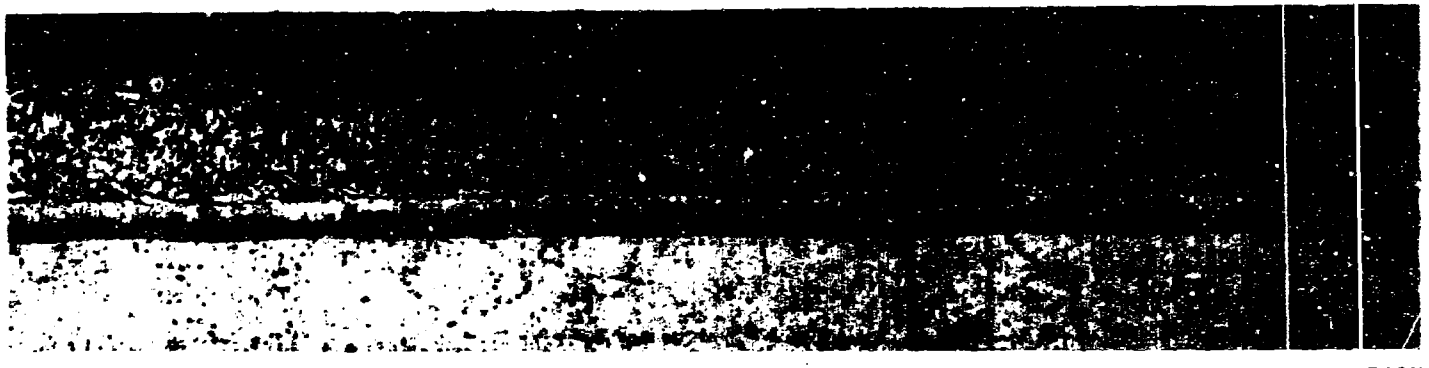

C-124-4 Si-20Cr-5Ti COATING ON D43 SEALED WITH Cu-10Si OVERCOAT 300X

Figure 101 Sealing of Coating Thermal Expansion Cracks

It has been shown (1) that it is feasible to coat and braze columbium alloy parts simultaneously in a single process cycle with the fused silicide coating. The advantages inherent in such a system are apparent and need not be described here. However, since the as-formed fused silicide coating consists of a mixture of intermetallic compounds, this coating shares in common with other coatings a characteristic brittleness which would preclude its use as a braze for specific types of joints or applications. For example, because of the high wettability and reactivity of the fused silicides, they tend not to form appreciable fillets, and it would therefore be doubtful if sound T joints could be made.

A double-lap-joint tensile test specimen was selected for evaluation of the fused silicide as a single-cycle combination coating-braze. The specimen geometry, shown in Figure 102, resulted from efforts to obtain a low shear-to-tensile area ratio so that failure would occur in the braze. The ratio for these specimens is 2.6:1. Initially, some specimens were assembled using various clearances and coating techniques. It was soon determined that the best joints resulted when the clearances were minimum and when no braze alloy was applied to the joint surface.

These specimens were made from Cb-752, because the thicker material was available in this alloy. The couplers were made by spot-welding three pieces of 0.032-inch sheet together. All parts were chemically cleaned in an acid bath consisting of equal parts of HNO_3, HF and H_2O. After assembly, the joint was sized by the application of pressure, and the entire sample was spray-coated with a Si-20Cr-5Ti slurry. Additional slurry was applied to the fillet areas of the joints by hand brushing. No slurry was applied to the joint surfaces. The coating-braze firing cycle was at 2580°F for one hour in vacuum.

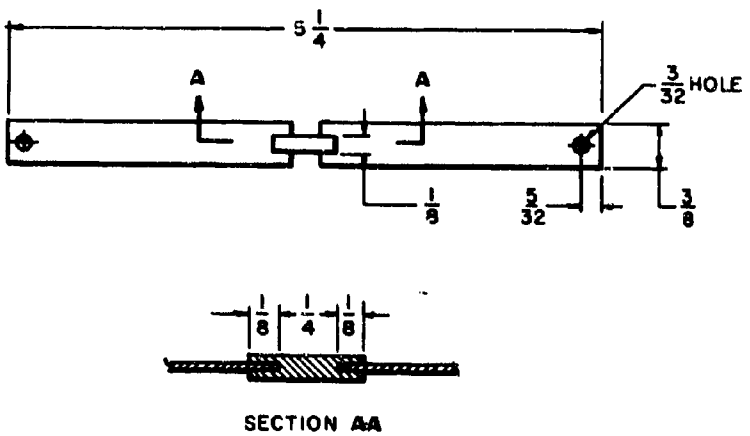

Figure 102 Double-Lap Brazed Joint Tensile Test Specimen

The apparatus used for the pull tests is shown schematically in Figure 103. At the start of the test the entire weight is supported by the hydraulic jack; at this point the balance reads 200 pounds. The power supply is then adjusted to yield the desired temperature. The return valve in the jack is then cracked open to permit the oil to bleed slowly from the main cylinder, thereby increasing the load on the sample while decreasing the load on the jack and balance. The breaking load is the difference between the initial load on the balance and the load just before failure of the sample. The rate of loading was about one lb/sec. At test temperatures from 1500 to 3000°F the sample was coupled directly to the coil, and the temperature was measured optically, by conservatively assuming a spectral emittance of 0.7 (at 0.65 micron). At temperatures below 1500°F, a silicon carbide susceptor was used, and the temperature was measured by a thermocouple. Three samples were tested at each of seven temperatures from room temperature to 3000°F. The results are given in Table XXIX and Figure 104.

In these tests, in contrast to earlier ones performed, and as a result of the reduction of the tensile-to-shear area ratio, all except one sample failed by shearing of the brazed joint; the values given are therefore ultimate shear stresses.

The range of test values at each temperature is probably attributable primarily to the fact that minor imprecisions in the specimens may result in appreciable errors in the shear area, or in misalignment, which can impose torsional or bending stresses on the braze in addition to the shear stresses. The data do indicate, however, that the Si-20Cr-5Ti coating braze has significant shear strength at all temperatures from room temperature to 3000°F.

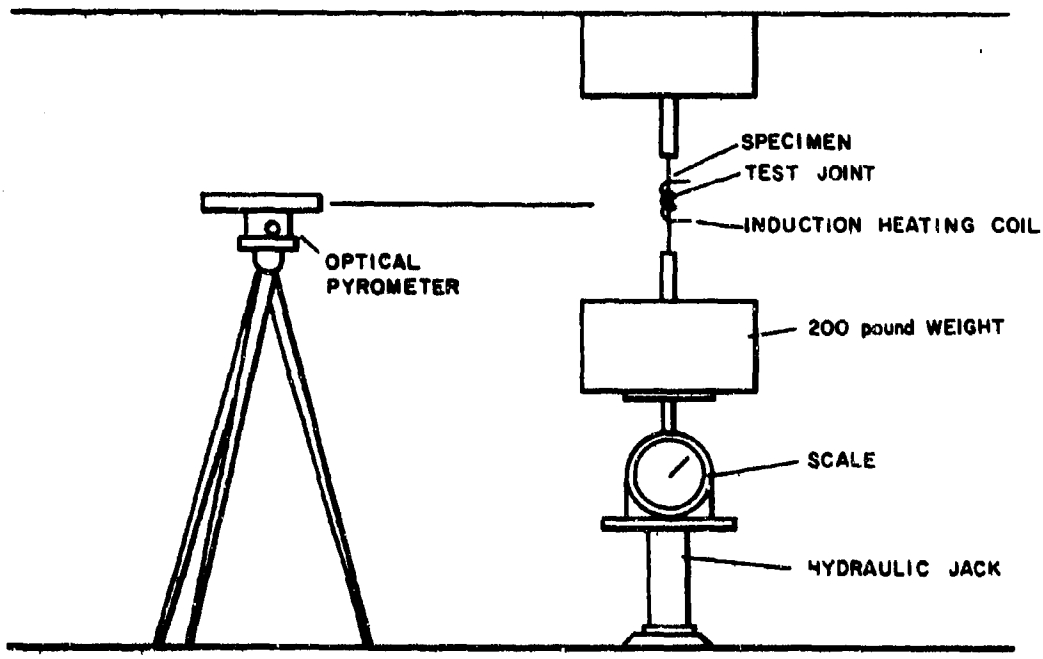

Figure 103 Schematic Arrangement of Elevated Temperature Pull Test Apparatus.

TABLE XXIX

ULTIMATE SHEAR STRENGTH OF Si-20Cr-5Ti COATING BRAZE

Test Temp. (°F)	Ultimate Shear Stress (psi)	Average Ultimate Shear Stress (psi)
RT	2710 3290 6420	4140
500	2840 4360 4860	4010
1000	3710 5100 6360	5060
1500	3480 7550 7840	6290
2000	3200 5870 6420	5160
2500	5540 5890 6020*	5820
3000	1340 1920 2180	1820

*Tensile failure at 15,700 psi T.S.

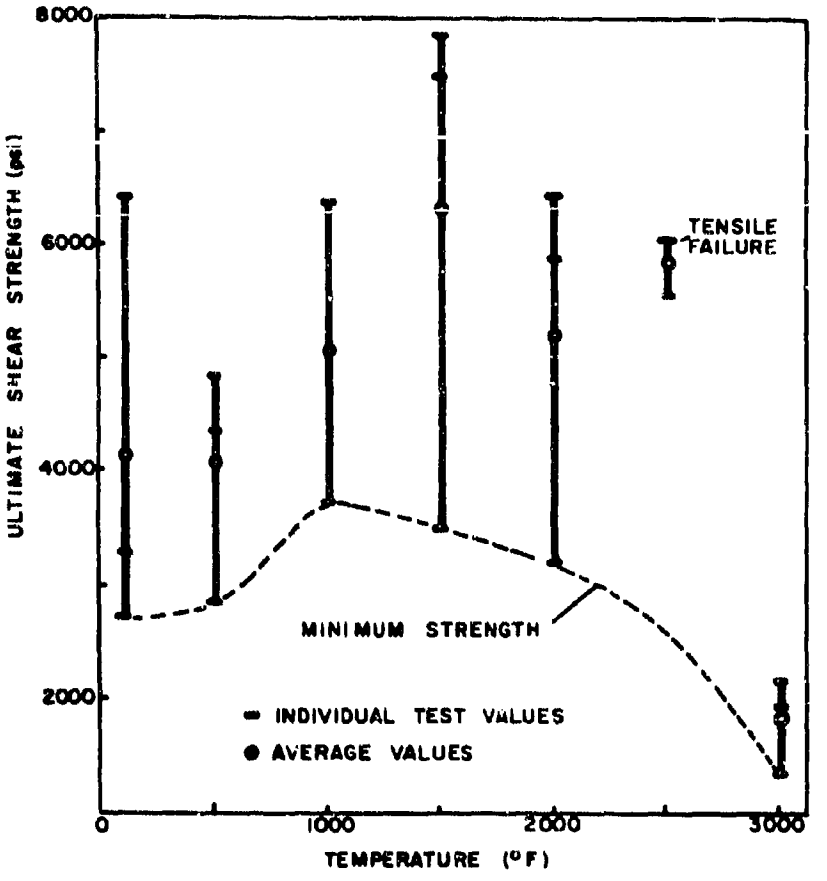

Figure 104 Ultimate Shear Strength of Si-20Cr-5Ti Coating-Braze Versus Temperature in Air (Cb 752 Substrate).

s. Duplex Fused Slurry Coating Systems

The single-cycle fused slurry silicides have demonstrated excellent protectiveness along with other attributes not commonly shared by other types of coatings. There are, however, potential advantages to be derived from a duplex slurry coating process even though it means some sacrifice in practicality. One objective of an investigation of duplex process is to determine if coatings with even better overall oxidation resistance could be obtained by this technique. This is possible since it is believed that resistance to some environments or test procedures is more related to the chemistry and structure of the lower coating layers, while in other environments the outermost layer is obviously of paramount importance. Another possiblity is that of using the first coating as a combination coating braze and the second coating as the highly oxidation-resistant silicide former. In this kind of system, a little more freedom of choice is permitted in that the braze need not be highly oxidation resistant but should form the basis for a highly modified oxidation resistant silicide layer to be

subsequently applied. This permits the use of somewhat more ductile braze alloys since they can be based on elements other than silicon.

Two alloys that have been cursorily evaluated as brazes for columbium alloys (8), and which may form a basis for a duplex fused slurry, coating-braze system, are Ti-8.5w/oSi and Ti(30-50)w/oCr. In view of the considerable developmental and evaluation effort directed in recent years at the Ti-Cr-Si duplex vacuum pack coating (9) and its demonstrated protectiveness, the initial efforts here focused on the Ti-Cr braze alloys in combination with Si-20Cr and Si-20Ti base overcoats.

The specific aim in the work undertaken initially was to braze and coat with a Ti-45Cr alloy in a cycle including a heat treatment equivalent to that used in the Ti-Cr-Si pack coating first cycle, so as to obtain a similar chemistry and morphology. After this step, an overcoat of Si-Cr, Si-Ti, or Si-Cr-Ti was fused on to result in an overall coating chemistry and morphology similar to that of the duplex vacuum pack coating. It was expected that this coating would uniformly cover all faying surfaces and recesses to any size part in a simpler, more economical, and practical way, while at the same time serving to braze detail parts into a unitized assembly.

Initial efforts were limited to a few exploratory experiments aimed at obtaining a fused Ti-Cr alloy coating. Coatings with a uniform appearance were obtained, but metallographically they were observed to be porous. Despite this porosity, however, a fused Ti-Cr coating overcoated with a fused Si-20Cr layer had a lifetime of 88 hours at 2500°F, including 44 thermal cycles.

A Ti-45Cr slurry further alloyed with two percent Ni was fired on a D43 substrate at 2300°F for 15 minutes. A dense uniform microstructure resulted, as shown in Figure 105. Several additional identical runs, however, produced coatings that were not fully dense.

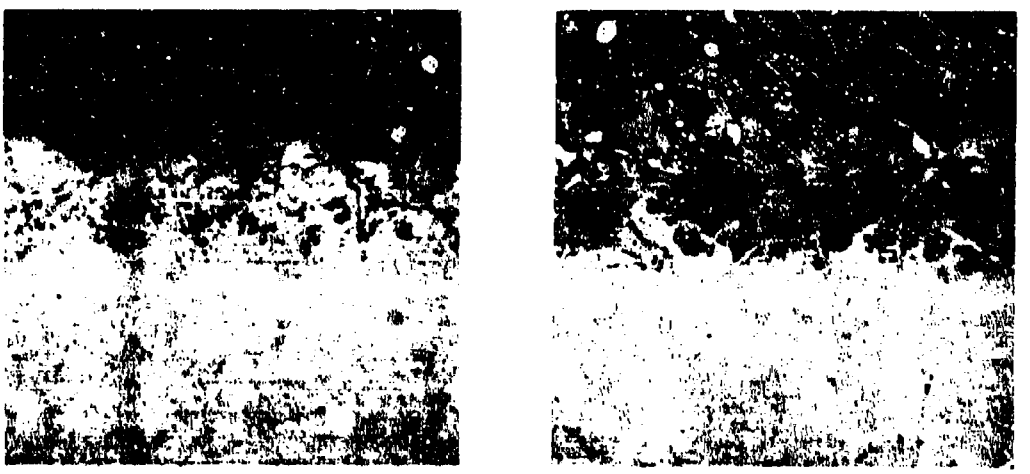

Figure 105 Ti-45Cr-2Ni Slurry Fired on D43 Alloy at 2300°F for 15 Minutes.

Fully dense Ti-45Cr coatings were obtained readily and reproducibly in either vacuum or argon by firing at 2600°F. Apparently all earlier efforts resulted in porous coatings because fusion had not occurred rather than because of vaporization.

Two batches of duplex fused (Ti-45Cr)-(Si-20Cr) coatings were made, but they were not satisfactory in slow cycling tests, both having characteristic lifetimes of but a few hours. It is believed that the Si-20Cr coating was excessively heavy in both cases in relation to the Ti-Cr coat. Attempts to apply heavier Ti-Cr coats (approximately 20 mg/cm^2 or more) encountered two principal difficulties. During the firing of these coatings, the molten coating tended to run to the bottom of the piece due to gravity. With the heavier coatings, brazing of the coupons to the suspension wires was also a problem. Substitution of quartz or alumina for tantalum for suspension purposes alleviated the latter problem, but the run-off problem was not readily overcome. Some success was achieved by revising the firing schedule to permit some initial reaction below the melting point, followed by a short excursion above the melting point, and then by a diffusion treatment. However, the processing parameters necessary to produce satisfactory and reproducible results have not been determined.

The photomicrographs in Figure 106 show a 20 mg/cm^2 Ti-45Cr coating after various heat treatments.

As an alternative process and as a demonstration of the potential usefulness of the duplex (Ti-Cr)-(Si-Cr) fused slurry coatings, a small batch of (Ti-Cr) vacuum pack - (Si-20Cr) fused slurry duplex coatings was prepared and tested. The Ti-Cr was deposited from a prealloyed Ti-50Cr KF activated pack in vacuum at 2300°F for eight hours. The Si-20Cr was sprayed over this and fused for 30 minutes at 2580°F in vacuum. The coating was very uniform in appearance. Two samples tested in the slow cycling furnace had lifetimes of 7 and 42 hours. Although this represents a considerable spread, the 42-hour lifetime indicates a significant potential for this system and for the all-slurry system as well. The combined pack slurry coating has potential merit on its own since it permits pack coating of detail parts with Ti-Cr alloy, followed by spot welding into an assembly, and finally by slurry coating the assembly with the Si-20Cr alloy. The detail parts are easier to pack coat since they are smaller and less intricate and have no faying surfaces. After assembly, faying surfaces could be readily coated by the liquid Si-20Cr alloy and the improved reliability associated with the fused silicides should then result.

It was determined, experimentally, that the maximum amount of Ti-50 w/o Cr that could be uniformly applied as a fused slurry on D43 was approximately 10 mg/cm^2. Heavier slurries tended to run off due to gravity effects. D43 coupons, precoated with a 10 mg/cm^2 of Ti-50 w/o Cr slurry, were subsequently coated with 5, 10, 15, and 20 mg/cm^2 of Si-20Cr. The resultant microstructures are shown in Figure 107.

Based primarily on these microstructures, a group of D43 coupons were coated with 10 mg/cm^2 of Ti-50w/o Cr, followed by 20 mg/cm^2 of Si-20Cr. Results of slow cyclic and high-temperature cyclic oxidation tests of these specimens are given in Table XXX.

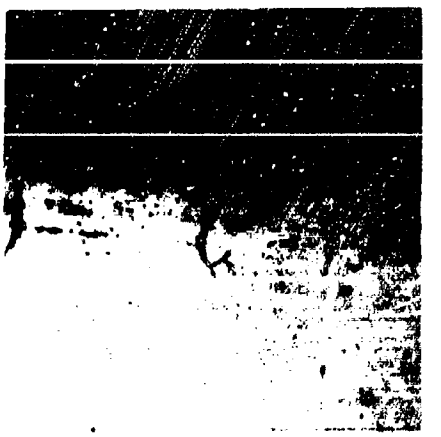

(a) 2600°F - 15 minutes (356-5)

(b) 2600°F - 15 minutes + 2600°F - 1 hour (356-1)

(c) 2600°F - 15 minutes +2500°F - 2 hours (356-2)

(d) 2600° F - 15 minutes +2400° F - 2 hours (356-3)

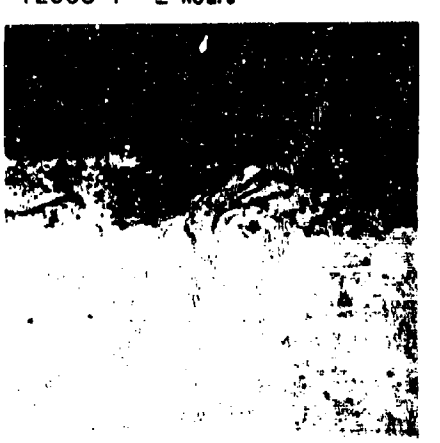

(e) 2600°F - 15 minutes +2300°F - 8 hours (356-4)

Figure 106 Ti-45Cr Slurry Coating on D43 After Various Diffusion Treatments (400X).

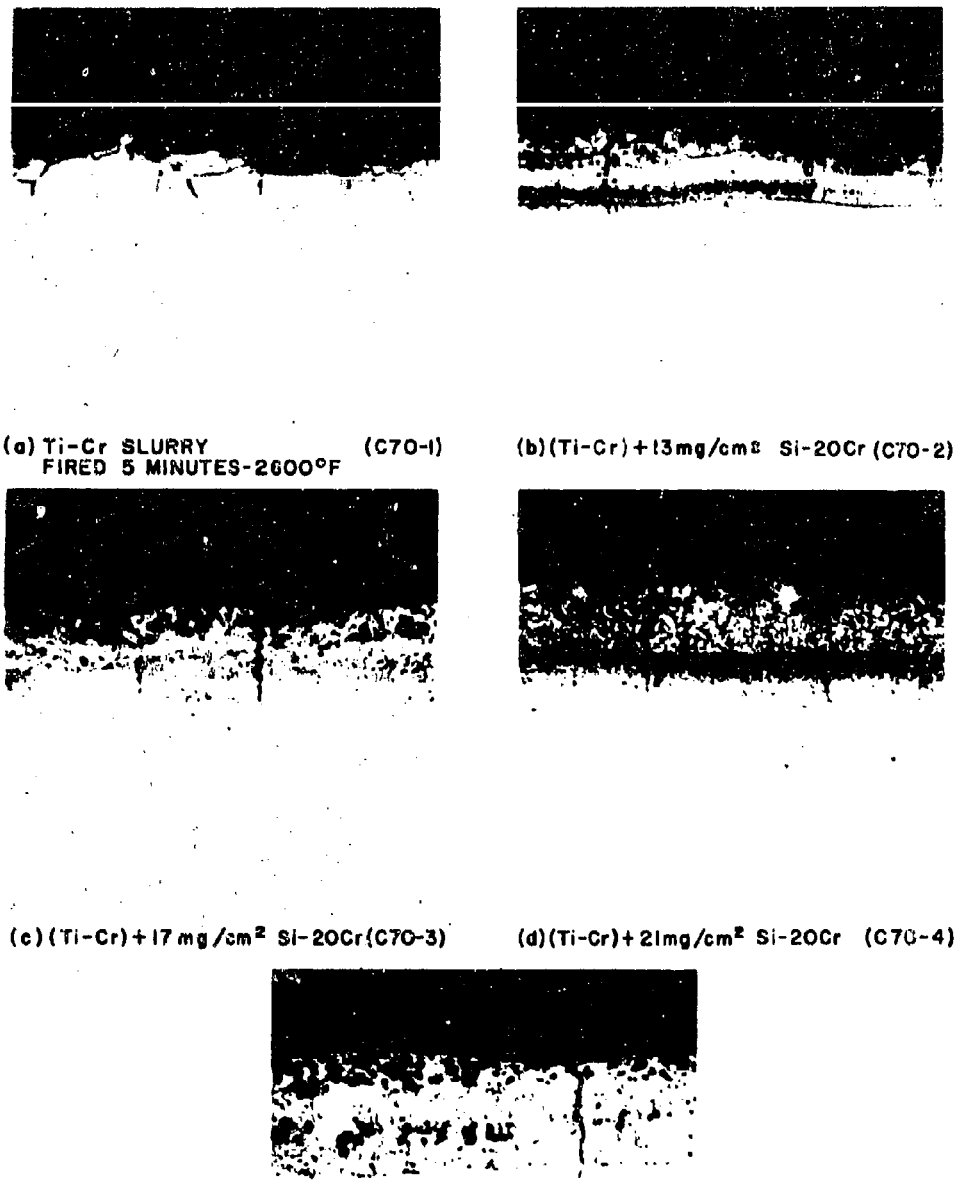

Figure 107 Photomicrographs of (Ti-Cr)-(Si-Cr) Duplex Fused Silicide Coatings on D43 (300X).

TABLE XXX

OXIDATION TEST RESULTS OF (Ti-Cr)-(Si-Cr) DUPLEX FUSED COATINGS ON D43 ALLOY

Slow Cyclic Oxidation Life (No. of 1-hour Cycles to Failure)	2400°F Cyclic Life (No. of 1-hour Cycles to Failure)	2500°F Cyclic Life (No. of 1-hour Cycles to Failure)
22[e]	26[e]	33[s]
22[s]	49[e]	40[s]
22[e]	70[e]	80[e]
30[e]	91[e]	80[s]
30[e]	119[e]	

[e] Edge Failure

[s] Surface Failure

These results indicate that this system has significant potential, particularly as a combination coating-braze. However, a great deal of additional work is necessary to optimize processing parameters, refine application techniques, and to thoroughly characterize its performance.

Earlier efforts described previously concentrated on forming uniform 4-mil-thick Ti-(40-60w/o Cr) coatings using mixtures of elemental powders in lacquer as the slurry. The primary difficulty involved gravity run-off of coatings of the desired thickness.

Subsequent efforts were aimed at exploring Ti-Cr base slurries with from 10 to 30 w/o additions of the refractory metals Cb, V, Mo and Ta. A number of such compositions, comprising mixtures of the elemental powders in lacquer, were applied to D43 sheet coupons by spraying and were subsequently fused in vacuum under varying conditions. The purpose of these tests was to determine suitable parameters for the production of a uniform, dense coating with a thickness of 3 to 4 mils. The results of these trial fusion runs are given in Table XXXI.

In general, with the systems studied, the fusion temperature was apparently quite critical. If too low a temperature was used, incomplete melting resulted. If too high a temperature was used boiling and/or gravity run-off occurred.

TABLE XXXI

TRIAL RUNS OF FUSED ALLOY UNDERLAYMENTS FOR DUPLEX FUSED COATINGS

Sample No.	Applied Composition	Fusion Treatment in Vacuum (°F)	Visual Examination		Metallographic Observations
			Surface	Gravity Blobbing	
30-1	40Ti-40Cr-20V	2730°, 5 min.	Shiny, smooth	Yes	Bumps, blow holes
30-2	40Ti-40Cr-20V	2550°, 5 min.	Shiny, small bumps	No	Good, except bumps
30-3	40Ti-40Cr-20V	2460°, 5 min.	Dull, rough	No	Porous
30-4	40Ti-40Cr-20Mo	2730°, 5 min.	Satin	No	Uneven surface
30-5	40Ti-40Cr-20Mo	2550°, 5 min.	Gray, smooth	No	Porous
30-6	40Ti-40Cr-20Mo	2910°, 5 min.	Gray, smooth	No	Bumps, blow holes
30-7	40Ti-40Cr-20Cb	2730°, 5 min.	Satin	Yes	Bumps
30-8	40Ti-40Cr-20Cb	2550°, 5 min.	Shiny, smooth	Yes	Good even coating
30-9	40Ti-40Cr-20Cb	2460°, 5 min.	Dull, rough	No	Poor coating
32-1	40Ti-45Cr-10V	2730°, 10 min.	Shiny, smooth	Yes	Thin due to blob
32-2	40Ti-45Cr-10V	2550°, 10 min.	Satin, bumpy	No	Blow holes
32-3	40Ti-45Cr-10V	2640°, 10 min.	Shiny, small bumps	Yes	Thin due to blob
32-4	45Ti-45Cr-10Cb	2730°, 10 min.	Shiny, smooth	Yes	Thin due to blob
32-5	45Ti-45Cr-10Cb	2550°, 10 min.	Satin, incomplete melt	No	Rough blow holes
32-6	45Ti-45Cr-10Cb	2640°, 10 min.	Shiny, smooth	Yes	Thin due to blob
32-7	45Ti-45Cr-10Ta	2730°, 10 min.	Shiny, smooth	Yes	Thin due to blob

TABLE XXXI (Cont)

TRIAL RUNS OF FUSED ALLOY UNDERLAYMENTS FOR DUPLEX FUSED COATINGS

Sample No.	Applied Composition	Fusion Treatment in Vacuum (°F)	Visual Examination		Metallographic Observations
			Surface	Gravity Blobbing	
32-8	45Ti-45Cr-10Ta	2550°, 10 min.	Satin, incomplete melt	No	Rough, holes
32-9	45Ti-45Cr-10Ta	2640°, 10 min.	Shiny, smooth	Yes	Thin due to blobbing
37-1	45Ti-25Cr-30V	2730°, 10 min.	Dull satin with bumps	No	Lumpy, holes
37-3	45Ti-25Cr-30V	2910°, 15 min.	Dull satin with bumps	No	Lumpy, holes
37-5	45Ti-25Cr-30V	2570°, 1 hr.	Gray, incomplete melt	No	Porous
37-7	45Ti-25Cr-30V	2650°, 15 min.	Gray, small bumps	No	Porous
37-8	45Ti-25Cr-30V	2595°, 15 min.	Shiny, smooth	No	Blow holes
37-2	45Cr-25Ti-30V	2750°, 10 min.	Light gray, bumpy	No	Lumps, blow holes
37-4	45Cr-25Ti-30V	2910°, 15 min.	Shiny, lumpy	No	Lumps, blow holes
37-6	45Cr-25Ti-30V	2570°, 1 hr.	Light gray, incomplete melt	No	Porous
37-12	45Cr-25Ti-30V	2650°, 15 min.	Gray, smooth	No	Lumpy, blow holes
37-13	45Cr-25Ti-30V	2705°, 15 min.	Gray, smooth	No	Lumpy, blow holes

The results of an initial metallographic examination of these samples is also included in Table XXXI. In many cases surfaces that appeared shiny and smooth visually were thin and rough when viewed microscopically. Therefore one must not rely to any great extent on visual observations.

The most satisfactory coatings of the group were the 40Ti-40Cr-20V, 40Ti-40Cr-20Mo, and 40Ti-40Cr-20Cb, all fired at 2550°F. The first two of these exhibited no gravity run-off (blobbing), but the coatings were not perfectly smooth and uniform. The 40Ti-40Cr-20Cb coating was very smooth and had the most uniform microstructure. However, this coating did blob.

It is believed that these are three systems which might be fruitfully pursued in any future efforts to produce duplex fused coatings for columbium alloys.

t. Mechanical Property Tests

The purpose of the tests described herein was to determine if the Si-20Cr-20Fe fused silicide coating had any pronounced effects on the tensile properties (especially the ductility) of the Cb752 alloy. Tests were performed on 0.010 and 0.032 inch thick Cb752 alloy, both coated and uncoated, at RT, 1100, 1500, 1850 and 2250°F, and at air pressures of 760, 1, 10^{-1}, 10^{-2}, and 10^{-4} torr. The tensile specimen shape is shown in Figure 108. Tests at 10^{-4} torr were performed in an Instron machine with a Brew vacuum furnace accessory in which the specimens were heated by radiation. All other tests were performed in the reduced pressure mechanical testing unit shown in Figure 109. With this unit the specimens were heated by an external furnace up to temperatures of 1500°F. At 1500°F and above self-resistance heating of the specimens was used. The tests were performed at a strain rate of 0.1 in/in/min, which is the same as that used by BMI (10) in their recent work.

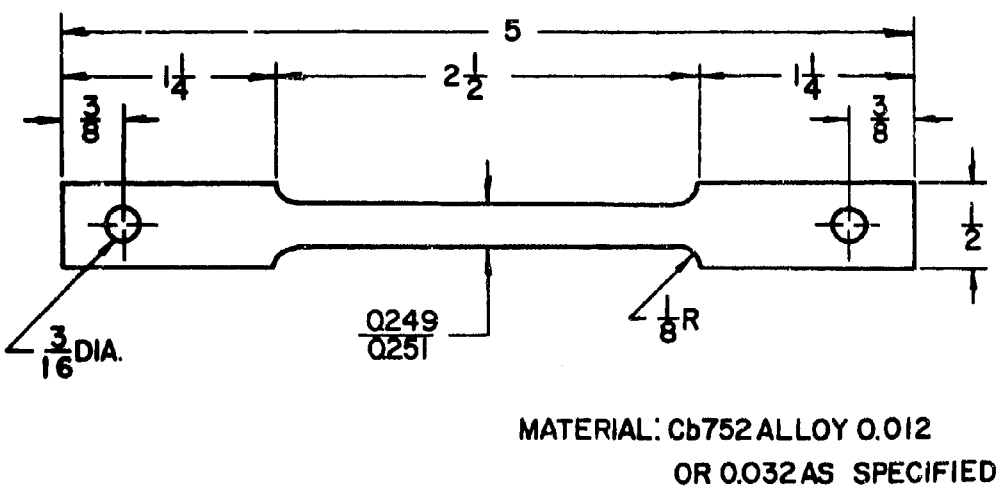

Figure 108 Tensile Test Specimen.

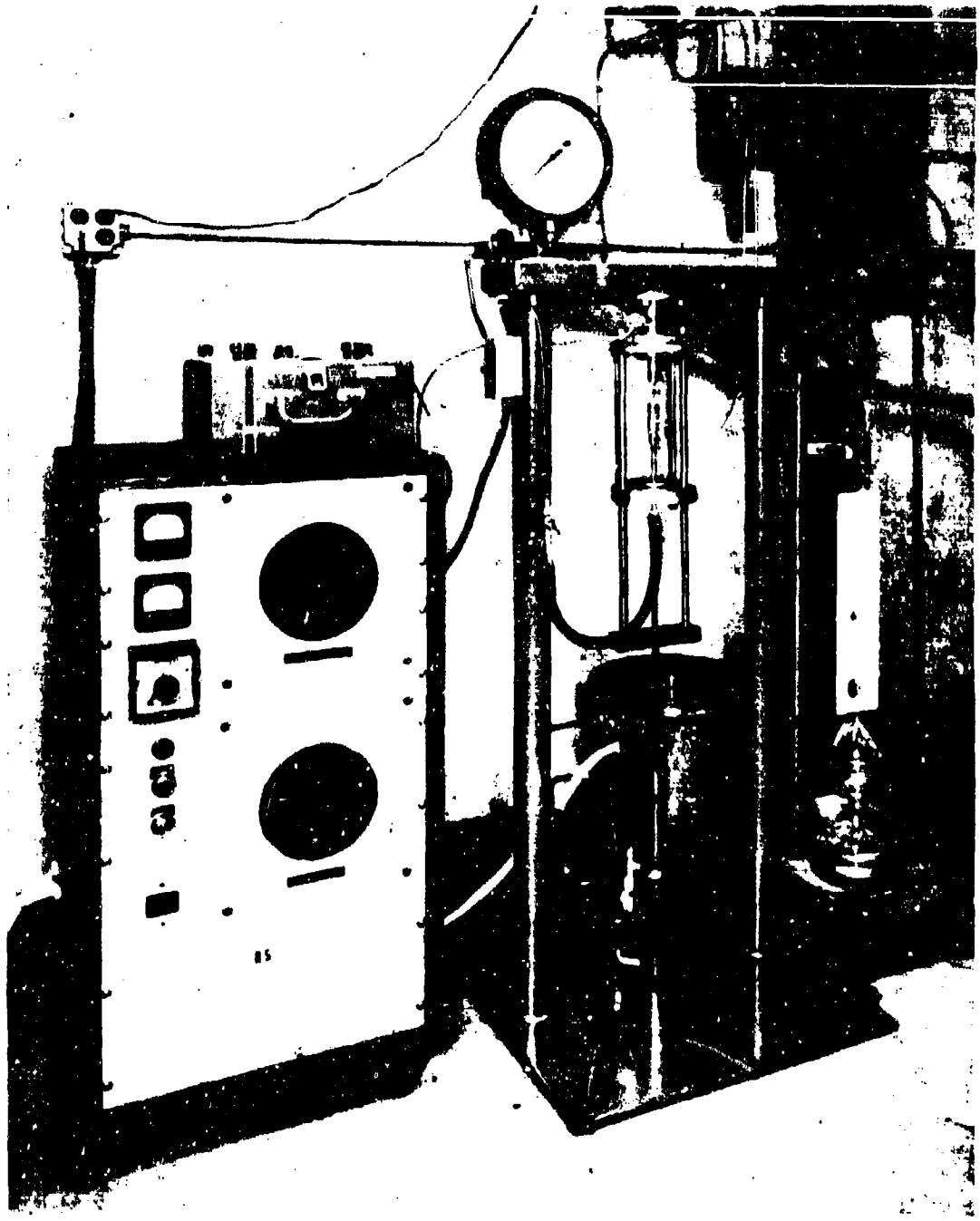

Figure 109 Reduced Pressure Mechanical Testing Unit.

Small gage marks were made with a punch at a spacing of one inch as a basis for elongation measurements. Although it was the elongation that was of primary interest, ultimate tensile stresses were also determined. The results are given in Table XXXII.

The degree of scatter (due to normal variations in properties as well as experimental error) inherent in test data of this type (particularly the elongation measurements) is such that they should be cautiously interpreted. The following observations should therefore be regarded as being somewhat speculative and tentative.

The presence of the fused silicide coating results in a loss of ductility to the 0.012-inch thick Cb752 alloy at temperatures up to and including 1500°F. This loss does not seem to be related to oxidation since it is manifest in vacuum as well as at air pressures up to one atmosphere. This may possibly be a notch sensitivity effect. At temperatures of 1850°F and 2250°F the presence of the coating causes no loss of ductility at pressures up to 1 torr. This may possibly indicate a notch brittleness transition temperature between 1500° and 1850°F. At atmospheric pressure there is a significant loss of ductility and this may be attributable to oxidation as shown in reference (10).

The thicker (0.032 inch) Cb752 alloy displayed greater initial uncoated ductility than the thinner material but it also showed a decrease in ductility at all temperatures (except 1850°F) due solely to the presence of the Si-20Cr-20Fe coating. It is not at all clear if oxidation may affect the ductility of such material when tested in air, since at 1100°F and 2250°F the loss of ductility was less than that experienced in vacuum tests, while at 1500°F and 1850°F the ductility losses were greater than in the vacuum tests.

Some concern has been expressed that attention has not been directed towards the evaluation of the effect of protective coatings on the impact resistance of high strength columbium alloys being developed as potential turbine blade alloys. Although the development of coatings for turbine applications is not specifically one of the major goals of this program, the fused silicide coatings have looked extremely promising in the evaluations at P & W (11) and it was intended to evaluate the effect of these coatings on the low-temperature impact resistance of XB88 and Cb132M. As an initial step, however, small uncoated pieces of each of these alloys were gripped in cantilever fashion in a bench vise and gently tapped with a small hammer. Both alloys shattered. Crude as this test was, there was no evidence that either of these alloys has any measurable impact bend ductility at room temperature.

Additional XB88 material was obtained from Westinghouse. This material had been heat treated to its optimum mechanical property condition. This material also exhibited zero ductility in the "impact test" described above.

TABLE XXXII

ELONGATION AND TENSILE STRENGTH OF Cb752 ALLOY

Temperature (°F)	0.012-Inch Thick Cb752 Alloy						0.032-Inch Thick Cb752 Alloy		
	Uncoated[a] 10^{-4} torr	Coated[b] 10^{-4} torr	Coated 10^{-2} torr	Coated 10^{-1} torr	Coated 1 torr	Coated 760 torr	Uncoated 10^{-4} torr	Coated 10^{-4} torr	Coated 760 torr
Room Temperature	21[c] (86)[d]	10.4 (77)	12 (81)				22.1 (79)	17.4 (79)	
1100	8.7 (59)	5.6 (52)	4.3 (56)	2.3 (52)	2.9 (56)	7 (42)	12.1 (55)	7.4 (52)	10 (47)
1500	8.3 (60)	2.6 (43)	3.8 (61)	3.0 (56)	3.1 (58)	5 (45)	14.3 (54)	9.6 (51)	5 (38)
1850	2.2 (62)	4.3 (50)	4.8 (56)	5.0 (58)	3.5 (55)	1 (42)	11.7 (43)	10 (44)	2 (38)
2250	6.5 (44)	5.2 (35)	3.2 (50)	5.9 (48)	4.3 (48)	1 (42)	28.2 (35)	4.8 (30)	9 (35)

[a] Uncoated material annealed 1 hr -2580°F 10^{-4} torr

[b] Coated with Si-20Cr-20Fe (R512E) 1 hr - 2580°F 10^{-4} torr

[c] Percent elongation in 1" gage length

[d] Ultimate tensile strength in thousands of psi (based on original uncoated cross section)

In order to demonstrate in a gross manner what effect the fused silicide coating might have on the impact ductility of a strong but ductile alloy, Si-20Cr-20Fe coated F-48 specimens were subjected to this same crude hammer test. Several specimens so impacted were completely ductile and were bent up to 90 degrees in this fashion, without the initiation of base metal cracks.

5. COATING OF COLUMBIUM ALLOY BRAZED HONEYCOMB PANELS (ASCEP)

Under an Air Force sponsored program bearing the acronym ASCEP (8, 12) (advanced structural concepts experimental program) the Martin Co. developed manufacturing processes for, and produced a number of columbium alloy brazed honeycomb panels. At the time that these panels were initially fabricated, the Ti-Cr-Si, two-cycle, vacuum-pack coating was selected as the best available coating. The development of the fused silicide coating system was not far advanced at that time.

Initially a study was made of the suitability of the Si-20Cr-5Ti fused silicide on ASCEP panels with the thought of evaluating the coating on a few spare panels in the course of the testing program. Later when testing of the Ti-Cr-Si coated panels showed that they were not adequate, a program to recoat all the columbium panels in the test vehicle was undertaken.

a. Evaluation of the Fused Silicides for Coating ASCEP Panels

Two types of specimens were supplied by the Martin Co. for the preliminary evaluation. One type of sample consisted of two pieces of D43 sheet (approximately 3 x 4 inches) brazed face-to-face with their B120VCA titanium braze alloy. The other sample type consisted of a 3 x 4-inch D43 face sheet and two 1 x 4-inch face sheets brazed to the former with same titanium braze alloy. In addition, however, the lap joint fillet areas were brazed with the Ti-8.5Si eutectic braze alloy which is used for repair purposes. These sheets were cut up into small coupons for coating, oxidation tests, and evaluation. Both the Si-20Cr-5Ti and Si-20Cr-5Ti-10Fe-10VSi_2 compositions were applied to groups of each type of specimen and tested as follows:

Temperature (°F)	Time (hours)	No. of Cycles
1600	98	38
1800	98	38
2000	98	38
2200	98	38
800-2500-800 (slow cycle)	8	8

Visual examination of as-coated coupons indicated a very strong reaction between the fused silicides and the Ti-8.5Si braze, resulting in a grossly wrinkled surface. Examination of this braze in the uncoated condition revealed considerable porosity in these areas which may be partly responsible for the resultant surface condition after coating. It is also clear that the interaction between the coating and the B120VCA braze is somewhat greater than that between the coating and the D43 alloy.

The Si-20Cr-5Ti coated sample failed between 82 to 98 hours in the 2200°F test. No other oxidation failures were observed. Despite the poor appearance of the coated Ti-8.5Si braze fillet, no evidence of accelerated oxidation was noted in these areas.

Photomicrographs of some of the coupons in the brazed, coated, and tested conditions are shown in Figure 110. The porosity of the Ti-8.5Si braze can be seen in these sections. The protectiveness of the coating to the D43 and to both the B120VCA and Ti-8-1/2 Si brazes is also demonstrated.

Some oxidation testing of prestressed coated samples was undertaken. The samples were 0.25 x 1.75 x 0.011-inch D43 before coating. They were coated with the Si-20Cr-5Ti slurry composition and prestressed to 50,900 psi at room temperature. The 0.2 percent offset yield strength of these composites was determined to be 58,800 psi which makes the prestressed value 87 percent of the yield strength. After prestressing, the samples were tested as follows:

Test Temperature (°F)	Time (hours)	No. of Cycles
1600	48	18
1800	48	18
2000	48	18
800-2500-800 (slow cycle)	8	8

No evidence of failure or accelerated oxidation was visually observed on these test samples. Photomicrographs of the as-coated and prestressed samples are given in Figure 111. It appears that the prestressing may cause additional transverse cracking of the coating. It may also be seen that the prestressing causes the cracks to propagate past the lower silicide to the coating-substrate interface and may also cause the cracks to widen somewhat.

Photomicrographs of the coupons oxidation tested after prestressing are presented in Figure 112. They show no evidence of accelerated attack in the cracks or any other indication that the protective properties of the coating have been affected by the prestressing.

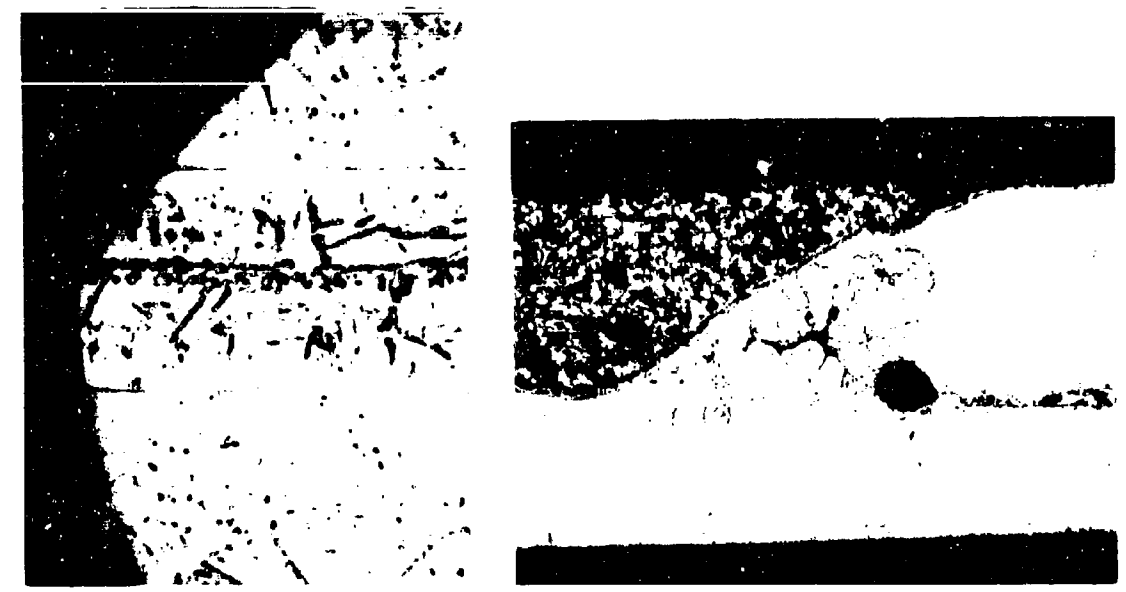

(a) EDGE 250x (b) FILLET 100x

AS BRAZED (28401-1)

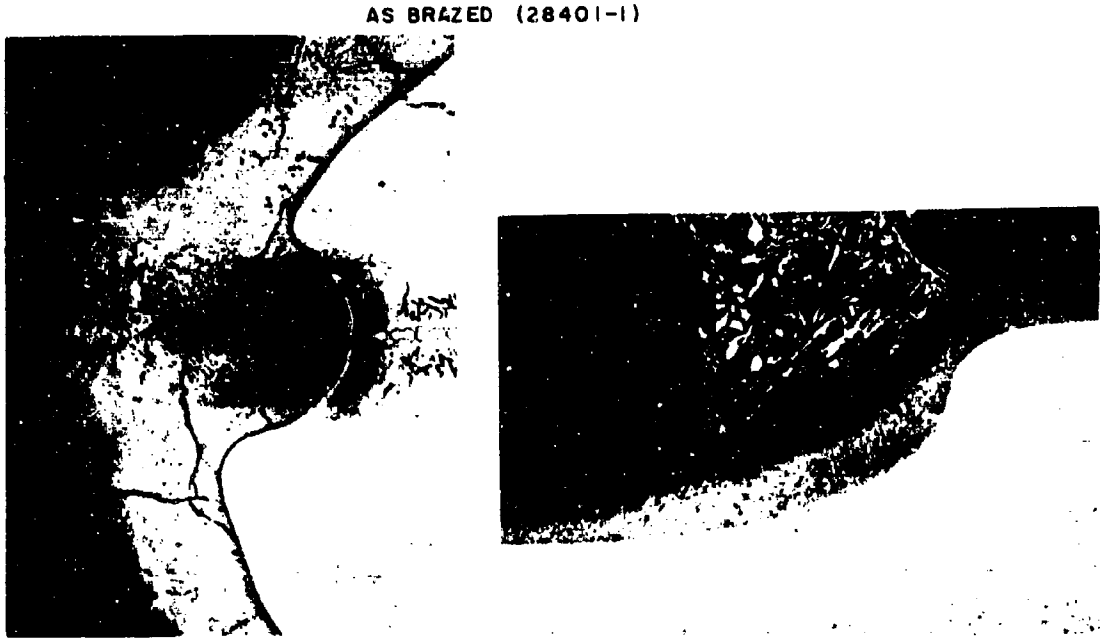

(c) EDGE 250x (d) FILLET 100x

AS COATED (28401-2)

Figure 110 Photomicrographs of Martin Brazed D43 Coupons in Brazed, Coated and Exposed Conditions.

(e) EDGE 250x (f) FILLET 100x
OXIDIZED 1800°F - 98 hours (38 cycles) (28401-5)

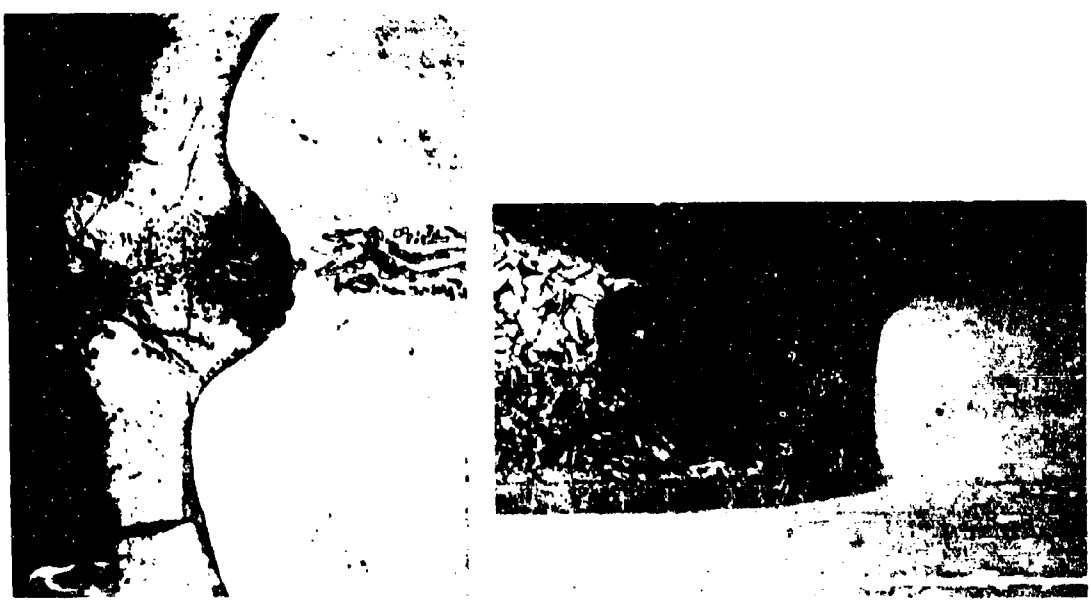

(g) EDGE 250x (h) FILLET 100x
OXIDIZED 8 ONE-HOUR SLOW CYCLES (28401-7)

Figure 110---Concluded

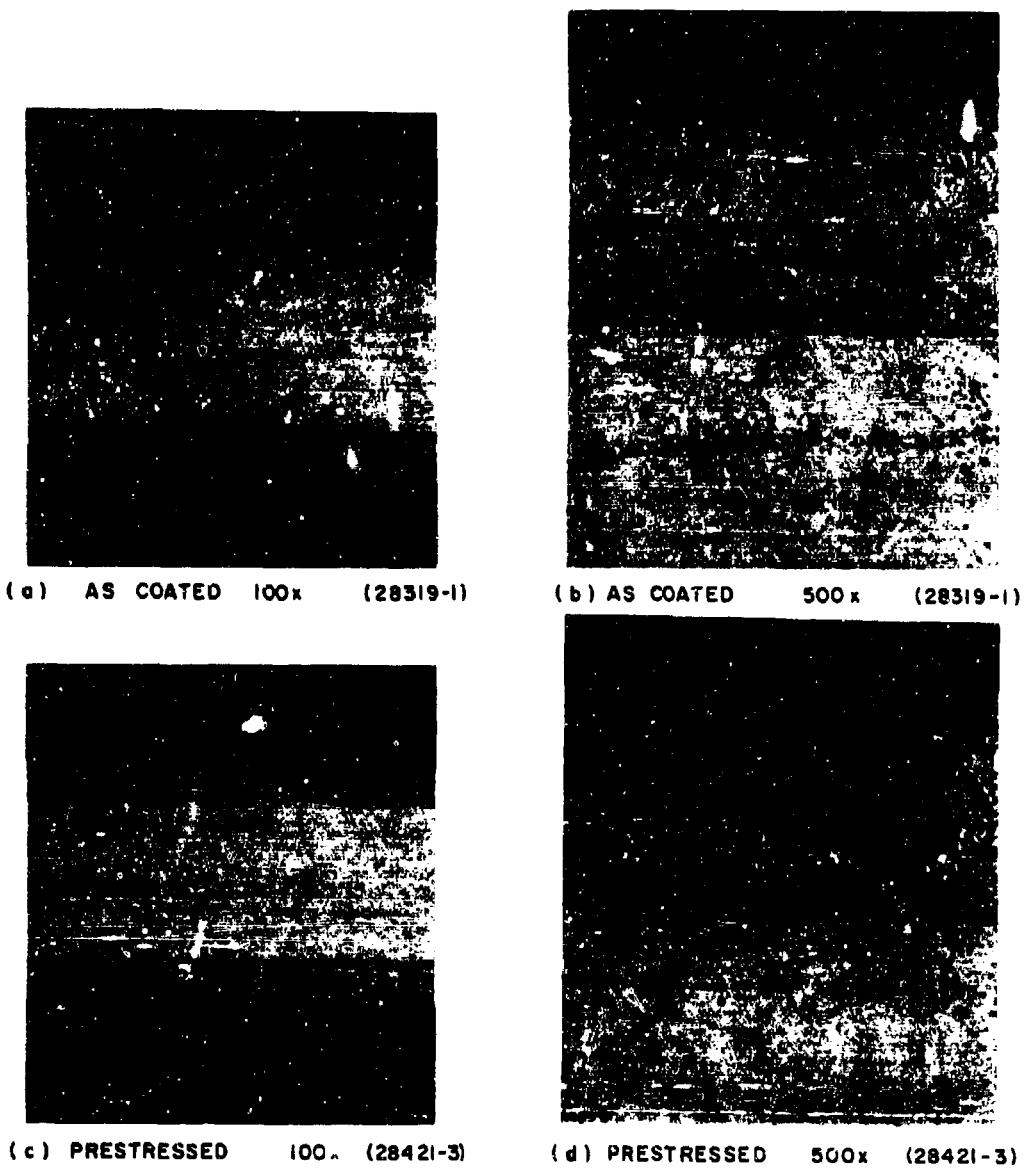

Figure 111 As coated and Prestressed Si-20Cr-5Ti Coated D43.

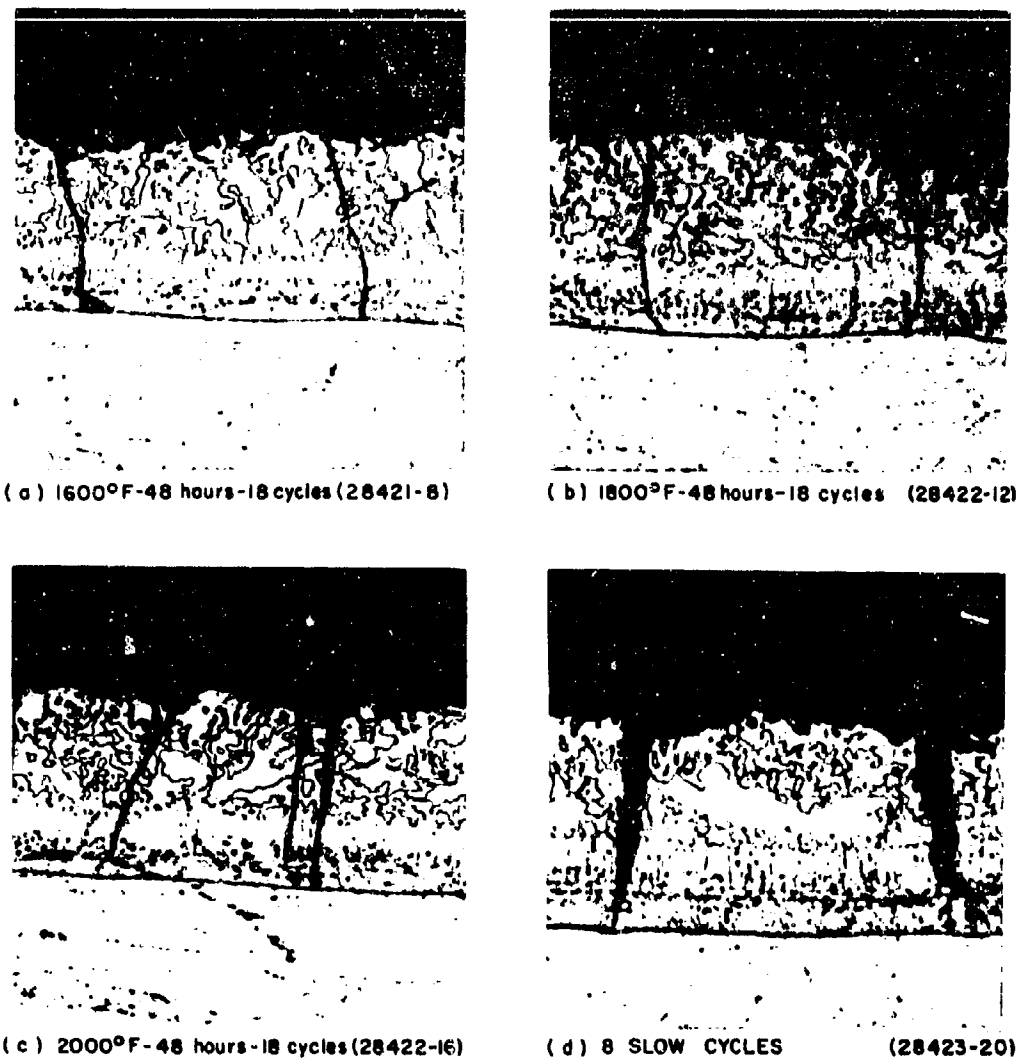

Figure 112 Si-20Cr-5Ti Coated D43 Oxidation Tested After Prestressing (500X).

As a result of the work described above, it was determined that two spare D-43 ASCEP panels would be coated with the Si-20Cr-5Ti fused silicide. The finished coated panels are shown in Figure 113. These spare panels were intended for replacement of one or more of the original Ti-Cr-Si vacuum-pack-coated panels in test at Wright-Patterson AFB if and when intermediate inspections indicated this to be desirable or necessary.

b. Recoating the ASCEP Test Vehicle

Subsequently it was determined that the Ti-Cr-Si coating applied to the ASCEP test structure panels was not comparable structurally or in protectiveness to the coating as it normally is applied to tabs in the laboratory. This probably was attributable primarily to early scale-up problems associated with the poor heat transfer characteristics of large coating packs. (The ASCEP panels had been the first pieces coated in a scaled-up vacuum-pack facility.)

A study was initiated with the aim of determining if the fused silicide coating could be used to repair or recoat the panels of the test structure so that the scheduled test could go forward. Preliminary examination of a portion of a panel removed from the test structure indicated that the Ti-Cr-Si coating was essentially undermined by oxidation at the coating-substrate interface and large areas had spalled off. Microexamination of portions with a fairly adherent coating showed a thick silicide coating with no underlying $CbCr_2$ laves phase, and no titanium diffusion zone. Photomicrographs illustrating both of these conditions are shown in Figure 114. Oxidation of the D-43 skin had occurred over large areas, particularly on the inner or back face.

Grit blasting tests showed that the back face could be readily cleaned at 60 psi, but that specific local areas, possibly the $CbCr_2$ phase, on the outer face, could not be completely cleaned using this procedure. It was decided, however, that use of higher blasting pressures might result in too much metal removal. Etching was also ruled out because of the possibility that dissolution of the titanium alloy braze in the joints would expose the uncoated honeycomb core.

Small tabs were cut from both the outer and inner surfaces, and after grit blasting, several of each were coated with the Si-20Cr-5Ti coating in two thicknesses (16 and 22 mg/cm^2) and the Si-20Cr-20Fe coating in the 16 mg/cm^2 thickness only. The two thinner coatings were tested through six ASCEP temperature profiles as shown in Figure 115, using the Reentry Simulator Equipment (see Figure 15). The Si-20Cr-5Ti coating on the outer surface tab developed two small pinhole failures during the first cycle. These did not, however, progress rapidly during the subsequent five cycles. The failures were obviously in areas where the original Ti-Cr-Si coating could not be completely removed. The Si-20Cr-5Ti coated inner surface tab was completely intact after the six cycles. The Si-20Cr-20Fe coated tabs developed the spalling outer layer characteristic of this coating during oxidation, but remained completely protective to both inner and outer surface tabs.

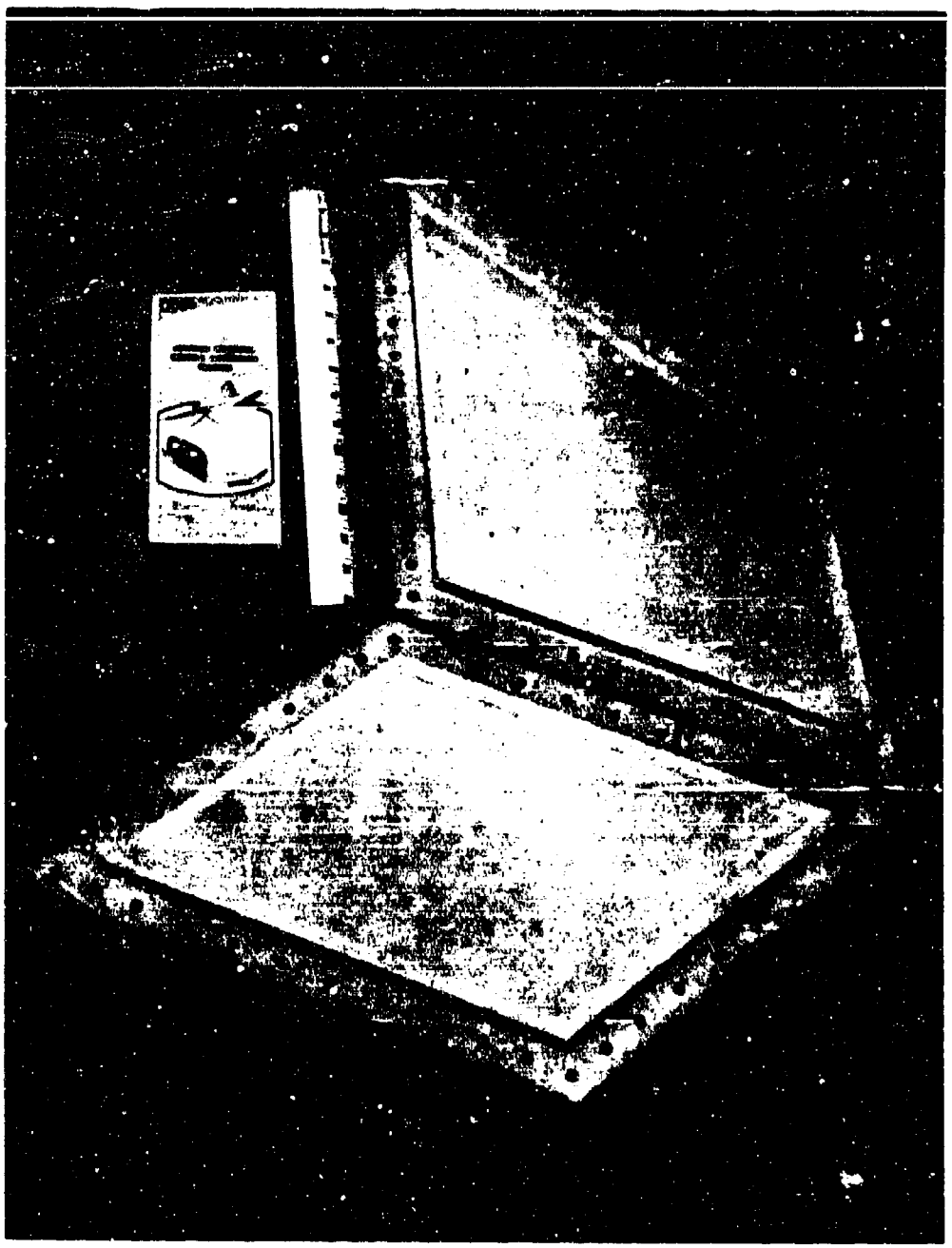

Figure 113 Brazed D43 Honeycomb Panels With Si-20Cr-5Ti Fused Silicide Coating.

(a) INTACT COATING

(b) SPALLED AREA SHOWING Cb_2O_5 MASS

Figure 114 Ti-Cr-Si Duplex Vacuum Pack Coated D-43 Honeycomb Panel Outer Sheet After 1 ASCEP Thermal Profile (300X).

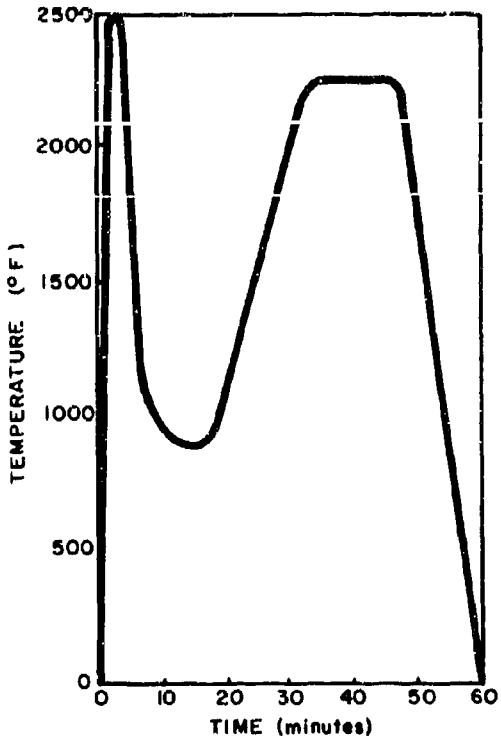

Figure 115 ASCEP Thermal Test Profile.

The thicker Si-20Cr-5Ti coated tabs were tested through seven ASCEP cycles. One of two outer surface tabs and the two inner surface tabs were not affected by this test. Microstructures of the stripped and recoated tabs in the as-coated and post-test conditions are shown in Figure 116. These structures appear normal in every respect, indicating perhaps that the Ti-Cr-Si coating was completely removed in these areas.

The remainder of the panel was grit blasted and coated with a 25 mg/cm^2 Si-20Cr-5Ti coating. The coating looked very good on the inner surface which had cleaned up much better. On the outer surface the coating had a generally good appearance, but there was evidence of macroscopic nonuniformities in those areas where portions of coating sublayers appeared to remain after the cleaning operation.

Based on the above described work, a decision was made to strip and recoat ASCEP panels on an as-required basis. Subsequently it was decided to strip and recoat all of the panels that comprise the ASCEP vehicle. The test vehicle contains 30 columbium alloy panels and their general size and shape are shown in Figure 117.

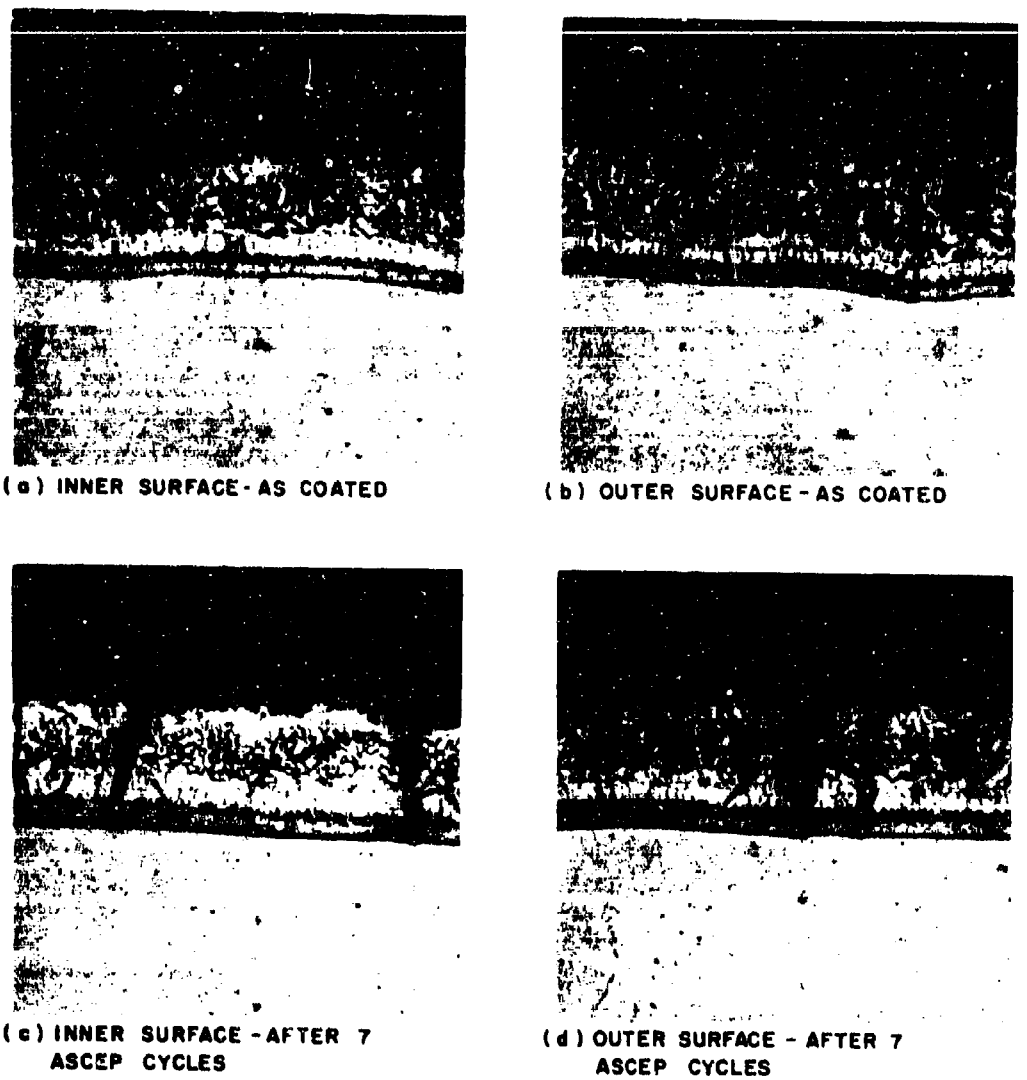

Figure 116 Photomicrographs of Stripped and Si-20Cr-5Ti Fused Silicide Coated ASCEP Panels.

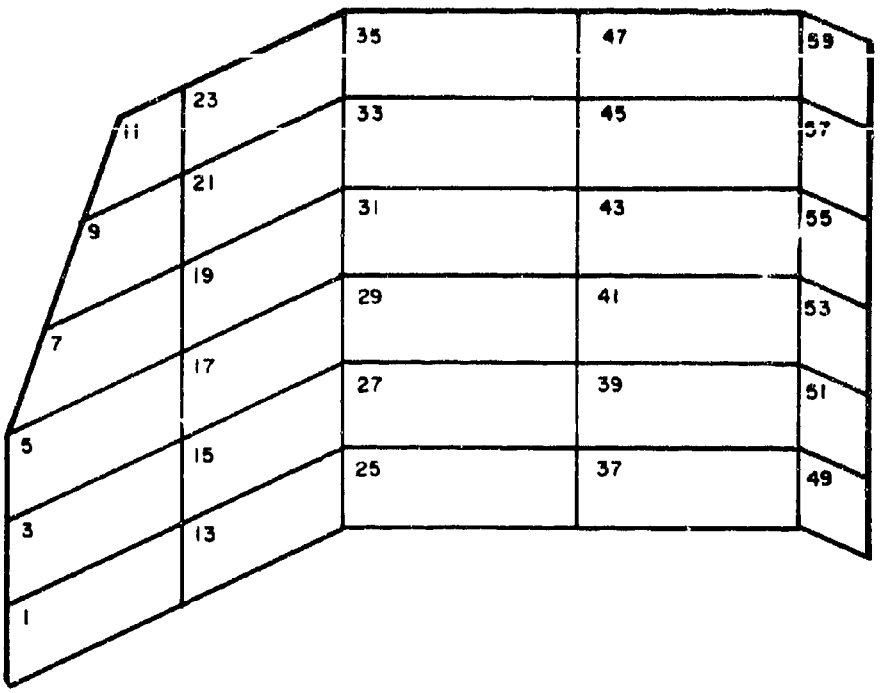

Figure 117 General Scale and Geometry Layout of ASCEP Panels. Scale Approximately 1/40.

On the basis of further tests it was determined that the panels were strong enough to withstand blasting at pressures up to 80 psi, and using aluminum oxide grit it was possible in most cases to strip most of the original Ti-Cr-Si vacuum pack coating. In some cases, areas of the $CbCr_2$ laves phase were very tenaciously adherent and could not be readily removed. Also the solid solution portion of the coating is for the most part not removed by the grit blasting.

After stripping the panels were given a gross leak check which consisted of immersing the panel in warm water and visually examining for air bubbles. Those panels that were determined to be leakers were returned to Martin for repair brazing.

A total of 43 individual panels were coated, nine of which were virgin panels with the remaining 34 being Ti-Cr-Si coated panels which required prior stripping. After stripping, 15 panels required repair brazing at Martin. In the course of repair brazing at Martin, one panel blew up, and during firing of the fused silicide coating, six of the repair-brazed panels blew up. Presumably, these blow-ups were due to the entrapment of gas in the core. Twenty-six of the stripped panels were satisfactorily coated.

The repair brazing of the stripped panels apparently presented problems. In order to effect the sealing of leaks at some points, it was necessary to use copious quantities of the Ti-8 1/2 Si braze. Consequently, the braze material in these areas was essentially unreacted and quite porous. When the large mass of porous braze reacted with the Si-20Cr-5Ti coating, a bubbly, permeable, fragile honeycomb of solid, intermetallic compound resulted. When this occurred, the bubbles were broken and brushed away, and these areas were subsequently recoated. This procedure was followed with five panels. Two of these five panels were found to leak after coating, necessitating another cycle of stripping, repair brazing and recoating. These panels (17-SN0008 and 23-SN0007) were Ti-Cr-Si coated, stripped, repair brazed, fused silicide coated, fused silicide repair coated, stripped, repair brazed, and fused silicide coated again. It should be realized that the skins of these panels may have been reduced in thickness by as much as 0.005 inch as a result of the numerous coating and stripping cycles to which they were subjected.

The first five panels received were surveyed by several Nondestructive Testing (NDT) techniques at AVCO in the initially coated condition, after stripping of the coating here, and again at AVCO after recoating with the Si-20Cr-5Ti fused silicide coating. Considerably more NDT work has been performed on these panels by AVCO (13) at various stages of processing and testing. Hopefully the NDT measurements will be later correlated with oxidation performance observations when the testing is completed.

Including repair coating runs, a total of 51 panel coating processing cycles were performed. A summary of the work performed is given in Table XXXIII.

The Si-20Cr-5Ti coating was applied to most of the panels by slurry dipping. The last five spare virgin panels delivered for coating were coated with the Si-20Cr-20Fe composition since it was definitely determined at that point in time that this coating was superior in protectiveness. The Si-20Cr-20Fe coating was applied by spraying in order to avoid the cost of the large volume of slurry necessary for dip coating.

The use of nondestructive testing techniques for in-process thickness control as well as for final coating thickness measurements was explored with the last two panels processed. The Dermitron instrument (refer to paragraph 7) was used to determine the thickness and uniformity of the as applied green slurry and of the finished coating after the fusion-diffusion treatment. The relationship between applied unit weight of green slurry and the Dermitron response is shown in Figure 118. A corresponding curve for the fired coating is shown in Figure 127.

A typical Dermitron scan of the outer or flat side of fuselage panel SP 0006 is shown in Figure 119. The numbers give the unit coating weight at each specific spot. The green coating was found to vary from 21-36 mg/cm^2 while after firing the variation was reduced to 26-38 mg/cm^2. By extrapolation of the curve of Figure 127, the coating thickness on the panel was determined to fall within the limits of 5.2 ±1 mil.

TABLE XXXIII

SUMMARY OF FUSED SILICIDE COATING[a] OF ASCEP PANELS

Category	Position No.	Serial No.	Mg/cm² Applied	Mg/cm² Diffused	Breakdown of Applied Coating Wt. (Mg/cm²) Dipped	Breakdown of Applied Coating Wt. (Mg/cm²) Over-spray	All Spray Raised Side	All Spray Flat Side	Min-Max (mg/cm²) Diff As Shown by Dermitron Raised	Min-Max (mg/cm²) Diff As Shown by Dermitron Flat	Min-Max Coating Thickness-Diffused by Micrometer on Flange (MILS)	Remarks
Virgin Panels	11	SP0001[b]	28.2	24.4	26.6	.6						Recoated
	55	SP0002	22.3	20.4								
	45	SP0004	28.6	25.2	24.0	4.6						
	wing	SP0003	28.1	24.8	24.9	3.2						
	wing	SP0004[c]	31.2	28.8			31.8	30.6			2.35-4.00	
	fuselage	SP0005[c]	29.4	27.1			28.0	30.9			2.55-3.60	
	wing	SP0005[c]	28.7	26.4			28.0	29.4			2.55-3.40	
	fuselage	SP0006[c]	32.4	30.0			35.0	29.8	22-42	19-38	2.90-4.35	
	fuselage	SP0007[c]	35.0	32.4			34.1	35.8	27-41	31-40	3.15-3.90	
Panels stripped of Ti-Cr-Si vacuum pack coating and fused silicide coated	3	SN0011	28.1	24.8	23.2	4.9						
	5	SP0002	28.5	24.9	24.2	4.3						
	7	SP0001	28.6	25.0	26.7	1.9						
	9	SN0001	28.4	25.0	24.7	3.7						
	9	SP0001	29.7	26.4	25.2	4.5						
	15	SP0001	28.7	24.9	26.0	2.7						
	19	SN0005	28.0	24.0	23.3	4.7						
	25	SN0012	27.9	24.7	26.7	1.2						
	27	SN0014	27.8	24.1	20.9	6.9						
	29	SN0004	28.8	25.4	23.5	5.2						
	31	SP0002	33.1	28.8	32.7	.4						Touch-up - no overspray
	35	SN0002	27.9	25.1	19.0	8.7						
	37	SP0003	35.3	31.7	34.7	.6						Touch-up - no overspray
	39	SN0013	28.5	25.0	26.7	1.8						
	41	SN0011	27.1	25.7	25.2	1.9						
	49	SN0007	28.9	25.6	26.1	2.8						
	55	SP0001	28.7	24.9	27.9	.8						Oversprayed - raised side only
	57	SN0004	28.2	25.1	22.5	5.7						
Panels stripped of Ti-Cr-Si vacuum pack coating, repair brazed at Martin and fused silicide coated	1	SN0010[d]	28.0	24.6	26.7	1.3						Repaired and relired final mg/cm² 26.3
	17	SN0008[e]	29.3	26.2			27.7	31.2				
	23	SN0007[f]	28.5	24.7	25.3	3.2						Repaired and relired 2x mg/cm² 28.1
	43	SN0009[d]	29.4	26.2	23.9	5.5						Repaired and relired mg/cm² 27.8
	47	SN0015	30.0	26.5								
	51	SN0008	29.3	26.2			27.7	31.2			2.65-4.55	
	53	SN0005	29.1	26.1	25.3	3.8						
	59	SN0001[d]	29.6	25.4	23.0	6.6						Repaired and relired mg/cm² 28.6

TABLE XXXIII (Cont)

SUMMARY OF FUSED SILICIDE COATING[a] OF ASCEP PANELS

Category	Position No.	Serial No.	Mg/cm²		Breakdown of Applied Coating Wt. (Mg/cm²)						Remarks
						All Spray					
			Applied	Diffused	Dipped + Over-spray	Raised Side	Flat Side	Raised	Flat		
Panels destroyed during reprocessing											
Blow-up during repair brazing	15	SN0001									
Blow-up during coating after repair brazing	7	SN0001	28.0		28.9						Blow up at 900°F
	11	SN0002	30.0		22.0 8.0						Blow up at 810°F
	13	SN0009	28.0	23.0	23.0 5.0						Blow up
	21	SN0002	28.7		21.0 7.7						Blow up at 1240°F
	33	SN0005									Blow up
	45	SN0006									Blow up
Panel Ti-Cr repair brazed and fused silicide coated for test purposes	55	SN0003	29.6	25.4							

[a] All panels coated with Si-20Cr-5Ti composition except as otherwise noted.

[b] Fused silicide stripped and recoated.

[c] Coated with Si-20Cr-20Fe composition.

[d] Double coated at repair brazed areas.

[e] Double coated at repair brazed areas, entire panel again stripped, repaired brazed and recoated.

[f] Double coated at repair brazed areas, local strip repair braze and local repair coat.

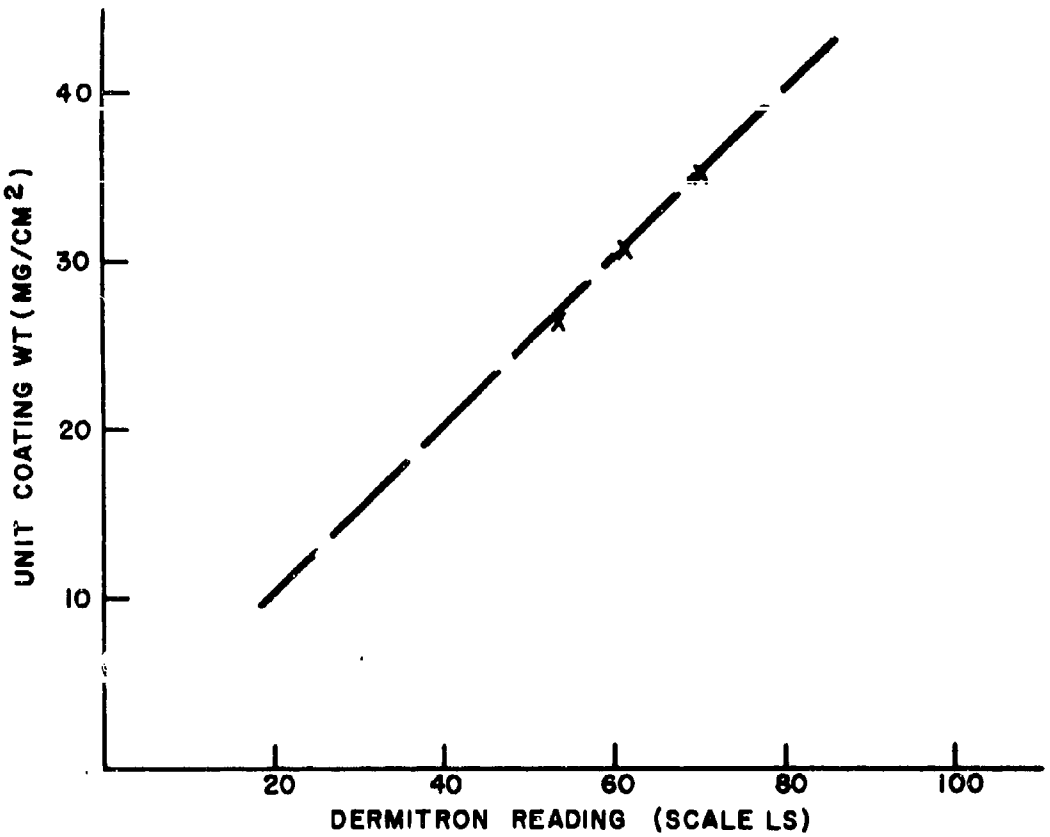

Figure 118 Green Coating Weight vs Dermitron Response (Si-20Cr-20Fe Coating on D43 Alloy)

For this panel the average unit green coating weight was determined to be 31.0 mg/cm^2 using the Dermitron while the actual average unit coating weight based on weight differences was found to be 32.4 mg/cm^2. After firing the Dermitron yielded an average unit coating weight of 30.2 as opposed to an actual figure of 30.0. The utility of this instrument and technique, particularly for determining the thickness uniformity of green coating, is considerable since it affords the opportunity to effect corrections in the processing of a specific part when these corrections can be most readily accomplished. The limitations of the instrument center on the availability of probes suitable for complex hardware shapes.

Figure 120 shows some photographs of one typical panel in the as-received condition (Ti-Cr-Si vacuum pack coated and oxidized through 1 ASCEP cycle), and after recoating with the Si-20Cr-5Ti fused silicide coating.

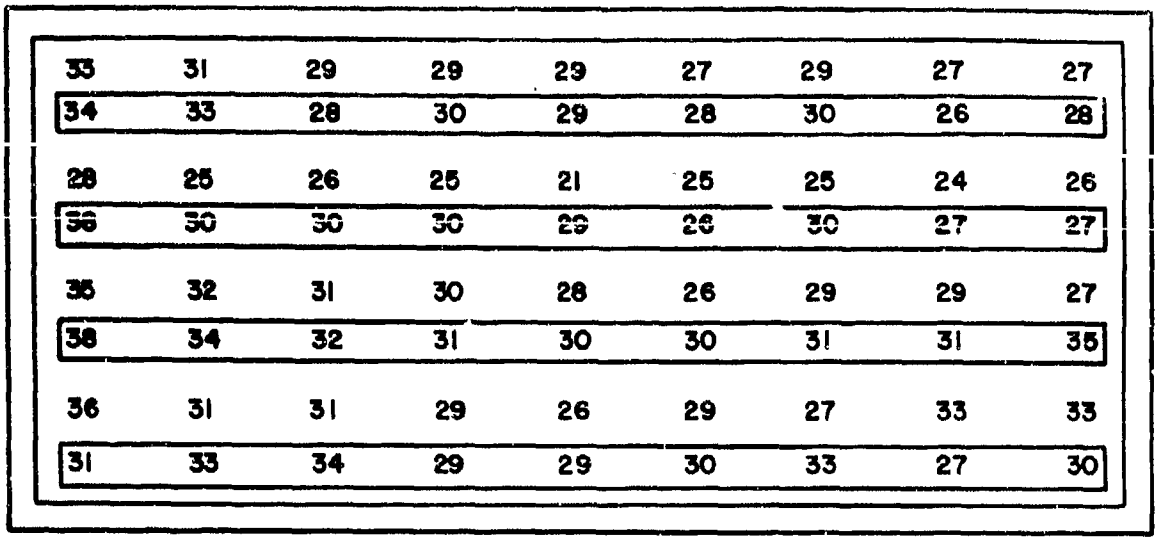

Figure 119 Coating Thickness by Dermitron on ASCEP Panel. Fuselage 0006 on Flat Side (Numbers Inside Boxes are After Diffusion) Final Thickness = 5.2 ± 1.0 Mils.

A virgin panel coated with the Si-20Cr-20Fe composition is shown in Figure 121. Photographs of virgin panels coated with the Si-20Cr-5Ti fused silicide were shown in Figure 113.

Prior to the initiation of testing of the ASCEP test structure the assembled vehicle was inspected by Sylvania personnel. Notes were made and 35 mm color slides were taken of numerous typical and atypical panels throughout the vehicle. In general no obvious defects were noted except for some chipping of the Ti-Cr-Si coating from the edges of the flush head screws holding the panels in place. There were differences in coloration resulting from the proof test oxidation cycle to which each panel had been subjected but, these differences are generally not relatable in any significant way to protectiveness. The Si-Cr-Fe coated panels were readily distinguishable from the Si-Cr-Ti panels after proof testing in that the former were rust colored while the latter were quite dark.

After the structure was heated through the ascent portion of the cycle, the heated surfaces of the fused silicide coated columbium alloy honeycomb panels were reinspected. Additional color slide photographs were taken of some of the same locations photographed before test. The panel in position 4, had ruptured during this ascent heating cycle but the failure of this panel could not be correlated with any prior visual or photograph observations. During the reentry heating cycle which was conducted subsequently, it is understood that another panel ruptured. These ruptures were similar to those occurring during reprocessing and are obviously caused by an internal gas pressure probably resulting from a leak in the brazed seal.

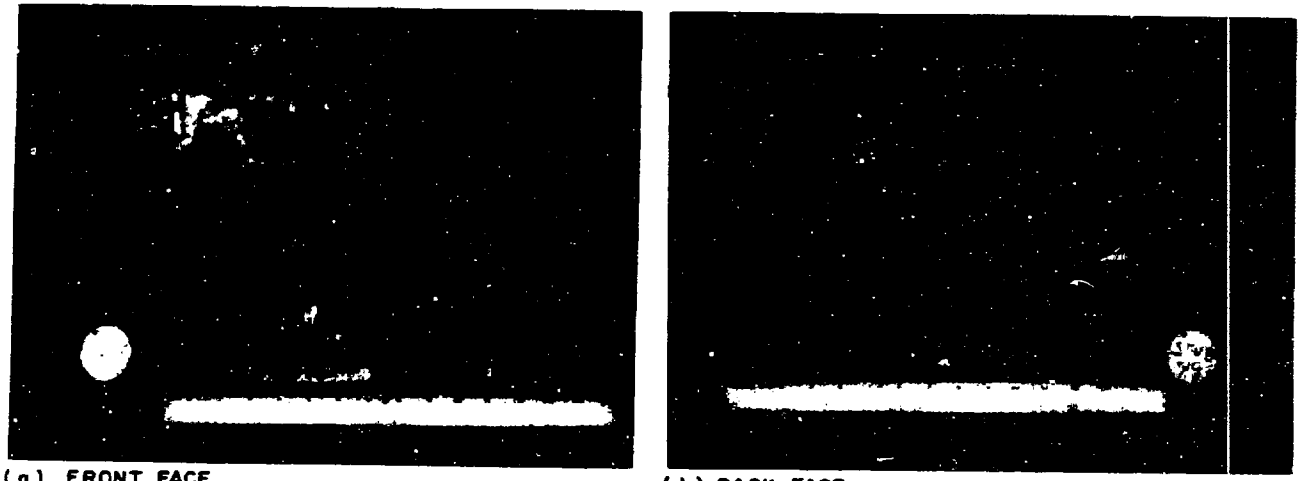

(a) FRONT FACE (b) BACK FACE

AS RECEIVED

(c) FRONT FACE (d) BACK FACE

FUSED SILICIDE COATED

Figure 120 ASCEP Panel 49-SN0007 As Received and After Stripping and Fused Silicide Coating.

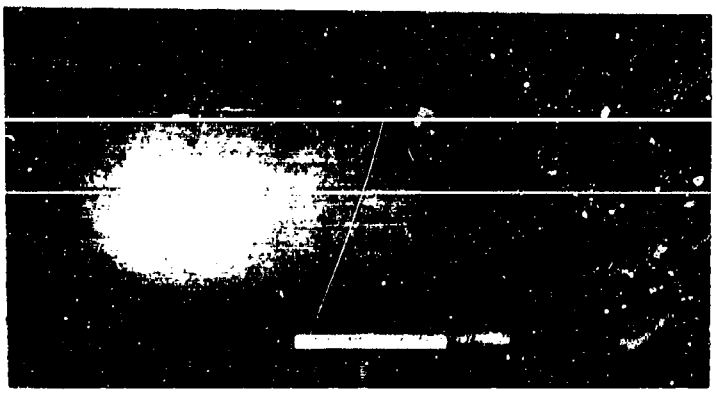

FRONT FACE

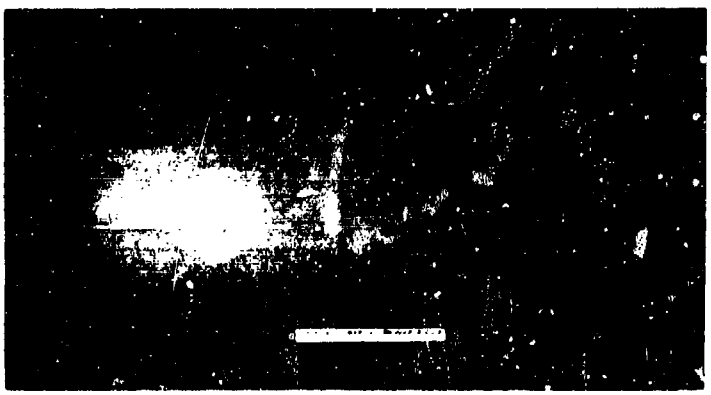

BACK FACE

Figure 121 ASCEP Virgin Fuselage Panel - SP0007 After Coating With Si-20Cr-20Fe Fused Silicide.

As of the date of this report, six additional no load ascent and reentry heat cycles were imposed on the vehicle. A number of additional panels failed either by "blowing up" due to internal gas pressure or by cracking of the skin from as yet undetermined causes. All of the virgin panels coated with the R512E (Si-20Cr-20Fe) composition have sustained the entire test schedule to date with no evidence of accelerated oxidation or of structural deficiency. Complete results of the testing of the ASCEP vehicle are described in reference (8, 12).

6. COATINGS FOR TANTALUM AND MOLYBDENUM ALLOYS

a. Characterization of Si-20Ti-10Mo Coated Tantalum Alloys

Although the advanced development of fused silicide coatings for columbium alloys was the primary goal of this program, an important secondary objective was the further development of this type of coating for tantalum and molybdenum alloys. Toward the end of the previous program a number of fused silicides were applied to tantalum and T-111 and cursorily screened for oxidation protectiveness using several oxidation tests (1). The composition that appeared most protective in those tests was Si-20Ti-10Mo, and it was decided to characterize the oxidation protectiveness of this coating more extensively.

The testing consisted of cyclic oxidation at 1000, 1600, 1800, 2000, 2600, 2700, 2800, 3000, and 3200°F. At temperatures through 2700°F the tests consisted of two 4-hour and one 16-hour cycle each day, while the 2800, 3000, and 3200°F tests consisted of 5 minute cycles and were performed in an oxyacetylene torch. All other tests (1000 to 2800°F) were conducted in electrically heated furnaces. It is believed that near black body conditions exist in the tubular test furnaces used and that the temperatures reported are therefore true temperatures. With the torch tests, a spectral emittance of 0.7 at 0.65 μ was assumed in arriving at the reported test temperature. The true brightness temperatures for the 3000°F and 3200°F tests were 2905°F and 3085°F respectively. The true temperatures probably fall somewhere between these sets of values. In other sections of this report when optical temperatures are cited they are true brightness temperatures. These test conditions and procedures by design conform closely to those employed by Solar (14) in evaluating their PA-8 tungsten-titanium modified silicide coating for tantalum alloys.

The results of these tests are given in Table XXXIV which also includes results on the PA-8 taken from Reference 14 for comparison.

The PA-8 coating was employed as a reference for comparison because there were no other silicide coatings available for tantalum alloys at the time of these tests. The Cr-Ti-Si vacuum pack coating (9) was developed primarily for columbium alloys and is most protective to them. On the basis of a brief study (9) of the protectiveness of that coating on Ta and Ta-10W, it would appear to be roughly comparable to the PA-8; however, these tests were limited to only three test temperatures (1800, 2500, 2700°F). The Sn-Al coating (15) is very protective to tantalum alloys, but must be considered in a separate class because its liquid phase and high unit weight limit its utility to applications where these properties do not deleteriously affect performance.

From the data in Table XXXIV the fused silicides appear to be considerably more protective to tantalum base materials than the PA-8 coating. If other factors such as unit weight, applicability to complex structures and reliability were considered, then the superiority of the fused silicides would be even more obvious.

TABLE XXXIV

CYCLIC OXIDATION PROTECTIVENESS OF FUSED SILICIDE COATINGS ON TANTALUM BASE MATERIALS

Test Temp. (°F)	Maximum Cyclic Oxidation Life[a]		
	Solar PA-8 on Ta-10W	Si-20Ti-10Mo on Ta	Si-20Ti-10Mo on T-222
1000	60 hours	158+ hours	158+ hours
1600	50 hours	158+ hours	158+ hours
1800	50 hours	158+ hours	158+ hours
2000	22 hours	158+ hours	158+ hours
2600	8 hours	28 hours	27 hours
2700	28 hours	28 hours	50 hours
2800	200 minutes	780 minutes	1200 minutes
3000	80 minutes	130 minutes[b]	95 minutes[b]
3200	17 minutes	10 minutes[b]	145 minutes[b]

[a] Results given are maximum lifetimes from among 3 samples.
[b] Test results are for single samples.
+ Indicates test stopped, samples not failed.

A number of representative photomicrographs of samples from these tests are shown in Figures 122 and 123. In the as-coated condition the outer portion of the coating appears to be quite porous. In Figure 123 the porous zone in most cases has been completely oxidized, resulting in fairly thick oxide scales. At 2600°F and above the scale is two-phased and becomes progressively more glassy.

b. Compositional Study of Coating for Tantalum and Molybdenum Alloys.

The objective in this area was to perform advanced evaluation tests of several fused silicide compositions identified in the previous program (1) as having good potential for the protection of tantalum (T-111) and molybdenum (TZM) alloys. Based on the results of the evaluation tests, the effort was then directed at optimizing promising coating compositions.

For the TZM alloy, three ternary systems, Si-Cr-V, Si-Cr-B, and Si-Cr-Fe, which had previously yielded good coating performance, were selected for these evaluations. For the T-111 alloy, only one ternary coating system, Si-Ti-Mo, has shown particular merit. A system which had not previously been looked at, and which was

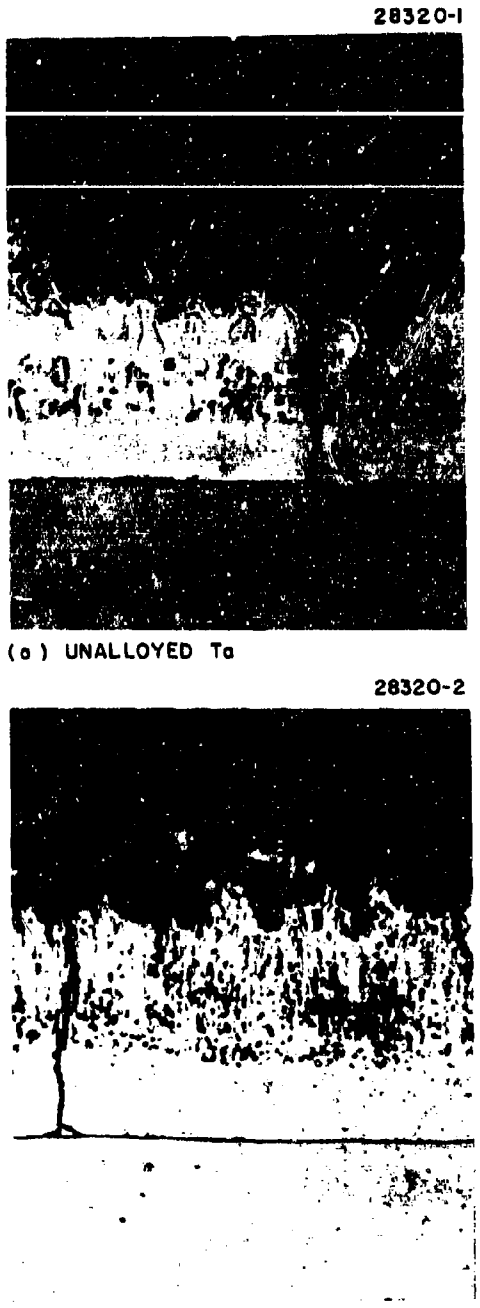

Figure 122 Si-20Ti-10Mo Fused Silicide Coating on Tantalum-Base Alloys; As-Coated Condition (500X).

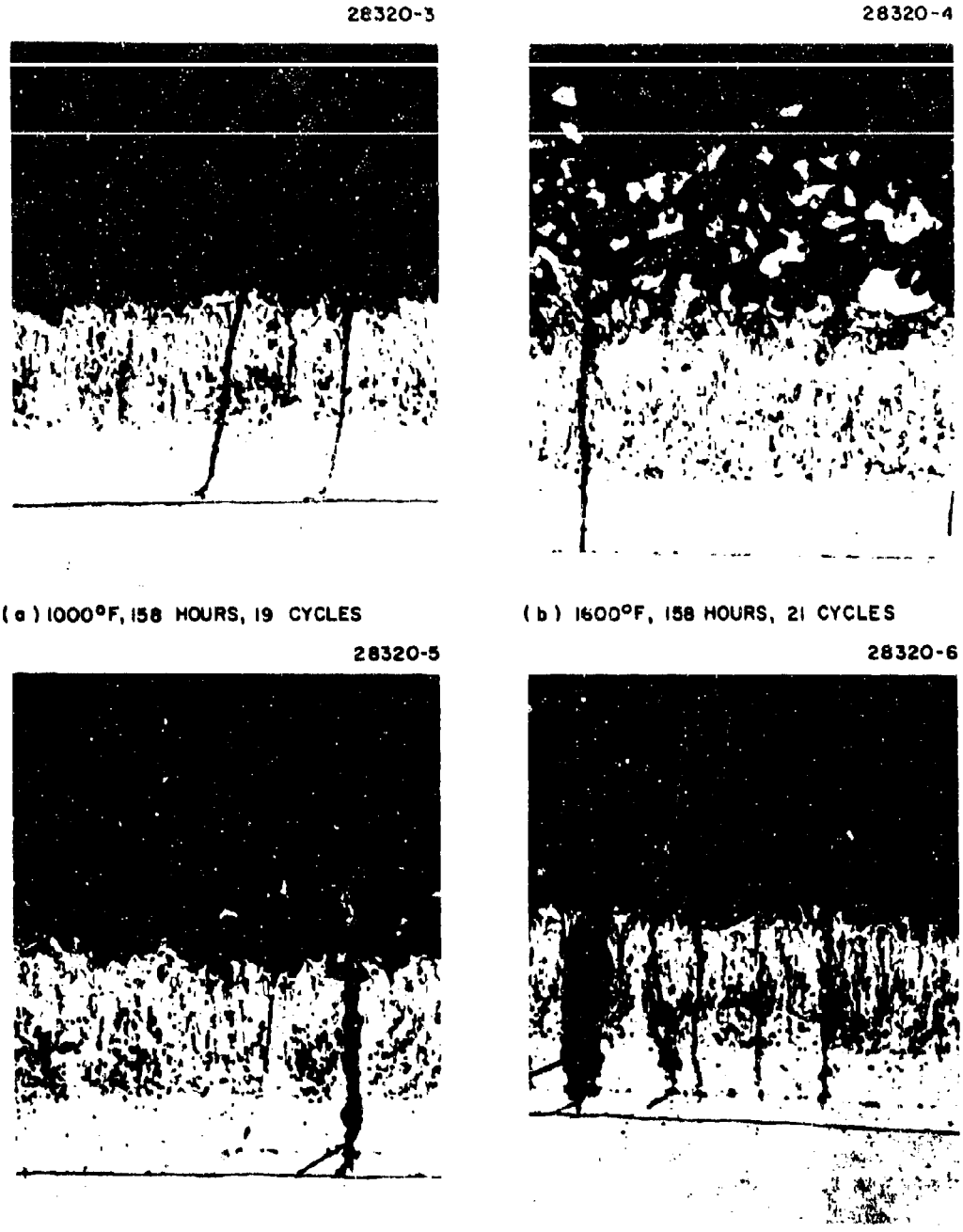

Figure 123 Si-20Ti-10Mo Fused Silicide Coatings on T-222 Alloy After Various Oxidation Exposures (500X).

28320-7

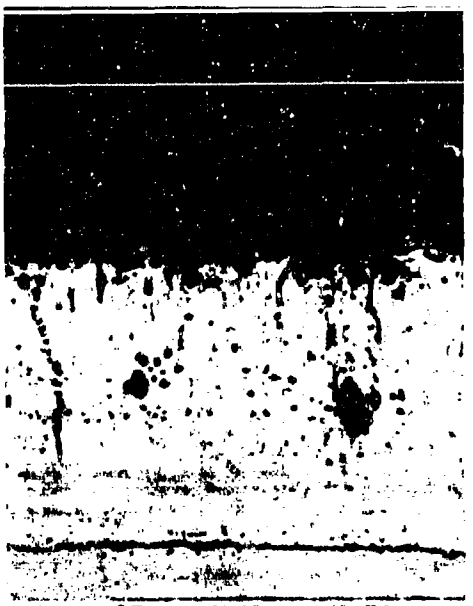

(e) 2600°F, 27 HOURS, 4 CYCLES

28320-8

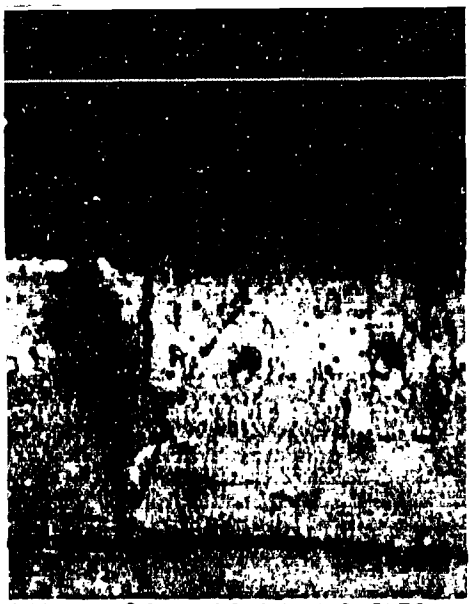

(f) 2700°F, 50 HOURS, 10 CYCLES

28321-1

(g) 3000°F, 95 MINUTES, 19 CYCLES

28321-2

(h) 3200°F, 145 MINUTES, 29 CYCLES

Figure 123---Concluded

thought to have potential merit for tantalum alloys, was Si-Ti-V. A third system selected for T-111 was Si-Ti-V-Mo.

Table XXXV lists the compositions chosen for initial coating trials and the results of these runs in terms of coatability. The three coatings selected for each base alloy are also indicated in the table. All the coatings containing vanadium or boron were not completely uniform and smooth, possibly indicating incomplete dissolution of these elements. As the concentration of these elements was reduced, the coatings which resulted were correspondingly smoother. Photomicrographs of the selected coatings are shown in Figure 124.

TABLE XXXV

RESULTS OF PRELIMINARY COATABILITY EVALUATION OF VARIOUS FUSED SILICIDE COATING COMPOSITIONS ON TZM AND T-111 ALLOYS

Base Alloy	Coating Composition	Visual Appearance After Vacuum Firing 1 Hour at 2580°F	Selected for Evaluation
TZM	Si-20Cr-10V	Some bumps in coating	
TZM	Si-20Cr-5V	Smoother than above	X
TZM	Si-20Cr-1B_4Si	Some bumps in coating	
TZM	Si-20Cr-1/2B_4Si	Smoother than above	X
TZM	Si-20Cr-10Fe	Smooth coating	X
T-111	Si-20Ti-10Mo	Smooth coating	X
T-111	Si-20Ti-10V	Very bumpy	
T-111	Si-20Ti-5V	Less bumpy than above	
T-111	Si-20Ti-3V	Few very small bumps	X
T-111	Si-20Ti-10Mo-10V	Very rough and bumpy	
T-111	Si-20Ti-10Mo-3V	Few very small bumps	X
T-111	Si-15Ti-10Mo-10V	Rough	
T-111	Si-10Ti-10Mo-10V	Rough	

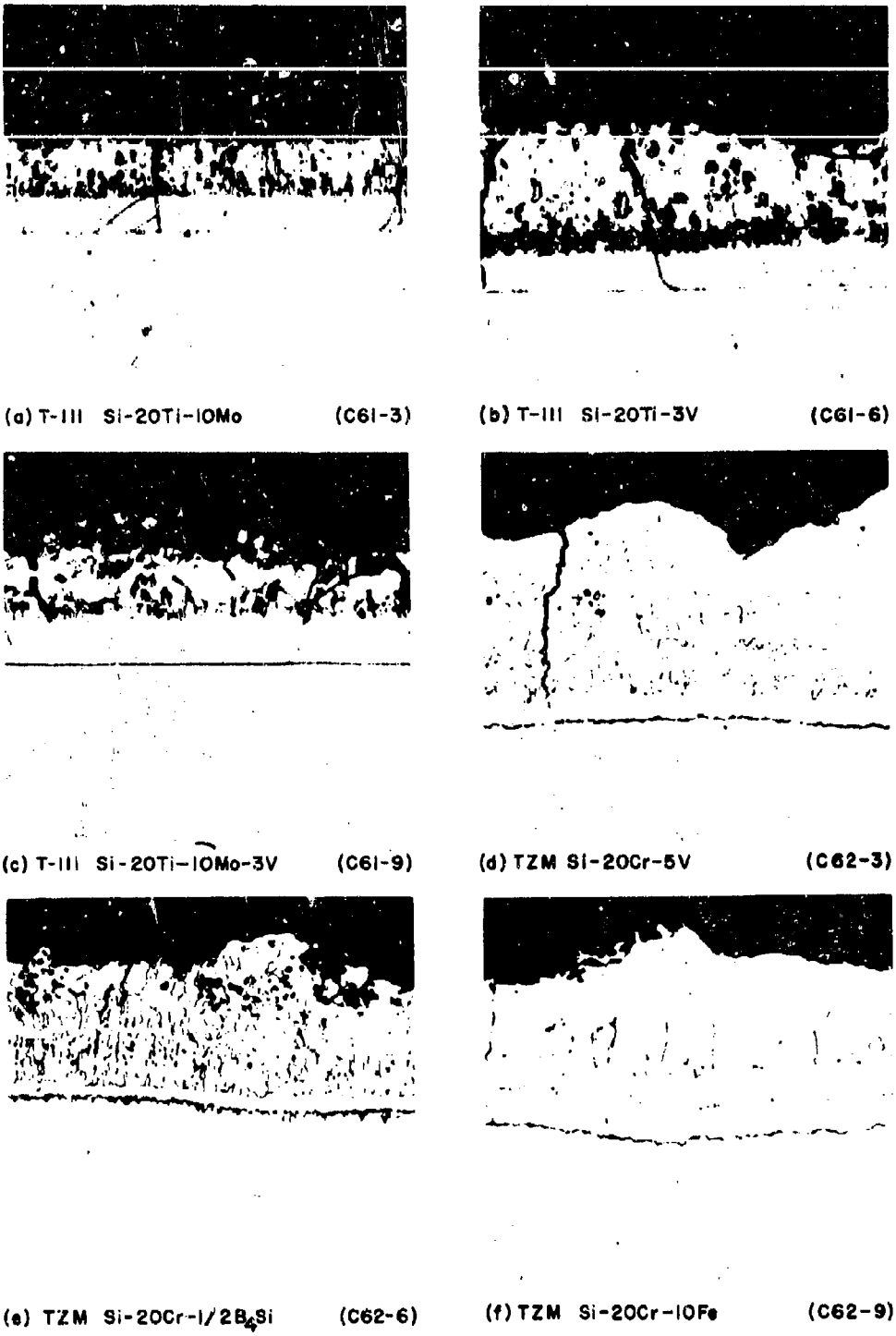

(a) T-111 Si-20Ti-10Mo (C61-3)

(b) T-111 Si-20Ti-3V (C61-6)

(c) T-111 Si-20Ti-10Mo-3V (C61-9)

(d) TZM Si-20Cr-5V (C62-3)

(e) TZM Si-20Cr-1/2B_4Si (C62-6)

(f) TZM Si-20Cr-10Fe (C62-9)

Figure 124 Photomicrographs of Fused Silicide Coated T-111 and TZM in As-Coated Condition (300X).

Batches of ten coupons each were coated with each of the selected compositions and evaluated by slow-cyclic oxidation testing in air and by reentry simulation testing. The same internal surface profile shown in Figure 36 was employed. The temperature profile was similar to that shown in Figure 36, but the maximum temperature was raised to 2800°F. The results of these tests are given in Table XXXVI.

TABLE XXXVI

SLOW CYCLIC OXIDATION AND REENTRY SIMULATION TEST DATA

Base Metal	Coating Composition	Slow Cyclic Oxidation Life 800-2500-800°F in 1 atm Air (No. 1-hour Cycles to Failure)	Reentry Simulation Life Internal Surface Profile 2800°F max. temp.
T-111	Si-20Ti-10Mo	14[e], 11[e]	9[e], 9[e,s]
T-111	Si-20Ti-3V	11[e,s], 11[e,s]	16[e], 16[e]
T-111	Si-20Ti-10Mo-3V	11[s], 14[e,s]	20[e], 128[r]
TZM	Si-20Cr-5V	21, 21	5, 5
TZM	Si-20Cr-1/2B_4Si	97, 97[+]	5[e], 5[e]
TZM	Si-20Cr-10Fe	55-75, 55-75	5[e], 16[e,s]

[+] Test stopped. Sample not failed.
[e] Edge failure.
[s] Surface failure.
[r] Reaction with boat.

The lifetimes reported for the coated T-111 are considerably shorter than those for the better compositions on the columbium alloys. The reentry tests in this case, however, were performed at 2800°F rather than 2500 or 2600°F. The Si-20Ti-10Mo-3V coating looks promising in view of the 128-hour life of one sample in the reentry test. As noted in Table XXXV, it did not appear as if all the vanadium went into solution during the fusion of this coating, and early failures can possibly be the consequence of the inhomogeneities resulting from the vanadium-rich bumps.

The results of the tests of the coated TZM specimens show very good lifetimes in the slow-cyclic test, but markedly shorter life in the reentry tests. Because of the volatility of MoO_3 the smallest pinhole in the coating results in the rapid loss of the substrate by sublimation. As a consequence of the volatility of the substrate oxide, it is quite difficult for the coating to heal any defect that penetrates the entire thickness of the coating.

Evaluation of the selected TZM and T-111 fused silicide coating systems was continued with the high-temperature oxyacetylene-torch testing of all six combinations. The results of these tests are given in Table XXXVII.

TABLE XXXVII

HIGH-TEMPERATURE OXYACETYLENE TORCH TESTS OF FUSED SILICIDE COATED TZM AND T-111 ALLOYS

		No. of 10-min. Cycles to Failure at Indicated Temperature*			
		3000°F	3100°F	3200°F	Melting Temp. (°F)
TZM	Si-20Cr-5V	4	3	1.2	3250
TZM	Si-20Cr-1/2B_4Si	25	8	3	3300
TZM	Si-20Cr-10Fe	32	5	6	3380
T-111	Si-20Ti-10Mo	27	10	1.5	3410
T-111	Si-20Ti-3V	13	3.2	1.2	3400
T-111	Si-20Ti-10Mo-3V	43	9	0.5	3450
T-111	Si-20Ti-10Mo-3V (prealloyed)	2	6	1.2	----

*Brightness temperature.

c. Coating for Tantalum for Over 3000°F Operation

A current need for coating for tantalum alloys that are protective at temperatures above 3000°F led to an investigation of the suitability of fused silicide systems in such high temperature environments. The Martin tantalum structures program required a coating that will protect T-222 alloy for 15 minutes at 2600°F, 15 minutes at 3200°F, and 1 hour at 3000°F, consecutively.

A number of coating compositions were applied to T-111 and/or T-222 alloy coupons and fired on under various conditions. The compositions looked at were Si-20Ti-10Mo, Si-5, 10, 20, 30 and 50Ta, Si-5, 10, 20, and 30Ti, and Si-20Ti-10Ta. The tantalum-containing coatings and the Si-5 and 10Ti coatings did not give satisfactory edge coverage, particularly to the 0.010-inch thick T-111 alloy. Even the Si-20Ti-10Mo coating on this thickness of T-111 resulted in some edge cracking, but reduction of the applied coating thickness from 30 to 20 mg/cm^2 resulted in essentially perfect edge coatings.

High temperature furnace tests were performed in a newly constructed graphite-rod resistance element furnace with a zirconia tube. Exploratory tests were conducted at 3200°F for one 15-minute cycle on Si-20Ti-10Mo, Si-20Ti, and Si-30Ti coated T-111 and T-222. The appearance of the samples after this exposure seemed to indicate, however, that the furnace atmosphere may not have been sufficiently oxidizing even though there were 1/2 inch diameter holes in the plugs at each end of the furnace. Identical tests were run with the plugs out and the samples were virtually destroyed by oxidation. Repeat tests at 3100°F yielded similarly poor results. Short time tests were conducted at 3100°F in an attempt to determine the sequence of events leading to the catastrophic oxidation observed. Examination of samples exposed for 1-1/2, 3 and 5 minutes at 3100°F indicated that the first appearance of a molten glassy phase occurred at the sample edges after 3 minutes. Since the coated edges of these samples were essentially crack-free, it was believed the problem was associated with reactions between the zirconia pad and the sacrificial coated sample, leading eventually to reactions with the top test specimen. A five-minute 3100°F test of a similar sample (Si-20Ti-10Mo coated T-111) resting on a quartz slab resulted in no visible molten glassy phase and no apparent attack of the coating or substrate. This test indicated that reactions between ceramic supports and the silica scale of the coatings was responsible for the furnace test failures noted above even when so-called sacrificial samples were used.

Investigations of support materials for the high temperature testing of fused silicide type coated tantalum alloys were continued. It appeared that silicide coated W was suitable for this purpose for furnace testing at 3200°F. All of the coatings previously tested were retested at 3200°F in contact with this support material, and all failed to survive a 15-minute cycle. There is a gross melting reaction between the oxide scale on the fused silicide coating and one or more of the complex silicides that comprise the coating at this temperature.

Torch tests of Si-20Ti and Si-20Ti-10Mo coated T-222 were performed at 3200°F and were halted after 30 seconds when the quite rapid growth of a molten phase appeared to indicate that failure was imminent. A composite photomicrograph of longitudinal section through the hot spot of the Si-20Ti coated T-222 specimen is shown in Figure 125. Higher magnification photomicrograph of two locations on the same specimen are shown in Figure 126. The section through the hot spot in Figure 126A appears to indicate that the oxide is attacking and dissolving the coating. The same thing is apparently happening at a point about 0.100 inch from the center of the hot spot where the temperature is estimated to be about 3150-3175°F true brightness. The attack is obviously less severe at this slightly cooler portion of the sample. Figure 126C shows a location estimated to be in 3000-3100°F range, and it is clear that no such attack of the coating by the oxide is occurring. It is interesting to note that in Figure 126A the oxide is lighter in color at the surface and black near the oxide-coating interface. In Figure 126B and C the oxide consists of two discrete phases, one of which is black and the other a light gray. The lighter colored phase is consistently observed extending to the surface.

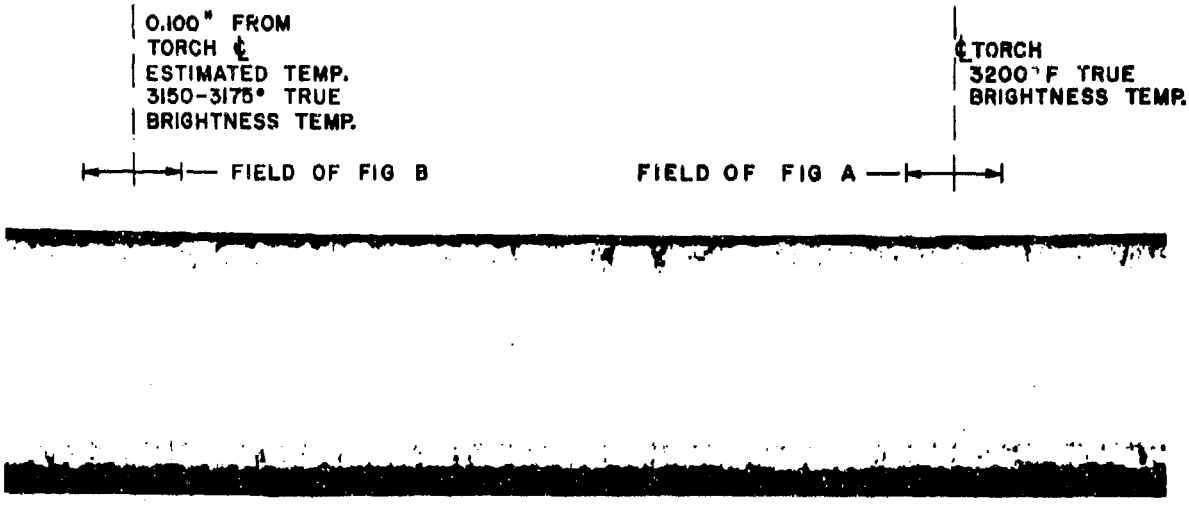

Figure 125 Photomicrograph of Si-20Ti Coated T-222 Oxacetylene Torch Tested for 30 Seconds at 3200°F (100X). (Reduced 50%).

X-ray diffraction analyses of Si-20Ti-10Mo coated T-222 alloy specimens exposed to various high temperature environments is given in Table XXXVIII. Since the microstructures of the Si-20Ti and the Si-20Ti-10Mo coatings are so similar it is believed that the analyses of Table XXXVIII will generally relate to both. Based on these results and other similar analyses performed on an earlier program (1), it seems safe to assume that the light colored oxide phase is TiO_2 and the black oxide phase is SiO_2. The melting points of SiO_2 and TiO_2 are approximately 3120°F and 3270°F. The eutectic between these phases occurs at 10 percent TiO_2 and melts at 2820°F. It is obvious that the scale in Figure 126A was completely molten and the SiO_2 (black phase) portion of the scale in Figure 126B was molten while neither oxide phase in Figure 126C appears to have been molten.

If the tantalum silicides are in fact soluble in their own "protective scales" at temperatures around 3200°F, this would obviously constitute a definite upper limit to the useful operating temperatures of this type of coating.

Apparently tungsten silicides are more stable with silica and this permits this system to retain its protectiveness to temperatures up to about 3600°F.

One should take cognizance of the fact that these tests were performed at atmospheric pressure. Reentry simulation tests performed at McDonnell at peak temperatures up to 3600°F have shown the Si-20Ti-10Mo coating to be more protective to T-222 alloy in that reduced pressure environment. If one is contemplating using coated tantalum alloys for reentry or hypersonic applications, it is questionable if the selection criteria should include atmospheric oxidation tests.

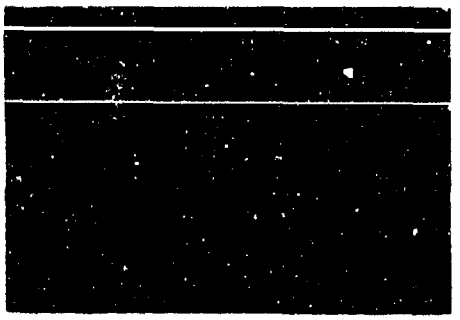

a) AT ℄ OF HOT SPOT 3200° T.B.T. *

b) 0.1" FROM HOT SPOT 3150-3175°F
ESTIMATED T.B.T.

c) 0.3" FROM HOT SPOT 3000-3100°F
ESTIMATED T.B.T.

*TRUE BRIGHTNESS TEMP.

Figure 126 Photomicrographs of Torch Tested Si-20Ti Coated T-222 Specimen Shown in Figure 125 (all 400X). (Reduced 45%).

TABLE XXXVIII

X-RAY DIFFRACTION ANALYSES OF Si-20Ti-10Mo COATED T-222

Sample Condition	Oxide Phases Detected		Other Phases Detected
	TiO_2 (Rutile) (Shifted)	SiO_2 (α crist)	
As coated	-	-	$TaSi_2$ (Shifted) + other unident. reflections Ta_5Si_3 (hex shifted)
Oxidized 2800°F - 8 hrs	(X)	X	+ other unident. reflections
Oxidized 3000°F - 1 hr	(X)	-	+ other unident. reflections
Oxidized 3100°F - 30 min	(X)	-	+ other unident. reflections
Oxidized 3200°F - 30 sec	(X)	-	$TaSi_2$ (Shifted) Ta_5Si_3 (hex shifted)

X Present.

(X) Strongest Reflections

7. NONDESTRUCTIVE TESTING

A "Dermitron", eddy-current type, nondestructive coating thickness instrument was cursorily evaluated for its applicability to fused silicide coatings on columbium alloys. Standards of 10, 20, and 30 mg/cm^2 Si-20Cr-5Ti coatings on D43 and Si-20Cr-20Fe coatings on Cb752 were prepared and it was established that this instrument could readily distinguish between these standards. The Dermitron reading is plotted against the applied unit coating weight for both coating systems in Figure 127.

The standards used for these tests were sectioned and metallographic coating thickness and base metal thickness measurements were made. This data were cross-correlated and curves relating applied unit coating weight to base metal consumption and coating thickness, and between Dermitron reading and coating thickness were constructed. These are shown in Figures 128 and 129.

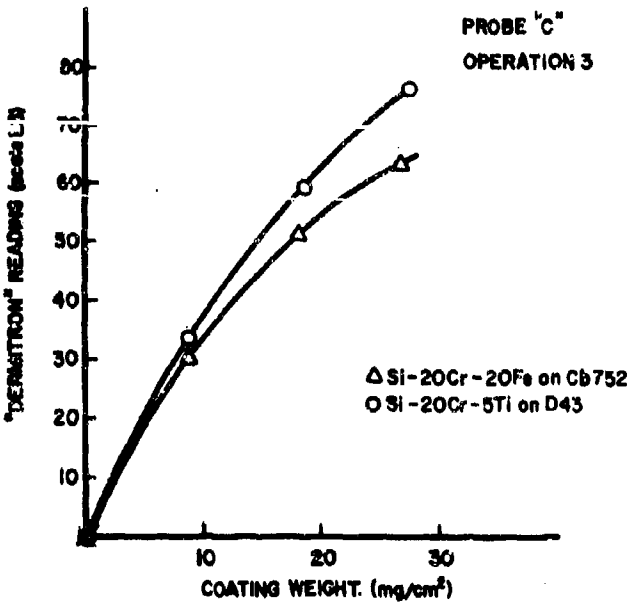

Figure 127 "Dermitron" Reading vs. Coating Weight.

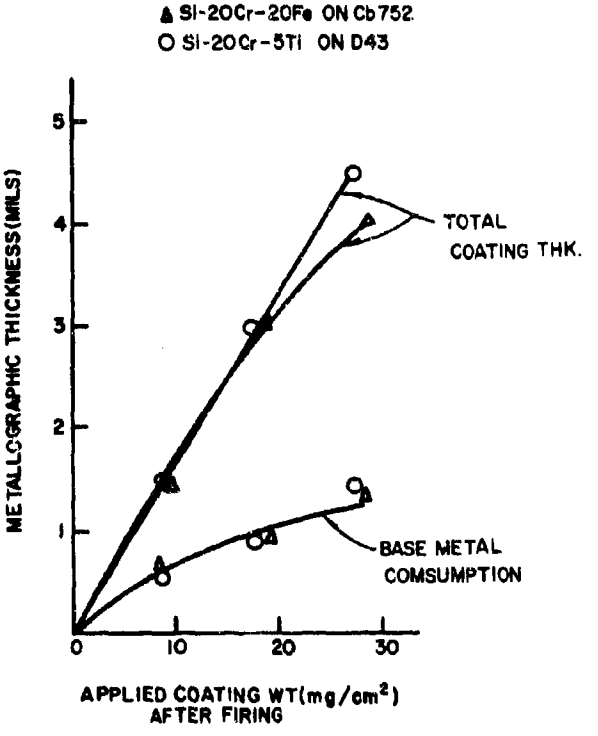

Figure 128 Metallographic Thickness and Base Metal Consumption vs. As-Applied Coating Weight.

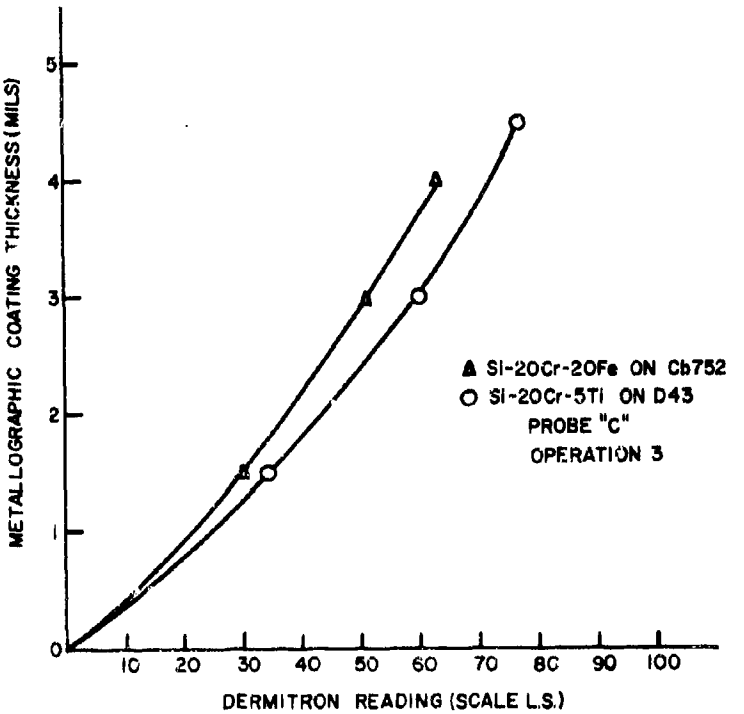

Figure 129 Metallographic Coating Thickness vs. Dermitron Reading

SECTION III

INDEPENDENT EVALUATIONS OF FUSED SILICIDE COATINGS

A great variety of test specimens and parts were coated for a number of outside laboratories and aerospace contractors for their independent evaluations. The circumstances involved in each agreement to provide coating services varied. Some were straight commercial transactions at a fixed price. In many instances the coating service was provided free to other AF contractors doing related R & D, while in still other cases the coating service was provided free with the understanding that the evaluation results would be made available to the AF and Sylvania, or made public. In any event the results of or references to outside independent evaluations detailed below cover those where there was an obligation to make the information public either through the evaluators own contractual obligations, or by virtue of their agreement to do so in return for free coating services.

1. LOCKHEED-CALIFORNIA CO. LOW PRESSURE EVALUATION.

The following specimens were coated for Lockheed under subject contract.

Item	Coating	Quantity
Cb752 coupons	Si-20Cr-20Fe (R512E)	120
Cb752 coupons	Si-20Cr-5Ti (R512A)	10
D43 coupons	Si-20Cr-20Fe (R512E)	10
D43 coupons	Si-20Cr-5Ti (R512A)	10

The object of the tests at Lockheed was to compare the fused silicide coating systems directly to other systems previously evaluated. In order to effectively accomplish this end the Lockheed-California Company funded the Material Sciences Laboratory at Lockheed Missiles and Space Company to perform tests which were identical to those made on other coating systems under a previously completed Air Force contract (4).

The results of their evaluations were reported on at the 12th meeting of the Refractory Composites Working Group (16); Figure 130, reprinted from this paper, summarizes the results of these tests. The conclusions of that paper are quoted below.

"While caution must be exercised in making claims for this coating system since other factors should be examined, it is apparent from the results of these tests that the Cb 752/R512E material system is superior to systems previously evaluated in the same way. An important conclusion is the probability that this system will

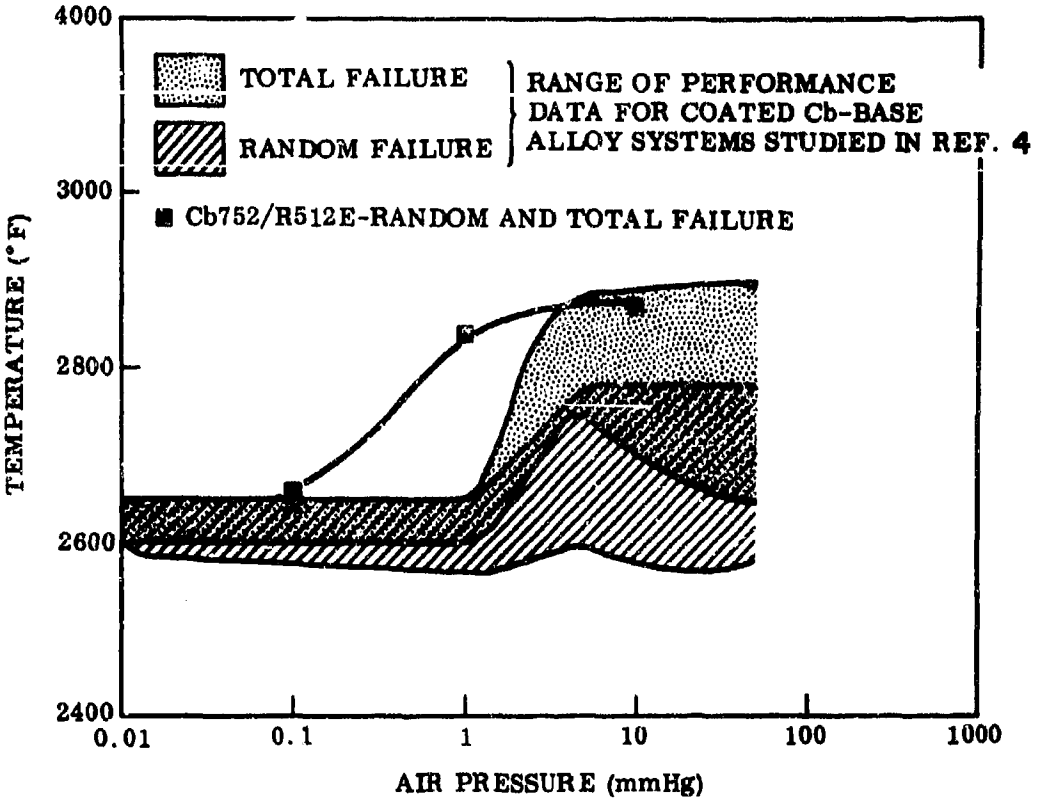

Figure 130 Maximum Temperature for 4-Hour Lifetime for Cb-752/R512E System and Coated Alloys Studied in Reference 4. Taken from Reference 16.

provide multiple useage capability for hypersonic and reentry vehicles particularly if the temperature is limited to 2500°F. There is also a margin of safety apparent which would permit overshoots due to guidance errors or aborts."

Services for the coating of a number of Ta-10W test specimens including several leading edge specimens for arc plasma tests were purchased by Lockheed under their contract NAS-1-7573.

2. UNIVERSITY OF DAYTON

Three batches of 0.020-inch thick D43 specimens were furnished by the University of Dayton for application of the Si-20Cr-5Ti (R572A) coating. The first batch consisted of two tensile specimens, 150 bend and oxidation test tabs (1-1/4 x 1/2) and three spot welded lap joint specimens. The other two batches each consisted of 50 bend and oxidation tabs.

The coating applied to all three batches was identical except for the nominal coating thickness. The first batch had a coating thickness of about 2.75 mils (15 mg/cm^2 unit weight), the second batch was 3.5 mils thick (19.5 mg/cm^2 unit weight), and the third batch was 4.4 mils thick (24 mg/cm^2 unit weight).

The bulk of their evaluation consisted of cyclic furnace oxidation testing and analysis of the resultant data by statistical methods (Weibull analysis). The results of their evaluation are reported on in Reference 17. Table XXXIX below is a summary of their findings.

TABLE XXXIX

RESULTS OF WEIBULL ANALYSIS OF CYCLIC FURNACE OXIDATION TESTS OF R512A COATED D43

Coating Thickness (MILS)	Expected Life (No. of 1 Hour Cycles to First Failure)			
	2400°F		2600°F	
	95% Reliability	70% Reliability	95% Reliability	70% Reliability
2.75 (15 mg/cm^2)	15	22	12	21
3.5 (19.5 mg/cm^2)	27	33	17	25
4.4 (24 mg/cm^2)	39	46	23	32

Thirty Cb 752 tensile specimens 0.030-inch thick, 2-1/2 inches wide, and 10-12 inches long were coated under subject contract with the R512E (Si-20Cr-20Fe) composition. These specimens are intended for stress oxidation tests in which discrete spot failures will either be repaired and/or carefully charted to determine the consequences of such failures as well as the effectiveness of repair procedures. Hopefully a better definition of coating failure will issue from these tests. Although testing has begun on this program, no results have as yet been reported.

The coating of 50 Cb 752 tubes 1-inch long by 1/2-inch O.D. by 0.033-inch wall thickness with the R512E (Si-20Cr-20Fe) coating was purchased by the University of Dayton for evaluation under their contract AF33(615)67-C-1262. These specimens are intended for arc plasma tests designed to determine the effects of simulated rocket environments on the protectiveness of the fused silicide coating. Various parameters such as gas composition, pressure, temperature, velocity, etc. are to be studied. No results have as yet been reported.

Forty-five Cb752 and 31 D43 tensile type specimens 0.018 inch thick were coated with the R512E (Si-20Cr-20Fe) composition under subject contract. These specimens are for creep-oxidation testing in air at 1800, 2200 and 2600°F for periods of time to 20 hours. No results of these tests have yet been reported.

3. NORTH AMERICAN ROCKWELL CORP.

Several batches of 31/32-inch diameter, 0.030-inch thick Cb752 specimens were coated with the R512E (Si-20Cr-20Fe) composition under subject contract. The total of 125 specimens coated were for evaluation of the coated samples optical properties (emittance) under their contract AF33(615)-3039. The results of this work are included in reference 18.

4. MC DONNELL-DOUGLAS CORP.

This company has a program for the "Evaluation of the Fused Slurry Silicide Coating Considering Component Design and Reuse" covered by contract AF33(615)-67-C-1574. More than 500 Cb752 specimens of various kinds will be coated by Sylvania with the R512E (Si-20Cr-20Fe) composition for evaluation by McDonnell. Essentially the object of this program is to determine the effectiveness of this coating system in its application to typical aircraft and aerospace type hardware and most specifically to joints. The first quarterly program report in this program is listed as reference 19.

5. AVCO SPACE SYSTEMS DIVISION

Various fused silicide coated specimens were purchased by this company from Sylvania for non destructive test development efforts under their contract AF33(615)-3877. These specimens included R512A (Si-20Cr-5Ti) coated B66 alloy and R512C (Si-20Ti-10Mo) coated T-111 alloy. The latest results of their efforts are reported in reference 13.

6. U.S. AIR FORCE

Under contract AF33(615)-68-C-0193 Sylvania is fabricating 171 T-222 tensile specimens and coating 104 of these specimens with the R512C (Si-20Ti-10Mo) composition for an AFML in-house mechanical property study at temperatures up to the maximum useful temperature of the system (3200°F).

7. APPLIED PHYSICS LABORATORY - JOHNS HOPKINS UNIVERSITY

Various columbium, molybdenum, and tantalum specimens were coated for this laboratory. This service was purchased by the above contractor under their contract Now 62-0604C. The results of the columbium alloy work are included in reference 20.

8. PRATT AND WHITNEY AIRCRAFT

This firm has a contract no. AF33(615)-2117 entitled "Evaluation and Improvement of Coatings for Columbium Alloy Gas Turbine Engine Components." This program includes a quite extensive evaluation of the fused silicide coatings for gas turbine applications. The tests performed included oxidation-erosion, thermal fatigue, and mechanical fatigue, to mention only a few. On the basis of these tests, fused silicide (Si-20Cr-5Ti) coated B66 air cooled vanes were evaluated in a test engine at turbine inlet temperature approaching 2400°F. The components were fabricated and coated during July and August 1968, and the test conducted during October-November. Reference 11 gives the results of this program.

9. SOLAR AIRCRAFT

Various small Cb752 panels and other specimens were coated with the R512E (Si-20Cr-20Fe) composition for Solar. This service was purchased from Sylvania under their contract AF33(615)-2304. The object was to determine the coatability of diffusion bonded joints in highly stressed thin gage structures.

10. MARQUARDT CORP.

Under contract NAS 9-6003 the Marquardt Corp. conducted a program entitled "Development of a Ductile Columbium Alloy Rocket Engine Combustion Chamber". In this program a number of coating and alloys were evaluated by various means including extensive engine testing. The results of their evaluation are given in Reference 21.

11. GRUMMAN AIRCRAFT ENGINEERING CORP.

This firm fabricated a tantalum alloy elevon on a company-funded program with coating services purchased from Sylvania. The parts were coated as details, and a final repair coat was given to the assembled structure. The R512C (Si-20Ti-10Mo) coating was applied to this assembly. The structure was given to the AF Flight Dynamics Laboratory - Wright Patterson AFB for testing under load at 3000°F in an oxidizing environment. A description of the structure is contained in reference 22. The test results have not been reported as of this date.

SECTION IV

GENERAL DISCUSSION AND CONCLUSIONS

The continuing development, optimization, and extensive characterization of the fused silicide type of coatings in this program, coupled with a substantial degree of outside independent evaluation, have demonstrated the inherent superiority of this type of coating in relation to the other types of coatings known and available.

Many idealized lists of properties presumably required of a protective coating have been constructed. In many instances, however, the properties listed are not true requirements, but are assumed to relate to the basic protectiveness of the coating. A list of true requirements for a useful coating really may consist of only two generalized items. The first requirement is that the coating have the necessary basic protectiveness in the broadest possible sense. The fulfillment of this condition may be determined by subjecting small, coated, test specimens to a variety of laboratory and simulated environmental tests, and then by careful examination and analysis of the specimens. The second requirement is that the coating be capable of being supplied to useful structures in such a manner that the full protective potential of the coating is realized.

It is believed that the data presented for the slow cyclic tests and the reentry simulation tests, supplemented with the outside independent evaluations referenced above, establishes the basic protectiveness of the fused silicide coatings for multimission reentry vehicle applications. Similarly, the wettability and flowability experiments, together with the Lockheed tests (16), and the demonstrations of the ability of this type coating to be applied to practically any size or shape or design of structure (refer to Appendix), clearly establishes its ability to achieve its potential in practice.

As far as the combined effects of low pressure and high temperature on the protectiveness of the fused silicide coating is concerned, the extensive reentry simulation testing performed here combined with the Lockheed (16) low pressure study give assurance of the enhanced protectiveness afforded by this coating system in comparison with other coatings.

The statistical reliability tests performed here (see paragraph 4.c of Section II) and at U.D.R.I. (17), the defect tolerance tests (see paragraph 4.f of Section II), and the repair studies, as well as the flowability and wettability tests, to name but a few, also are convincing evidence of the essential reliability and practicality of this system.

Although it is in no way essential to the present utility of the system, it would be extremely useful to future coating development efforts to know why the fused silicide coatings are superior in most, if not all respects, and some speculation on this subject therefore appears warranted. Anyone who has studied intermetallic compound coatings for any time will no doubt have had his attention focused on the network of transverse cracks that is common to all such coatings. It is common knowledge that these cracks are the result of thermal stresses arising from the large difference in thermal expansivities between refractory metals and their silicide or aluminide coatings; (the coatings have the higher expansivity). It has been the stated objective of many workers to match the expansivities of coating and base metal, and although this is admittedly a worthy goal it does not appear to be readily achievable. It should be quite obvious, therefore, that the oxidation process in and around these cracks is quite crucial and probably determines to a large degree the protectiveness of the coating.

In a single cycle pack cementation coating, the coating in general is only slightly alloyed, and the oxidation resistance of the M_5Si_3 sublayer, or diffusion zone as it is sometimes referred to, is poor at all temperatures. In addition the slightly alloyed MSi_2 has fairly good oxidation resistance at elevated temperatures but probably will be oxidized more rapidly at some intermediate to low temperature. When such a coating is exposed to an oxidizing environment at a very high temperature, two factors work together to prevent rapid oxidation at the base of this crack. First, if the exposure temperature is higher than the coating application temperature, then the cracks will be held tightly closed. Secondly, at elevated temperatures the MSi_2 outer phase will oxidize rapidly enough to seal or bridge over the crack with oxide thereby preventing oxidation at the base of the crack. As the exposure temperature is lowered, however, the oxidation rate of the MSi_2 outer layer will be reduced (at least until a "pest" range is reached), and simultaneously the cracks will open thereby exposing the less oxidation resistant M_5Si_3 layer. This process results in undermining of the coating longitudinally as well as oxidation penetration into the base metal at that point.

In the case of the fused silicide coatings the outer layer consists of MSi_2 and M_5Si_3, the latter being substantially alloyed. This layer has a moderate oxidation rate somewhat higher than a corresponding single-cycle coating outer layer which is composed essentially of MSi_2. Additionally, the coating sublayer, which is M_5Si_3 substantially alloyed with chromium and other additives, is moderately oxidation resistant. So, in this case we have conditions which are more favorable to effect sealing of the thermal expansion cracks in these coatings over the whole temperature spectrum, i.e. the outer layer and sublayer materials are comparably and moderately oxidation resistant.

The reliability of the fused silicides can probably be attributed to several factors. First of all, as demonstrated in the wettability tests, it is quite unlikely that uncoated areas may inadvertently result. Also it is hard to imagine a grossly inhomogeneous coating resulting from the reaction of a molten alloy with a homogeneous base, since a substantial part of the reaction takes place before solidification. The fact that the reaction goes forward to some extent while the coating remains liquid

also tends to result in better edge coverage. In addition, it is not possible to have unreacted or partially reacted coating materials adhering to the part after processing which can readily happen with the pack cementation process. In the fused silicide process, if fusion occurs, all coating materials are almost instantly reacted. Since one can safely exceed the actual fusion temperature of the as-applied coating by 200°F or more, there is little danger in practice of not completely fusing the coating.

There is little question that the fused silicide coatings will penetrate the faying surfaces of any joint better than any other coating applied by any other process, and will thereby afford greater protection to these joints than the other coatings. However, the extent to which the protective life of the coated joint approaches the basic protective life of the coating will depend on factors such as the stiffness of the joint, the length of catilevered faying sheet, the weld and/or rivet spacing, the faying surface gap, the flatness of faying sheets, the thicknesses and thickness ratios of mating parts, etc. These factors and many others will determine whether the joint will be effectively sealed or if the faying surfaces will each have a separate, tapered coating. The latter case can be particularly harmful since it can lead to early failures at the thin coating areas deep in the faying surfaces. It has been demonstrated (23) that short stiff joints can be effectively coated and protected; it remains to define design limitations which will assure this desired end. It is expected that the program now in progress at McDonnell will begin to fill this gap (19).

Although there remains a great deal of work that can be done to advantage, it is believed that the fused silicide coatings can now be applied to many reentry vehicle components with confidence that they will satisfactorily protect these structures through many reuse cycles.

SECTION V

RECOMMENDATIONS FOR FUTURE WORK

1. MANUFACTURING SCALE-UP STUDY

This study would focus on developing improved methods of applying the slurry uniformly to large and/or intricate hardware. Although presently developed methods for applying the fused silicide coatings are superior to other procedures in this regard, they could be improved substantially. Much practical knowledge has been gained concerning the effect of process and part variables on the uniformity of slurry applied coatings but this knowledge is for the most part qualitative. Therefore it is usually necessary to make a number of trial coating runs in order to determine coating conditions on any specific day for a particular slurry and piece of hardware. The ability to inspect the "green" slurry by NDT methods as explained in Paragraph II 5a (pp. 188-192) has been most helpful in this regard although additional work is needed in this area as well (see recommendation 2 below).

Parts of simple geometry such as flat panels of the ASCEP type appear to be amenable to spray coating methods. However automatic spray gun indexing and operation would be necessary to assure uniform coating thicknesses. This method of slurry application is potentially the most economical for the coating of small quantities of parts of any size if the part geometries are suitable. The availability and suitability of automatic spray equipment should be evaluated. Design modifications and/or redesign should be carried forward as indicated by the evaluation of the uniformity of applied slurry to typical panel shapes.

Many, if not most, refractory metal parts can not be readily spray coated and must be coated by dipping. Slurry coating thickness in dipping is a function of temperature, composition, type and concentration of additives, powder size and distribution, withdrawal rate, withdrawal angle, length of part, drainage and part surface condition. This list constitutes some of the more prominent process parameters and part variables that significantly affect the dip coating process. If uniform reproducible coatings on complex parts are to be achieved with a minimum of trial and error and in a systematic and economical manner, then the relationships between these factors and coating uniformity (in both composition and thickness) must be quantified.

Another important question about slurry coating is the shelf life of large expensive slurries. It has been noted here that while the compositions Si-20Cr-5Ti and Si-20Cr-20Fe (R512A and R512E for columbium alloys) appear to be stable for periods exceeding one year, the Si-20Ti-10Mo (R512C for tantalum alloys) deteriorates in storage in a matter of a few weeks. No experience has been acquired with other compositions. For slurry compositions of interest the shelf life should be determined and where this life is found to be impractially short, methods for retarding deterioration should be studied.

2. NONDESTRUCTIVE TESTING

Emphasis should be on methods for examining critical areas such as faying surfaces, corners, crevices, joints, and internal surfaces. Methods for measuring

"green" slurry thickness for in-process control should also be improved and refined.

3. COATINGS FOR COLUMBIUM ALLOY GAS TURBINE ENGINE COMPONENTS

This effort should focus initially on optimizing the fused silicide for this specific application in view of the very promising results obtained so far in the P&W evaluation program (11).

APPENDIX I

Following are the raw data on which the Weibull Cumulative Failure plots of Figure 8 (p. 32) were based. The curves of Figure 8 are constructed by plotting X (slow cyclic lifetime) against F(x) (% less than cumulative frequency). The intercept for any given lifetime therefore gives a figure indicating "less than that percent of the specimens had failed at that time". The reader is referred to references (2) and (3) for details of the Weibull distribution function and its applicability to this specific type of data.

Si-20Cr-20Fe Coating on D43

X hours to first failure	No. of Specimens	f(x)	% cumulative frequency	F(x)	% less than cumulative frequency
54	1		5		0
55	1		10		5
59	7		45		10
60	4		65		45
64	3		80		65
65	2		90		80
68	2		100		90

Si-20Cr-20Fe-10VSi_2 on D43

X hours to first failure	No. of Specimens	f(x)	% cumulative frequency	F(x)	% less than cumulative frequency
11	1		5		0
29	1		10		5
43	1		15		10
47	3		30		15
48	1		35		30
51	3		50		35
56	3		65		50
61	1		70		65
63	1		75		70
64	2		85		75
67	1		90		85
70	2		100		90

APPENDIX II

Following is a group of photographs illustrating the ability of the fused silicide coatings to be uniformly applied to real hardware regardless of its size, shape, or complexity.

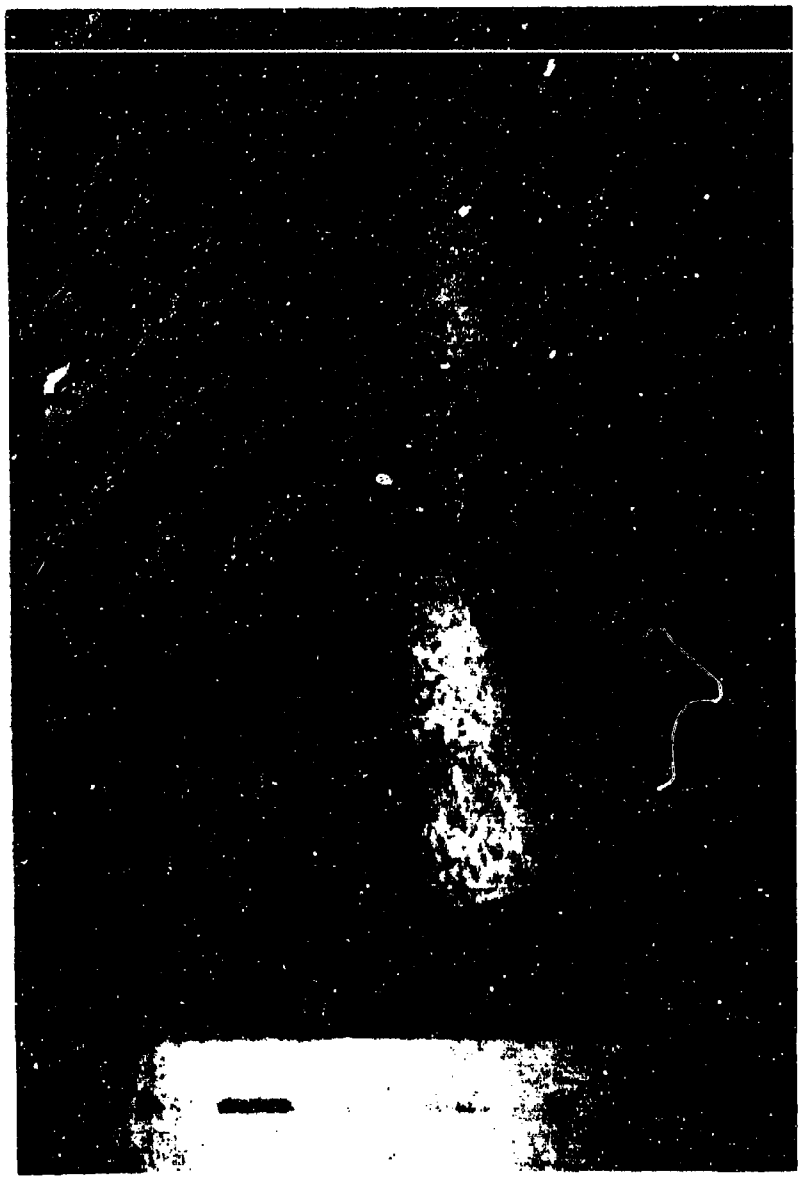

Figure 131 Marquardt SCb-291 Thruster Coated With Si-20Cr-5Ti (R512A).

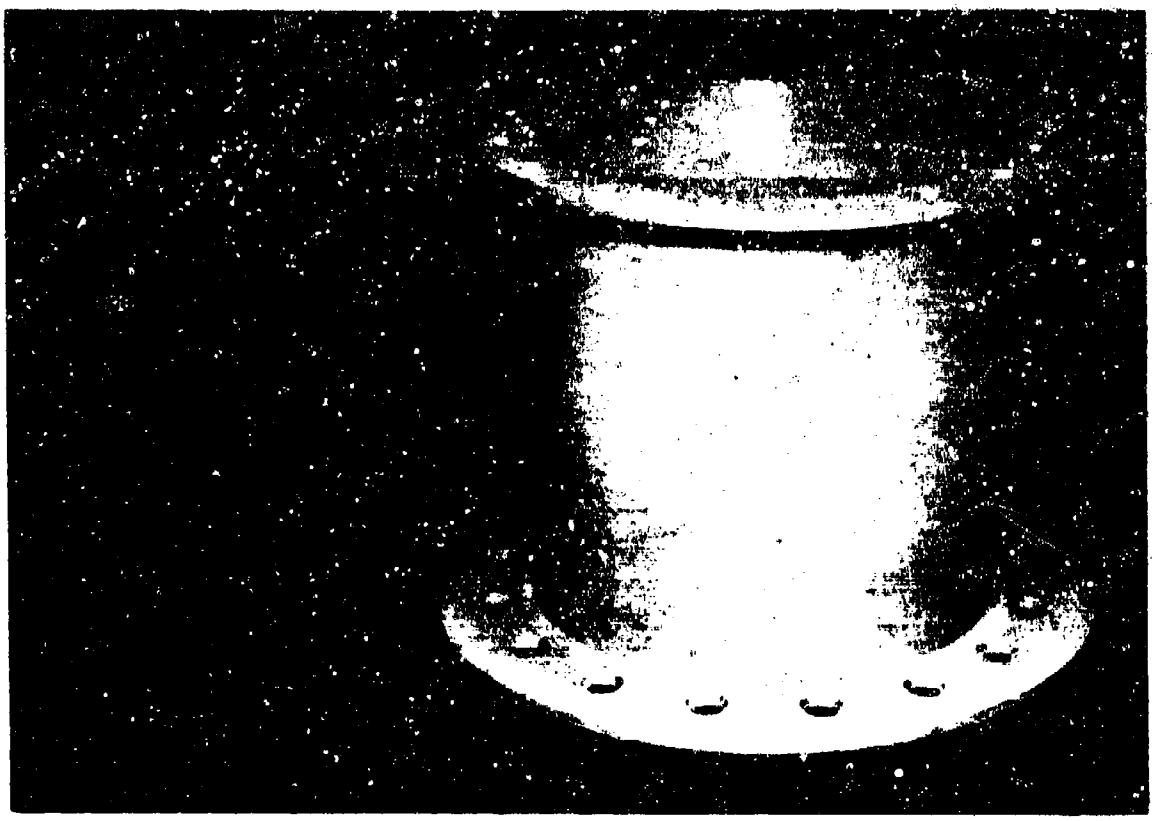

Figure 132 Marquardt Ta-10W Rocket Motor Case Coated With Si-20Ti-10Mo (R512C).

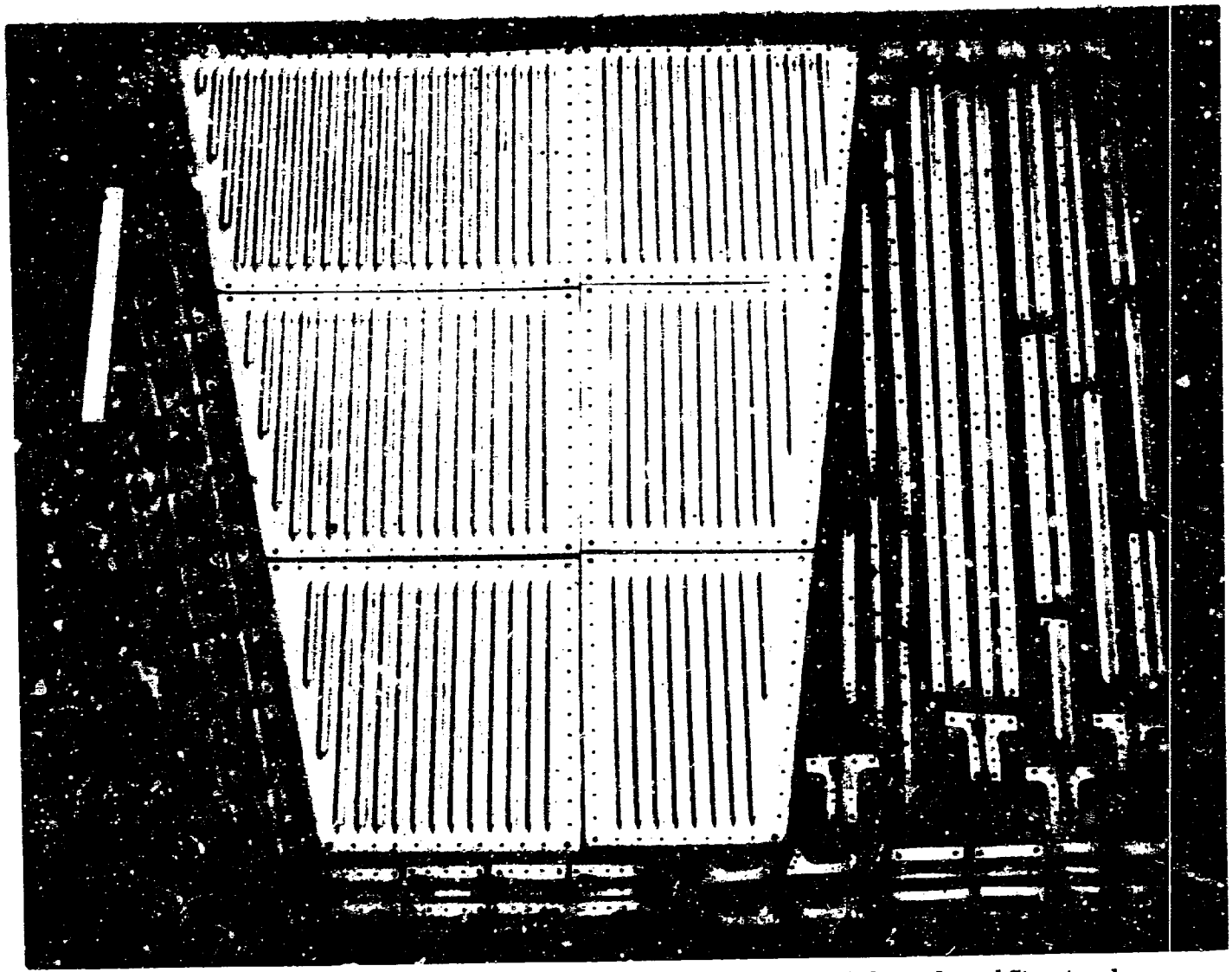

Figure 133 Lockheed Cb-752 Columbium Alloy Electron Beam Welded Panels and Structural Members Coated With Si-20Cr-5Ti (R512A).

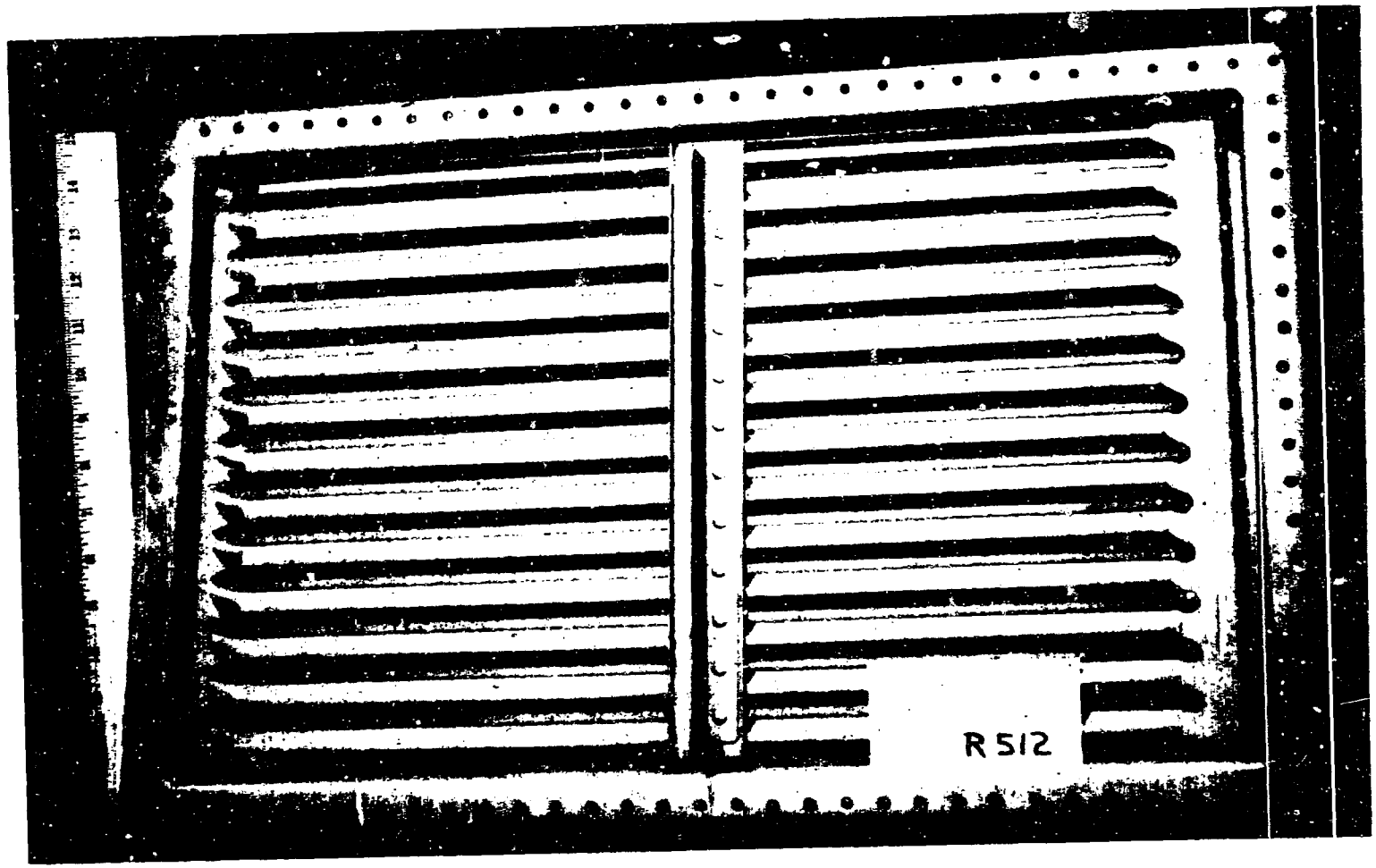

Figure 134 Grumman Ta-10W Tantalum Alloy Spot Welded and Riveted Corrugated Panel-Coated With Si-20Ti-10Mo (R512C).

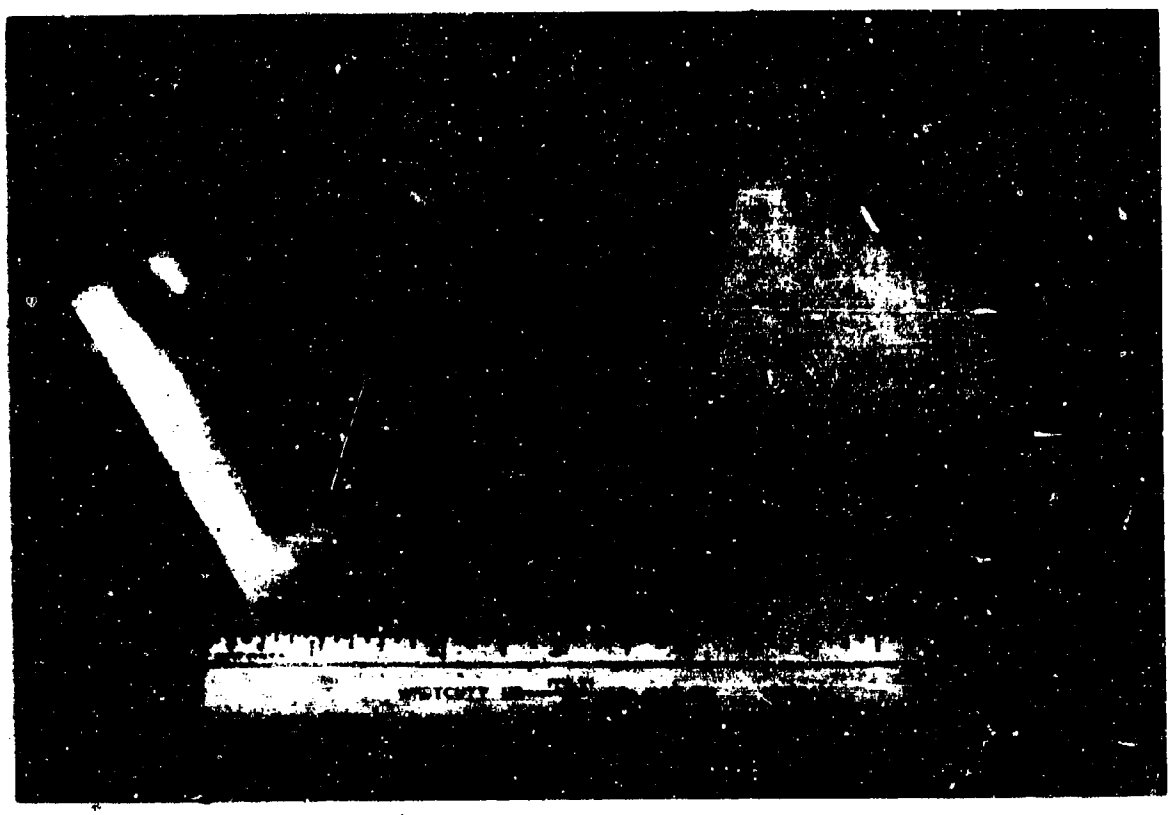

Figure 135 Pratt & Whitney Simulated Turbine Vane Test Specimens D43 Columbium Alloy Coated With Si-20Cr-5Ti (R512A).

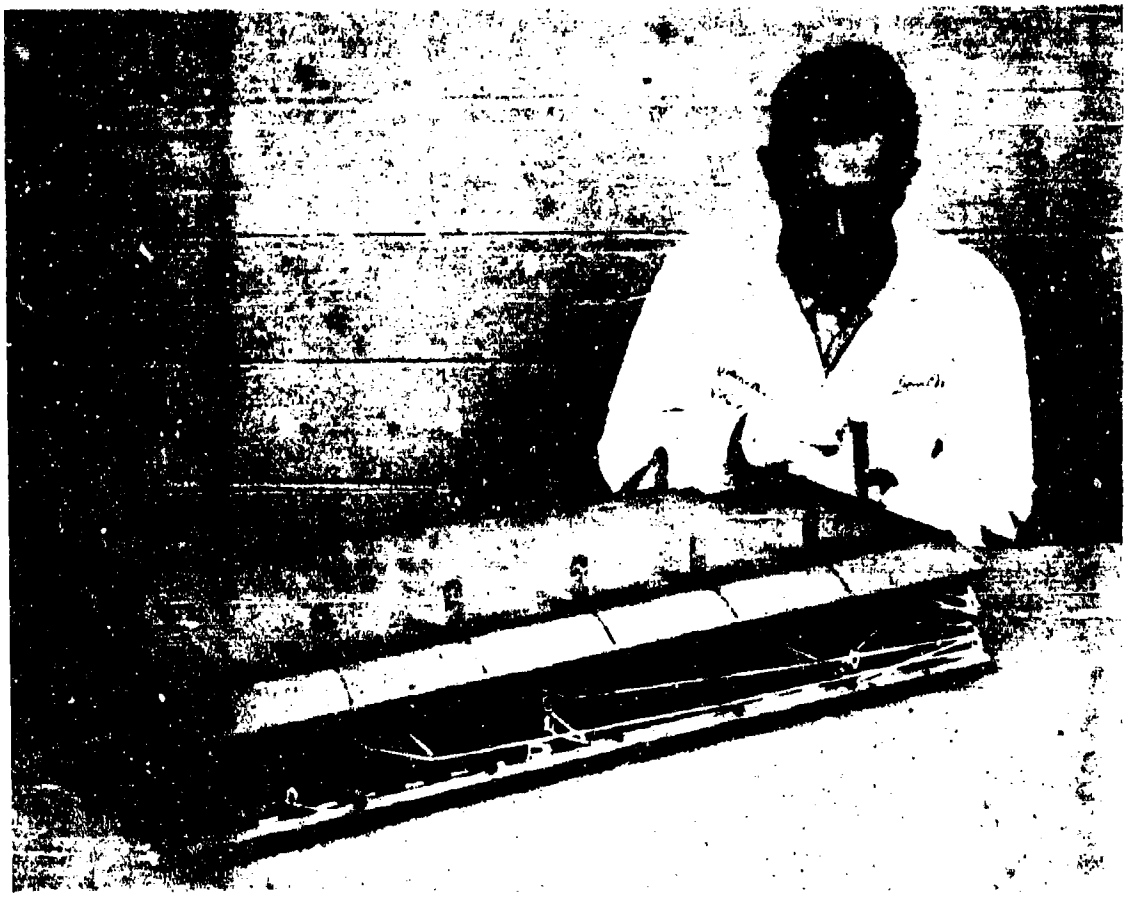

Figure 136 Grumman Ta-10W Tantalum Alloy Test Elevon Coated With R512C (Si-20Ti-10Mo).

REFERENCES

1. S. Priceman and L. Sama, "Development of Slurry Coatings for Tantalum, Columbium, and Molybdenum Alloys," AFML-TR-65-204, September 1965.

2. W. Weibull, J. Appl. Mech 18(3), 293-7 (1951)

3. J. Wurst, "Development of Testing Techniques for Evaluating High Temperature Coating Systems," Plating, October 1964.

4. R. A. Perkins and C. M. Packer, "Coatings for Refractory Metals in Aerospace Environments," AFML-TR-65-351, September 1965.

5. A. R. Stetson, "Ductile Coatings for Columbium Alloys," Contract AF33(615)-1598. Phase 1 Progress Report 3, dated May 1965.

6. H. W. Lavendel, "Investigation of Modified Silicide Coatings for Refractory Metals with Improved Low Pressure Oxidation Behavior," AFML-TR-65-344, August 1965.

7. R. W. Bartlett, "Investigation of Mechanisms for Oxidation Protection and Failure of Intermetallic Coatings for Refractory Metals," ASD-TDR-63-753, June 1963.

8. A. M.Norton, "Advanced Structural Concepts Experimental Program - Volume II - Materials Manufacturing Process Development and Fabrication AFFDL-TR-67-146, July 1968.

9. J. D. Gadd, "Advancement of Protective Coating Systems for Columbium and Tantalum Alloys," AFML-TR-65-203, April 1965.

10. B. C. Allen, E. S. Bartlett, and B. A. Wilcox, "Elevated Temperature Ductility Minima and Creep Strengthening of Coated and Uncoated Columbium Alloys" Technical Report AFML-TR-66-89, Part II, February 1967.

11. J. F. Hollaway and H. A. Hauser, "Evaluation and Improvement of Coatings for Columbium Alloy Gas Turbine Engine Components" AFML-TR-66-186, Part 1, July 1966 and Part 2, May 1968.

12. C. R. Wilks, "Advanced Structural Concepts Experimental Program - Volume III - Experimental Evaluation", AFFDL-TR-67-146, July 1968.

13. R. C. Stinebring and T. Sturiale "Development of Nondestructive Methods for Evaluating Diffusion-Formed Coatings on Metallic Substrates", Technical Report AFML-TR-66-221, September 1966.

14. A. R. Stetson, H. A. Cook, and V. S. Moore, "Development of Protective Coatings for Tantalum Base Alloys," AFML-TR-65-205, Part 1, June 1965.

15. L. Sama, "High Temperature Oxidation Resistant Coatings for Tantalum Base Alloys," ADS-TDR-63-160, February 1963.

16. M. G. Childers "Behavior of Sylcor R512E Coated Cb 752 Columbium Alloy in a Low Pressure Environment" Summary of the 13th Refractory Composites Working Group Meeting, Seattle, Wash., July 1967.

17. J. C. Wurst, et al "The Evaluation of Materials for Aerospace Applications" AFML-TR-67-165, June 1967.

18. K. O. Bartsch "The Role of Emittance in Refractory Metal Coating Performance" AFML-TR-66-55, Part 1, August 66, Part II, September 1968.

19. B. G. Fitzgerald "Evaluation of the Fused Silicide Coating Considering Component Design and Reuse", Contract F33(615)-67-C-1574, Report Nos F904 and G103, November 1967, March 1968.

20. R. O. Weiss, et al "An Evaluation of Coated B66 Columbium Alloy at Elevated Temperatures" Journal of Spacecraft & Rockets, Vol 5, No. 2, February 1968.

21. E. Ritchie "Development of a Ductile Columbium Alloy Rocket Engine Combustion Chamber", Report No. S-843, Contract NAS 9-6003, September 1967.

22. M. L. Yafee "Tantalum Elevon Built for 3000°F Test" AviationWeek and Space Technology, January 1, 1968.

23. L. Yates, "Selection of Materials for high L/D Reentry Vehicles," SAE Aeronautic and Space Engineering and Mfg. Meeting, Los Angeles, October 1966.

UNCLASSIFIED

Security Classification

DOCUMENT CONTROL DATA - R & D

(Security classification of title, body of abstract and indexing annotation must be entered when the overall report is classified)

1. ORIGINATING ACTIVITY (Corporate author)
Sylvania Electric Products, Inc.
High Temperature Composites Laboratory
Hicksville, New York 11802

2a. REPORT SECURITY CLASSIFICATION
Unclassified

2b. GROUP

3. REPORT TITLE
Development of Fused Slurry Silicide Coatings for the Elevated-Temperature Oxidation Protection of Columbium and Tantalum Alloys

4. DESCRIPTIVE NOTES (Type of report and inclusive dates)
Final Report

5. AUTHOR(S) (First name, middle initial, last name)
S. Priceman
L. Sama

6. REPORT DATE	7a. TOTAL NO. OF PAGES	7b. NO. OF REFS
July 1968	229	23

8a. CONTRACT OR GRANT NO.	9a. ORIGINATOR'S REPORT NUMBER(S)
AF33(615)-3272	AFML-TR-68-210
b. PROJECT NO. 7312	
c. Task No. 731201	9b. OTHER REPORT NO(S) (Any other numbers that may be assigned this report)
d.	

10. DISTRIBUTION STATEMENT This document is subject to special export controls and each transmittal to foreign governments or foreign nationals may be made only with prior approval of the Metals and Ceramics Division (MAMP), Air Force Materials Laboratory, Wright-Patterson AFB, Ohio 45433

11. SUPPLEMENTARY NOTES	12. SPONSORING MILITARY ACTIVITY
	Air Force Materials Laboratory Air Force Systems Command Wright-Patterson AFB, Ohio 45433

13. ABSTRACT Improved fused silicide coatings for columbium alloys were selected on the basis of slow cyclic oxidation tests. Several coating compositions were broadly characterized in terms of their structure and chemistry by means of x-ray diffraction and electron microbeam probe techniques and in terms of their applicability and performance by experimental analyses of wettability and flowability, faying surface penetration, coating repair, mechanical property tests, slow thermal cycling, furnace and torch oxidation, arc plasma tests, low temperature cycling, low pressure - high temperature exposures, reentry simulation and statistical reliability analyses. The coating composition Si-20Cr-20Fe was the best for columbium alloys using the above combined criteria. More than 40 typical full scale columbium alloy aerospace structural panels were coated for reentry evaluation. During the course of the program several experimental compositions were utilized and procedures modified in accordance with panel fabrication requirements. These included stripping and repair brazing. Improved coating compositions and application techniques were used in the latter stages on virgin panels. Demonstrations are also presented which show the applicability of the process to the coating of threaded fasteners.

The compositions Si-20Ti-10Mo and Si-20Cr-1/2B_4Si were identified as better compositions for tantalum and molybdenum alloys on the basis of various higher temperature tests. The maximum useful temperature of these systems is approximately 3200°F.

The feasibility of using the fused silicides as a one-step combination coating-braze was demonstrated, and shear strength tests on such joints were carried out at temperatures in the range of room temperature to 3000°F.

This abstract is subject to special export controls and each transmittal to foreign governments or foreign nationals may be made only with prior approval of the Air Force Materials Laboratory (MAMP), Wright Patterson AFB, Ohio 45433.

DD FORM 1 NOV 65 1473 (PAGE 1)

S/N 0101-807-6801

UNCLASSIFIED

Security Classification

3ND PPSO 13152

14. KEY WORDS	LINK A		LINK B		LINK C	
	ROLE	WT	ROLE	WT	ROLE	WT
Protective Coatings						
Columbium						
Tantalum						
Molybdenum						
Slurry Coatings						
Oxidation						
Environmental Testing						